Sorptive Removal of Carbofuran and 2,4-Dichlorophenoxyacetic Acid (2,4-D) Pesticides from Water Using Sustainable Biochars Derived from Agricultural Byproducts

**Thesis submitted to Jawaharlal Nehru University
in partial fulfillment of the requirements
for the award of the degree of**

Doctor of Philosophy

By

VINEET VIMAL

**School of Environmental Sciences
Jawaharlal Nehru University
New Delhi-110067, India
2019**

Certificate

This is to certify that the research work embodied in this thesis entitled **"Sorptive removal of Carbofuran and 2,4-Dichlorophenoxyacetic acid (2,4-D) Pesticides from Water Using Sustainable Biochars Derived from Agricultural Byproducts"** is submitted to Jawaharlal Nehru University for the award of the degree of Doctor of Philosophy. This work is original and has not been submitted in part or in full for any other degree or diploma to any university/institution.

Vineet Vimal

Vineet Vimal

(Candidate)

22/7/2019

AL Ra_ 2/7/19

(Dean, SES)

Prof. Dinesh Mohan

Dr. Dinesh Mohan
Professor
School of Environment Sciences
(Supervisor)
Jawaharlal Nehru University
New Delhi-110067, India

प्रो. एल. रामानाथन/Prof. AL. Ramanathan
डीन / Dean
पर्यावरण विज्ञान संस्थान
School of Environmental Sciences
जवाहरलाल नेहरू विश्वविद्यालय, नई
Jawaharlal Nehru University, Ne

Dedicated to

My Family

Acknowledgements

This part of my thesis is dedicated to all the heavenly and worldly beings which made it happen. Starting with the God who has been with me all the time. He gave me strength to withstand everything that came across me in this journey His answers to my prayers made my belief on him further stronger. I owe a lot you, God! Keep up the grace. I hope to do something good for the society someday.

I would like to express my heartfelt gratitude and respect to my PhD supervisor Prof. Dinesh Mohan, School of Environmental Sciences, Jawaharlal Nehru University, New Delhi. I don't think I have enough words to describe his personality and stature. An accomplished scholar, a supporting guide, an understanding person- there are many facets of him. Yes, he gets annoyed too but not like losing cool but like making you do the work. I simply cannot thank him enough for taking me under his supervision and guiding me all through it despite shortcomings from my side. Sir, you truly guided me from despair to triumph!

I am also very grateful to Prof. H.B. Bohidar, School of Physical Sciences, JNU and Prof. J.K. Tripathi, School of Environmental Sciences, JNU, members of my doctoral committee for their useful inputs in my research work.

I would also like to convey my sincere regards to Prof. A.L. Ramanathan, Dean, School of Environmental sciences, JNU for his support and role in overseeing day to day happenings of our school. I convey similar regards to Prof. I.S. Thakur and Prof. S. Mukherjee too who happen to be Ex-deans of our school. Thanks to all of you for keeping the interests of student community your top priority.

I am immensely obliged to Padamshree Prof. R.K. Sinha, my supervisor during M.Sc. dissertation at Central university of South Bihar (Camp office-Patna). I express my utmost respect to him for raising academic interest in me and guiding me towards research. I owe similar regards to Dr. Prashant and Dr. Rajesh Kr. Ranjan, assistant professor, Central University of South Bihar, Gaya. Thank you sirs for inspiring me and showing me the way ahead in life.

Talking about my lab and lab mates, I would simply say that they were the best one could get. Sufficient resources to start with, helping hands to continue with and golden hearts to keep you motivated- major ingredients of our lab. I express my hearty thanks to

my amazing seniors, Ankur Sarswat, Rupa Sharma, Shalini Rajput, and Rahul Kumar for their continuous assistance in work and exclusive lessons for life. I will always cherish the memories of our time together in the lab, visit to the canteens, and zero to infinite kind of discussions on almost everything. Thanks to Hemant, my batchmate too for being a good companion and teaching me so many things. Our stay together in Brahmaputra hostel was awesome and so were our visits to Shambhoo Da's dhaba!

I would specially like to mention about Manvendra Patel, Vaishali Chaudhary and Abhishek Kumar Chaubey- motivated scholars adding sparks to our lab. You guys are excellent. No words can suffice my gratitude and appreciation to all three of you for helping me out in my work and thesis writing. Thanks for being there for me when it was needed the most. I would also like to thank my other labmates Kumar Abhishek, Prachi singh, Kwai Kut, Kamal, Preetiva, Jonathan, Anand, Jahnavi, Tej and Supriya for keeping spirited surroundings. Altogether, lab number- 205, School of Environmental Sciences, JNU will always be a part of my life.

My research work has also been assisted by instrumentation facilities at IIT Roorkee and IIT, Bombay along with advanced instrumentation research facility (AIRF), JNU. Thanks to all the staffs there for this help. I would also like to thank University Grant Commission (UGC) for research fellowship during my PhD. My sincere regards to Guite sir, Uma sir, Vinod bhai, Khagendra ji and Rawat ji from SES for their help and support. I am also very thankful to Anil Sharma ji, Sonu labs for his quick response logistics support.

My life in JNU has been lot more than work and lab. Good peoples around and vibrant hostel life make even dull moments lively. I would like to name and thank few good people around- Sughosh Madhav, Rohit Gautam, Saurabh Sonwani, Naveen Kumar, Namrata Priya, Arif Ahmad, Maroof Azam, Thupstan Angchuk, Shraddha Sharma and Amit Singh Patel for their constant encouragement and appreciation to me. I would have similar regards for my hostel mates Sumeer Ranjan, Amit kumar Dash, Qamar Haider, Yogender Singh, Gaurav Jha, Saurabh kumar Singh, Dheerendra kumar Jha, and Avinash Kumar Singh. I am very lucky to have you guys in my life. Stay connected! Contrary to general belief of JNU being all about high level academics, political activism, and tiresome research I found JNU very compassionate, soulful, and enjoying. It was great being part of JNU!

My family has always been the greatest pillar of support for me. I wouldn't have imagined myself being in such a reputed university if not for my family. I bow my head in deep respect to my father, Dr. Ram Baboo Yadav and my mother, Vimala devi for supporting me through thick and thins of my life. I cannot thank them enough for the upbringing they gave me. It was all their inspiration, motivation, encouragement, and blessings which kept me going. I am equally thankful to my elder brothers, Amit Kumar Achal and Sumit Kumar Suman for being covers of my life. They saved me from everything, just to read and move ahead in life. I would also like to express my sincere gratitude to my younger brother, Navneet Kumar Naveen for his support all these years. His modesty, kindness and ability to reason me out of doubts will always be acknowledged. I would also like to thank my Badi Bhabhi, Dimple Yadav and Chhoti Bhabhi, Kiran Yadav for all the love and blessings. A special thanks to my nephews, Raj and Anmol for being unlimited sources of joy and happiness in hard times. I am sure about getting the same strength and support from all of you forever.

Finally, I would like to thank everyone who waved at me, smiled at me and greeted me. Cheers to all of you! You guys strengthened my belief of world still being a good place to live in.

Contents

Chapter 3: Characterization of CSBC and CCBC

Chapter 7: Conclusions and recommendations

References

List of Figures

List of Tables

CHAPTER 1

INTRODUCTION AND LITERATURE REVIEW

1. Introduction

Water has always been the center point of life on the Earth. This is evident as life originated in ocean and major ancient civilizations flourished near rivers. Even in the modern times water is crucial for human well-being and sustainable development (WWAP, 2015). Conclusively, water is not only responsible for emergence of life but it is also required for continuance of life. With water being vital to mankind and all other life forms on the earth, it automatically becomes the most stressed resource among available ones (McNabb, 2017). In words of Luna Leopold, a great visionary in water resource management, "Water is the most critical resource of our lifetime and our children's lifetime. The health of our waters is the principal measure of how we live on the land" (Darapu et al., 2011).

Quantitatively about three-fourth of earth's surface is covered by water, with 1386 million cubic kilometers being the volume of water inside earth's hydrosphere (Cassardo and Jones, 2011). Oceanic water consists of Earth's 97% water which is saline, while remaining 3% is fresh water. Amongst freshwater, ice caps, glaciers and permanent snow cover in the polar regions; groundwater, and river systems, lakes and reservoirs accounts for 69%; 30% and 0.3% of available volume, respectively (Du Plessis, 2017). Both the oceanic water and freshwater contribute to the livability of our planet. Freshwater is required for domestic, agricultural, industrial and recreational purposes (Kibona et al., 2009). Importance of freshwater increases as its availability on the earth is limited and most of its uses cannot be replaced with use of oceanic water.

The quality of water being used is however an important issue as degradation in water quality reduces its utility for human being and other organisms (Sikhlomanov and Rodda, 2003). Degraded water refers to the water which has undergone physical, chemical or microbiological degeneration in quality (O'Conner et al., 2008). Also, any change in biological, chemical and physical properties of water that has a harmful effect on human health and living things can be termed as water pollution (WHO, 1997). Overpopulation, rapid urbanization, advanced agricultural practices and modern technology are enlisted as some of the potential reasons for degradation in water quality and quantity around India and world (CPCB, 2010). Apart from these, expeditious

industrialization is also considered as one of the major contributors to water pollution and its subsequent impacts (Ebenstein, 2012).

Water pollutants include suspended solids and sediments, nutrients and agriculture runoff, pathogens, organic pollutants, inorganic pollutants (salts and metals), thermal pollutants, radioactive pollutants and nanopollutants (Das et al., 2018). These are distinguished broadly as geogenic and anthropogenic on the basis of their origin (Grützmacher et al., 2013). Geogenic pollutants are present in the rock matrix naturally and they entered surface and sub-surface water through rock-water interactions. Natural phenomena like weathering of rocks, soil erosion and atmospheric deposition of particles along with a variety of climatic factors, redox conditions and flow congestions contribute to the Geogenic water pollution (CGWB, 2014). Major geogenic pollutants include arsenic, fluoride, iron, manganese, chromium, nitrate, salinity agents, selenium, strontium, and radon (Chouhan and Flora, 2010; CGWB, 2014). Water pollution due to anthropogenic activities can take place as domestic sewage, municipal wastewater; urban runoff, storm water, agricultural runoff, and industrial effluents (UN, 2015). Sources of water pollution are also categorized on the basis of their conveyances i.e. point and non-point sources, when the conveyance is discrete and diffused, respectively (Dressing et al., 2016). Individual discharge sources like industrial effluents are considered as point source (EEA, 2018) while pollutants discharged over wide area such as urban and agricultural runoffs are non-point sources (USEPA, 2005; USEPA, 2003).

Different pollutants viz. arsenic (Bhowmik et al., 2018), fluoride (Babu et al., 2015), nitrate (Suhag, 2016), sulfate (Satapathy et al., 2017), phosphate (Kundu et al., 2015); heavy metals like lead (Ventrimurughan et al., 2017), cadmium (Idrees et al., 2018), chromium (Rangasamy et al., 2015), and mercury (Tadiboyina and Ptsrk, 2016); dyes (Elango et al., 2017), pharmaceuticals like antibiotics (Diwan et al., 2018), personal care products (Balakrishna et al., 2017), and pesticides like organophosphates (Kumar et al., 2016), organochlorines (Gupta et al., 2016) and carbamates (Somashekhar and Manjunath, 2015) have been reported from ground and surface water in India.

Though the nuisance created by any of these pollutant can't be undermined nowadays, but pesticides are standout as major class attributing to water pollution. Threats posed by pesticides to water quality are very high due to their toxicity,

persistence and tendency to bioaccumulate (Nicolopoulou-Stemati et al., 2016). Increased use of pesticides for maximizing agricultural output, maintenance of sports turfs and protection of degradable structure of buildings has resulted in pesticides finding their way into various environmental matrices (Aktar et al., 2009; Zolgharnein et al., 2011).

A pesticide is a substance or mixture of substances used to prevent, destroy, repel or mitigate any pest, or is a growth regulator, defoliant, desiccant, or nitrogen stabilizer (USEPA, 2018). Pesticides can be broadly classified as botanicals (natural pesticides like pyrethrum and azadirachtin), inorganic (arsenic, sulphur, and copper) and synthetic pesticides (organochlorines, organophosphates), on the basis of origin and chemical nature (Stănescu, 2014). Classification of pesticides based on their chemical structures (Bernardes et al., 2015) is given below.

Table 1.1. Classification of pesticides on the basis of chemical structure

Categories	Example
Organophosphates	Chlorpyrifos, dichlorvos, diazinon, malathion, parathion
Organochlorines	DDTs, HCHs, endosulfan, heptachlor, aldrin, endrin
Carbamates	Carbaryl, aldicarb, carbofuran, methomyl, fenubocarb
Pyrethrins/pyrethroids	Cyfluthrin, cypermethrin, allethrin, resmethrin, permethrin
Benzoic acid derivatives	Dicamba, 2,4,6-TBA, polychlorobenzoic acid, chloramben
Triazines	Atrazine, simazine, cyanazine, melamine,
Phenoxyactic derivatives	2,4-D, MCPA, 2,4,5-T, MCPA-thioethyl, 3,4-DA, 4-CPA
Dipyridyl derivatives	Diquat, Paraquat
Glycine derivatives	Glyphosate, glyfusinate
Dithiocarbamates	Maneb, ziram, thiram, metal sodium

Pesticides are also distinguished into various categories viz. insecticides, herbicides, acaricides, rodenticides, nematicides, molluscicides, termaticides, fungicides, bactericides, algicides and virucides on the basis of target organisms. Some pesticides are also categorized on the basis of their function viz. repellent and desiccant (Yadav and Devi, 2017). Herbicides and insecticides constitute the major fraction of total pesticides used worldwide with their share being 36 and 25%, respectively (Qurattu and Reehan, 2016). Pesticide use has shown consistent increase over a period of time (Zhang, 2018).

These are imperative for agricultural production and shield crops against pests responsible for upto one-third of pre-harvest loss (Popp et al., 2013). Pesticides also helped in abating vector borne diseases i.e. malaria, dengue and Chagas by controlling mosquitoes, flies and mites population (Van den Berg, 2012). Though pesticides are applied against specific target organisms but pesticides along with their metabolites often affect non-target organisms (Simon-Delso et al., 2015). Occurrence and fate of pesticides and their metabolites in these environmental matrices are affected by their properties i.e. solubility, mobility and half-life along with ambient physical factors such as drainage, rainfall, microbial activity, soil temperature, treatment surface, and application rate (Agrawal et al.,2010). Once after reaching the environment, the pesticides and their residues tend to stay for plausible duration. However, human and non-target organisms living around the contaminated site are highly susceptible to their harmful effects (Damalas and Eleftherohorinos, 2011). Hence, pesticides are a potential threat to human health and environment (Zhang et al., 2007).

Considering their hazardous nature, pesticides have been extensively monitored and reported in different environmental sphere i.e. soil (Alonso et al., 2018), sediment (Ndunda et al., 2018), air (Pozo et al., 2017), surface water and groundwater (Li et al., 2018*). They reach these spheres via spray drift and surface runoff from agricultural fields (Zhang et al., 2018). Leaching and redeposition from atmosphere also add to pesticide contamination of environment (Tiryaki and Temur, 2010). They are also reported from drinking water (Klarich et al., 2017) and edibles like milk, honey, fruits and vegetables (Hadian and Eslamizad, 2018). In the natural environment pesticides are subjected to diverse fate viz. 1) biological and non-biological transformations (oxidation, reduction, hydrolysis, comparative metabolism and conjugation) (Crosby, 1973), 2) inter and intra-matrix transport (Gavrilescu, 2005), 3) degradation by microbes and sunlight (Matsumura, 1982), 4) uptake and adsorption (Chiou et al., 2001), 5) mineralization (Nair et al., 1993) and 6) volatilization (Bailey and white, 1970). Movement of pesticides in the environmental spheres is given in Figure 1.1. Pesticide characteristics such as solubility, persistence and affinity, governs its fate in the soil-water system. A pesticide with high water solubility, lower affinity for soil and longer persistence period has tendency to reach and contaminate both the surface and groundwater (Gavrilescu, 2005). Such cases

of pesticide contamination of water are widely reported around the world and are enlisted in Table 1.2.

1. Evaporation
   Spray drift
   Wind erosion
2. Regional transport
3. Dry deposition
4. Runoff
5. Percolation/seepage
6. Effluent
7. Precipitation
8. Downstream flow
9. Groundwater discharge to stream
10. Sorption-desorption onto biota
11. Sorption-desorption onto bed sediment
12. Sorption to suspended particles
13. Settling-resuspension
14. Mixing
15. Burial
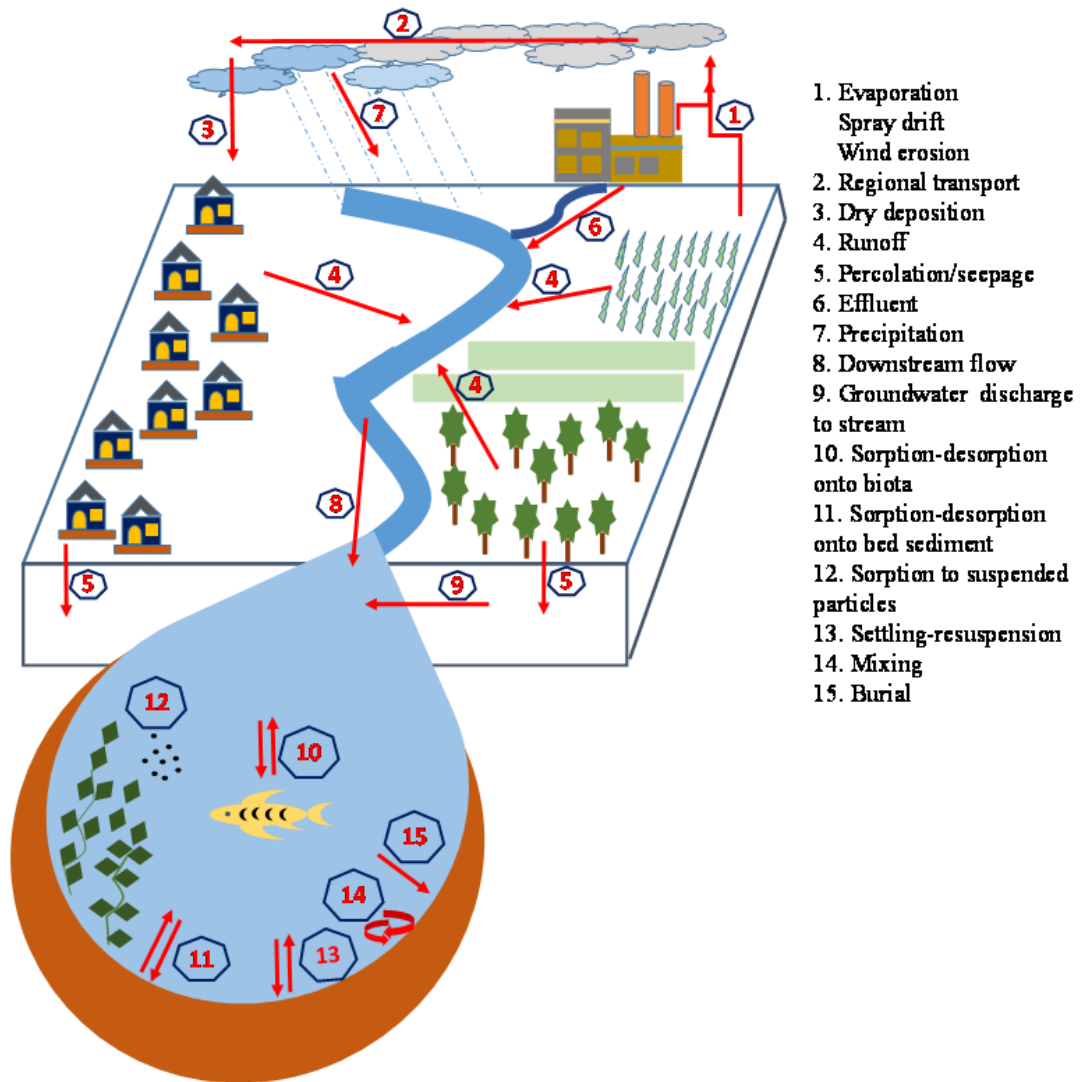
Figure 1.1 Movement of pesticide in environment (modified from Majewski and Capel, 1995)

Table 1.2: Pesticides reported in surface and ground water around the world

Pesticides	Country	Water source	Concentration (µg/L)	Reference
Acetachlor Alachlor Chlorpyrifos	Serbia	Surface water (drainage canal in agricultural field)	0.02-0.41 0.05-0.78 0.07-0.92	Lazic et al., 2013
Atrazine Tebuconazole Diethyltoluamide	Argentina	Groundwater (sub-surface streams)	1.4 0.035 0.701	Geronimo et al., 2014
DDT DDE Endosulfan carbofuran	Pakistan	Surface water (Ravi river tributaries)	0.034-0.045 0.033-0.046 0.108-0.123 0.028-0.040	Akhter et al., 2014
OCPs (HCHs,heptachlor, dieldrin, Aldrin)	China	Groundwater (underground Nansan river)	3.1 – 5.369	Alam et al., 2014
Imidacloprid pp'-DDD Phenthoate Diazinon Chlorpyrifos Endosulfan o, p'-DDT	China	Groundwater (near yellow river region)	58.915 2.596 2.170 1.198 0.946 0.665 0.280	Lei et al., 2014
Isoprothiolane Fenobucarb Fipronil	Vietnam	Surface water and groundwater (Mekong river delta region)	8.49 2.32 0.41	Chau et al., 2014
Diuron Metolachlor Simazine Imidacloprid	Australia	Surfacewater (stormwater harvesting scheme, Salisbury)	0.033-0.063 0.009–0.014 0.075–0.015 0.006–0.017	Page et al., 2014
2,4-D	Spain	Groundwater (Catalonia region)	0.001-0.016	Kock-schulmeyer et al., 2014
OCPs	Lebanon	Groundwater	14.2	El-Osmani et al., 2014

(HCHs, DDTs, Aldrin and Endrin)		(drinking water in Akkar plains)		
Heptachlor Dieldrin	Polland	Groundwater (Opole protected region)	15970 1940	Głowacki and Ciesielczuk, 2014
Endosulfan sulfate	Togo	Groundwater	0.116	Mawussi et al., 2014
Glyphosate AMPA Terbuthylazine Diuron 2,4-DB 2,4-D Terbutryne Metolachlor Malathion Linuron Dieldrin Simazine Terbuthylazine Cadusafos Azoxystrobin Bentazone Pendimethalin Endosulfan sulfate Alachlor	Italy	Surface and groundwater	167 70 30 28 20 18 16.47 16 13.13 478.03 221 29.05 24.96 18.96 16 15.36 10.71 10.2 10.8	Meffe and De Bustamente, 2014
HCHs DDTs Heptalchors Hexachlorobenzene Aldrins Endrins	China	Shallow groundwater (Taihu lake region)	0.011-0.198 0.007-0.482 0.005-0.228 0.003–0.065 BDL-0.359 0.001-0.159	Wu et al., 2014a
HCHs DDTs	China	Groundwater (Yangtze river delta)	0.123 0.323	Wu et al., 2014b
Atrazine-L	USA	Groundwater	0.004-0.27	Katz et al., 2014

Deethyl atrazine Alachlor Metachlor Simazine Tebuthiruron		(Floridian aquifers)	0.004-0.29 0.0045-0.52 0.0038-0.27 0.004-0.013 0.008-2.1	
Glyphosate	Mexico	Surface water (agriculture intensive tropical region)	36.7	Ruiz-Toledo et al., 2014
pentachlorophenol atrazine diuron fenarimol	Guiana	Groundwater	0.418 0.420 0.258 0.121	Vulliet et al., 2014
Mancozeb Carbofuran	Columbia	Surface water (Ventaquemada, Boyacá region)	50 40	Camacho et al., 2015
Carbofuran	Serbia	Surface and ground water (Danube River and tributaries)	Occurrence reported	Radovic et al., 2015
Carbofuran	Nigeria	Surface water (Owan river, Edo state)	0.03	Ogbeide et al., 2015
Carbofuran	Argentina	Groundwater (El cardalito stream region)	Occurrence reported	Bedmar et al., 2015
Carbofuran	Pakistan	Surface water (Ravi river, Head Balloki)	0.85 (dry season) 0.70 (wet season)	Mehboob et al., 2015
Clorpyrifos-ethyl diazinon	Kenya	Surface water (Lake Naivasha)	2.5 3.3	Otieno et al., 2015
Isoprothiolane fenobucarb fipronil.	Vietnam	Ground water (Drinking water in Mekong delta,)	8.49 2.32 0.41	Chau et al., 2015
Diazinon, DDT Fenitrothion Cyfluthrin Diazinon Dieldrin	Saudi Arabia	Surface water and groundwater (Dams and wells in Jazan area)	0.098 (surface water) 0.104 0.321 0.394 0.117 (groundwater) 0.005	Al-Hatim et al., 2015

Fenthion			0.472	
HCHs DDTs	China	Surface water and groundwater (Yellow river estuary region)	In Surface water HCHs- 18.57 DDTs- 9.79 In groundwater HCHs-34.74 DDTs-10.78	Li et al., 2015
HCHs DDTs	China	Groundwater (Hangzhou-Beijng region)	0.0027-0.011 BDL- 0.0015	Li et al., 2015
Carbofuran Glyphosate	Srilanka	Groundwater (Drinking water from well water, Padavi-Sripura region)	More than 1	Jayasumana et al., 2015
Pirimiphosmethyl	Lebanon	Groundwater (South Litani region)	0.301	Youssef et al., 2015
OCPs (α-HCH, δ-HCH, o, p'- DDD, Aldrin, Endosulfan-sulfate and HCB)	China	Groundwater (Xiaodin sewage irrigation area, Tiyun city, Shanxi province)	13.91-103.23	Li et al., 2015
2,4-D Trifluralin Atrazine Diazinon Metribuzin Acetachlor Prometryn Tertbutryn Metachlor	Hungry	Surface water and groundwater	0.01-1.00 0.80-10 0.50-15 0.01-0.90 0.10-1.00 0.020-6.30 0.10-10.00 0.01-1.00 0.001-56.00	Székács et al., 2015
Thiamethoxam, Chlorantraniliprole, Phenthoate	Bangladesh	Surface water (Prawn-rice concurrent system)	Occurrence reported in 25 % of sample size	Sumon et al., 2016
CarbofuranBentazon	Brazil	Surface water (Santa Catarina region)	5.16 135.93	Vieira et al., 2016

Carbofuran	Saudi Arabia	Groundwater (Al-Qassim region)	0.3	Al-wabel et al., 2016
Metalaxyl, Penconazole, Tebuconazole, Myclobutanil, Triadimenol	Spain.	Surface and groundwater (La Rioja region)	Occurrence reported (concentration up to 25.52)	Herrero-Hernández et al., 2016
Glyphosate AMPA	Canada	Groundwater (Nottawasaga river watershed, Ontario,)	0.663 0.698	Van Stempvoort et al., 2016
Trifluralin	Turkey	Groundwater (Farmer well in Turgutbey irrigation project Thrace region)	7.14- 79.2	Cebi et al., 2016
Carbofuran	Spain	surface water groundwater (Castellon region)	0.38	Pitarch et al., 2016
HCHs methoxychlor	China	Groundwater (Krast water system)	0.213 0.037	Zhang et al., 2016
Carbofuran	Burkina faso	Surface water and groundwater (lakes and borewell)	More than 0.1	Lehmann, 2017
Aldicarb Acetachlor	Pakistan	Groundwater (Drinking water in Khyber Pakhtunwa province	30 10	Qureshi and Rehman, 2017
Carbofuran	srilanka	Shallow ground and surface water (Mahaweli river basin)	2.2	Aravinna et al., 2017
HCHs Heptachlor	China	Groundwater (Yangtze river basin)	2 5.8	Pan et al., 2017
Triazine (tertbuthylazine)	Spain	Surface water (Júcar river)	9	Menchen et al., 2017
Endosulfan Lindane	Chile	Surface water (Nuble river)	0.12-2.68	Montory et al., 2017
Omethoate, Methamidophos Diazinon	China	Surface water and groundwater (Jianghan plain region)	0.054 0.032 0.028	Wang et al., 2017
Chlordane-gamma,	USA	Wastewater stream	0.026-0.071	Nguyen et al., 2017

Chlordane-Alpha Trans-Nonachlor		(south California region)	0.028-0.087 0.011-0.049	
Simazine atrazine	Europe	Groundwater	0.015 0.035	Sassine et al., 2017
Glyphosate	Mexico	Groundwater (Hopelchén, Campeche region)	0.44-1.21	Rendón-von Osten and Dzul-Caamal, 2017
Carbofuran	China	Surface water (Yangtze and Huangpu river, Shanghai)	0.03-0.14 (with 70-83% occurrence frequency)	Sun et al., 2018
Carbofuran	Brazil	Surface water (Sao Laurenco river, Camp Verde)	0.20 (35% occurrence frequency)	Berton et al., 2018
HCHs Heptachlor	China	Surface water (Shying river)	0.021-0.061 0.012-0.077	Bai et al., 2018
Endrin aldehyde BHCs Heptachlor	Phillipines	Surface water (Pampanga river)	1.314 0.149 0.028	Navarrete et al., 2018
Methyl parathion Atrazine Simazine Malathion	Egypt	Groundwater (Shallow Nile delta aquifer)	Occurrence reported	Masoud et al., 2018
2,4-D Atrazine	China	Surface water (Fu river in Northern plains)	3.00 0.96	Brauns et al., 2018
Carbofuran	China	Groundwater (agricultural region in Chuncheong)	0.116	Lee et al., 2018
Methamidophos Dichlorovos Chlorpyrifos	Pakistan	Drinking water (Peshawar basin)	0.12-52.34 0.0-3.46 0.0-19.12	Ali et al., 2018
Endrin δ-lindane	Mexico	Groundwater (Yucatan region)	3200 10860	Rodríguez et al.,2018

γ-lindane α-lindane Heptachlor			5230 6530 13610	
2,4-D MCPA Chlopyralid	Canada	Groundwater (Prairie province)	0.025-0.361 0.026-1.293 1.153-7.121	Munira et al., 2018
Atrazine Acetachlor Ametryne Metolachlor	China	Surface, ground and drinking water (Sugarcane producing Guangxi region)	0.585 0.311 0.341 1.312	Li et al., 2018
DDT Methylparathion	Lebanon	Groundwater (Akkar region)	0.39 44.6	Chaza et al., 2018
Glysphosate AMPA	Argentina	Surface and groundwater (El Crespo basin, pampas region)	0.4 0.2	Okada et al., 2018
Glyphosate	USA	Surfacewater (Urban, mixed runoff from agricultural watershed, Hawaii)	Occurrence reported (96 and 65% in storm and base flow conditions, respectively)	Steven et al., 2018
HCHs, heptachlor and Heptachlor epoxide (OCPs)	China	Surface and groundwater (Huixian karst wetland, Guilin)	0.137, 0.138 and 0.004 in lake, canal and shallow groundwater, respectively	Fu et al., 2018
Atrazine Tertbuthylazine Carbamazepine	Africa.	Groundwater (Drinking water sources)	0.15 0.15 0.0015	Gwenzi and Chaukura, 2018
Pyrimethanil Cyprodinil	Chile	Surface water (Cachapoal river basin)	0.937 0.644	Climent et al., 2018

1.1. Pesticide Remediation Methods

1.1.1. Coagulation-flocculation

Colloidal components (size less than 10 µm) of water, both inorganic as well as organic are removed by coagulation and flocculation. Both these processes are employed in tandem, firstly the surface charge over the colloid is neutralized by use of suitable coagulant. Then, this coagulated mass is mixed, followed by aggregation of smaller colloids into "flocs" leading to flocculation (USEPA, 2001). Apart from charge neutralization, complexation and entrapment also assist in coagulation process. These flocs are large and they tend to settle down under gravity (Matilainen et al., 2010). Significant removal of hydrophobic and lipophilic pesticides containing low molecular weight, acidic functional group such as carboxyl and carbonyl can be achieved by coagulation-flocculation (Krasner et al., 1996). Some common coagulants groups are inorganic electrolytes i.e. aluminum chloride, ferrous sulfate, alum and ferric chloride; organic polymers and synthetic polyelectrolytes (Niti et al., 2013).

Coagulants used for coagulation-flocculation not only facilitate but also add advantage to this process making it easy to handle. Different coagulants ensure a wide range of pH being taken care of during application. Some of the coagulants form heavier flocs and enable faster settling. The major drawbacks of the process include high pH dependence, secondary pollution via sludge, and cost factors.

1.1.2. Advanced oxidation processes

Advanced Oxidation Processes (AOP) includes the setup for particular chemical reactions resulting into the generation of highly reactive oxidizing species, which enables oxidation and mineralization of any pesticide or other recalcitrant organic molecules into CO_2 and inorganic ions. Basic principle of AOP systems involve generation of strong oxidizing agent viz. hydroxyl radical (HO•) with high oxidation potential of 2.8 V. This hydroxyl radical leads to formation of pesticide intermediates via electron transfer, hydrogen removal, or by adding double bonds and aromatic rings. Finally, these intermediates undergo additional reaction to yield end products i.e. CO_2 and H_2O. Extent of pesticide degradation via AOPs is dependent on their chemical structures. The oxidation processes may or may not involve the use of light. The C-H bond and sulfides (-S-); double bonds (-C=C-) in alkenes and polyenes; carbonyl groups (-C=O); phenols

(Ar-OH); aryl chlorides (Ar-Cl); nitroaromatic group ($-C_6H_4NO_2$) being susceptible to absorption of light (even sunlight) undergoes photochemical reactions eventually (Bartolomeu et al., 2018). These AOPs have added advantages as there are different ways to produce hydroxyl radicals as per quality of wastewater to be remediated and treatment requirements. AOPs include heterogeneous photocatalysis, homogenous Fenton and photo-Fenton along with methods based on ultraviolet light (UV), and H_2O_2 or O_3 or TiO_2 combinations to produce hydroxyl radicals (Badawy et al., 2006). AOPs are particularly effective against the biologically toxic pollutants and preferred for being non-selective. They can remove many pesticides in a single go and also accelerate the same when applied in combination with solar, UV or ultrasonic radiations.

1.1.2.1 Fenton process

Fenton's process is oxidation process effective for pesticide remediation. It works on the principle of oxidative pesticide degradation via reaction with highly reactive hydroxyl radical produced from H_2O_2 (hydrogen peroxide) in the presence of Fe^{2+}/Fe^{3+} as a catalyst following equation given below. Both ferric and ferrous salt can be for generation of hydroxyl radical, however mechanism of generation of OH radical is different. Ferrous salt generates hydroxyl ion in single step as described in Equation 1.1 while ferric salt involves two-step process for hydroxyl radical generation as described in Equation 1.2.

$$Fe^{2+} + H_2O_2 = Fe^{3+} + {}^{\bullet}OH + {}^{\bullet}OH \qquad\qquad (1.1)$$

$$Fe^{3+} + H_2O_2 = Fe^{2+} + HO_2{}^{\bullet} + H^+$$

$$Fe^{2+} + H_2O_2 = Fe^{3+} + {}^{\bullet}OH + {}^{\bullet}OH \qquad\qquad (1.2)$$
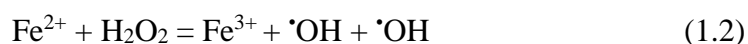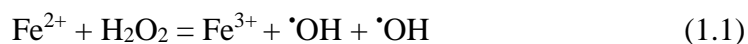
Effectiveness of Fenton's process for pesticide degradation depends on factors like concentration of H_2O_2 and Fe^{2+} along with pH of the reaction system (pH~3-5). Other than pesticides Fenton's process is also reported to be very helpful in remediation of different organic compounds from groundwater and wastewater (Barbusiński and Filipek, 2001). A major drawback of Fenton process is formation of sludge.

1.1.2.2 Electrochemical degradation

Electrochemical degradation has been endorsed for breakdown of toxic and bio-refractory organic pollutants such as pesticides. During the process non-biodegradable

organic compounds are converted in relatively innocuous end products like CO_2 and H_2O via hydroxyl radical mediated electro-conversion and electro-combustion (Bouya et al., 2012). The process involves destruction of pesticides by reaction with the hydroxyl radical formed on the anode surface from oxidation of water and suitable cathode in presence of electrical current (galvanostatic scheme). Some of the prominent anode materials used are Pt for thiamethoxim, SnO_2 for cypermethrin, PbO_2 for 2,4-D and boron doped diamond (BDD) for methyl parathion degradation (Samet et al., 2010). The efficiency of electrochemical degradation is the function of anode characteristics, electrolyte used, applied current density current density and initial concentration of pesticides. The major advantages of this technique include feasible application in flowing systems and immobilized catalyst for ease in separation (Bouya et al., 2012). However, synthesis and timely replacement of the electrode serve as the deterrent to this process.

1.1.2.3 Photocatalytic degradation

Photocatalytic degradation deals with breakdown of pesticides in the presence of semiconductor photocatalyst (TiO_2, ZnO), energetic radiation source and suitable oxidizing agent (oxygen/air) (Ahmed at al., 2011). The principle of this technique involves in-situ generation of hydroxyl radicals ($^{\bullet}OH$) under given conditions. These hydroxide radicals are then used to convert different pesticides and organic compounds relatively non-toxic end products as CO_2 and H_2O. Photocatalytic process are differentiated into homogeneous and heterogeneous systems according to the phase of reactants and catalysts used. Though, visible-light irradiation is enough for the process to operate, the presence of UV radiation can increase the efficiency (Badawy et al., 2006). Photocatalytic degradation of pesticides depends on the pH of the solution, nature and composition of catalyst, organic substrate type and concentration, light intensity, catalyst loading, ionic composition of waste water, types of solvent, oxidant concentration, and calcinations temperature (Shakthivel et al., 2003). This method is considered as an effective as well as inexpensive for pesticides remediation (Devipriya and Yashodharan, 2005). However, major technical barriers in the process are the limited catalytic activity of photocatalyst used, incomplete degradation of pollutants in consideration, generation of innocuous end-products and reduced feasibility for large scale application (Dong et al., 2015).

1.1.2.4. Ultra-sound combined with Photo Fenton

Ultra-sound combined with photo Fenton refers to the sonochemical reaction pathways which involves degradation of pesticides and other organic compounds via hydroxyl radicals and heat mediated reactions. Here, hydroxyl radicals are produced by the sonolysis of water as the solvent inside the collapsing cavitation bubbles under extremely high temperature and pressure. The quantity and rate of hydroxyl radical generation is further enhanced by mixing Fenton, Fe (II)/H_2O_2 and Fenton like, Fe (III)/H_2O_2 catalysts. Generated hydroxyl radicals can react with pesticides, or even recombine to form H_2O_2 inside the cavitation bubble and at interface. Fraction of pesticides decomposition may also take place adjacent to the collapsing bubble due to the high local temperature and pressure (Katsumata et al., 2011). Rapid degradation of pesticides and easy sample handling are among main advantages of ultrasound assisted photo Fenton process.

1.1.2.5. Ozonation

Ozonation refers to the chemical oxidation technique for water treatment using molecular ozone, O_3 with high oxidation potential of 2.07 V (in comparison to hydrogen electrode) (Ikehata and Gamal El-Din, 2005). Molecular ozone reacts selectively with unsaturated bonds, aromatic systems and amino groups present in the pesticides (Broséus et al., 2009). Degree of pesticide degradation by ozonation is affected by pesticide concentration, ozone dose/exposure and pH of the reaction system. Ozone reacts with organic contaminants through both a direct reaction with molecular ozone or through indirect reactions with free radicals (including the hydroxyl radical $^\bullet OH$ produced by the decomposition of ozone). The rate of $^\bullet OH$ formation depends on the water matrix, especially its pH, alkalinity, type and content of natural organic matter (von Gunten, 2003). The major disadvantage of the process is high cost for the generation of ozone.

1.1.3 Biological degradation

Biological degradation or biodegradation refers to the enzymatic breakdown of the substance by the living microbial activity which may take place in-vivo or in-vitro (Ortiz-Hernadez et al., 2013). Pesticide remediation through this technique involves the alteration of pesticide residue structure to remove toxicological properties followed by complete breakdown of these organic pesticides into constituent inorganic components

(Meleiro-Porto et al., 2011). The microbial assisted degradation may be part of energy derivation, detoxification or it also may be part of the co-metabolism (Becker and Seagren, 2010). Metabolic breakdown by microbes may include three steps-1. Transformation of pesticides via oxidation, reduction or hydrolysis to yield water soluble and less toxic intermediates, 2. Conjugation of sugar and amino acid to these pesticide intermediates and, 3. Conversion of intermediates generated into non-toxic secondary conjugates. The enzymes required for these include hydrolytic enzymes, peroxidases, oxygenase, which can be intracellular or extra-cellular in nature and are produced generally from fungi and bacteria (Ortiz-Hernández et al. 2011). Breakdown of the pesticide by a particular microbe group depend on their nature, genetics and chemical behavior of different enzymes. Presence of various microorganism with diverse metabolism and their ability to function in adverse conditions favors biological degradation of pesticides (Megharaj et al. 2011). Biological degradation of pesticide can be aerobic as well as anaerobic with different pathways and end products i.e. hydrolysis products of parathion are different in case of aerobic and anaerobic degradation (Abo-Amer, 2012). Specificity of microbes for a particular substrate and occasional transformation of less toxic pesticides intermediates into hazardous products and longtime duration often limits the applicability of process (Singh and Walker, 2006).

1.1.4. Membrane processes

Membrane separation is among the most advanced techniques applied to concentrate and separate molecular or ionic compounds in their aqueous state. This process is significantly effective against water pollutants with less molecular mass and other ionic species (Bhattacharya, 2006). Membrane techniques can be applied in both crossflow and dead-end mode (Karabelas and Plakas, 2011). The membrane-based separation techniques are differentiated on the basis of driving force involved i.e. applied pressure and electrical potential. Pressure-driven membrane processes include microfiltration (MF), ultrafiltration (UF), nanofiltration (NF) and reverse osmosis (RO). These processes are differentiated on the basis of pore size of the membranes and applied pressure gradient. The pore size of membrane (in nm) varies as MF (50-1000)>UF(10-50)>NF(2)>RO(1) whereas pressure gradient (in bar) follows MF(0.1-2)>UF(1-5)>NF(5-

20)>RO(10-100) (Singh, 2006). Electric potential driven process includes electrodialysis membrane technique that employs electrical current and membranes for selective permeability of ions. Mass transport in electrodialysis is driven by the electrochemical gradient across the membranes, whereby negatively charged cation-exchange membranes (CEM) and positively charged anion-exchange membranes (AEM) are arranged in alternate sequence between two electrodes viz. cathode and anode (Niti et al., 2013). Membrane material and its characteristic like charge, porosity, molecular cut-off weight, degree of desalination affect the electrodialysis. Pesticide characteristic like molecular weight, size, polarity, and its behavior in aqueous solution along with pH, ionic strength and presence of organic matter in feed solution also affects the electrodialysis process (Karabelas and Plakas, 2011).

Electrodialysis via membranes for pesticide remediation are suitable for large scale continuous operations with its longer durability. The major drawbacks of this process include costly feed water, membrane fouling, and need of pretreatment (Strathmann, 2012).

1.1.5 Ion-exchange

Ion exchange is a process in which ions with similar charge from solid phase adsorbent (mostly resins) are replaced by adsorbate ions from solution through electrostatic interactions to maintain electro-neutrality. It is characterized by two-way influx of ions viz. from solution to adsorbent and vice-versa based on the relative affinities of adsorbent (Kammerer et al., 2010). In organic compounds like pesticides the ion exchange may occur due to charge based interactions as well as hydrophobic interactions (Humbert et al., 2008). Efficiency of ion exchange process for separation is affected by properties of adsorbent resin i.e. crosslinking and swelling. Nature of exchanging ion i.e. charge/valency, size, polarizability along with factors like concentration of solution also affects the performance of ion-exchange process (Kumar and Jain, 2013). However, large size and less surface density on the surface of pesticides reduce the ion exchange efficiency. This process edges over other processes in terms of regeneration of resins, cost factors, and energy consumption. Major shortcomings of this process are low efficiency against chlorinated pesticides and the presence of micro-

organisms. Disposal of loaded pesticide after regeneration is also a major concern (Foo and Hameed, 2010).

1.1.6 Adsorption

Adsorption is a phase transfer removal phenomenon whereby the target compound present in aqueous phase are transferred to the solid phase, known as adsorbent. The progress of the adsorption process can be characterized by four consecutives steps that is, 1) Transport of the adsorbate from the bulk liquid phase to the hydrodynamic boundary layer, 2) Transport through the boundary layer to the external surface of the adsorbent, 3) Transport into the interior of the adsorbent particle (intraparticle diffusion, pore diffusion and/or surface diffusion, 4) Energetic interaction between the adsorbate molecules and 5) final adsorption (van der Waals interactions, hydrogen bonding, electrostatic attractions). The effectiveness of the process is function of adsorbate (liquid) and adsorbent (solid) interaction. Often the surface area, pore size and functional groups on the adsorbent define these interactions (Mohan et al., 2014).

The advantages of adsorption process over other above- mentioned techniques are the low capital, ease of set up, easy scale up, no additional power and chemical requirement. Since, the effectiveness of process is directly correlated with the physical and chemical characteristic of adsorbent, various adsorbent such as activated carbons, mineral oxides, polymer resins, nanomaterials, zeolites, bio-sorbents, biochar etc. are being utilised. Some of the common adsorbent used for the removal of organic and inorganics are described below.

1.1.6.1. Biosorbent

Biosorbents are biomolecules which are capable of binding and concentrating different ions and molecules (Volesky, 2007). They may be dead or live biomass, but the uptake process for them is metabolism independent (Bilal et al., 2018). Biosorbent may be in the form of freely-suspended cells, immobilized biomass, and living biofilms (Wang and Chen, 2006). The functional groups present in biomass (carboxyl, phosphate, hydroxyl, amino, thiol) along with monovalent cations ($H^+/Na^+/K^+$) enable adsorption, absorption, ion-exchange, complexation and coordination (Gadd, 2009). Biosorbent and adsorbate association is affected by molecular size, charge, solubility, hydrophobicity, and reactivity of later along with age, individual cell size, wall composition, and

extracellular secretion of former (Wu and Yu, 2007). Physico-chemical conditions of the sorption system such as pH, speciation, competition among the intermediates and temperature bio sorbent's efficiency. Apart from this nutrient availability and maintenance of optimal growth condition is essentially requisite for the functioning of the biosorbent in the living system (Gadd, 2009). Biosorbents are highly selective, efficient, cost-effective, and have good removal capacity with vulnerability against highly toxic waste as the main disadvantages (Aksu, 2005**).**

1.1.6.2. Inorganic adsorbents

Inorganic adsorbents include clay minerals, zeolites, and their modified forms. These all have a high surface area and serve as good adsorbent for organic and inorganic pollutants (Uddin, 2017). Clay minerals are formed by weathering of primary minerals (Ugwu and Igbokwe, 2019). They are also known as oxide adsorbent (Chang, 2016). They can be engineered from aluminium and iron via precipitation of hydroxide followed by dehydration (Barbosa et al., 2017). Adsorption capacity of clay minerals having abundance of –OH groups takes a dip against anionic adsorbate due to electrostatic repulsion (Gitari and Mudzielwana, 2018). Zeolites are naturally occurring crystalline hydrated aluminosilicate which can be modified at industrial scale. Their microporous surface provides high surface area for sorption process (Li and Yu, 2014). Properties of zeolites are decided by silica to alumina ratio in it (Jiang et al., 2018). These properties enable zeolite to perform cation exchange, molecular sieving, catalysis and sorption. However, application of zeolites as an adsorbent for pesticides is limited as large organic moieties of pesticides molecules don't fit into zeolite's micropores (Wang and Peng, 2010).

1.1.6.3. Polymer resins

Polymeric adsorbents, often known as resins are porous solids with considerable surface areas and have distinctive adsorption capacities for organic molecules based on Van der waal attraction, H-bonding and polarisation of π electrons of aromatic nuclei (Kyriakopoulus et al., 2018). They are produced by co-polymerization. The polymer adsorbents shows a narrow pore-size distribution and the surface is relatively homogeneous (Samiey et al., 2014). Polymeric adsorbents have limited adsorption capacities due to involvement of weaker interaction forces. Their use also faces setback

as they are costly, require longer time duration for completion of adsorption process, and have separation and regeneration related problems (Chen et al., 2016).

1.1.6.4. Nanomaterials

Nanomaterials refers to the materials having constituent particle or structure of size ranging from molecular level i.e. 1 nm to 100 nm. These nanomaterials are characterised by size order of nanoscale with high surface area to volume ratio (Riu et al., 2006). They can be modified extensively and have surface and magnetic properties better than their corresponding bulks. Some of the prominent nanomaterials are single wall (SW) or multiple wall (MW) carbon nanotubes (CNT), crystalline metal oxides, fullerenes and graphene (Firozjaee et al., 2018). These nanomaterials are highly effective as adsorbent for pesticides but tend to have production and application constraints. Controlling the structural properties and physicochemical characteristic of nanomaterials is one of them. Oxidation, dissolution of nanomaterials i.e. metal oxides along with their tendency to agglomerate in solution makes their application troublesome in adsorption process (Perreault et al., 2015).

1.1.6.5. Activated carbons

Activated carbons (ACs) are the group of carbonaceous adsorbents characterised by large surface area and presence of well-developed pore structures (Yang and Hu, 2001). They are very efficient against variety of organic and inorganic pollutants. Activated carbons are produced by two step process, 1) carbonisation of biomass or other materials of vegetable origin and 2) activation of carbonised material (Valix et al., 2004). During first step, pyrolytic decomposition of feedstocks leads to removal of loosely bound oxygen and hydrogen and development of pores. In the second step the carbonised mass is activated physically or chemically to enhance the porosity and increase the total surface area grossly. Physical activation involves high temperature treatment in the present of some oxidising gas such as steam and CO_2 whereas chemical activation involves exposure to chemicals like KOH, H_2SO_4, $ZnCl_2$, and H_3PO_4 (Rodríguez Correa et al., 2017). ACs production process parameters such as temperature, residence time, activation time; steam, gases and chemical involved significantly affect its properties (Angın et al., 2013). Activated carbons have also been used effectively for aqueous remediation of pesticides (Gupta et al. 2011) but their higher production cost, relatively

lesser removal capacity per unit surface area and losses during regeneration pushes for some other viable and sustainable option (Lata et al., 2015).

1.1.6.6 Biochar

Term 'Biochar' is relatively new to the scientific jargon. Different definitions have been put up to describe the biochar. According to Lehmann and Joseph, (2009) it is a carbon rich product when biomass such as wood, manure or leaves is heated in a closed container with little or unavailable air. They also suggested the operational difference between charcoal and biochar in terms of end use i.e. charcoal is used as fuel and energy whereas biochar is meant for carbon sequestration and environmental management. According to McLaughlin et al., (2009) biochar is a term used to designate charcoal or biocarbon destined for addition to soils. Shackley et al., (2012) defined biochar as the porous carbonaceous solid produced by the thermochemical conversion of organic materials in an oxygen depleted atmosphere that has physicochemical properties suitable for safe and long-term storage of carbon in the environment. Similarly, biochar can also be described as the biomass that has been pyrolysed in a zero or low oxygen environment applied to soil at a specific site that is expected to sustainably sequester C and concurrently improve soil functions under current and future management, while avoiding short and long-term detrimental effects to the wider environment as well as human and animal health (Verhiejen et al., 2010). According to European biochar certificate (EBC) biochar is defined as a heterogeneous substance rich in aromatic carbon and minerals which is produced by pyrolysis of sustainably obtained biomass under controlled conditions with clean technology and is used for any purpose that does not involve its rapid mineralization to CO_2 and may eventually become a soil amendment (EBC, 2012). According to International biochar initiative (IBI), biochar is a solid material formed by the thermochemical conversion of biomass in oxygen-limited environment (IBI, 2015). Most of the definitions are attributed to biochar development condition and its application in soil.

Traditionally biochar has been associated with environmental management strategies i.e. soil enhancement, waste management, climate change mitigation and energy generation (Lehmann and Joseph, 2009). But nowadays uses of biochar have been diversified i.e. catalysts, absorbents for removal of contaminant from soil and water, fuel

cell constituent, gas capture and as precursor material for producing activated carbon (Qian et al., 2015). Apart from these nanocomposites based engineered biochars and designer biochar with specific and controlled properties meant for particular purposes as healthcare are also gaining momentum (Ok et al., 2015). Physico-chemical properties of a biochar produced i.e. composition, particle and pore size distribution are highly dependent on thermochemical conversion conditions such as temperature, ramp rate, residence time; and feedstock characteristics. Different thermochemical processes for production of biochar along with pyrolysis conditions and yield distribution are given in Table 1.3.

Table 1.3. Techniques for biochar production and corresponding yields

Process	Temp	Residence time	Products		
			Solid (biochar) (%)	Liquid (bio-oil) (%)	Gas (Syngas) (%)
Fast pyrolysis	300-1000	Short (<2sec)	75	12	13
Intermediate pyrolysis	~500	Moderate (10-20 sec)	50	25	25
Slow pyrolysis	100-1000	Long (5-30 min)	30	35	35
Gasification	>800	Moderate (10-20 sec)	5	10	85

Feedstocks used for biochar production are generally forest residues from logging activities and waste from dead wood stocks; mill residues from lumbering, sawmills, pulp and veneers workshops and field crop residues as straw, husk, cobs, and stover along with urban wastes such as litters, yard trimmings, site clearing**,** pallets, wood packaging (Lehmann et al., 2006). These feedstocks can also be classified as animal feedings, agricultural materials, food wastes, woody materials, animal litters and solid wastes (Ahmed et al., 2016). On the basis of origin these feedstocks can be either of plant origin (rich in cellulose, hemicellulose and lignin), animal origin (litter, manures) or waste (sludge) (Sun et al., 2017). Plant biomass used as feedstock for biochar are differentiated into woody and herbaceous based on lignification (Rossatto et al., 2014). Biochar from woody biomass have higher degree of carbonization and percentage yield (Wang et al., 2015) but biochar from herbaceous biomass have edge over them in terms of feedstock's availability i.e. large quantity of agricultural by-products and crop residues (Wang et al., 2013). India having traditional farming system with a variety of crops every year can use

its agricultural byproducts and crop residues as sustainable source for biochar production and other purposes.

Rice (*Oryza sativa*), maize (*Zea mays*) and sorghum (*Sorghum bicolor*) are among most valued food crops of India. Importance of these three crops can be understood both in terms of area under cultivation for these crops as well their production. Average yearly production of 108.5 million tons (in 431.3 lac hectares), 25.27 million tons (in 89.70 lac hectares) and 4.51 million tons (in 53.7 lac hectares) was reported for rice, maize and sorghum respectively during years-2015-2018 (DACFW, 2018). Along with the crop yield, the byproducts or residue produced i.e. husk, straw, stover, cob, and stalks of these crops are also of great significance (Daioglou et al., 2016). Estimates of by-products produced from these crops can be assessed using residue to production ratio (RPR) values. RPR is the gravimetric ratio of residue (by-products) to the actual crop yield (Murli et al., 2008). On the basis of production of respective crops and individual RPR value of by-products i.e. rice straw (1.5), rice husk (0.2), corn stalk (2), corn cob (0.33), sorghum cob (0.5), sorghum husk (0.2), and sorghum stalk (1.7) the total by-product generated can be quantified using following Equation 1.3 (Hiloidhari et al., 2014):

Quantity of by-products generated (in tons) = crop production (tons) x RPR.   (1.3)

Portions of these by-products are used as animal fodder and fiber while some have great fuel value. But sizeable fraction of these by-products remain unused and end up rotting in the field which emit harmful gases. All these factors lead to the search for more effective management of these agricultural products i.e. conversion into some sustainable product which can solve many problems simultaneously. Thermal conversion of these by-products into biochar and their use for aqueous remediation of pesticides is one such approach.

Biochars developed from rice husk (Mayakaduwa et al., 2017), corn cobs (kearns et al, 2014) and sorghum bagasse (Lima et al., 2017) has been used for water remediation and soil amendment. Variation in surface properties of biochar produced from corn stover (Rajkovich et al., 2011; Holm et al., 2014), corn cobs (Bourke et al., 2007; Dume et al., 2015), and rice husk (Jindo et al., 2014) at different temperature has been studied. Increase in surface area with increase in pyrolysis temperature is a common phenomenon. An observed trend of higher surface area of biochars produced at higher temperature and

their significant removal efficiency for aqueous pesticides adsorption motivates higher temperature for pyrolysis i.e. 900°C in present study.

1.2. Carbofuran

Carbofuran is a broad spectrum insecticide which is very effective against ticks, mites, and nematodes. It kills the organism ingesting it directly or coming in contact (Plangklang and Reunsang, 2010). On application, it enters into plant and is transported by the sap. When insects or other pests feed on plant parts, they are poisoned (Hodgson et al., 1991). Carbofuran was developed in 1960's and patented in 1965 by agricultural chemical division of Food Machinary Corporation (FMC), USA under the trade name, Furadan (Budvari, 1989It is applied on variety of crops such as strawberries, alfalfa, grapes, soybeans, and wheat. Carbofuran is also used to control soil dwelling and foliar feeding insects in sugarcane, sugar beet, maize, rice and coffee. (Trotter et al., 1991). Carbofuran is highly effective against green grasshoppers, brown plant hoppers, stem borers and whorl maggots, white flies, leaf miners, ants, mealy bugs, scale insects, cockroaches, wasps and aphids (Otieno et al., 2010b). It is effective against both nymphs as well as adults and can kill them in 20 minutes (Suett, 1986).

Carbofuran functions by inhibiting the acetylcholinesterases (AChE, choline hydrolase), the enzyme group responsible for hydrolysis of neuro-transmitting agent acetylcholine (AChE) into acetic acid and choline (Fukuto, 1990). Plasma pseudocholinesterases are also inhibited by carbofuran (Goel and Aggarwal, 2007). This inhibition is reversible (Gupta, 1994) and occurs due to inability of carbamylated enzyme (formed by association between carbofuran and alcohol moiety of AChE) to catalyze acetylcholine hydrolysis (Wilson and Harrison, 1961). Inhibition of AChE leads to its excessive accumulation at the synapses and neuromuscular junctions. This results in overstimulation of muscarinic and nicotinic acetylcholine receptors, which can ultimately lead to death due to respiratory failure (Gupta, 1994; Goel and Aggrawal, 2007). AChE can recover rapidly from this carbofuran induced inhibition by dissociation of methylmercury moiety from enzyme (O'Brien et al., 1966).

Carbofuran is classified as highly hazardous to human beings (WHO, 2004). It is classified based on acute oral rat LD_{50} value which is as low as 8 mg/kg for carbofuran (Health and Welfare Canada, 1987). Acute exposure to carbofuran, through dermal

contact, inhalation or ingestion can result into high toxicities and even death in some cases (Otieno et al., 2010a). Carbofuran is also reported to be mutagenic, genotoxic, terartogenic and affects the embryo (Tamrakar et al., 2007). It also exhibits placental transfer and is even reported to be found in milk of goats (Gupta, 1994). It does not tend to bioaccumulate as have relatively moderate water solubility and low K_{ow}. In fish, it disrupts enzymes and lipid metabolism. Honeybees and earthworms are also affected by its use. It is readily taken up by the plants and transported to areas with rapid transpiration rate (Eisler, 1985).

Due to widespread use, carbofuran and its metabolites have been found in air (Hall et al., 1997), soil (Farahani et al., 2008), groundwater (Tariq et al., 2004), surface water (Otieno et al., 2010b) and food (Bhargavi et al., 2006). Major source of carbofuran in environment is its application as insecticide. About 90% of total pesticides application does not reach to the target organisms and gets dispersed into air, soil and water (Moses et al., 1992). In addition, carbofuran can also reach directly to the surrounding environment from production sites (Sriramchari, 2004). It is stable under neutral or acidic conditions but unstable in alkaline medium (WHO, 2004). It has tendency to volatilize from water and moist soil due to low vapor pressure and low Henry's constant (Deuel et al., 1979; Siddaramappa et al., 1978). Carbofuran is relatively mobile in soil and in runoff due to high water solubility and low adsorption coefficient (Arias et al., 2008).

Carbofuran enters the aquatic environment through direct spray or broadcast of granular formulations, drift deposition of spray formulations and in runoff from treated field (Trotter et al., 1991). It may also reach aquatic bodies through rainwater and atmospheric redeposition (Richards et al., 1987). In aquatic environment, it can display persistence or undergo hydrolysis, microbial degradation, volatilization, photodecomposition, plant mediated deposition. Moreover, carbofuran accumulation and elimination can also take place in aquatic biota (Trotter et al., 1991).

Figure 1.2. Shows the different carbofuran metabolites present in water, soil and biota. 3-hydroxycarbofuran, 3-ketocarbofuran, carbofuran phenol, 3-hydroxycarbofuran-7-phenol, 3-ketocarbofuran-7-phenol and 2-3 dihydro-2, 2- dimethyl benzofuran 4, 7-diol are the major metabolites reported in environmental attributes (Eisler, 1985). 3-hydroxycarbofuran and 3-ketocarbofuran are the major metabolites present in soil and

water, (Eisler, 1985). They are found to be very toxic to target as well as non-target organisms (Azizullah et al., 2011). The carbofuran phenol, 3-hydroxy-7-carbofuran phenol and 3-keto-7-carbofuran phenol are formed through phenyl ring oxidation/reduction and hydroxylation reactions. The methyl hydroxylation reactions of carbofuran forms N-hydroxy methylcarbofuran and 3-hydroxy-N-hydroxymethyl carbofuran (Otieno et al., 2010a).

Carbofuran is reported in ground/surface water in many parts of world including Bangladesh (given in Table 1.2). The maximum concentration of carbofuran permitted in drinking water prescribed by WHO is 3µg/L (WHO, 2004). According to USEPA, the maximum contaminant level goal (MCLG) of carbofuran in water is 40 µg/L (USEPA, 2014).
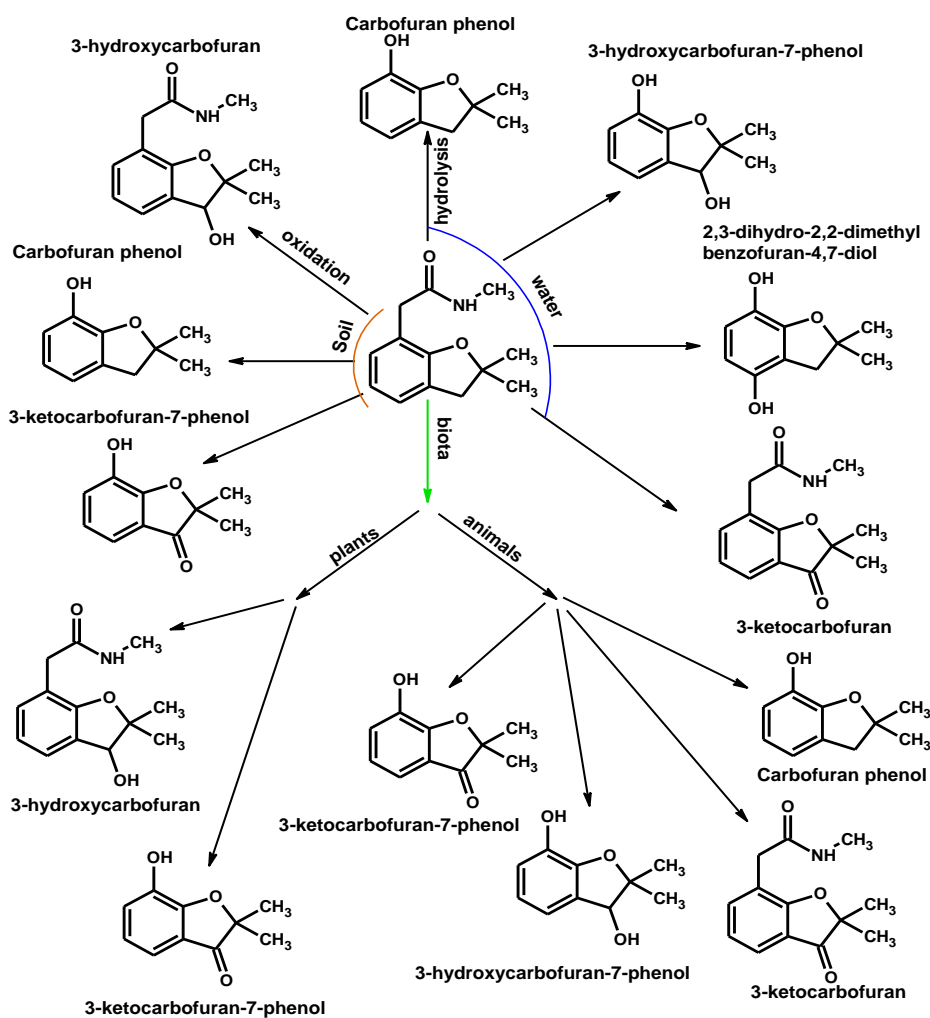
Figure 1.2 Fate of carbofuran in environment

There are many techniques for carbofuran analysis including liquid chromatography-mass spectrometry (LCMS) (Soler et al., 2008), gas chromatography coupled with mass spectrometry (GCMS) (Petropolou et al., 2006), gas chromatography (GC) (Wong and Fisher, 1975), gas-liquid chromatography (GLC) (Agrawal and Gupta, 1999), high pressure liquid chromatography (HPLC) (Lawrence and Leduc, 1977), flow injection spectrophotometry (Waseem et al., 2007) and simple spectrophotometric methods (Jan et al., 2003; Bhargavi et al., 2006). Spectrophotometric method can be either indirect or direct. Indirect spectrophotometric method involves detection of some metabolite viz. methylamine from hydrolysis of carbofuran (Jan et al., 2003) or detection of some coupling agent as 4-bromoaniline, 4-methylaniline and 4-aminobenzaldehyde (Harikrishna and Naidu, 2005), diazotized dapsone (Nagaraja and Bhaskara, 2006), diazotized p-aminoacetophenone (Tamrakar et al., 2007) with carbofuran. Direct method includes detection of carbofuran at a specific wavelength as in work done by Salman and co-workers (Salman et al., 2011a, Salman et al., 2011b).

1.2.1. Sorptive removal of carbofuran

Among various approaches employed for aqueous remediation of carbofuran, adsorption serves as a low cost, eco-friendly and significantly effective method at different operational conditions. Carbofuran remediation has been reported by 1) biosorbent as microchlophyte *Chlorella vulgaris* (Hussein et al., 2017); 2) agricultural adsorbents i.e. water chest nut shells (Memon et al., 2007), orange peels (Chen et al., 2012) and modified maize wastes (Foo, 2016); 3) polymeric adsorbents i.e. calix-arene based impregnated resin (Memon et al., 2015) and *p*-tetranitrocalix based modified silicon (Memon et al., 2014); 4) industrial waste i.e. flyash (Kumari and Saxena, 1988), blast furnace sludge, dust and slag (Gupta et al., 2006); inorganic adsorbents i.e. calcium phosphate (Ramdane et al., 2014) and animal bone meal (Roudani et al., 2014); and carbonaceous adsorbents i.e. activated carbons (Salman and Hameed, 2010) and biochars (Vithanage et al., 2016). Carbonaceous adsorbents are preferred because of their relatively better removal efficiency based on higher surface area. Common availability of their precursors and ease of production are added advantages of these adsorbents. Activated carbons (ACs) derived from various feedstocks i.e. rice straw (Chang et al., 2011), palm fronds (Salman, 2013), coconut fronds (Njoku et al., 2014), date seeds

(Salman et al., 2011a), banana stem (Salman and Hameed 2010a), and *Canariums chweinfuthii* seed shell (Titus et al., 2013) have been studied extensively for aqueous carbofuran remediation. Sorptive removal of carbofuran from water mediated by commercially available activated carbon, CAC (Salman et al., 2011b) and granular activated carbon, GAC (Salman and Hameed, 2010b) have been also reported. Biochar, a relatively new adsorbent derived from thermal degradation of natural and synthetic organic material has also been employed for carbofuran remediation. Biochar are often cost effective than activated carbons as additional activation (thermal or chemical) isn't required. In terms of surface area too they are comparable to activated carbons and in some cases the adsorption capacity per unit area is better than activated carbons.

First study for aqueous removal of carbofuran using rice husk and tea waste (spent) biochar has been reported by Vithanage et al., (2015). Here rice husk (RHBC700) and tea waste (TWBC700) biochars were developed from pyrolysis of respective biomasses at 700°C. Physicochemical characteristics of these biochar were determined using proximate and ultimate analyses. It was observed that the carbon content of these biochar were promising (through carbon content TWBC>RHBC). The molar H/C and O/C of obtained biochars as indicators of aromaticity and polarity respectively were also well within the guidelines laid by IBI for biochar. Surface areas of 342.2 and 377.0 m^2/g were reported for TWBC700 and RHBC700, respectively. Kinetic study with 1g/L biochar dose at initial carbofuran concentration of 50 mg/L (pH~5.0) revealed the equilibrium adsorption capacities (qe) of 10.7 and 23.9 mg/g for TWBC700 and RHBC700, respectively and obtained experimental data was found to be in agreement with non-linear pseudo-second order model (R^2>0.95). Better fitting of pseudo-second order model suggested abundance of adsorption sites on biochar surface and initial carbofuran solution being used lesser than their respective sorption capacities. Thermodynamic study of TWBC700 and RHBC700 biochar-carbofuran association suggested the exothermic and spontaneous nature of the adsorption process based of negative value of standard enthalpy change (ΔH°) and standard Gibbs free energy change (ΔG°) at all temperatures (25, 35 and 45°C)

Mechanism of the adsorption process was also explained and functional groups involved in adsorption process onto biochar were estimated using FTIR. Both physical

processes i.e. porous diffusion, H-bonding, and π^+-π interactions as well as chemical interactions i.e. electrostatic and electrophilic attractions were involved in completing the adsorption process. Porous diffusion and pH-based protonation-deprotonation of carbofuran are considered as primary mechanism involved in adsorption process. Broad peaks at 3370-3420 cm^{-1} in TWBC700 and RHBC700 spectra are attributed to O-H stretching vibrations of alcohol, phenols and carboxylic acids. Similarly, intense peak at 1050-1100 cm^{-1} in TWBC700 and RHBC700 spectra corresponds to phenolic O-H whose intensity reduces in carbofuran loaded TWBC700 and RHBC700 spectra with these groups acting as donor and acceptor in H-bonding. π^+-π interactions between electron rich graphene surface of biochars and protonated amino group of carbofuran is represented by typical peaks of C=N (1560 cm^{-1}) and C-N (1218 cm^{-1}) in loaded TWBC700 and RHBC700. Donor-acceptor π^+-π interactions are also evident from the appearance of peaks at 1460 and 1630 cm^{-1} corresponding to C-N and C=O respectively in loaded TWBC700 and RHBC700.

Another set of biochars, RHBC300, RHBC500 and RHBC700 produced from rice husk at different temperature i.e. 300, 500 and 700°C along with one steam activated biochar, RHBC700S were used for aqueous removal of carbofuran (Mayakaduwa et al., 2016a). Surface areas of these biochars were in order of RHBC300 (68.77m^2/g) <RHBC500 (169.81 m^2/g) <RHBC700(236.74 m^2/g) <RHBC700S (251.47 m^2/g). Isotherm study with adsorbent dose of 1 g/L at initial carbofuran concentration range of 5-100 mg/L at pH~5.0 revealed the equilibrium adsorption capacities (qe) of 30.73, 48.75, 132.87 and 160.77 mg/g for RHBC300 RHBC500, RHBC700 and RHBC700S, respectively and obtained experimental data was found to be in agreement with non-linear Langmuir as well as Freundlich isotherm model (R^2>0.90). Better fitting of Langmuir as well as Freundlich isotherm model suggested that the adsorption of carbofuran is a favorable process governed by both physisorption and chemisorption that occurs between carbofuran molecules and heterogeneous RHBC surface. Physical and chemical processes i.e. H-bonding and dipole-dipole interactions governing the carbofuran sorption onto RHBC700S was confirmed by FTIR analysis of this biochar before and after adsorption process. Appearance of peak at 1630 cm^{-1} corresponding to H-O-H bending, disappearance of characteristic peak from 739 cm^{-1} and shifting of peak

from 3420 to 3440 cm^{-1} corresponding to OH-bonded groups in carbofuran loaded RHBC700S suggested above mentioned mechanism for carbofuran adsorption.

Similarly, TWBC300, TWBC500 and TWBC700 produced from spent tea waste at different temperature i.e. 300, 500 and 700°C were used for aqueous removal of carbofuran (Mayakaduwa et al., 2016b). Surface areas of these biochars were in order of TWBC300 (2.28 m^2/g)>TWBC500 (1.57 m^2/g) <TWBC700 (342.22 m^2/g). pH study performed at 3,5,7 and 9 suggested that the removal was maximum at pH 5 (acidic) with electrostatic attraction between protonated carbofuran molecule and negatively charged biochar surface. Beyond 5 adsorption was seemingly reduced due to deprotonation of carbofuran molecule at alkaline pH. Isotherm study with adsorbent dose of 1.5 g/L at initial carbofuran concentration range of 5-100 mg/L at pH~5.0 revealed the equilibrium adsorption capacities (qe) of 54.71, 48.73 and 22.74 mg/g for TWBC300, TWBC500, TWBC700, respectively and obtained experimental data was found to be in agreement with non-linear Freundlich and Tempkin isotherm model (R^2>0.90). Another statistical function for error estimation based on chi-square (X^2) was used to determine the fitting of Freundlich and Tempkin was found to be lesser than 5 (X^2<5). Better fitting of Freundlich and Temkpin isotherm model suggested that the adsorption of carbofuran is a chemical process predominantly governed by electrostatic attraction that occurs between carbofuran molecules and TWBCs surface.

1.3. 2,4-Dichlorophenoxyacetic acid (2,4-D)

2, 4-Dichlorophenoxyacetic acid or 2,4-D is one of the most commonly used pesticide in the world. It is a systemic pesticide, categorized as herbicide which is used for post emergence control of annual and perennial broad-leaved weed in cropland and water bodies (WHO, 2004). 2,4-D can be directly sprayed on foliage and stem of the broadleaf plant. It can also be applied to the soil in granular or aqueous form from where it is absorbed by the roots and translocated to meristem areas (Munro et al., 1992). It is used against susceptible weeds in major crops as corn, wheat, oats, barley, rye, and sorghum and most of the grasses. It is quite effective against broad leaved weed on land such as dandelions, plantain, clover and chickweed as well as aquatic weed i.e. duckweed and water hyacinth. Biological action of 2,4-D includes change in cell wall characteristics as plasticity and permeability; impact on protein synthesis and increase in ethylene

production. These factors result into symptoms like stunted growth of roots and stems; vascular tissues i.e. xylem and phloem degeneration; ceasing of leaf growth and curls (Song, 2014). At molecular level 2,4-D results into alterations in synthesis of RNA and DNA along with associated changes in intracellular calcium concentration (Chinalia et al., 2007). Basically uncontrollable and unsustainable growth causes stem curl, leaf weathering and plant grows itself to death (Walker, 1998).

Chemically 2,4-D lies in phenoxyalkanoic acid group of auxinic herbicide family (Grossmann, 2009). It is among first synthetic auxins synthesized by academic and industrial laboratories during 1940s (Song, 2014). Post development in USA during 2nd world war it gained notoriety as constituent of Agent Orange used during Vietnam War (Greig, 1995).2,4-D was introduced in India soon after its synthesis in 1940s. But its large scale use started with its import in 1960s (Choudhury et al., 2016). 2,4-D is registered under section 9(3) of the Insecticides Act, 1968 and has been approved for use in 8 crops i.e. paddy, maize whet, sorghum, potato, sugarcane, citrus fruit and grapes. Maximum residual level (MRL) of 2,4-D in all these crops is set except for sugarcane (CSE, 2013). Frequent use of 2,4-D is attributed to its high selectivity and strength. It is manufactured by a four step process; 1) phenol neutralization, 2) NaMCA production, 3) condensation and 4) final ageing (Bovey and Young, 1980). It is manufactured and marketed with different trade names i.e. Aqua-Kleen, Baragge, Weedone, Salvo, Plantgard. It is marketed in different forms i.e. simple acid (2,4-D), salts (DEA, DMA, IPA, and TIPA and esters (EHE, IPE). Different formulations of 2,4-D includes water-dispersible powder, granule and concentrate. Effect of 2, 4-D on non-target organism is considered as moderately hazardous. It has been placed in group II as per toxicity level i.e. oral and dermal LD_{50}value for rat (mg/kg body weight) is 50-2000 and 200-2000, respectively. Acute toxicity of 2,4-D measured as oral, dermal and inhalation dose is 639, >1600 and 1.79 mg/kg, respectively. Sub-chronic exposure of laboratory animals to 2,4-D may result into eye irritation along with damage to thyroid, kidney, adrenal glands, testes and ovary. In human 2, 4-D are reported to induce cancer and other respiratory diseases after long exposure (Charles et al., 1996).2,4-D may also function as endocrine disrupter and lead to reduction in serum production (Rawlings et al.,1998).

Though applied against particular target organism 2,4-D like other pesticides are reported to find their way into air, water, soil, sediment through direct application spray drift and surface runoff. Processes like hydrolysis, photolysis, volatilization, microbial degradation and aerobic-anaerobic metabolism govern the fate of 2,4-D and its metabolite in environment. Apart from this, rainfall and irrigation pattern along with wind direction and intensity round the area decide the stay of 2,4-D in environment (Wafa et al., 2011). Major metabolites of 2,4-D (Figure 1.3) reported from water, soil and biota include 2,4-Dichlorophenol (2,4-DCP), chlorohydroquinone, 1,2,4-benzentriol, 4-chlorophenol, 2,4-Dichloroanisol (2,4-DCA), 2,4-Dichloro-5 hydrophenoxyacetic acid, succinic acid and 2,4-Dichlorocatechol (Walters, 1999). Especially 2,4-D contamination of water is mediated via direct application for agricultural purposes, forestry, right of-way, or turf land and surface runoff (IARC, 2015).
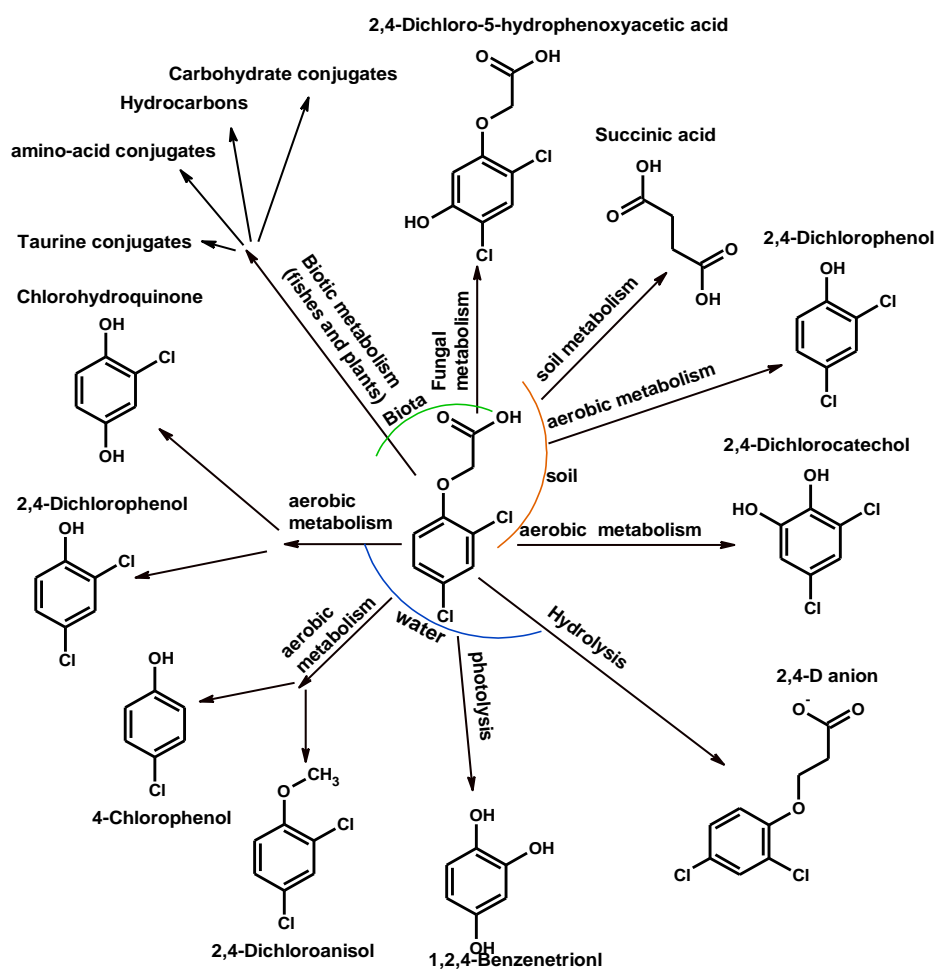
Fig.1.3 Fate of 2,4-D in environment

The maximum concentration of 2,4-D permitted in drinking water prescribed by WHO is 30 µg/L (WHO, 2004). According to USEPA, the maximum contaminant level goal (MCLG) for2,4-D in water is 70 µg/L (USEPA, 2014). Similarly BIS limit for 2,4-D in water is 30 µg/L (BIS, 2012).

Quantitative determination of 2,4-D in environmental and biological samples can be done by different methods as capillary electrophoresis (Raks et al., 2015), gas chromatography (GC) (Jiménez, 2013), liquid chromatography/ tandem mass spectrometry (LC-MS/MS) (Chamkasem and Morris, 2016), high-performance liquid chromatography (Kashyap et al., 2005), electrode assisted potentiometric method (El-Beshlawy, 2015), immunogenetic/electrophotochemical sensors (Dequaire et al., 1999; Shi et al., 2011) and UV spectrophotometry (Salman and Al-Saad,2012). Use of spectrophotometric methods for 2,4-D estimation is old. It is based on molar extinction coefficient (ε) i.e. measure of strength of adsorption of a particular wavelength by a chemical species (Bandurski, 1947). 2,4-D concentration in water can be determined directly (Salman and Al-Saad,2012) or via some transformation product i.e. 2,4-DCP (Shah et al., 2006).

2,4-D and its metabolites have been found in surface, ground and wastewater in different parts of the world. Its presence has been reported in water in Canada (Munira et al., 2018), China (Brauns et al., 2018), Hungry (Szekacs et al., 2015), Spain (Kock-Schulmeyer et al., 2014), USA (MDH, 2016), Mexico (Felix-Canedo et al., 2013), Iran (Pirsaheb et al., 2013) and Australia (Mitchell et al., 2005). 2,4-D have also detected in Indian water i.e. Okhla, New Delhi (Aleem and Malik, 2005). 2,4-D can be removed from water using several methods such as adsorption, photo-catalytic degradation, combined biological oxidation, photo-Fenton, advanced oxidation processes, aerobic degradation, nanofiltration (with membranes), ozonation, coagulation, fluid extraction, and solid-phase extraction (Trivedi et al., 2016).

1.3.1. Sorptive removal of 2,4-Dichlorophenoxyacetic acid

Sorptive removal of 2,4-D has been reported by different adsorbents. These adsorbents belong to different adsorbents groups such as 1) biosorbent i.e. macro fungi (*Sojar caju and Sojar florida*) (Alam et al., 2000), *penicillium chrysogenum* and pristine biomass (Deng et al., 2009); 2) polymeric adsorbents i.e. MEIX resin (Ding et al.,2012),

NDA-99 and styrene divinyl benzene copolymers (amberlite-XAD-4) (Qiua et al., 2009); 3) industrial waste i.e. bottom ash (Alam et al., 2000), modified slilica gel factory waste (Koner et al., 2012), blast furnace sludge, dust and slag (Gupta et al., 2006); 4) inorganic adsorbents i.e. calcined hydrotalcite (Pavlovich et al., 2005), dodecaylammonium (Ackay et al., 2005), Zn-Al-Cl layered double hydroxides (LDH) (Legrouri et al., 2005), zeolite (Venkatkrishnan et al., 2006) and polygorskite (Xi et al.,2010), 5) metal organic framework (MOF) (Jung et al., 2013), 6) nanoadsorbents i.e. single wall carbon nanotubes (SWCNTs) (Bazrafshan et al., 2013), iron oxides nanoparticles (Tang et al., 2015) and rice husk nanomaterials (Abigail and Chidambaram, 2016) and 7) carbonaceous adsorbents i.e. high area carbon cloth (Ayranchi and Hoda, 2004), activated carbons (ACs) (Njoku et al., 2013) and biochars (Essandoh et al., 2017).

Extensive studies about 2,4-D adsorption onto activated carbon have been done. Different carbon active materials i.e. ACF400 (Chingombe et al., 2006), SAC (Gupta et al., 2006), GAC (Aksu and Kabasakal, 2005; Kim et al., 2008; Zahoor, 2013), PAC (Aksu and Kabasakal, 2005) are used successfully for aqueous 2,4-D remediation. Chemically modified activated carbons (Denghahi et al., 2011; Li et al., 2018) along with activated carbon derived from different sources i.e. phenolic resins (Diaz-Flores et al., 2006), particle board (Cansado et al., 2017), corn cob (Njoku and Hameed,2011), date stones (Hameed et al., 2009), palm fronds (Salman et al., 2011), banana stem (Salman et al., 2011), Langsat fruit (Njoku et al., 2005), pumpkin seed hull (Njoku et al.,2013), coconut shell (Njoku and Hameed, 2014), groundnut shell (Trivedi et al., 2016a), banana leaf (Salman and Khadim, 2017); willow, miscanthus, flax, and hemp (Doczekalska et al., 2018) have also been applied successfully aqueous removal of 2,4-D. But despite the greater surface area and subsequent greater adsorption capacity the activated carbon tend to have some production based and application condition related constraints. Along with normal pyrolysis activated carbons requires specific thermal and chemical activation which increases their production cost. Moreover the removal of 2,4-D by such activated carbon have been mostly reported at lower pHs. It has been also observed that the adsorption capacity per unit area of activated carbon is comparatively lower with wide difference between their respective surface area and adsorption capacities. To overcome these shortcoming and put forward a cost effective, application friendly and sustainable

adsorbent biochars come into ploy. First of all, common wood charcoal obtained from market was applied for 2,4-D removal. The near-neutral pH of 5.6-6.0 was used for this adsorption study. The removal efficiency and removal capacity of wood charcoal was reported to be 92. % and 0.70 mg/g, respectively. This adsorption process was best fitted by the Freundlich isotherm model (Alam et al., 2006).

Rice straw biochars (acid modified) produced at different temperature were employed for 2,4-D adsorption and its controlled release (Lu et al., 2012). For rice straw biochar preparation, rinsed and dried rice straw was pyrolysed at 200, 350 and 500°C. Surface area of produced biochars i.e. RS200 (2.1 m^2/g), RS350 (20.6 m^2/g) and RS500 (128 m^2/g) were determined using BET surface area analyzer while other surface properties were assessed using attenuated total reflection infrared (ATR-IR) spectroscopy. All three biochars were reported to have -C=O, -C-O and –OH as prominent functional groups. CHNS analysis with H/C and O/C ratio suggested the increase in aromaticity and carbonization with increase in pyrolysis temperature. The isotherm experiments with these biochars; RS200, RS350 AND RS500 at pH~3-3.5 and 2,4-D concentration ranging from 60-300 ppm yielded adsorption capacity of 13.48, 19.80 and 8.8 mg/g, respectively. Data obtained was best fitted by Freundlich isotherm model. In one similar study by Li and co-workers (Li et al., 2013) poplar wood was pyrolysed at temperature 200, 350 and 500°C and studied for 2, 4-D adsorption. Poplar wood biochar, PW200, PW350 and PW500 were reported with surface area of 1.0, 4.03 and 30.6 m^2/g. Isotherm studies revealed that the adsorption capacities of 10, 24 and 11 mg/g for PW200, PW350 and PW500, respectively and data obtained here too was best fitted by Freundlich model.

Kearns et al., (2014) studied the aqueous removal of 2,4-D using laboratory made as well as field-collected biochars. Laboratory biocharswere obtained from feedstock i.e. wood chips, bamboo, corn cobs, and rice straw at different pyrolysis conditions viz. temperature (350, 400, 500, 600, and 700°C) and residence time (4, 6, and 96 hr). Field collected biochars viz. Basudha, Punpun, Sal, Coconut, Logan, and rice straw made through traditional kiln methods in rural Thailand. BET surface area for different biochars obtained from wood chips, bamboo, corn cobs and rice straw were found to range within 2.4-516, 4.7-510, 2.3 and 20.6-128 m^2/g, respectively. Similarly BET

surface area for field collected chars as Basudha, Punpun, Sal, Coconut, Longan and Rice straw was reported to be 404, 333, 197, 90.9, 4.0 and 10.85 m^2/g, respectively. Their adsorption capacities are reported in order of basudha (54.6 mg/g)> rice straw (34.2 mg/g)>punpun (3.63 mg/g)>sal (1.20 mg/g)>longon (0.64 mg/g)>coconut (0.49 mg/g). Here, it was observed that with increase in pyrolysis intensity, (either by increasing pyrolysis temperature or by increasing the residence time) surface area of the biochar also increased. During batch studies at pH~ 7, initial 2,4-D concentration 10 mg/L, biochar dose 0.005-10 g/L and equilibrium time of 2-4 weeks, wood chips, bamboo, corn cob and rice straw exhibited experimental adsorption capacity of 21.3, 13.75, 0.43 and 0.77 mg/g , respectively. Adsorption capacity for raw wood chips, bamboo, corncob and rice straw was reported to be 4.68, 3.0, 0.11 and 0.21 mg/g, respectively and when compared it was always lesser than adsorption capacity of corresponding char. For field collected chars, the adsorption capacities are reported in order of Basudha (54.6 mg/g)> rice straw (34.2 mg/g)>punpun (3.63 mg/g)>sal (1.20 mg/g)>Longon (0.64 mg/g)>coconut (0.49 mg/g). This study suggests that both the biochars, laboratory made as well as field collected are good at aqueous 2,4-D removal.

Similarly, the aqueous removal of 2, 4-D by groundnut char was studied by Trivedi et al., (2016a). Groundnut shell were ground, sieved (85 BSS mesh size) and pyrolysed at temperature of 650°C with heating rate of 20°C/minute and for residence time of 2 hours in an nitrogen environment for preparation of biochar (GSC). The BET surface area of this biochar was reported to be 43 m^2/g. They reported the Langmuir adsorption capacity of 3.0 mg/g for groundnut char. Trivedi and co-workers (Trivedi et al., 2016b) also reported the adsorption of 2, 4-D onto cotton plant char. For the preparation of this biochar cotton plant were dried at 110°C for 24 hours and then pyrolysed at 650°Cat heating rate of 20°C/minute and for residence time of 2 hours in nitrogen environment. Cotton plant char (CSC) obtained was reported to have BET surface area of 109 m^2/g. CSC was reported to have maximum adorption capacity of 3.93 mg/g with Langmuir as best fitting isotherm adsorption model. Both the above mentioned studies were done at basic pH and upto 2,4-D concentration of 100 mg/L.

Various biochar obtained from different feedstock and at different pyrolysis conditions were applied the aqueous removal of 2,4-D from water (Mandal et al., 2017).

Here biochar were obtained from tea waste (TW-BC), burcucumber (BU-BC), oakwood (OW-BC) and bamboo (B-BC). The pyrolysis condition for first two biochars i.e. TW-BC and BU-BC included temperature of 700°C with heating rate of 7°C/minute for 2 hours under nitrogen flow of 5 ml/minute. A part of TW-BC produced was further activated under flow of steam (5 ml/minute) to develop steam activated biochar (TW-BCS). Other two biochars i.e. OW-BC and B-BC were produced under similar pyrolysis condition but at temperature of 400°C. The surface areas of these biochar, TW-BC, TW-BCS, BU-BC, OW-BC and B-BC were reported to be 421.3, 576.1, 2.3, 270.7 and 475.6 m^2/g, respectively. FTIR analyses of these biochar for assessment of their bulk surface characteristic indicated the presence of C-H, C=O, carboxyl, phenolic and other oxygen containing functional groups. X-ray photoelectron spectroscopy (XPS) was also done to recognize the specific functional group. It was observed that the oxygen content of steam activated biochar was greater than the other biochars. Also the –COOH with greater oxygen proportion was more abundant in TWBCS. In a batch adsorption experiment with biochar dose- 2.5 g/L and 2,4-D concentration- 100 mg/L at pH~7 the adsorption capacities were reported to follow the order, TW-BCS>OW-BC>BU-BC>B-BC>TWBC. Adsorption capacities were reported to be 58.85, 42.67, 28.92, 26.66 and 10.05 mg/g for TW-BCS, OW-BC, BU-BC, B-BC and TWBC, respectively. The adsorption data was found to be in agreement with Freundlich isotherms model.

Phenoxy herbicide, 2,4-D adsorption onto switchgrass biochar was studied by Essandoh and co-workers (Essandoh et al.,2017). Here, pH study done at biochar dose of 1 g/L and 2,4-D concentration 40 mg/L revealed that the adsorption of 2,4-D onto biochar was best at pH 2 with only slight reduction till pH 8 followed by abrupt decrease at pH 10. This variation in percent removal was attributed to electrostatic repulsion between negatively charged carboxylate anion of 2,4-D at and protonated functional groups of biochar at higher pH~10. Kinetic concentration studies at 2,4-D concentration i.e. 100,200 and 300 °C suggested that the pseudo-second order rate equation fitted the experimental data best. Similarly, data obtained from iostherm studies were found to be in agreement with Freundlich and Langmuir isotherm models with highest Langmuir adsorption capacity of 134 mg/g at 45°C.

1.4 Research objectives

The objective of the present study was to develop sustainable biochars from agricultural byproducts and use them as economically an ecologically viable adsorbent for removal of pesticides from water. The specific objectives of this study are as follows:

1. Selection of precursor material and their thermal conversion into biochar using slow pyrolysis.

2. Characterization of developed biochars using BET surface area analysis, CHNS analysis, powder X-ray diffraction (XRD), Fourier transform infrared spectroscopy (FTIR), scanning electron microscopy (SEM) and energy dispersive analysis (SEM-EDX), transmission electron microscopy (TEM) and inductively coupled plasma atomic emission spectrometry (ICP-AES).

3. Sorption equilibrium studies and kinetic studies for carbofuran and 2,4-D remediation at different pHs, adsorbent doses, adsorbate concentrations and temperatures

4. Modeling of the kinetic and sorption data using various rate kinetic equations (pseudo first and pseudo second order rate equations) and isotherm models (Langmuir, Freundlich, Temkin, Sips, Redlich-Peterson, Toth, Koble-Corrigan and Radke-Prausnitz).

5. Determination of thermodynamic parameters i.e. change in standard enthalpy ($\Delta H°$), standard entropy ($\Delta S°$) and standard free energy ($\Delta G°$).

6. Column studies for up scaling and designing fixed bed reactor for pesticides adsorption and regeneration of spent biochars using suitable desorbing agents.

1.5. Structure of thesis

The thesis is organized as chapters in following manner.

This thesis is composed of seven chapters. The first chapter contains introduction and literature review related to various aspects of this study. It also bears the objectives of this study. Second chapter informs about the materials and methods used in this study. Third chapter of this thesis includes the characterization of biochar using various analytical techniques. Fourth chapter of this thesis bears results from carbofuran adsorption studies onto the biochars. It includes mechanism for carbofuran adsorption, pH optimization studies, kinetic and isotherms studies along with respective modeling;

and thermodynamic studies for carbofuran adsorption. Fifth chapter of this thesis describes 2,4-D adsorption studies onto the biochars in batch mode. It also explains 2,4-D sorption mechanism, its pH optimization, kinetic and isotherms studies along with thermodynamics. Chapter 6 of this thesis bears results from adsorption studies in column mode and desorption studies. Chapter 7 summarizes this study. It bears conclusions and recommendations for future.

CHAPTER 2

MATERIALS AND METHODS

2. Materials and methods

2.1 Carbofuran

Carbofuran is a white crystalline powder.
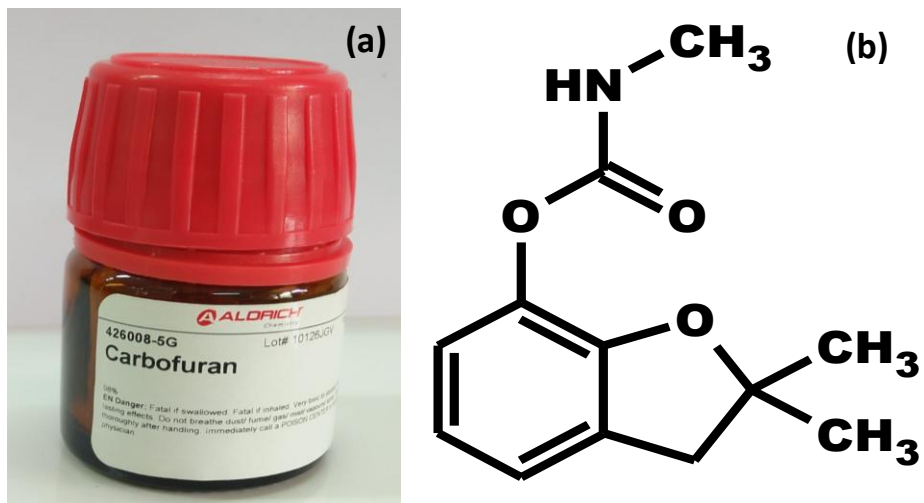
Figure 2.1 (a) Carbofuran (98%) from Aldrich (b) Molecular structure of carbofuran.

2.2 2,4-Dichlorophenoxyacetic acid

2,4-D is also a white crystalline powder.
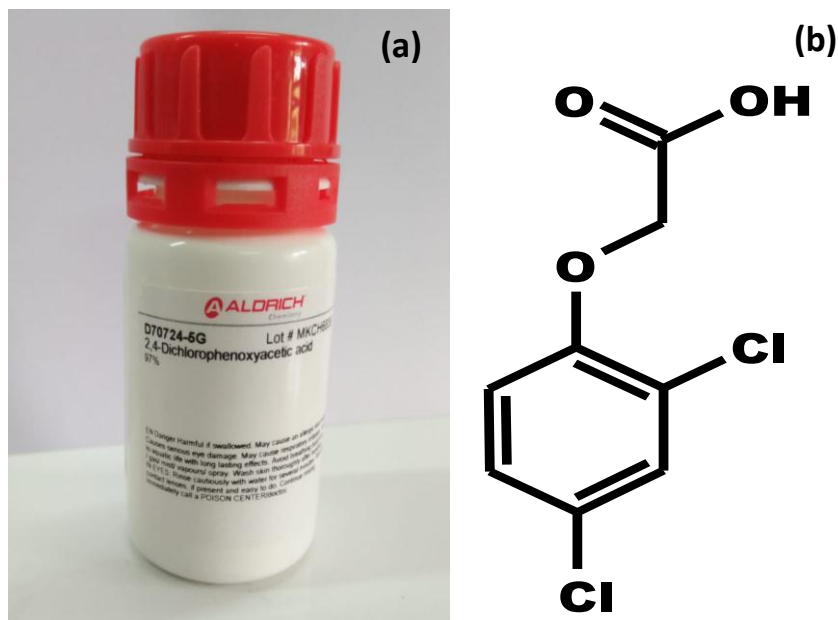
Figure 2.2 (a) 2,4-D (97%) from Aldrich (B) Molecular structure of 2,4-D.

Table 2.1 Physico-chemical properties of Carbofuran and 2,4-Dichlorophenoxyacetic acid (Evert, 2002; Walters, 1999)

Common Name	Carbofuran	2,4-Dichlorophenoxyacetic acid (2,4-D)
Molecular formula	$C_{12}H_{15}NO_3$	$C_8H_6Cl_2O_3$
Molecular weight (g/mol)	221.26	221.04
Density/ specific gravity	1.18 (at 25°C)	1.42 (at 25°C)
Water solubility (ppm)	351 (at 25°C)	677 (at 25°C)
Melting point (°C)	150-152	140.5
Vapor pressure	54×10^{-6} mm Hg (25°C)	14.0×10^{-6} mm Hg (25°C)
pK_a	3.78 11.98	2.81
Octanol-water partition coefficient (Log K_{OW})	2.32	2.81
Henry's law constant (atm m^3/mol)	4.5×10^{-10}	9.75×10^{-8}
Hydrolysis half-lives (days)	27.7 (pH 7 , 25°C)	39 (pH 7 , 25°C)
Aqueous photolysis half-life (days)	7.95×10^3	13
Soil photolysis half-life (days)	138	393
Field dissipation half-life (days)	13.0	59.2
Adsorption coefficient (Koc)	7-123	20-136
Trade Names	Furadan 4F or 3G, Niagara 10242, Brifur, Crisfuran, Chinifur, Cuarterr, Yaltox, Pillarfuran, Kenofuran.	Aqua-Kleen, Baragge, Weedone, Salvo, Plantgard

2.3. Reagents and equipment

Chemicals used in the experiments were either of analytical reagent (AR) grade or guaranteed reagent (GR) grade. Carbofuran (purity- 98%) and 2,4-D (purity- 97%) were obtained from Sigma-Aldrich, India. Ethanol (absolute) with 99% purity was obtained from Merck, Germany. Similarly, concentrated HNO_3 and NaOH (98%) were ordered from Merck, India. Nylon syringe filters (non-sterile, pore size ~ 0.2μm) used for phase separation after adsorption process were obtained from Axiva sichem biotech, India. Whatman filter paper no.1 and 41 with pore size of 11 and 2.5μm respectively were obtained from GE healthcare UK limited, UK for filtration.

Different instruments and equipment were used in the present study at different steps viz. development of biochar, characterization of biochar, experimental set-up for adsorption process and pesticide analysis. High end Thermo-Scientific muffle furnace (model-Thermolyne Eurotherm 2416) was used for pyrolysis of biomass. Brass test sieves from Jayant Scientific, India having different B.S.S. and ASTM calibration were used with sieve-shaker from Scientech, India for uniform sorting of adsorbent particle. A digital hot air oven (model Scientech Instruments, India) was used to dry the material. Locally made china-clay mortar-pestle, Buchner funnel and Borosil desiccator were used for grinding, filtration and storage of biochars, respectively. Characterization of the biochar was done using proximate and ultimate analysis along with respective instrument for BET, SEM, TEM, FTIR, XRD, and ICP-AES. For the adsorption experiments, all the chemicals and adsorbents were weighed on Mettler Toledo balance (model AB 265-S/FACT). All the pH measurements of solution and samples were done by Thermo Scientific pH meter (model ORION 5 STAR). Water bath incubator shakers from Macro Scientific (models- MSW 275 and 275R) and Scientech, India (model-RC51000) were used or mixing adsorbent and adsorbate at constant temperature and speed of 120-150 rpm. Measurement of carbofuran and 2,4-D concentration in samples was done by UV-Vis spectrophotometer (model Lambda 35, Perkin Elmer).

2.4. Development of biochar

Biochars were developed from the slow pyrolysis of biomass (agricultural byproducts like corn stover and corn cob in this case). Corn stover and corn cob were collected from agricultural field post-harvest in Bhikhanpur village, Gaziabad, Uttar Pradesh, India.

After collection both these were segregated and sun-dried separately for 2 weeks. Sun drying was done to reduce the moisture content of the biomass as much as possible. After drying both the biomasses, corn stover were cut into small size of 1-2 cm and pyrolysed separately at 900°C (ramp rate-10°C/min and residence time of 30 minute) in quartz crucibles in muffle furnace to form biochar. Residence time was selected precisely to ensure maximum carbonization. The gases and vapors formed during pyrolysis were allowed to escape via exhaust pipe. After pyrolysis the biochars were left overnight to cool by itself. Post cooling both these obtained biochar were crushed using mortar-pestle and sorted with standardized sieves. These sorted biochar particle were washed and filtered with double distilled water to remove any possible color leach. No color leaching was ensured by spectrophotometric analysis of filtrate obtained from washing. After washing biochars were oven dried and sieved again with 30-50 BSS mesh size sieves to ensure uniform particle size. Developed biochars were kept in air-tight containers placed in desiccators till further use. The biochar obtained from corn stover and corn cob as feedstocks were named as CSBC and CCBC, respectively. Complete process of development of CSBC and CCBC from their respective feed is given in Fig 2.3.

Four different agricultural products i.e. rice husk, corn stover, corn cob and sorghum stem were screened for use as precursor for biochars development. Biochar derived from them viz. RHBC, CSBC, CCBC and SSBC were used for aqueous removal carbofuran and 2,4-D removal at different pH i.e. 2, 4, 6, 8 and 10. Biochar doses, particle size, and initial carbofuran/2,4-D concentration kept for this study were 5 g/L, 30-50 B.S.S. (mesh size), 5 mg/L and 25°C, respectively at 25°C. It was observed that percent carbofuran adsorption was maximum at pH 6 for all the biochars with value being 82.93, 83.94 80.52 and 82.73% for RHBC, CSBC, CCBC and SSBC, respectively. Similarly, percent 2,4-D adsorption for RHBC, CSBC, CCBC and SSBC were 34.91, 72.52, 72.29 and 64.19%, respectively.

Thus, on the basis of performance of CSBC and CCBC in preliminary adsorption experiment corn stover and corn cob were selected as precursor for development of biochars.
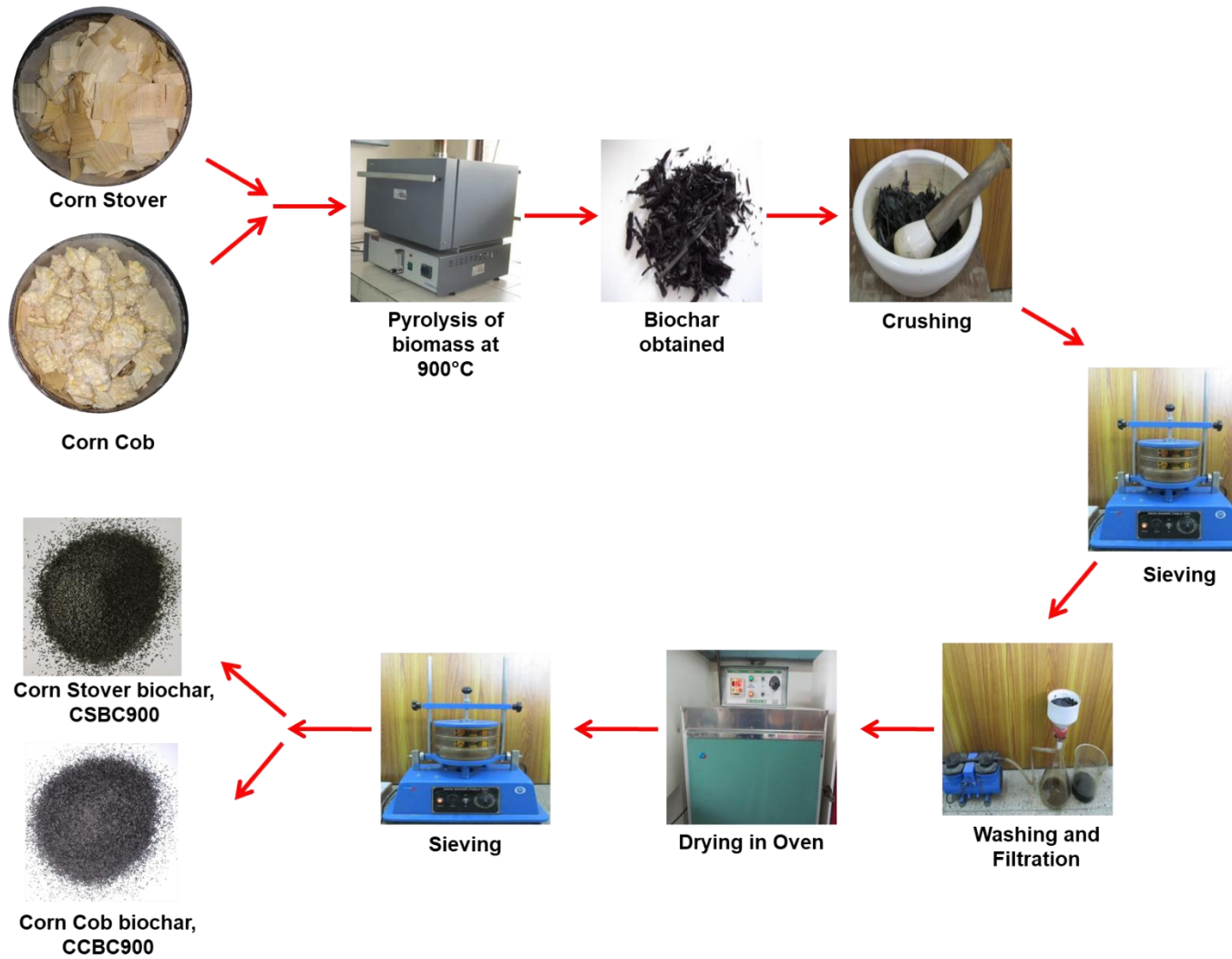
Figure 2.3 Development of corn stover (CSBC) and corn cob (CCBC) biochars.

2.5. Characterization of CSBC AND CCBC

2.5.1 Proximate analysis

Carbon, hydrogen, nitrogen and sulfur were analyzed using Elementar CHNS analyzer (model Vario-El-III). Oven dried samples were used for analysis. The carrier gas used in the combustion reactor was helium at a flow rate of 80 ml min^{-1}. Ultrapure oxygen at 20 ml min^{-1} flow rate was used as the fuel gas. Analysis was performed at a furnace temperature of 980 °C and 115 °C of GC oven temperature with an actual combustion temperature of 1800 °C in the reactor. .

pH and conductivity of the biochar were determined by process mentioned in Novak et al, 2009 and Cantrell et al., 2012. For this, the mixture of biochar and double distilled water was shaken in water bath at 25 °C for 24 hours. After this the mixtures were filtrated and measurements were taken with pH meter and conductivity meter. Percentage yield, moisture content, and ash content were also determined using standard processes (Mašek et al., 2013; Novak et al., 2009).

2.5.2 Ultimate analysis

The ultimate analysis of CSBC and CCBC were done using inductively coupled plasma emission spectrometer (ICP-AES) by Spectro analytical instruments, GmbH, Germany (model ARCOS, simultaneous ICP spectrometer). It involves the principle of emission spectrophotometry where energy at specific wavelength characteristic to electronic configuration of a particular atom after fall from excited state to ground sate is taken into consideration (Van de weil, 2003). For determining Si (silica), biochars were dissolved in hydrofluoric acid. ICP-AES determined the elements present in the biochar in terms of weight percentage.

2.5.3. Specific surface area and pore characteristic

The specific surface area and pore characteristic of the biochars were determined using BET surface area analyzer. The principle of this analysis technique is an extension of Langmuir adsorption theory of monolayer adsorption into multilayer adsorption with given hypothesis: 1) layered adsorption of gas molecules on a solid surface which is infinite and continuous, 2) no interaction between adjacent adsorption layers and 3) application of Langmuir theory to each layer (Park and Seo, 2011). In practice, the

amount of gas adsorbed on surface of material gives the information about total surface area (S_t) using given equation (Brame and Griggs, 2016):

$$S_t = \frac{W_m N A_{cs}}{M} \tag{2.1}$$

where, W_m is the weight of adsorbate in the monolayer, N is the Avogadro's number, A_{cs} is the cross sectional area of adsorbate, and M is the molecular weight of adsorbate gas. From total weight of this material the specific surface area is derived using equation:

$$SSA = \frac{S_t}{W} \tag{2.2}$$

where, S_t and W are the total surface area and weight of sample taken for analysis, respectively.

Specific surface area and pore characteristics of CSBC and CCBC were estimated using nitorgen adsorption-desorption isotherms performed at 77 K with a Quantachrome BET surface area and pore volume analyzer (Autosorb 1C) (Fig X). For this the biochar samples were degassed in vacuum at 303 K for 24 h followed by exposure to nitrogen gas at various vapor pressures. Adsorbed nitrogen per unit biochar weight was plotted against its relative vapor pressure (P/Po) ranging from 0.01 to 0.1. The adsorption-desorption data was fitted onto Brunauer-Emmett-Teller equation to determine the surface area.

2.5.4. Scanning Electron Microscopy (SEM)

SEM is used to observe the pore structure and surface morphology of the material. It involves the scanning of the sample by focused beam of electrons to produce the image. Electron beam is used instead of light for SEM as its wavelength is smaller than the light which enables better resolution (Lin et al., 2014). A SEM assembly includes an electron source, anode, condenser lens, scanning coils, objective lens and secondary electron detector arranged in vacuum (Figure 2.4) (Peiris, 2014). The working principle of SEM involves thermionic emission of electrons from electron source which are drawn forward and accelerated by the anode. Now, these electrons are concentrated into beam and directed to the sampleby the lens system i.e. condenser and objective lens. Condenser lens meets these elections first and guides them into a beam determining their size and thus defines the resolution of microscope (Peiris, 2014). Objective lens, on the other hand comes afterwards and focusses the electron beam onto the sample. Scanning coils are

arranged between these two lenses which rasters the converging electron beam from condenser lens onto the samples. Later SEM images are processed using the information provided by secondary and backscattered electrons reflected from near surface region of sample to the detector (Everhart-Thornley detector) (Frank et al., 2012).
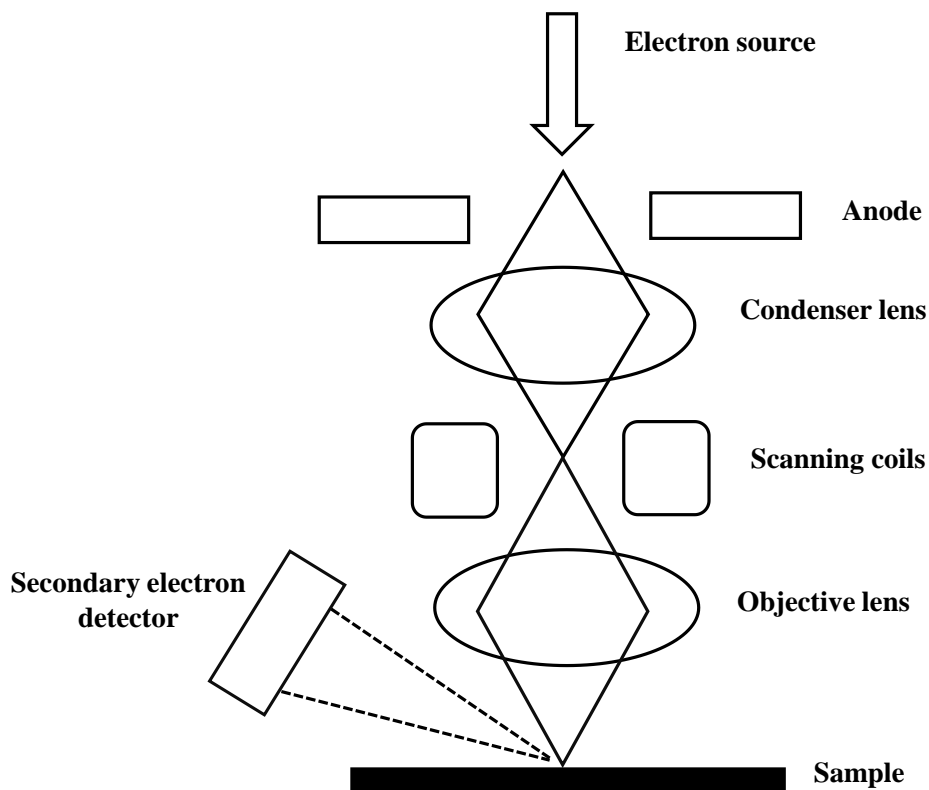
Figure 2.4 Schematic diagram of SEM (modified from Peiris, 2014).

Surface morphology of CSBC and CCBC were studied by using the SEM (model Zeiss, EVO 40), operating at 20,000 KV/mA voltage. For this, small quantity of biochars were dispersed in ethanol in separate centrifuge tubesand these suspensions were ultra-sonicated for 30 minutes. Post ultra-sonication, a drop of each suspension containing biochars was mounted on separate aluminum stub using double sided carbon tape. Thereafter the biochars were coated with a thin layer of gold nanoparticles to make it conductive. Surfaces characteristic of biochars were determined through grayscale micrographs obtained at different magnifications.

2.5.5. SEM-EDX

SEM-EDX uses the same arrangement as SEM and differs only in terms of signals generated from electron beam-sample interaction which are used to process to information. SEM-EDX uses the X-ray produced from the transition of electron from higher energy shell to positively charged hole of the atom. These positive charged holes arein turn formed by knocked off electron from particular energy shell of atom by high energy electron beam (Scimeca et al., 2018).

Energy of the X-ray produced is dependent on the atomic number and characteristic to the energy difference between these two shells participating in transition (Rades et al., 2014). Thus the X-ray emitted by different elements serve as their unique fingerprint based on their atomic number and hence can be used to identify the type of elements existing in the sample. These X-rays are detected by different detectors i.e. Si/Li detector and silicon drift detectors (SDDs).

2.5.6 TEM

TEM is also a type of electron microscope which produce images from information processed by beam of electron transmitted through the samples. The thickness of sample analyzed should be very less (<150 nm) as the incident beam of electrons is required to pass through it. TEM is used to determine the crystal structure, internal morphology and stress state of the material (Nanakoudis, 2019). The assembly of TEM includes electron source, arrangement of lenses for determining shape and path of electron beam and image on fluorescent screen (Figure 2.5). TEM produces image in 2D and its resolution is better than SEM (~50 pm) (Kaech, 2002).

TEM (model JEOL 2100F) was used for assessing the internal morphology of CSBC and CCBC and operated at an accelerating voltage of 200 KV. For sample preparation, biochars were taken in separate centrifuge tubes and suspended in ethanol and ultra-sonicated for 1 hour. A drop of the ultra-sonicated suspension was placed on the copper grid and viewed at various magnifications. High-resolution transmission electron microscopy (HRTEM) was done for detailed structural analysis. The HRTEM investigates the crystallinity of any material by the crystal lattice fringes analysis
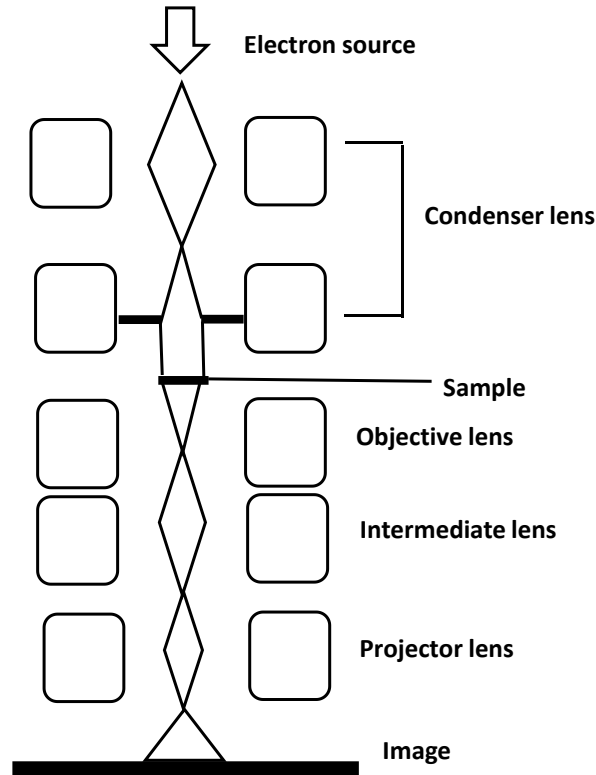
Figure 2.5. Schematic diagram of TEM (modified from Marturi, 2013).

2.5.7 X-Ray Diffraction

XRD analysis is done to gather the information about mineral components of the material along with the arrangement of atoms in crystal i.e. crystallinity. This technique is based on the interaction of X-ray radiation with the constituent atoms of a material. The spacing between the atoms is in order of wavelength of X-ray (0.1-100 A°) and hence can be used as the diffraction grating for the X-rays as discovered by Von Laue (Eckert, 2012). Relationship between the spacing between atoms of a crystal lattice and angle of diffraction of X- ray when it strikes the crystal given by W. L. Bragg (Bragg, 1913) is given in Equation 2.3.

$$n\lambda = 2d\mathrm{Sin}\Theta \qquad (2.3)$$

Where, n is an integer representing reflection's order , λ is the incident X-ray's wavelength , d is the interplanar spacing and Θ is the angle of diffraction for X-ray.

The device which does the diffraction analysis of the material is known as X-ray diffractometer. This diffractometer basically detects the X ray diffraction from the material and represents the diffraction intensity as a function of diffraction angle (2Θ)

i.e. plot of intensity vs 2Ө known as diffractogram. Working of the XRD involves components such as source of X-ray beam, primary X-ray optics, goniometer, sample holder, diffracted beam collimator and detector. A X-ray powder diffraction system from PANalytical model X'Pert PRO was used to obtain the X-ray diffraction (XRD) pattern of CSBC and CCBC at 45 kV and 40 mA using Cu-Kα (λ=1.5406 Å) radiation. The samples were scanned at 2Ө range of 5.0250-89.9750° (where, Ө is diffraction angle) with a 0.05° step size and ~3 seconds scan speed.

2.5.8 Fourier Transform Infra-Red spectroscopy (FTIR)

FTIR spectroscopy helps in determination of functional groups present on the surface of the sample. It also provides specific information about the vibration and rotation of the chemical bond and molecular structure based on their characteristic adsorption of infrared radiation (Jaggi and Vij, 2006). This characteristic adsorption is at definite wavelength and frequencies and corresponds to the vibrational transitions of the chemical bonds when they come across infrared radiation (King et al., 2004). In simpler words, infrared (IR) spectrum is unique to the sample and serves as fingerprint with absorption peaks corresponding to the vibrational frequencies of the bonds present in the sample. So, different chemical bonds and subsequently different compounds can be identified using FTIR spectroscopy (Coates, 2006). The components of FTIR include source of IR radiation, collimator for generation of parallel IR beams, interferometer (assembly of beam splitter and two mirrors arranged perpendicular to each other) for spectral encoding, sample chamber and detector (Figure 2.6).
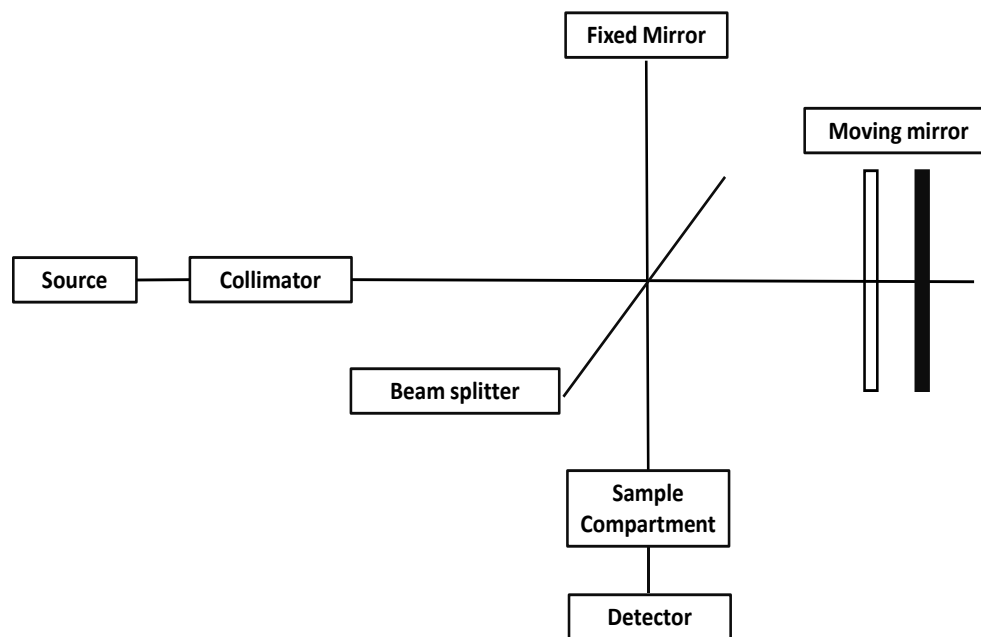
Figure 2.6 Schematic diagram of FTIR (Macdonald, 2018).

Functional groups present on CSBC and CCBC, before and after carbofuran and 2,4-D adsorption were determined by FTIR (model Nicolet 1100) using pellet method. For this, small quantity of biochar was crushed and mixed homogenously in 1:20 ratio with potassium bromide (KBr) using pestle-mortar. The mixture was pressed into pellets in a steel dye set by a hydraulic press. FTIR spectra of biochar samples were recorded from 500-4000 cm^{-1} in transmittance mode.

2.5.9 pHzpc

Point of zero charge (pHzpc) refers to the pH at which surface charge over the adsorbent becomes zero. It helps in determination of the charge present over adsorbent in a solution at particular pH (Singh et al., 2016). At pH = pHzpc, the charge of the positively charged functional groups on the sorbent surface are equal to that of the negatively charged functional groups. Information about pHpzc also helps in understanding the behavior of biochar in solution based on its functional group's ionization and their interaction with adsorbate at particular pH. When pH > pHzpc, adsorbent surface is negatively charged and binds with positively charged chemical species whereas at pH < pHpzc, sorbent surface positively charged and could interact with negative species (Fiol and Villaescusa, 2009).

pHzpc for CSBC and CCBC was determined through pH drift method using 0.01N NaCl solution. For this, definite weight of biochars (0.25g) were added to 50 ml of 0.01N NaCl solution at different pHs (2-10) in separate plastic beakers (pHs were adjusted using 0.01N HCl solution and 0.01N NaOH). These biochar suspensions were thoroughly agitated for 24 hours in a water bath shaker. Afterwards the initial and final pH were measured using pH meter measured using pH meter and graph between initial pH and ΔpH (pH$_{initial}$ - pH$_{final}$) plotted for pHzpc determination.

2.6. Carbofuran and 2,4-D analysis in water UV-Visiblespectrophotometer

Analysis of carbofuran and 2,4-D in water is done by UV-Visible spectrophotometer. It is device for qualitative and quantitative analysis of various inorganic and organic compound based on absorption of light in ultraviolet and visible range (210-900 nm) of electromagnetic spectrum (Mohammed, 2018). It measures the intensity of the absorbed light as a wavelength's function. UV-Visible spectrophotometer follows Beer-Lambert' law which relates the attenuation of light to the compound's properties (Hardesty and Attili, 2010). According to Beer-Lambert's law light absorbance shows direct proportionality to the concentration with plot between absorbance and concentration being straight line (Swinehart, 1962). Thus, Beer-Lambert's law quantifies the adsorption of light according to Equation 2.4.

$$A = \varepsilon Cl \tag{2.4}$$

Where, A is the absorbance (no unit as $A = \log_{10} P_0/P$), ε is the molar absorbance (L mol^{-1} cm^{-1}), C is the concentration of solution (mol l^{-1}) through which light is passing and l is the path length (cm) of light (width of cuvette).

Working of UV-visible spectrophotometer is based on 5 major components i.e. source of light, sample holder, monochromator, detector, and the interpreter (Figure 2.7). Deuterium arc (190-330 nm) and a tungsten filament lamp (330–800 nm) are used to generate a light beam in given spectral range. Monochromators are used for definite optical path with least possible optical aberrations. Nowadays, grating monochromators are also used in reflection mode to separate the spectral lines of interest from others. Sample holder consist of the compartments where cuvettes containing the reference and sample solution are kept i.e. reference and sample cell, respectively. Detector enables the conversion of light into proportional electrical signal for spectrophotometric response.

Phototubes, photomultiplier tubes, diode ray detector and charged coupled devices are some of the detectors used these days. Finally the interpreter converts these electrical signal into respective concentrations using standard equations of graph plotted between specific concentration and absorbance.
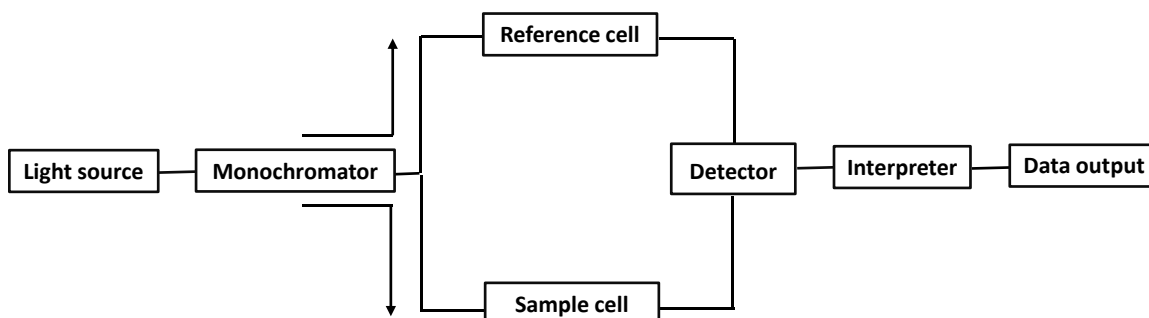
Figure 2.7. Schematic diagram of UV-visible spectrophotometer (modified from Gong et al., 2009)

UV-visible spectrophotometer from Perkin Elmer (model Lambda 35) was used for carbofuran and 2,4-D assessment in water.

2.6.1. Maximum absorbance (λmax)

Absorption maxima represents the most absorbed wavelength of scanned spectrum which is represented by peak in intensity. It is was determined by scanning the sample solutions of carbofuran and 2,4-D across UV region (320-190 nm) of electromagnetic spectrum. To check any possible fluctuation in adsorption maxima, the scanning was done at various pHs i.e. 2-10 and concentrations (1-110 ppm). Adsorption maxima obtained for carbofuran and 2,4-D is determined to be 275 and 284 nm, respectively. Absorption maxima near to these value were used by different research groups for carbofuran and 2,4-D analysis. (Vithanage et al., 2015; Mandal et al., 2017)

2.6.2 Calibration curve

Once the absorption maxima was obtained the standardized calibration curve was plotted with absorbance against specified concentration to quantify the concentration of carbofuran and 2,4-D in water samples.

2.7. Sorption experiments

In the sorption experiment, biochars i.e. CSBC and CCBC were agitated with separate solutions of pesticides i.e. carbofuran and 2,4-D to ensure proper contact between adsorbent and adsorbate. These experiment were performed batch wise at different

solution pHs, dosages of biochars, adsorbate concentration and temperature. Concentration of carbofuran and 2,4-D before and after adsorption were determined using double beam UV-visible spectrophotometer. Percentage carbofuran and 2, 4-D removal and adsorption capacities of biochars, q_e (mg/g) were calculated by Equation 2.5 and 2.6, respectively.

$$\text{Percent removal} = \frac{(C_o\text{-}C_e)}{C_o} \times 100 \qquad (2.5)$$

$$\text{Adsorption capacity, } q_e = \frac{(C_o\text{-}C_e)}{W} \times V \qquad (2.6)$$

Where, C_o and C_e are pesticides concentration at initial & equilibrium stage, respectively. V is the pesticide solution's volume, while, W represents the biochar's weight taken for the adsorption purpose.

2.7.1 Effect of initial pH

The effect of solution pH on the adsorption of pesticides by biochar was performed from pH 2-10. During this experiment 0.25g of CSBC and CCBC was used to remediate fixed pesticide concentration of 10ppm. The desired solutions for this experiment were achieved using 0.1M NaOH and 0.1M HCl for alkaline and acidic pHs, respectively. Study of pH versus adsorption efficiency or adsorption capacity enables the pH optimization for further studies

2.7.2 Sorption kinetic experiments

Kinetics deals with the adsorbent-adsorbate interaction at varied system condition as the function of time. It tell about the two important aspect of adsorption i.e. mechanism of adsorption and potential rate controlling step which may be either mass transfer or some chemical reaction process (Nethaji et al., 2013). Kinetic experiments were carried out to understand the effect of biochar doses and initial pesticide concentration on adsorption process.

2.7.2.1. Effect of adsorbent dose

After the pH optimization through pH studies, all experiments onwards were carried out at this optimized pH. For studying the effect of adsorbent dose, different doses of the biochars were mixed with 50 mL of the working solution at 25 °C. pH and

initial carbofuran concentration used for assessing dose kinetics of adsorption process were kept at 6 and 10 mg/L, respectively. Different doses of CSBC i.e. 2.5, 5.0 and 6.0 g/L, and CCBC i.e. 4.0, 6.0 and 8.0 g/L were used for dose kinetics studies for carbofuran removal. For studying the kinetics of aqueous 2,4-D remediation CSBC and CCBC dosages taken were 2.5, 5.0 and 7.0 g/L; and 3.0, 5.0 and 7.0 g/L, respectively. The residual pesticide concentration at different time intervals was determined for each of the adsorbent dose. This study provides the optimum dose of the biochars required for carbofuran removal at the given pH.

2.7.2.2. Effect of adsorbate concentration

The effect of initial pesticide concentrations were determined by varying the adsorbate concentration. For this, a fixed quantity of biochar (optimized through dose kinetic study) was mixed to 50 ml of pesticides solutions with 5, 10 and 20 mg/L concentrations.

2.7.2.3 Kinetic models for adsorption

(a) Pseudo-first order model

The pseudo-first order equation given by Lagergen (Lagergren, 1898).

$$\ln \frac{q_e - q_t}{q_e} = -k_1 t$$

$$q_t = q_e\left(1 - e^{-k_1 t}\right) \tag{2.7}$$

Where, k_1 (min^{-1}) is the first order adsorption rate constant, q_e and q_t are the adsorbed amounts of adsorbate, at equilibrium and at time "t" respectively.

(b) Pseudo-second order model

The pseudo-second order equation shows that the adsorbate's amount on adsorbent's surface and the adsorbate's amount that is adsorbed at equilibrium influences the sorption kinetics (Ho et al., 1999). The rate of the reaction is directly proportional to the active sites number on the surface of adsorbent. The pseudo-second order equation can be written as

$$\frac{t}{q_t} = \frac{1}{k_2 q_e^2} + \frac{t}{q_e} \tag{2.8}$$

$$\text{Initial adsorption rate} = k_2 q_e^2 \text{ (mg g}^{-1}\text{ min}^{-1})$$

Where, k_2 is rate constant of pseudo second order adsorption (g mg^{-1} min^{-1}). k_2 and q_e values were determined from the plots at different adsorbent doses and pesticides concentrations.

2.7.3 Sorption isotherm studies

Sorption isotherm studies involve equilibrium experiments done at constant temperature. The motive of these studies is to understand the transfer of adsorbate material to adsorbent from solution phase in equilibrium state at particular temperature (Gholizadeh et al., 2013).

2.7.3.1. Sorption isotherm models

Sorption isotherm model represents the curve which describes the movement of adsorbate from solution phase to adsorbent at equilibrium, at constant temperature and pH. It is expressed in the terms of amount adsorbed on the adsorbent and residual concentration of adsorbate in the solution (Foo and Hameed, 2010). The parameters obtained from these isotherm models are helpful in designing and set-up of fixed bed reactors.

(a) Freundlich

This model is non-ideal, reversible and not restricted to formation of monolayer. Instead it assumes the adsorption process to be multilayer with non-uniform distribution of adsorption heat and affinities over heterogeneous surface. Here, adsorption at sites with greater binding energy takes place first, followed by adsorption at binding sites whose binding energy decreases exponentially as the adsorption process proceeds. The non-linear form of Freundlich adsorption model (Freundlich, 1907) is given in Equation 2.9.

$$q_e = K_F C_e^{\frac{1}{n}} \tag{2.9}$$

Where, q_e is adsorbate's amount adsorbed per unit biochar's weight (mg/g), C_e is equilibrium adsorbate concentration (mg/L), K_F is the constant which indicates biochar's relative adsorption capacity (mg/g) and $1/n$ is another constant which represents adsorption intensity.

(b) Langmuir

Langmuir isotherm model is a verifiable model which assumes the adsorption process to be monolayer where a single adsorbate molecule binds with one of the localized sites which are identical and equivalent with no lateral interaction and steric hindrance between them. This model denotes occurrence of homogenous adsorption where each adsorbed molecule has equal enthalpy and sorption adsorption energy. Here the adsorption sites are also supposed to bear equal affinity for adsorbate molecules with no movement of adsorbate on the surface of adsorbent. The non-linear form of Langmuir adsorption model (Langmuir, 1918) is provided in Equation 2.10.

$$q_e = \frac{Q_a b C_e}{1 + b C_e} \tag{2.10}$$

Where, qe is the adsorbent's amount adsorbed per unit biochar's weight (mg/g), C_e is equilibrium adsorbate concentration in mg/L, Q_a is monolayer capacity of adsorption (mg/g) and b is constant related to net enthalpy.

(c) Temkin

Tempkin adsorption isotherm model takes adsorbent-adsorbate interactions in account, exclusively. It assumes that the heat of adsorption of molecules which is function of temperature reduces linearly other than logarithmically as the surface coverage increases. Also, it is characterize by uniform distribution of binding energy up to a limited value of maximum binding energy. However, these assumptions have limitations at upper and lower extremes of concentration. The non-linear form of this model (Tempkin and Pyzhev, 1940) and is mentioned in Equation 2.11.

$$q_e = \frac{RT}{b_T} \ln a_T C_e \tag{2.11}$$

Where, q_e is amount of solute adsorbed per unit weight of adsorbent (mg/g). a_{T_e} and b_{T_e} are the Temkin constants related to heat of sorption with unit being l/g and J/mol, respectively (Inam et al., 2017). C_e is the equilibrium concentration in solution in mg/L. R is universal gas constant and T is absolute temperature

(d) Sips

It is a combined form of Freundlich and Langmuir isotherm. It is derived for heterogeneous adsorption system and has higher concentration related limitation

associated with Freundlich isotherm. So, at lower concentration this empirical model becomes Freundlich isotherm while it becomes it predicts occurrence of monolayer adsorption following assumptions of Langmuir isotherm at higher concentration. This model as other models are affected by pH, concentration and temperature. Non-linear form of Sips model (Sips, 1948) is given in Equation 2.12.

$$q_e = \frac{K_{LF} C_e^{n_{LF}}}{1 + (a_{LF} C_e)^{n_{LF}}} \qquad (2.12)$$

Where, q_e is the adsorbate's amount of adsorbed per unit biochar weight (mg/g), Ce is equilibrium concentration (mg/L); K_{LF}, a_{LF} and n_{LF} are the Sips constants.

(e) Redlich-Peterson

It is a hybrid isotherm comprising of both Langmuir and Freundlich models. It is versatile as it can be applied to both heterogeneous as well as homogenous system over a wide range of concentration. This model has linear dependence on concentration in the numerator and exponential function in the denominator to represent adsorption equilibrium. This model approaches Freundlich isotherm at higher concentration where β tends to zero while it is in agreement with Langmuir model ta lower concentration with β value nearing 1. Non-linear form of this isotherm model (Redlich and Peterson, 1959) is given in Equation 2.13.

$$q_e = \frac{K_{RP} C_e}{1 + \alpha_{RP} C_e^{\beta_{RP}}} \qquad (2.13)$$

Where, q_e is the adsorbate's amount adsorbed per unit biochar weight (mg/g), Ce is equilibrium concentration (mg/L); K_{RP}, α_{RP} and β_{RP} are the Redlich-Peterson constants. Value of exponent, β, ranges from 0 to 1.

(f) Toth

It is empirical equation which enhances fitting of experimental data to Langmuir isotherm model. It is useful in describing heterogeneous adsorption systems, and is applicable at extremes of both, high and low concentrations. Non-linear form of Toth isotherm model (Toth, 2000) is given in Equation 2.14

$$q_e = \frac{K_T C_e}{\left(1 + B_T C_e^{\beta_T}\right)^{\frac{1}{\beta}} T} \qquad (2.14)$$

Where, q_e is the adsorption capacity of adsorbent per unit (mg/g), and Ce is the adsorbate concentration at equilibrium (mg/L). K_T, B_T and β_T are Toth constants

(g) Koble-Corrigan

It is an empirical three parameters model which incorporates both the Langmuir and Freundlich isotherm models for representing equilibrium adsorption data (Koble and Corrigan, 1952). Non-linear form of this isotherm is represented in Equation 2.15.

$$q_e = \frac{AC_e^{\eta_{KC}}}{1+bC_e\eta^{KC}} \tag{2.15}$$

Where, q_e is the adsorbate's amount adsorbed per unit biochar weight (mg/g), C_e is equilibrium concentration (mg/L); A, b and η^{KC} are the Koble-Corrigan constants. This isotherm model behaves as Freundlich isotherm model when the value of $C_e \lll 1$. Also, at $C_e \ggg 1$, the amount of adsorbate per unit weight of adsorbent at equilibrium is represented by A/b.

(h) Radhke-Prausnitz

This model fits well to the sorption experiment data of a large concentration range. Non-linear representation of this model (Radke and Prausnitz, 1972) is given in Equation 2.16.

$$q_e = \frac{abC_e^{\beta}}{a+bC_e^{\beta-1}} \tag{2.16}$$

Where, q_e is the adsorbate's amount adsorbed per unit biochar weight (mg/g), C_e is equilibrium concentration (mg/L); a, b and β are the Radke and Prausnitz constants. At lower adsorbate concentration, Radke-Prausnitz isotherm model behaves as linear isotherm i.e. Henry's Model while at higher adsorbate concentration it behaves as Freundlich isotherm. Similarly, Radke-Prausnitz model behaves as Langmuir isotherm model with parameter value i.e. $\beta=1$.

2.7.4. Adsorption Thermodynamics

Thermodynamic constants such as $\Delta G°$, $\Delta H°$, and $\Delta S°$ were calculated to understand the energy dynamics involved with the adsorption process at different temperature using Equation (2.17, 2.18 and 2.19), respectively (Sharma et al., 2017)

$$\Delta G° = -RT\ln b \tag{2.17}$$

$$\Delta H^\circ = R \left(\frac{T_1 T_2}{T_1 - T_2} \right) \ln \frac{b_1}{b_2} \qquad (2.18)$$

$$\Delta S^\circ = \frac{\Delta H^\circ - \Delta G^\circ}{T} \qquad (2.19)$$

Where R is universal gas constant (8.314 J/mol K), and T is the absolute temperature (K), ΔG° is Gibbs free energy change, ΔH° is standard enthalpy change and ΔS° is standard entropy change.

CHAPTER 3

CHARACTERIZATION OF CSBC AND CCBC

3.1 Proximate analysis

The major outcomes of the elemental analyses of corn stover biochar (CSBC) and corn cob biochar (CCBC) includes their carbon content of 82.12 and 78.37% which is well above the mark specified for typical class I biochar who are supposed to have carbon content greater than 60% (IBI, 2014). A remarkably higher carbon content can be attributed to the high pyrolysis temperature at which most of the volatile matter escapes leaving behind the carbon component. Proximate analyses and ultimate analyses with major elemental components and their ratios for CSBC and CCBC are mentioned in Table 3.1. Molar H/C ratio are used for evaluating aromaticity i.e. decrease in molar H/C signifies increase in aromaticity (Mayakaduwa et al., 2016b). Molar H/C ratio for CSBC and CCBC is 0.15 and 0.20, respectively which mean later has lesser condensed aromatic structure than former. Nonetheless, molar H/C ratios of both the biochars being less than 0.3 suggests that they have abundance of highly condensed aromatic ring arrangement (Mayakaduwa et al., 2016b). Also, smaller H/C ratio of CSBC than CCBC suggests higher degree of carbonization for former than the later (Vithanage et al., 2015). The other elemental ratio i.e. molar O/C which is measure of polarity of biochar is reported to be 0.081 and 0.158 for CSBC and CCBC, respectively. It suggests that the CCBC is more hydrophilic than the CSBC (Vithanage et al., 2015). Ash content of CSBC and CCBC are found to be 6.39 and 2.72%, respectively.

3.2 Ultimate analysis

Percent composition of elements present in CSBC and CCBC are given in Table 3.2. SiO_2 was found more in CSBC than CCBC i.e. 20.67 and 9.77%, respectively. Other element oxide in noticeable amount was phosphate in CSBC which was 1.02%. Other elemental oxides i.e. Al_2O_3, CaO, Cr_2O_3, CuO, Fe_2O_3, K_2O, M_gO, MnO, Na_2O, NiO, ZnO and P_2O_3 contributed less than 1% to total elemental composition of CSBC and CCBC.

3.3 pHzpc

pHzpc was determined on the basis of deviation in final pH from initial pH. Plots between initial pH and change in pH (ΔpH) for CSBC and CCCBC are given in Figure 3.1 (a) and (b), respectively. The pH value at which ΔpH= 0 was taken as pHzpc. It was found to be 7.9 and 7.75 for CSBC and CCBC, respectively.

3.4 Surface area and micropore properties

BET Surface area of the CSBC and CCBC were found to be 204.9 and 222.9 m^2/g, respectively from their nitrogen adsorption-desorption plots [Figure 3.2 (a)-(b)]. Total micropore volume of 0.097 and 0.105 cubic cm^3/g were estimated for CSBC and CCBC respectively using Dubinin-Radushkevich (DR) equation. The average pore diameter was obtained from cumulative value of Barret-Joyner-Halenda (BJH) isotherm. Average pore diameter is found be 1.88 and 1.90 nm, respectively for CSBC and CCBC. According to IUPAC pore size classification, average pore diameter for micropores, mesopores and macropores is 0-2, 2-50 and more than 50 nm, respectively (Zdravkov et al., 2007). Both CSBC and CCBC can be classified as microporous material as average diameter of their pores is less than 2 nm. In general, the surface area of the biochars increase with increase in pyrolysis temperature above 500°C (Rodríguez-Vila et al., 2018). Similarly the pore size also decreases with increase in pyrolysis temperature (Tan et al., 2018). But at higher temperature beyond 750°C the sintering of pores may take place which decreases the overall surface area (Lehmann and Jospeh, 2015). As CSBC and CCBC are produced at 900°C they may not have surface area as high as expected due to sintering.

3.5 Scanning electron microscopy (SEM)

Surface morphology of the produced biochars were studied using SEM and SEM-EDX imaging techniques. SEM micrographs of CSBC and CCBC at various magnifications are given in Figure 3.5 (a) and 3.5 (b), respectively. CSBC and CCBC well display their high pyrolysis temperature induced surface morphologies in these micrographs. Both the biochars have shown possessing honeycomb like structures at high magnifications. These honeycomb structure are basically constituted by mesopores and micropores which are formed due to breakdown of lignin, cellulose and hemicellulose along with volatilization of some organic components. In the micrograph of higher magnifications distinguished availability and elaborate structural morphology of pores can be seen. Numerous pores of irregular shapes are present and which increases the surface area. Micropores present on surface of CSBC and CCBC are in agreement with results of pore size and pore volume assessment obtained from BET analysis. These

figures also meets the general assumption that biochar produced at high temperature generally have higher surface area and smaller pores.

However, exfoliation of the porous structure and possible ash deposition can also be observed in micrographs of CSBC and CCBC at higher magnifications. This may cause reduction in its total surface area. Furthermore, presence of magnesium, phosphorous and silica in relatively high amount can be ascertained from SEM-EDX image of CSBC [Figure 3.5(a)]. Presence of these elements in CSBC is in agreement with the results obtained from ICP-AES which is discussed earlier in this chapter. Similarly, SEM-EDX of CCBC also shows presence of silica which is confirmed by results obtained from ICP-AES [Figure 3.5(b)]. SEM-EDX mapping of CSBC and CCBC confirms carbon and nitrogen as major constituent elements of biochars which have been previously confirmed by CHNS analysis [Figure 3.6 (a-d) and 3.7(a-d)]. Limited oxygen content in both the biochars is ascertained by SEM-EDX and mapping. This observation can be attributed to the high pyrolysis temperature i.e. 900ºC for both the biochars at which most of their oxygen containing functional groups are lost. This results into abundance of carbon rich polyaromatic moiety in CSBC and CCBC (Keiluiweit et al., 2010)

Exfoliation, blocking of pores and presence of silica can be related to the high temperature pyrolysis. Metal oxides present in the feedstocks melt at this high temperature causing disorientation of the surface structures which decreases the surface area (Brown et al., 2012). All three of these meet our observations here and justify the moderate surface area of the CSBC and CCBC.

3.6 Transmission electron microscopy (TEM)

TEM is used to access the crystallinity and layering present in the biochars. TEM micrographs of CSBC and CCBC are given in Figure 3.8 (a-d) and 3.9 (a-d), respectively. Existence of multilayered structure in both the biochars is noticeable. However, these layered structures seem to be crumpled in some micrographs [Figure 3.8 (c) and 3.9 (d)]. This can be caused by condensation of biochar structure at high pyrolysis temperature. Thus, graphene sheet like layered structure of biochar is affected by high temperature induced condensation (Sahoo et al., 2018). No visible crystallinity whatsoever was

observed in TEM micrographs of either biochars. This confirms the highly amorphous nature of CSBC and CCBC.

3.7 Fourier transform infrared (FTIR) spectroscopy

FTIR spectra of the material bear peaks corresponding to different functional groups present in it. Sharpness of such peaks, in turn, corresponds to the quantitative value of functional groups. Combined graph of spectra from corn stover biochar before adsorption and after adsorption of carbofuran and 2, 4-D onto it is given in Figure 3.10. Here in this figure, we can see that most of the peaks are common in all the three FTIR spectra. Also, there is only minor shifts in intensity whatsoever after adsorption. Starting from the lower wavenumbers, the distinct peaks at 602 and 656 cm^{-1} are present in all the three spectra which are attributed to substituents of aromatic rings (Claoston et al., 2014). Similarly the sharp peak at 752 cm^{-1} corresponds to out of plane aromatic C-H vibration which may be due to dehydration and aromatization (Wu et al., 2012). In general the peaks between 1000-600 cm^{-1} are characteristic of aromatic C-H wagging vibrations (Tarazzi et al., 2016). Other sharp peak at 1400 cm^{-1} may be due to aromatic C$^{1/4}$ C stretching (Takaya et al., 2016). All these peaks suggest abundance of aromatic structures in corn stover biochar due to pyrolysis at high temperature. The peak lying between 1000-1200 cm^{-1} i.e. 1121 and 1192 cm^{-1} in all the spectra are attributed majorly to functional groups like C-O, P-O or O-Si-O (Wang et al., 2017). A broad peak at 3136 cm^{-1} is also present in all the three spectra and corresponds to O-H stretching (Zhu et al., 2015). Two distinct peak of relatively lower intensity are present in carbofuran loaded biochar at 1629 and 2268 cm^{-1}. These can be attributed to the N-H bend (Claoston et al., 2014) and C≡C or C≡N bonds (Zama et al., 2017), respectively. The former peak at 1629 cm^{-1} is also sometimes attributed to aromatic C-C and C-O bond (Wang et al., 2017). The appearance of peaks corresponding to N-H bond and aromatic C-C along with C-O suggests the adsorption of carbofuran onto the corn stover biochar. Two of the peaks unique to the 2,4-D loaded biochar i.e. 3745 and 3852 cm^{-1} are well beyond 3500 cm^{-1} and correspond to –Si-OH stretching (Aragao and Messaddeq, 2008).

FTIR spectra for CCBC was nearly flat and has lesser number of peaks (Figure 3.11). Two peaks were obtained at 1635 and 1578 cm^{-1} in CCBC. Peaks at 1632 cm^{-1} may be attributed to plane bending of N-H bond in amide group (Çagler et al., 2018)

while peak at 1578 cm^{-1} can be due to aromatic C=C stretching vibrations (Herath et al., 2016), respectively. No new peaks were observed in the FTIR spectra of carbofuran and 2,4-D loaded CCBC.

3.8 X-Ray Diffraction (XRD) spectroscopy

XRD was carried out to understand the mineral composition and crystallinity of the biochars. Diffractograms for CSBC and CCBC (before and after adsorption) obtained through plotting 2Ө against intensity are given in Figure 3.12 and 3.13, respectively. Diffractograms of CSBC and CCBC were very similar to each other and very little change was observed in them even after pesticide absorption. This similarity may be due to their common plant biomass origin. Little change in diffractogram after adsorption may have been obtained due to lesser loading of pesticides. Not many sharp peaks were obtained in diffractogram of either biochars except at 72.54° which may be attributed to silicate (SiO_2) (Mohan et al., 2014). Absence of many sharp peaks corresponds to amorphous nature of both the biochars. Amorphous nature of CSBC and CCBC can be further confirmed by broad peaks at 23.77° and 43.96°corresponding to diffused graphite bands obtained from higher degree of carbonization (Odette and Yin-Ping, 2014) and calcite ($CaCO_3$) (Mohan et al., 2018), respectively. Presence of silica and calcium mineral peaks were in accordance with results earlier through ICP-AES analysis.

Table 3.1. Physico-chemical characteristics of the CSBC and CCBC.

Biochar→ Particulars↓	CSBC	CCBC
pH	8.03	8.09
Conductivity (μ S/cm)	34.60	29.33
Ash content (%)	6.39	2.72
Percentage yield (%)	15	18
Moisture content (%)	8.55	9.69
Carbon (%)	82.12	78.37
Hydrogen (%)	1.046	1.362
Nitrogen (%)	1.42	0.94
Sulpher (%)	0.035	0.017
Oxygen (%)	8.989	16.591
Molar H/C	0.15	0.20
Molar O/C	0.081	0.158

Table 3.2. Elemental composition (as % oxides) of the CSBC and CCBC.

Elements (as oxides)	Elemental composition (%)	
	CSBC	CCBC
Al_2O_3	0.23771	0.2549
CaO	0.44169	0.1964
Cr_2O_3	0.00077	0.0008
CuO	0.00356	0.0030
Fe_2O_3	0.00919	0.0092
K_2O_3	0.34497	0.4148
MgO	0.04967	0.0637
MnO	0.01485	0.0033
Na_2O	0.58680	0.5297
NiO	0.00028	0.0002
ZnO	0.00614	0.0067
P_2O_3	1.02713	0.4688
SiO_2	20.67395	9.7767
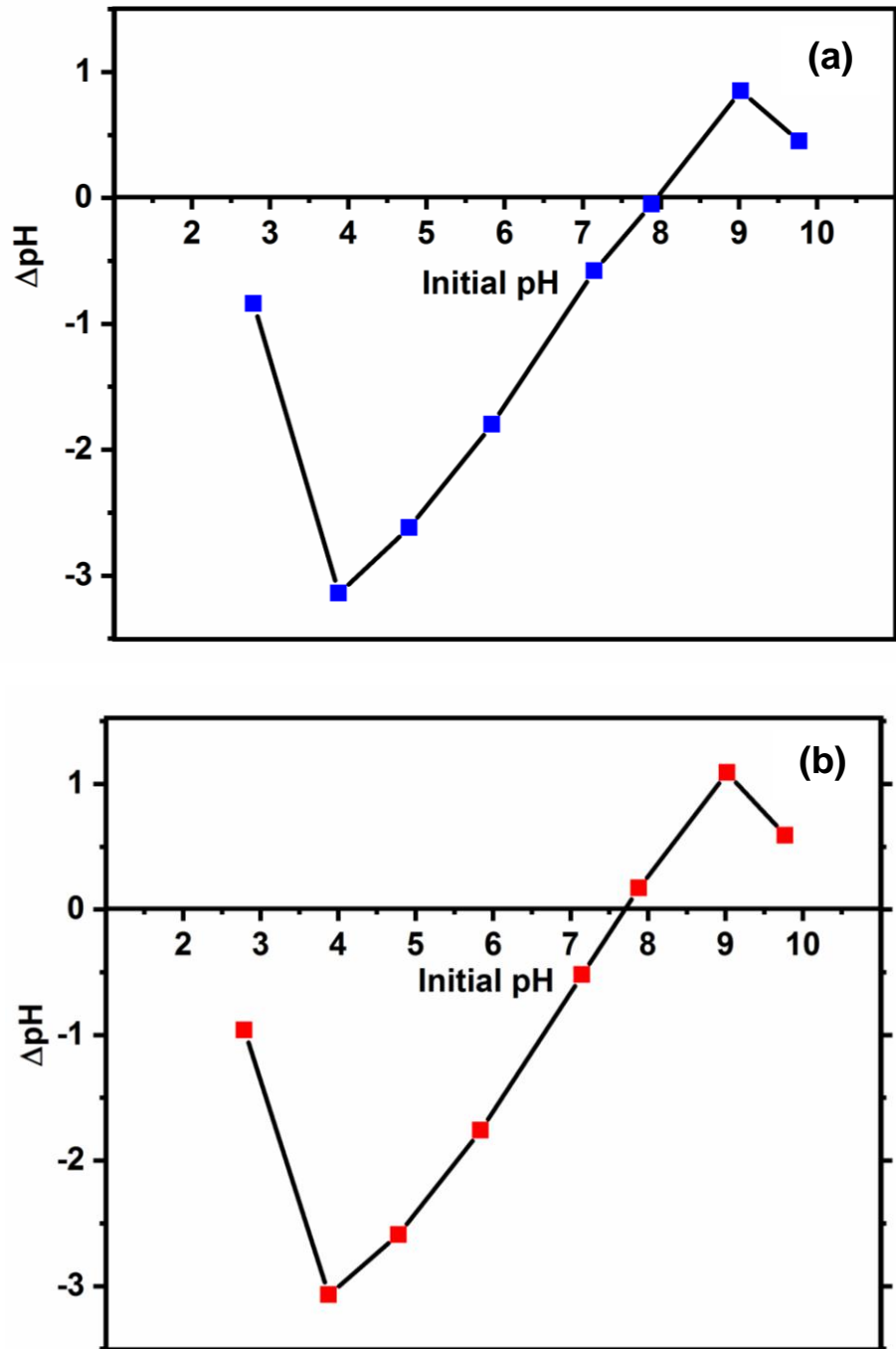
Figure 3.1 pHzpc determination of (a) CSBC and (b) CCBC.
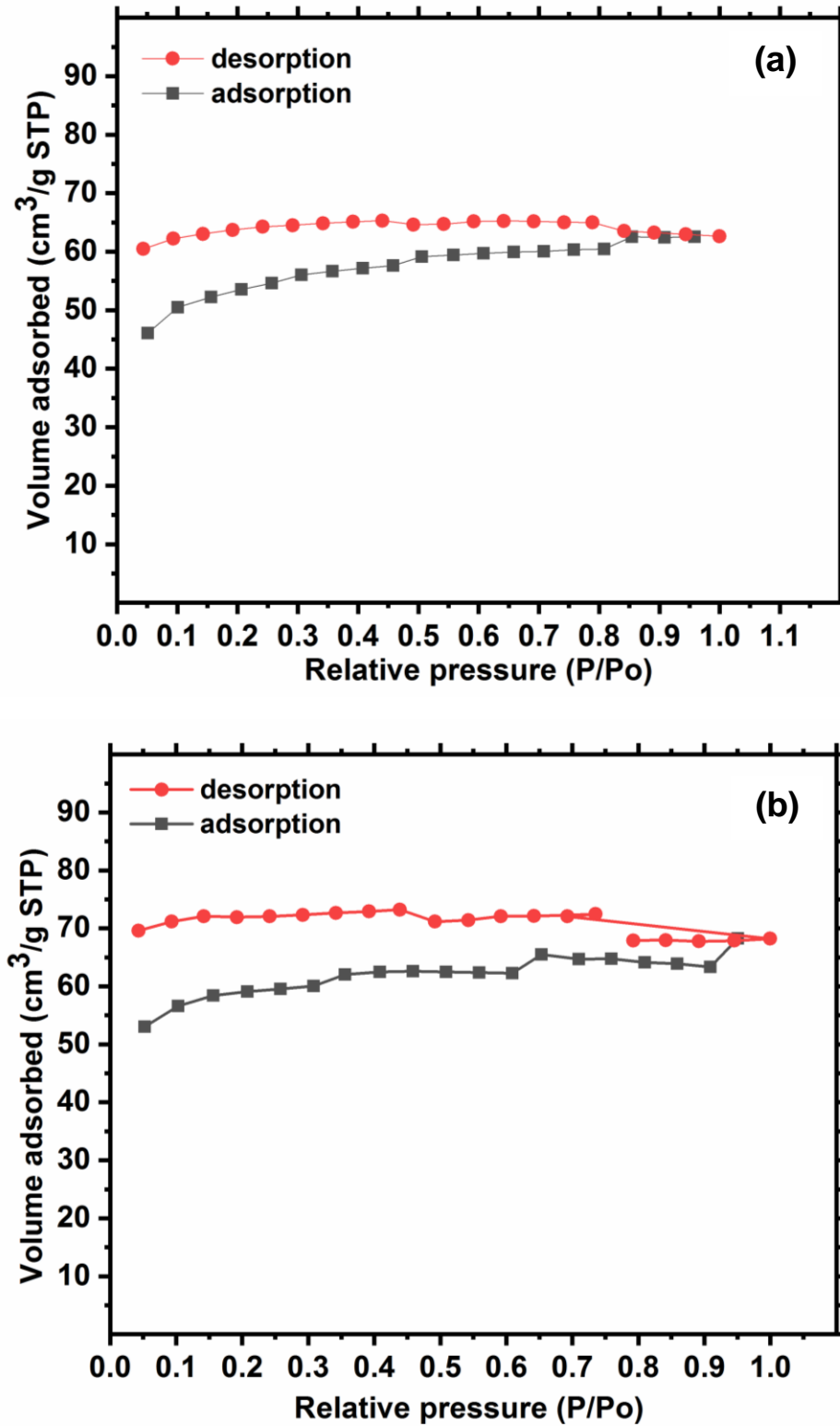
Figure 3.2 Nitrogen adsorption-desorption plots of (a) CSBC and (b) CCBC.
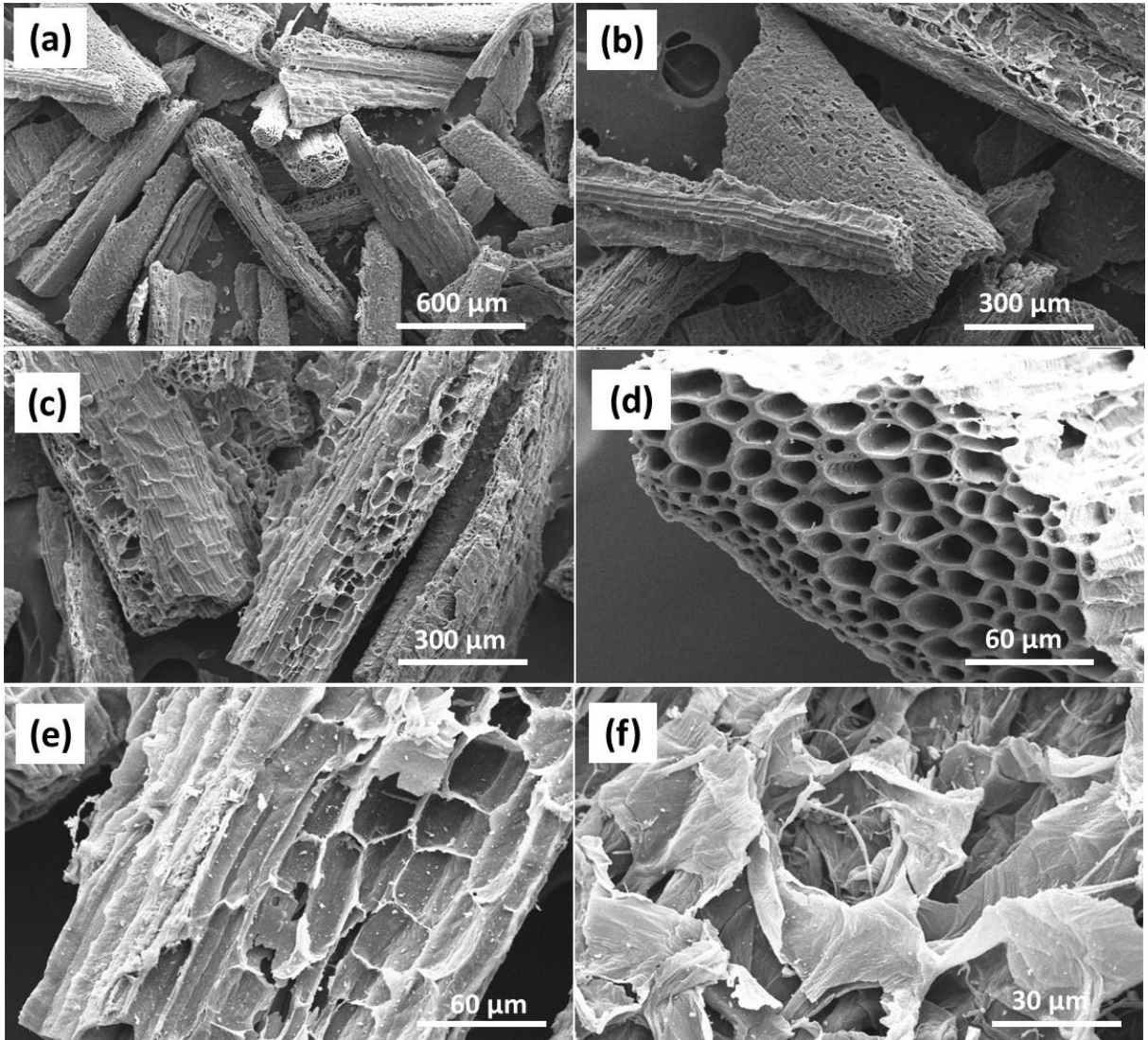
Figure 3.3 SEM micrographs of CSBC at magnifications at (a) 100X, (b) 200X, (c) 250X, (d) 1KX, (e) 1KX and (f) 2 KX magnifications
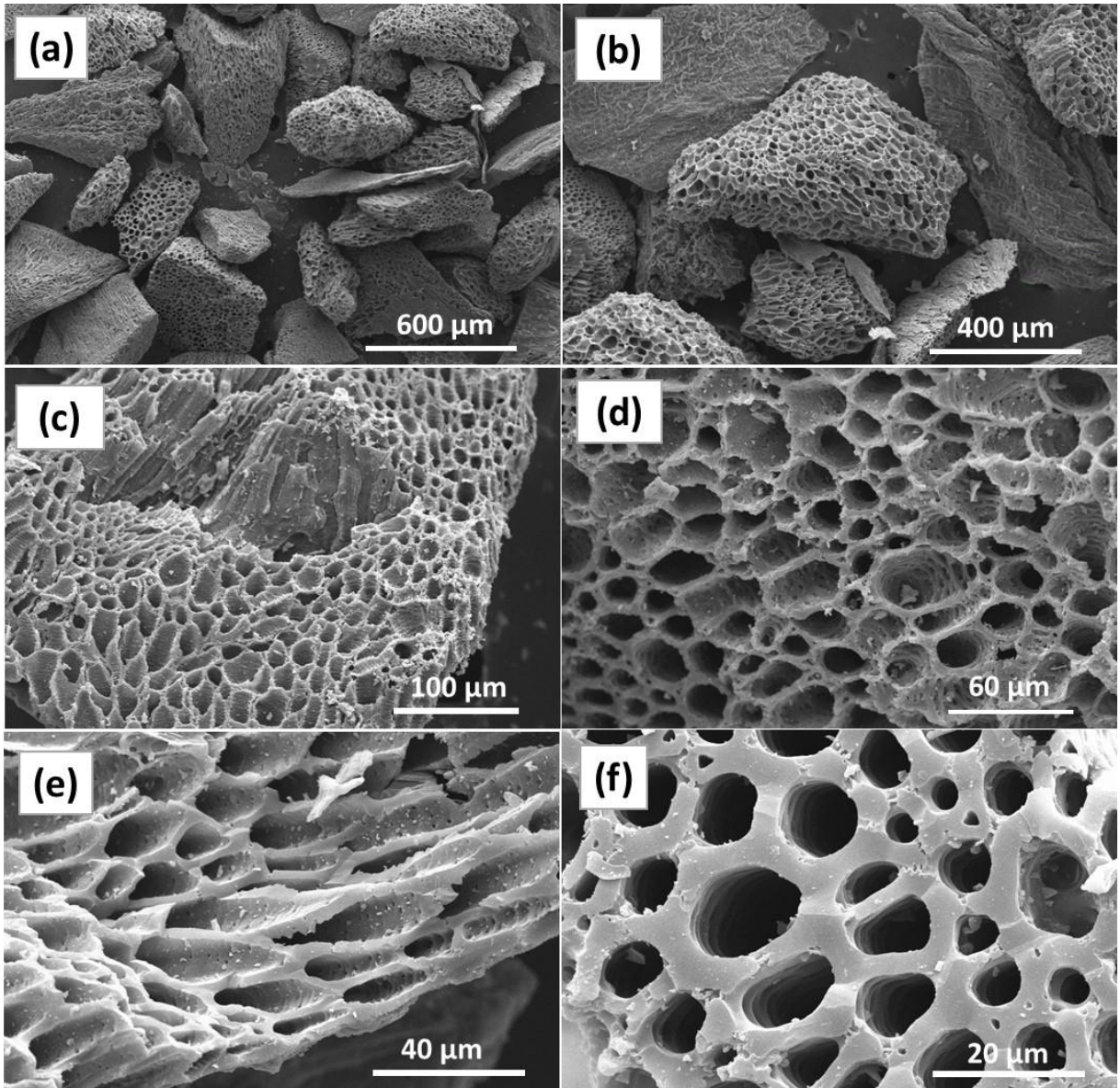
Figure 3.4 SEM micrographs of CCBC at magnifications at (a) 100X, (b) 200X, (c) 500X, (d) 1KX, (e) 2KX and (f) 4 KX magnifications
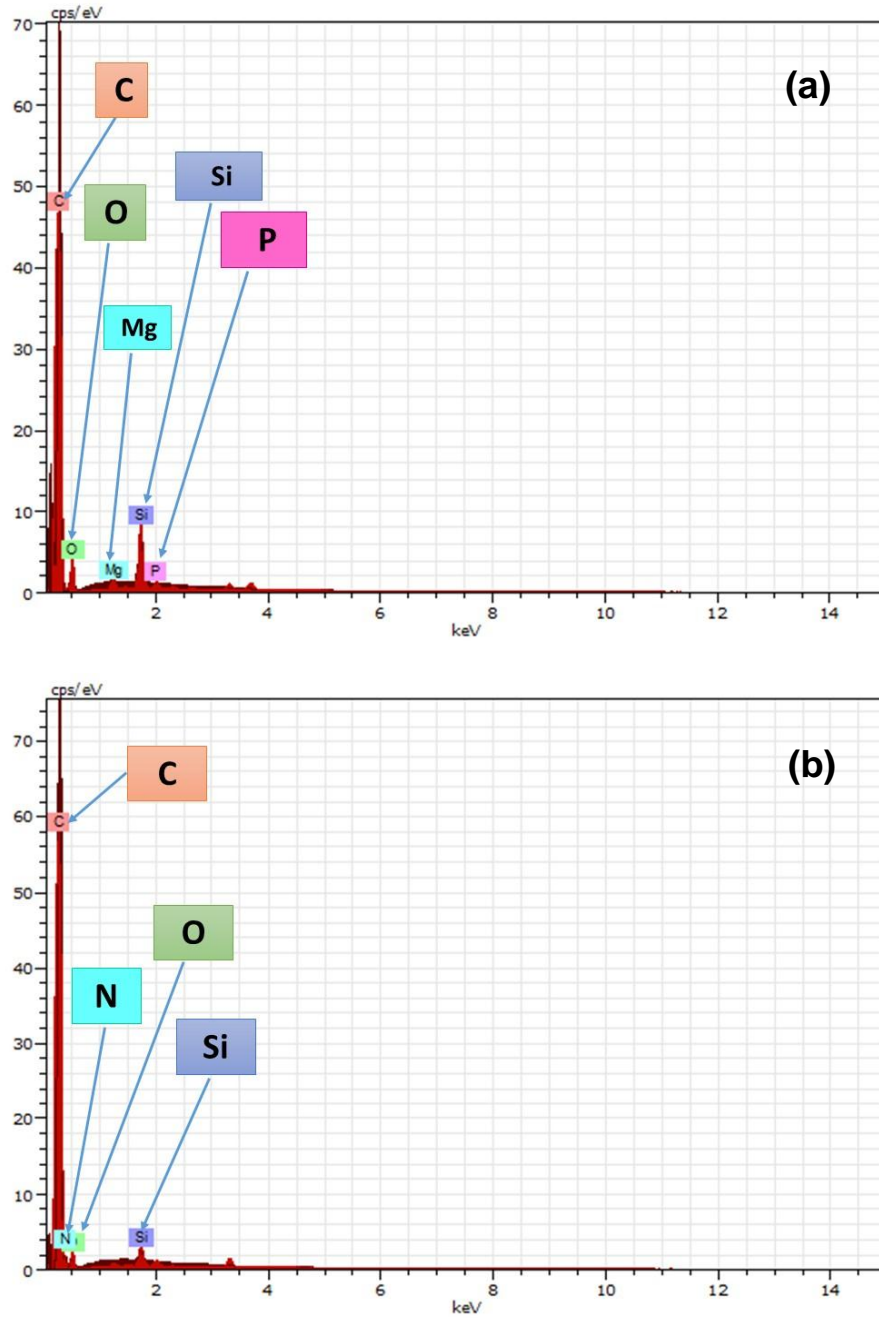
Figure 3.5 SEM-EDX graphs of (a) CSBC and (b) CCBC.
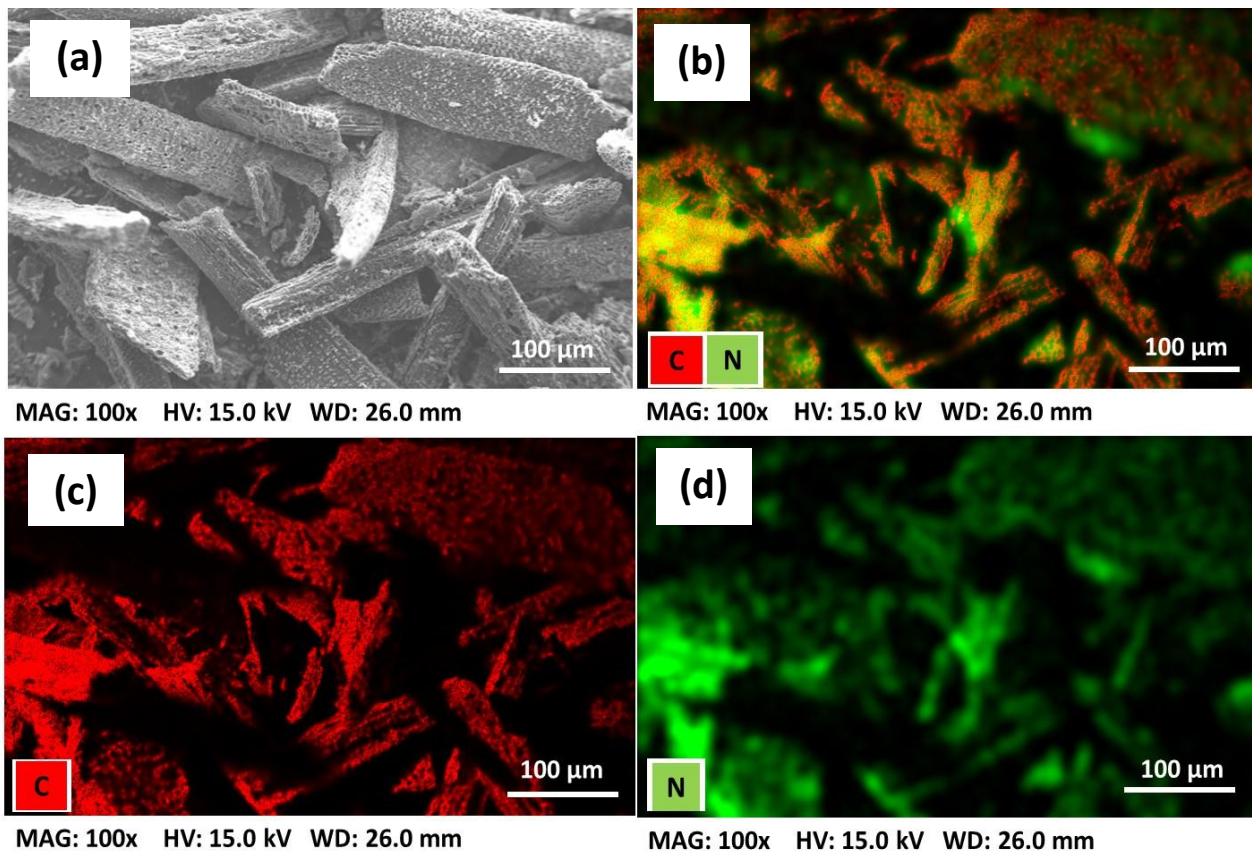
Figure 3.6 SEM mapping images (a) at 100X, (b) carbon and nitrogen, (c) carbon and (d) nitrogen of CSBC.
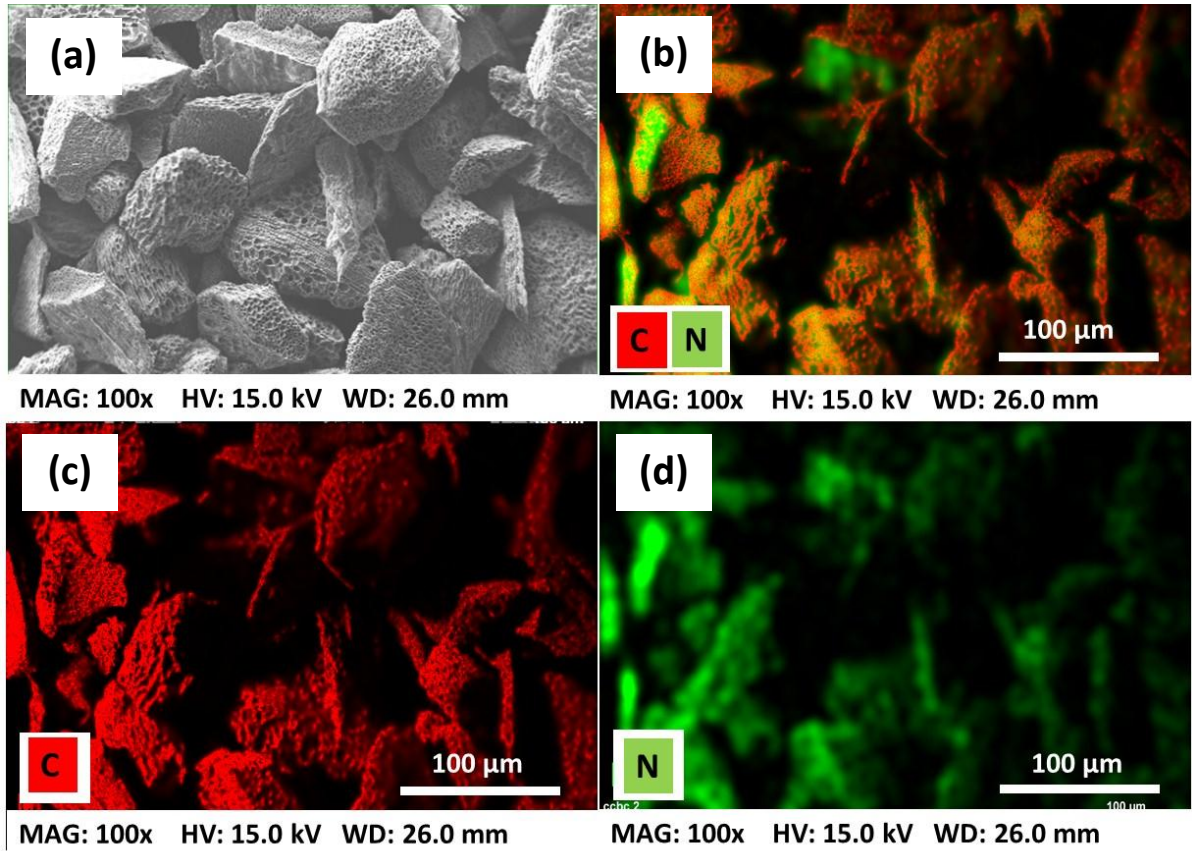
Figure 3.7 SEM-EDX mapping image (a) at 100X, (b) carbon and nitrogen, (c) carbon and (d) nitrogen of CCBC.
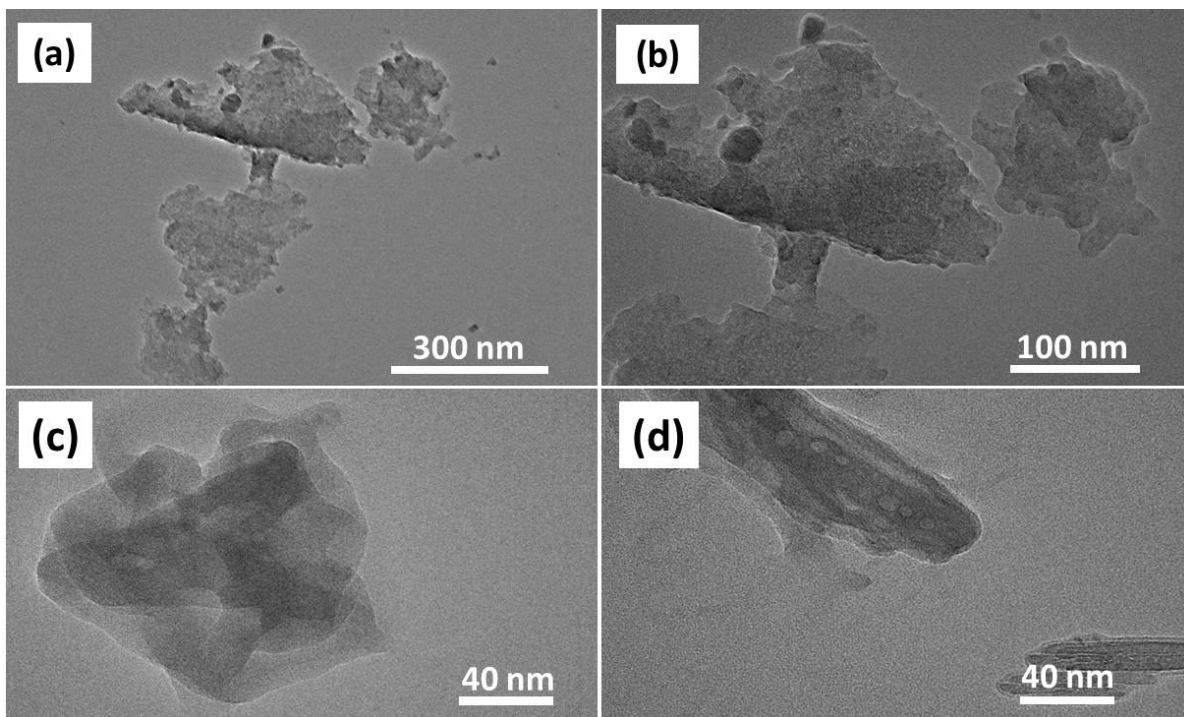
Fig 3.8. TEM micrographs of CSBC at (a) 25000X, (b) 50000X, (c) 100000X and (d) 100000X magnifications.
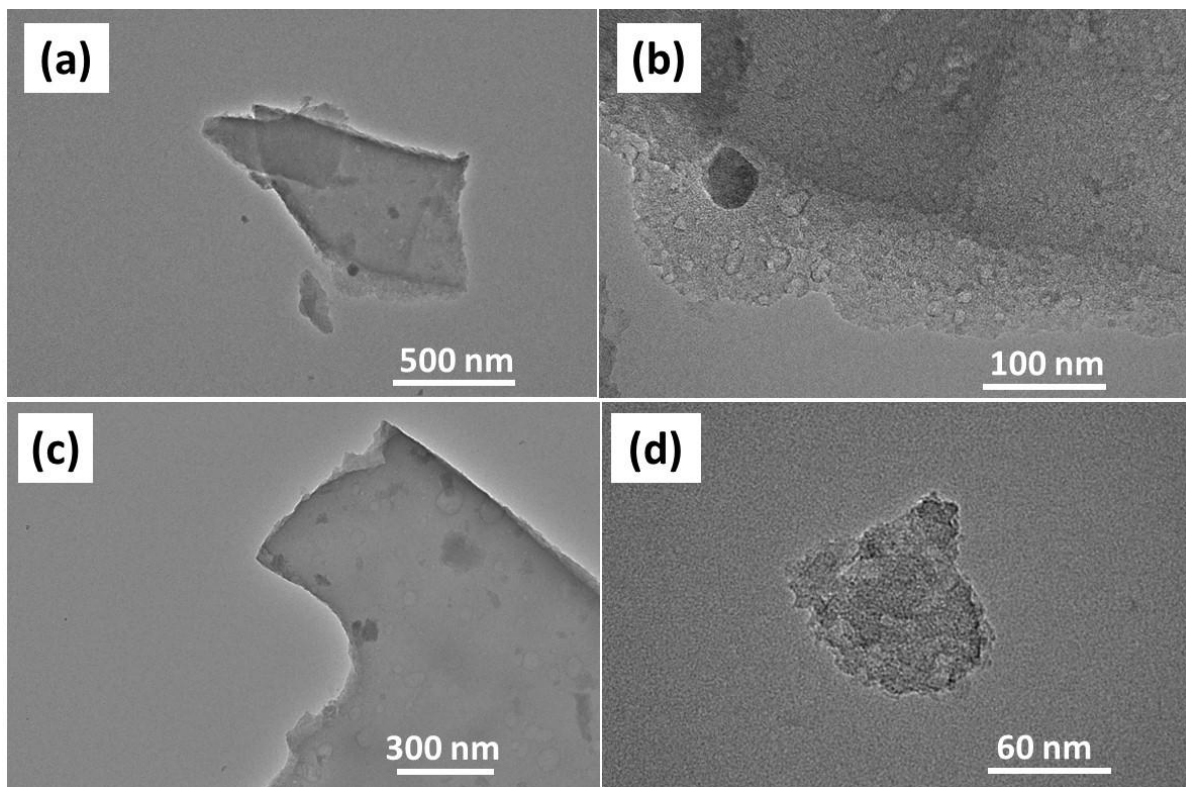
Fig 3.9. TEM micrographs of CCBC at (a) 10000X, (b) 50000X, (c) 100000X and (d) 100000X magnifications.
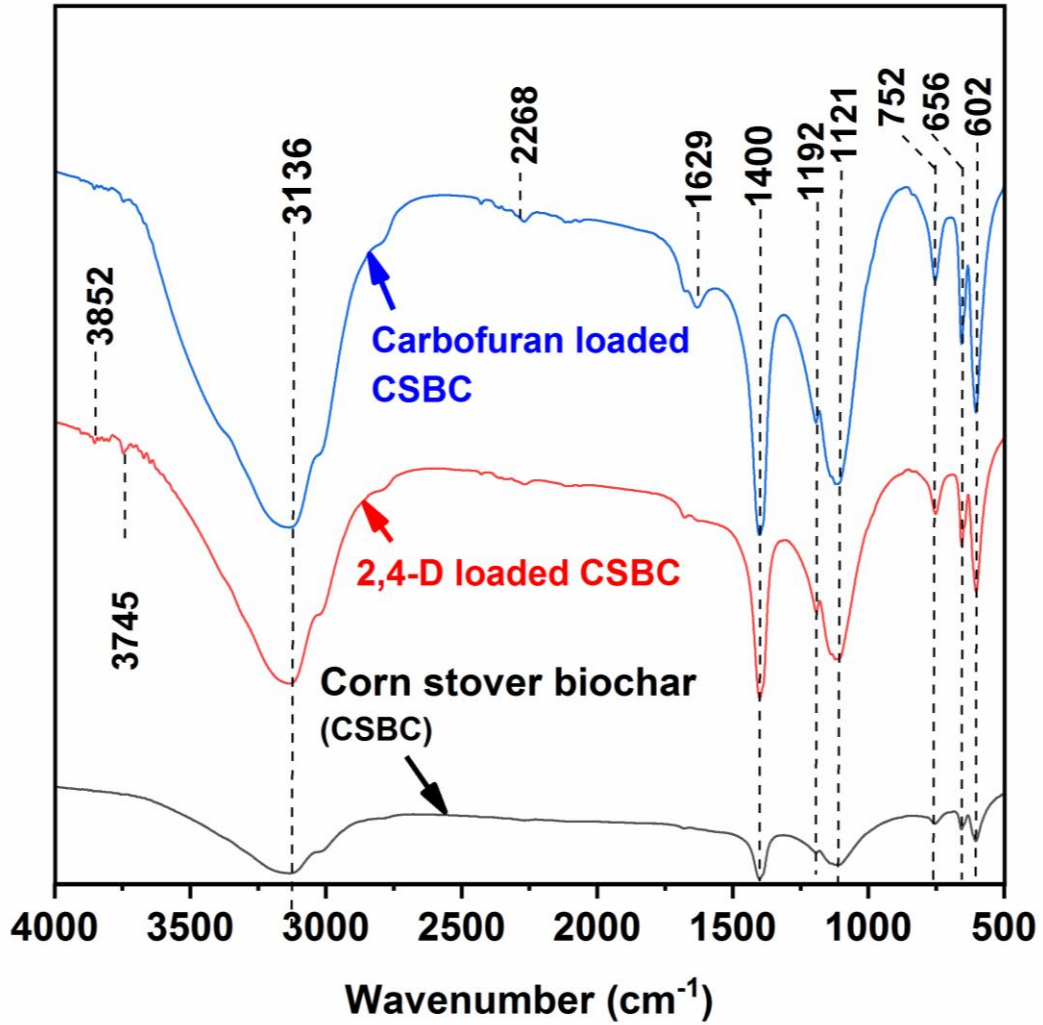
Fig 3.10. FTIR spectra of CSBC, carbofuran loaded CSBC and 2,4-D loaded CSBC.
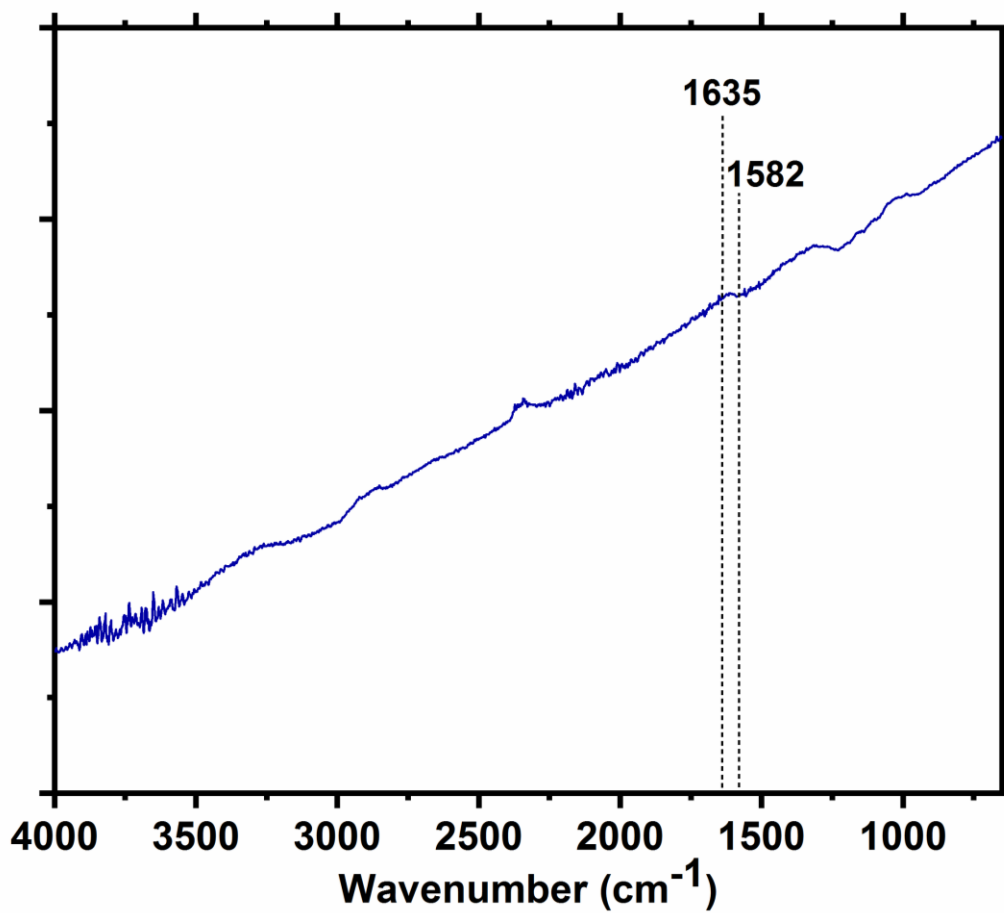
Fig 3.11 FTIR spectra of CCBC
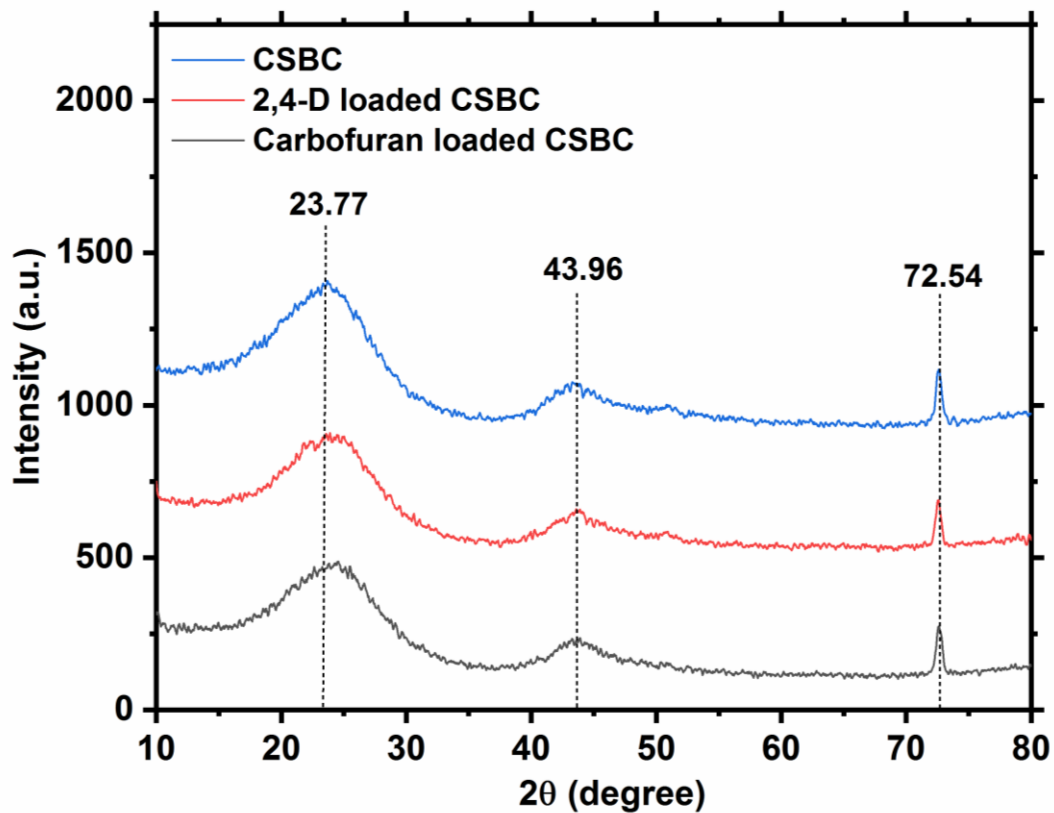
Figure 3.12 X-ray diffractograms of CSBC, carbofuran loaded CSBC and 2,4-D loaded CSBC.
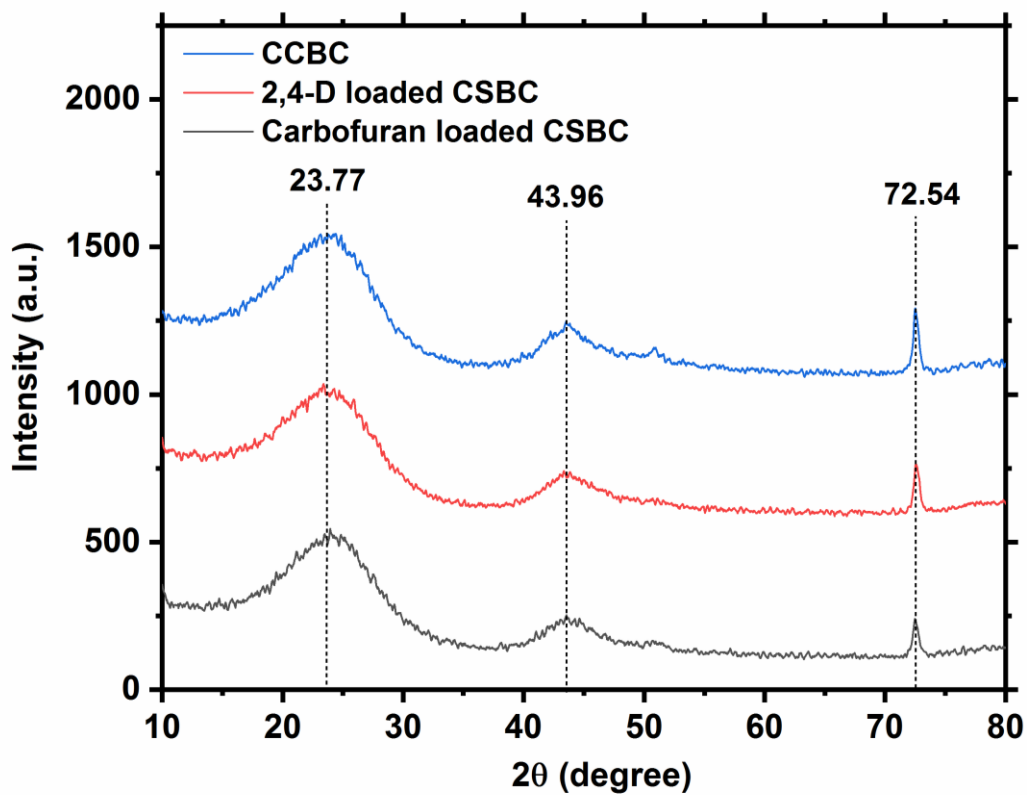
Figure 3.13 X-ray diffractograms of CCBC, carbofuran loaded CCBC and 2,4-D loaded CCBC.

CHAPTER 4

CARBOFURAN ADSORPTION ON CSBC AND CCBC

4.0 Sorption studies for Carbofuran removal

Carbofuran sorption studies onto CSBC (corn stover biochar) and CCBC (corncob biochar) were done in batch mode. Removal studies were performed at different pHs, biochar dosages, initial carbofuran concentration, contact time and reaction temperatures. Batch sorption studies were carried out to optimize carbofuran adsorption and to describe the mechanisms involved in it.

4.1. Effect of pH

Apart from the properties of the adsorbent and adsorbate, the adsorbent-adsorbate interaction is greatly affected by the solution pH. This effect is due to change in behavior of adsorbate, and possibly the adsorbent too with change in pH of the solution in which they are present. Though sometimes the change is trivial and can be ignored within the small range but it certainly has to lay an impact when considered across extremes of pH. Carbofuran adsorption onto the CSBC (Figure 4.1) does not change much from pH 2 to 10. Unlike other similar studies the removal is lower (75.60%) at pH 2 and increases with increase in pH (80.64% at pH 4.0, 82.25% at pH 6.0 and 81.08 % at pH 8.0. Further increase in pH to 10 decreases the percent adsorption to 72.19%. Carbofuran adsorption on CCBC displays similar trends of variation in percentage adsorption with change in initial pH (Figure 4.2). Here percent removal was 56.05 % at pH 2 which increased until 61.72 and 63.59% at pH 4 and 6 respectively. Afterwards at pH 8 and 10 the order of variation is reversed and percent adsorption reduces marginally to 57.57 and 53.77%, respectively. Furthermore, the equilibrium pH remains nearly the same for initial pH 2 and 10 but increases considerably in intermediate range of pH i.e. 4, 6 and 8. This increase in equilibrium pH along initial pH 4 to 8 is more in case of CSBC than CCBC.

4.2. Mechanism of carbofuran adsorption onto CSBC and CCBC

Adsorption of carbofuran onto CSBC and CCBC can either be a physical process or a chemical process or it may be both. Physical processes involved in sorption here include porous diffusion, H-bonding and π^+-π interactions whereas chemical processes involved here include electrophilic and electrostatic interactions [Figure 4.3 (a-g)]. pH dependent speciation of carbofuran [Figure 4.3 (a)] and surface charge characteristic of biochars based on their pHzpc are major factors guiding the electrostatic interactions. The pHzpc of CSBC and CSBC are 7.90 and 7.75 respectively which means that the biochars

will be positively charged when solution pH < pHzpc and negatively charged when solution pH > pHzpc. At lower pH, carbofuran molecules acts as weak acid and is present in protonated form (pKa_1- 3.78). With the increase in pH beyond 3.78 carbofuran releases H^+ and turns into unprotonated (neutral) carbofuran molecule. Thus, the decrease in removal efficiency of either biochars at pH 2 can be attributed to the repulsion between positively charged carbofuran molecule and positively charged surface of CSBC and CCBC. Small increment in carbofuran removal is observed with increase in solution pH from 2 to 4 for both biochars which is further continued at pH 6. This trend suggests that the neutral carbofuran is also getting adsorbed. Here the adsorption can be attributed to the H-bonding interaction between the carbofuran molecules and surface oxygen sites of biochars.

H-bonding interactions are present at all the pH from 2-6. Protonated as well as neutral carbofuran molecules are involved in H-bonding. Protonated carbofuran acts more as H-bond donor with protonated carbonyl carbon and nitrogen as H-bond donor sites. Carbofuran with protonated nitrogen is stronger H-bond donor due to development of resonance based positive charge. Protonated carbofuran can also act as H-bond acceptor using its ether oxygen in 5-membered (furan) ring. Hence, Adsorption of protonated carbofuran adsorption can also take place at pH < pHzpc and at positively charged biochar surface [Figure 4.3 (b)]. Neutral carbofuran, on the other hand is a better H-bond acceptor and undergoes H-bonding with oxygen sites of CSBC and CCBC [Figure 4.3 (c)]. Decrease in carbofuran removal for both the biochars while moving from pH 6 to pH 8 and 10 might be related to electrostatic repulsion between deprotonated carbofuran molecule which is a weak base (pKa_2-11.98) at higher pH and negatively charged biochar surfaces as pH > pHzpc [Figure 4.3 (g)]. Apart from this, ionization of oxygen functionalities of biochar viz. phenolic, hydroxyl and some carboxylic groups based on solution pH also affects the H-bonding [Figure 4.3 (d)]. Biochar surface functional group i.e. –OH acts as H-donor in hydrogen bond with N-H group of neutral carbofuran at solution pH > pHzpc but subsequently, gets deprotonated at higher pH (pH > pHzpc) and acts as H-acceptor in the same H-bonding (Vimal et al., 2019).

Adsorption process is also assisted by electrophilic interaction in acidic medium where protonated amine group of carbofuran binds to phenolic aromatic ring of biochar

surface at ortho and para positions. Similarly, carbonyl carbon (C=O) is likely to attack the electron reach oxygen atom of phenolic OH group at lower pH. Sorption onto CSBC and CCBC can also occur through π-π^+ interactions between their electron rich graphene like surfaces and protonated carbofuran acting as π-electron donor and π-acceptor, respectively [Figure 4.3 (e)]. Carbofuran diffusion in the pores of CSBC and CCBC is adds to its sorption [Figure 4.3 (f)]. High BET surface area (204.9 and 222.9 m^2/g for CSBC and CCBC, respectively) and abundance of micro, meso and macro pores (average pore diameter- 1.90 nm for both the biochars) enables significant carbofuran adsorption onto CSBC and CCBC (Njoku et al., 2014).

4.3 Sorption kinetic studies for carbofuran removal

Sorption kinetic studies were conducted at different biochar dosages, initial carbofuran concentration and contact time. Sorption kinetic studies establishes the adsorption process as function of time.

4.3.1 Effect of biochar doses on carbofuran removal

Percent carbofuran removal was increased with increase in CSBC doses (68% at 2.5 g/L, 85% at 5 g/L and 88 % at 6 g/L) after 24 hours. Dose kinetic studies for carbofuran adsorption onto CCBC were conducted at 4, 6 and 8 g/L. Percent carbofuran adsorption was 48% at CCBC dose of 4 g/L which increased up to 59% with increase in CCBC dose to 6 g/L. Increase in biochar dose to 8 g/L resulted into further increase in percent carbofuran removal up to 65%. It is observed that most of adsorption is completed in 5 hours but percent removal keeps on increasing with time. A significant hike in percent removal is also observed with increase in contact time from 12 hour to 24 hour at all the doses. This trend can be attributed to the better interaction between carbofuran and biochar surfaces with increase in contact time. With the increase in biochar dose the specific sites for carbofuran adsorption are increased. So, the percent carbofuran removal increases with increase in CSBC [Figure 4.4 (a)] and CCBC [Figure 4.4 (b)] doses.

4.3.2. Effect of initial concentration of solution on carbofuran removal.

Kinetic sorption studies were also conducted at different initial carbofuran concentration. At the end of equilibrium time (24 hour), percent carbofuran removal by CSBC was found to be 83, 79 and 64 % at initial carbofuran concentration of 5, 10 and

20 mg/L, respectively. Similar results were obtained for carbofuran adsorption onto CCBC where percent carbofuran removal shows a decrease from 59% to 57% with increase in initial carbofuran solution from 5 to 10 mg/L. On further increasing the initial carbofuran solution to 20 mg/L, this percent removal further dips to 40%. Thus, a decrease percent carbofuran removal was observed with increase in initial carbofuran concentration.

Increase in adsorption capacities of CSBC and CCBC were recorded with increase in initial carbofuran adsorption. Adsorption capacity (qe) of CSBC was found to be 1.70, 3.48 and 4.19 mg/g at carbofuran concentration 5, 10 and 20 mg/L [Figure 4.5 (a)]. Similarly, adsorption capacity of CCBC was found to be 0.67, 1.15 and 1.24 at carbofuran concentration of 5, 10 and 20 mg/L, respectively [Figure 4.5 (b)]. Thus, CSBC and CCBC adsorption capacities were found to be in positive correlation with initial carbofuran concentration. This relationship between the adsorption capacities of biochars and initial carbofuran concentration can be ascribed to the higher concentration gradient working as driving force and ensuring use of full sorption capacity of biochars (Salman et al., 2011a). Similar results was obtained by Salman, 2013. It was also observed that adsorption by CSBC was faster than that by CCBC as most of the adsorption took place in 5 hours and 10 hours for former and later, respectively.

4.4. Kinetic modelling

Pseudo-first order and pseudo-second order kinetic equations were applied to the experimental kinetic data. Best fit equation was selected on the basis of agreement between data obtained from the model and experimental sorption data along with the regression coefficient. The feasibility of sorption process along with nature of sorption i.e. physical adsorption or chemical adsorption is described by the kinetic models.

4.4.1 Pseudo-first order kinetic model

Results obtained from kinetic sorption studies at different biochar doses and initial carbofuran concentration are evaluated using pseudo-first order kinetic equation. The rate constants (K_1), adsorption capacities (q_e) obtained through kinetic model and correlation coefficients (R^2) for carbofuran adsorption onto CSBC and CCBC are provided in table 4.1 and 4.3 (at different biochar doses); and table 4.2 and 4.4 (at different carbofuran concentration). As mentioned in the tables, the experimental q_e value

doesn't seems to be near q_e value obtained by pseudo-first order model. Also, the value of correlation coefficient is quite away from unity which suggest that the experimental data is not in agreement with the data obtained through pseudo-first order rate equations. Linear pseudo first order kinetic plots [log (q_e-q_t) vs t] for carbofuran adsorption onto CSBC and CCBC at different dose and initial concentration are given in figure 4.6 (a, b) and 4.7 (a, b), respectively. Data points in these plots seem to be skewed with no definite trends. Thus, pseudo-first order rate equation cannot explain carbofuran adsorption kinetic onto CSBC and CCBC.

4.4.2 Pseudo-second order kinetic model

Results obtained from kinetic sorption studies at different biochar doses and initial carbofuran concentration were also fitted to pseudo-second order kinetic equation. The rate constants (K_2), adsorption capacities (q_e) obtained through kinetic model and correlation coefficients (R^2) for carbofuran adsorption onto CSBC and CCBC are given (at different biochar doses); and table 4.2 and 4.4 (at different carbofuran concentration). It is very clear from these tables that the experimental q_e value is very close to q_e value obtained by pseudo-first order model with a correlation coefficient very close to unity ($R^2 > 0.99$) for all biochar doses and initial carbofuran concentration. Proximity of R^2 value to 1 suggests that the pseudo-first order rate model fits the kinetic data well. Thus, experimental data is in agreement with the data obtained through pseudo-second order rate equations. Linear pseudo-second order kinetic plots [t/q_t vs t] for carbofuran adsorption onto CSBC and CCBC at different dose and initial concentration are given in Figure 4.8 (a, b) and 4.9 (a, b), respectively. Thus, on the basis of better fitting of kinetic data to pseudo second order rate equation, it can be concluded that chemisorption is rate limiting step for carbofuran adsorption onto CSBC and CCBC.

4.5. Sorption isotherm studies for carbofuran removal

Carbofuran adsorption isotherm studies for CSBC [Figure 4.10 (a)] and CSBC [Figure 4.10 (b)] were conducted at 25, 35 and 45°C. Isotherms studies on CSBC were performed with biochar dose and initial carbofuran concentration of 5 g/L and 5-110 mg/L at pH - 6 i.e. optimized through pH study. Similarly, biochar dose selected for isotherm studies of carbofuran adsorption onto CCBC was 6 g/L whereas concentration range for the same was 5-100 mg/L. Both the studies were carried out for 24 hours. As

mentioned earlier in kinetic studies part, more than 50-60% of final absorption was completed within 5-6 hours but adsorption process continued with slow pace till it reached equilibrium after 24 hour.

4.5.1. Isotherm modeling

Various isotherm models like Freundlich, Langmuir, Temkin, Sips, Redlich-Peterson, Toth, Koble-Corrigan and Radke-Prausnitz were applied to data obtained for equilibrium studies performed at constant temperature. These models graphically represent the mathematical correlation between amount adsorbed on adsorbent and residual concentration of solution at equilibrium (Foo and Hameed, 2010).

Non-linear Freundlich plots for carbofuran adsorption onto CSBC and CCBC are given in Figure 4.11(a) and (b), respectively. Here, it can be observed that Freundlich isotherm fits better to carbofuran adsorption onto CCBC ($R^2 > 0.95$) than that to CSBC ($R^2 > 0.92$). Also, the value of $1/n$ as measure of adsorption intensity or surface heterogeneity is below 1 which means that the sorption process is chemical in nature (Foo and Hameed, 2010). Parameters from Freundlich and other isotherm models for carbofuran adsorption onto both biochars are given together in Table 4.5.

Non-linear Langmuir plots for carbofuran adsorption onto CSBC and CCBC are given in Figure 4.12 (a) and 4.12 (b), respectively. As per assumptions Langmuir adsorption is monolayer. So, the adsorption capacity obtained through Langmuir isotherm is called monolayer adsorption capacity. Monolayer adsorption capacities for CSBC and CCBC were found to be increasing with increase in temperature from 25-45°C i.e. 6.39, 7.99 and 12.33 mg/g; and 6.57, 6.81 and 11.95 mg/g, respectively. Correlation coefficient for carbofuran adsorption onto CSBC ($R^2 > 0.93$) is better than that of CCBC ($R^2 < 0.90$). Similar results of rise in adsorption capacity as temperature increases are also obtained by many researchers (Salman and Hameed, 2010; Njoku et al., 2014).

Non-linear Temkin isotherm plots for biochars CSBC and CCBC are given in Figure 4.13 (a) and 4.13 (b), respectively. Temkin isotherm gives different fitting to carbofuran adsorption onto CSBC and CCBC. While its fit is reasonable for former ($R^2 < 0.95$) but becomes poor in case of later ($R^2 < 0.90$). One significant inference derived from this model is endothermic nature of this adsorption process as value of b_{Te} is positive (Inam et al., 2017).

Non-linear plots of Sips isotherm fitted to carbofuran adsorption onto CSBC and CCBC are given in Figure 4.14 (a) and 4.14 (b), respectively. It is observed that the Sips isotherm model fits the carbofuran adsorption data well with $R^2 > 0.90$ for both the biochars and at all the temperatures.

Adsorption data is also well fitted by Redlich-Peterson and Koble-Corrigan ($R^2 > 0.95$) and are given in Figure [4.15 (a), (b)] and [4.16 (a), (b)], respectively. Toth [4.17 (a), (b)] and Radhke-Prausnitz [4.18 (a), (b)] isotherm model also fit the adsorption data with reasonable R^2 value which is more than 0.90 for both biochars and at all temperatures.
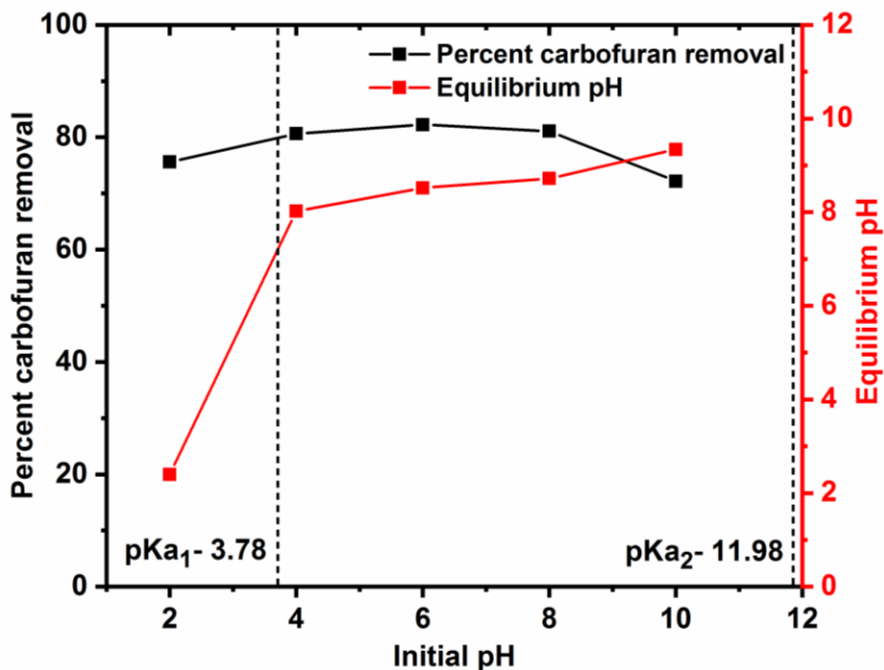
Figure 4.1 Effect of pH on Carbofuran removal by CSBC [Initial carbofuran concentration= 10 mg/L; CSBC dose= 5 g/L; T= 25°C]
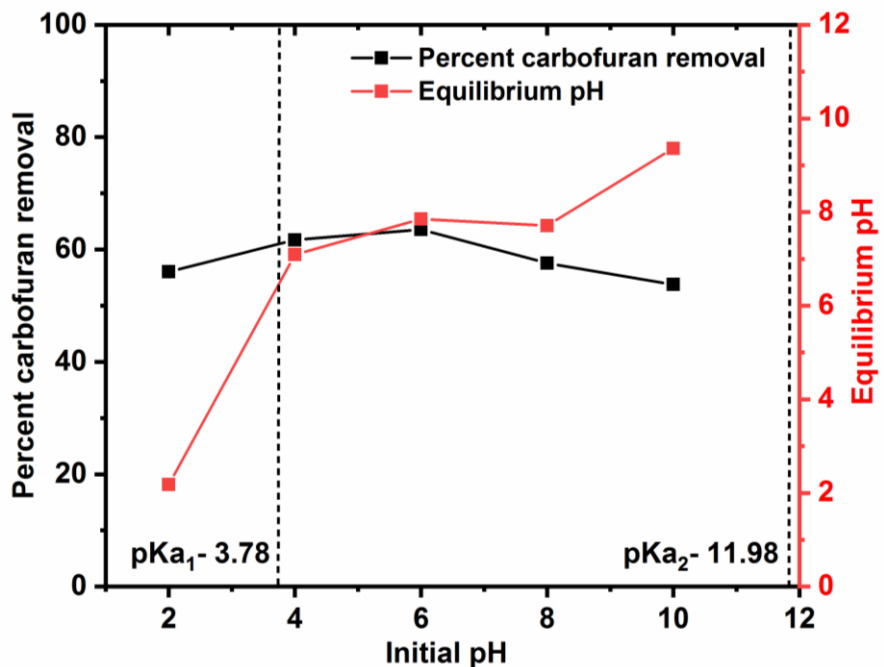
Figure 4.2 Effect of pH on Carbofuran removal by CCBC [Initial carbofuran concentration= 10 mg/L; CCBC dose= 5g/L; T= 25°C].

pKa$_1$ = 3.78

pKa$_2$ = 11.95
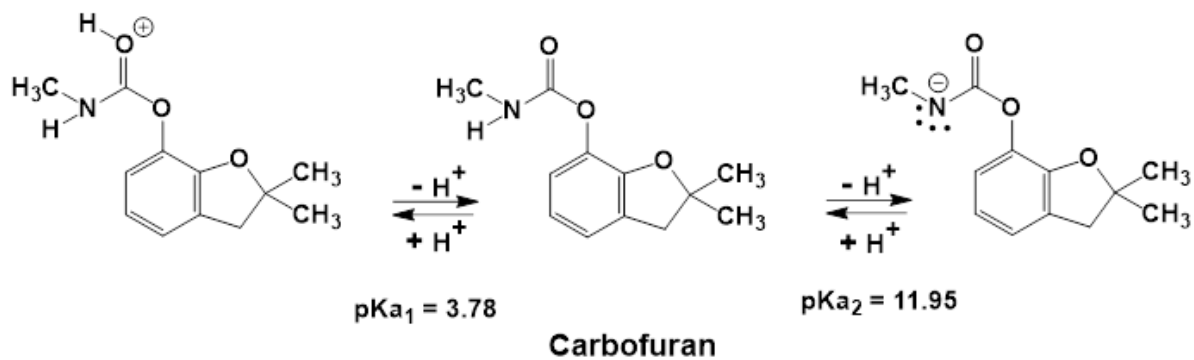
Carbofuran

Figure 4.3 (a) Carbofuran speciation in aqueous solution.

Biochar (Phenolic group)

Protonated Carbofuran
(low pH range)

Strong H-bond

Protonated Carbofuran
(low pH range)

Mono H-bonding

Biochar (Lactone group)
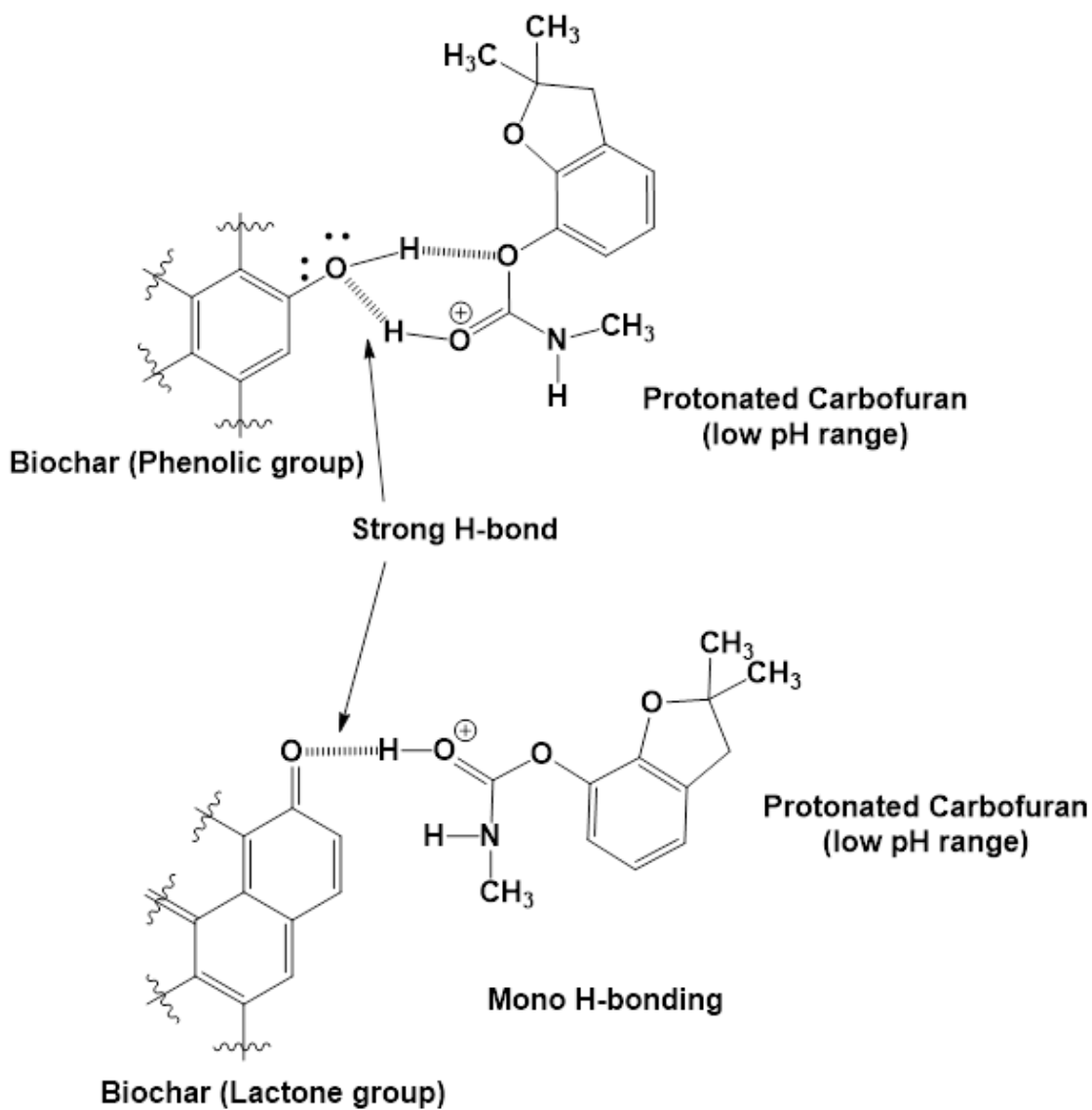
Figure 4.3 (b) Hydrogen bonding between protonated and neutral carbofuran with biochars.
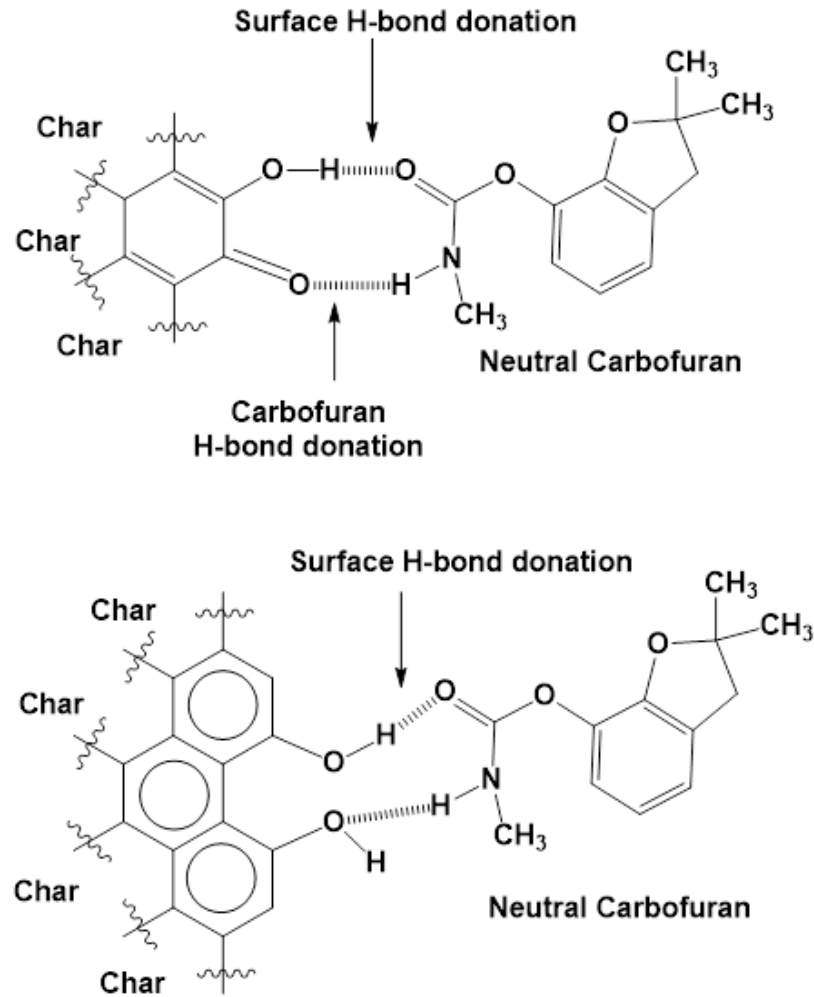
Figure 4.3 (c) Chelation type bonding between neutral carbofuran and biochars.
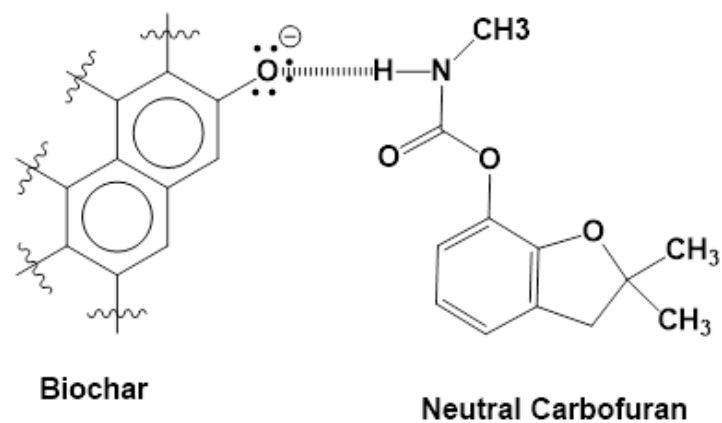
Figure 4.3 (d) Bonding between negatively charged biochar at high pH with carbofuran.
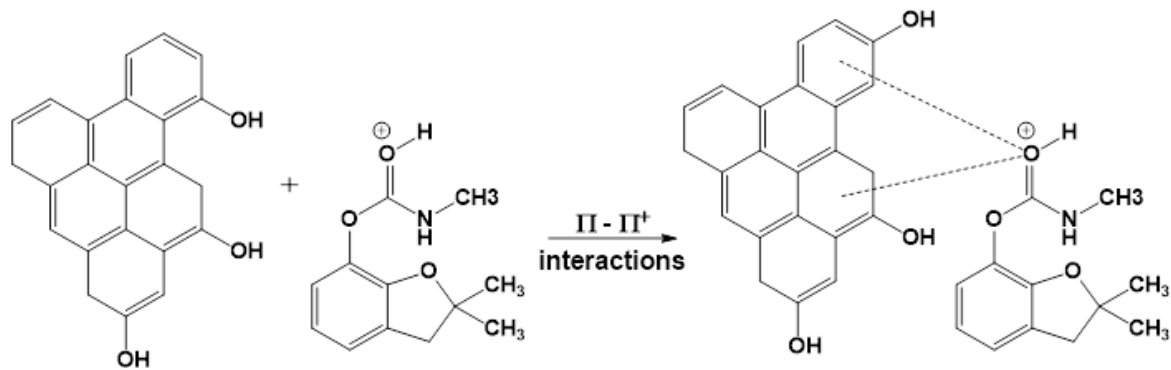
Figure 4.3 (e) Carbofuran sorption onto biochar via π-π electron donor-acceptor interactions.
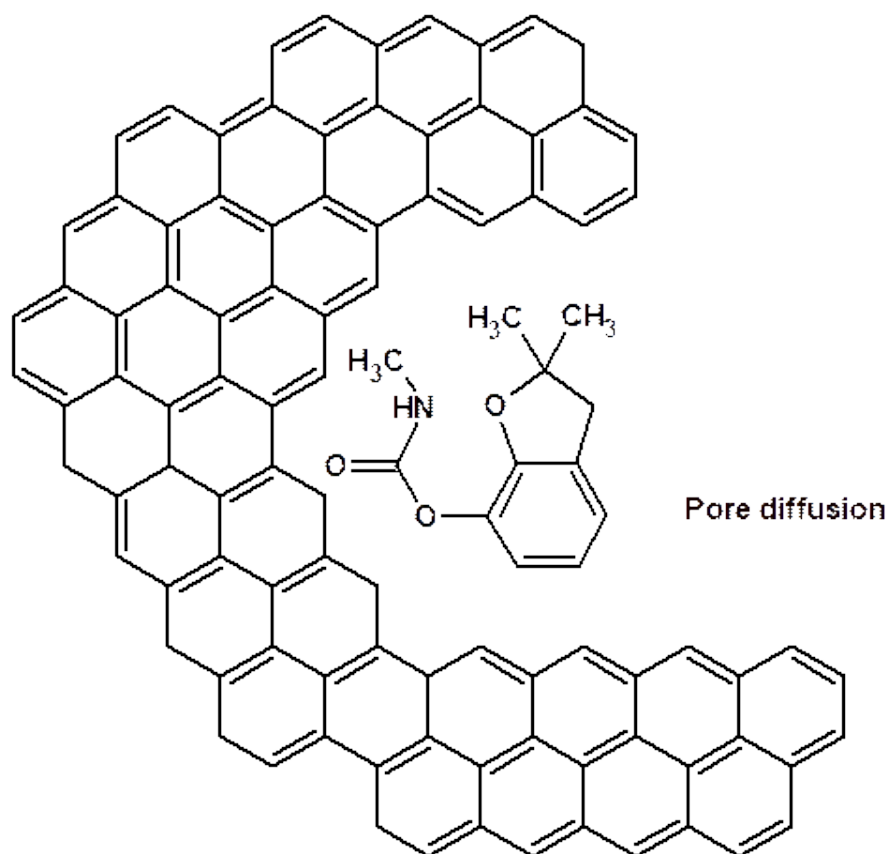
Figure 4.3 (f) Carbofuran diffusion into biochar pores [benzene rings on the left side show the biochar's aromatic structure].
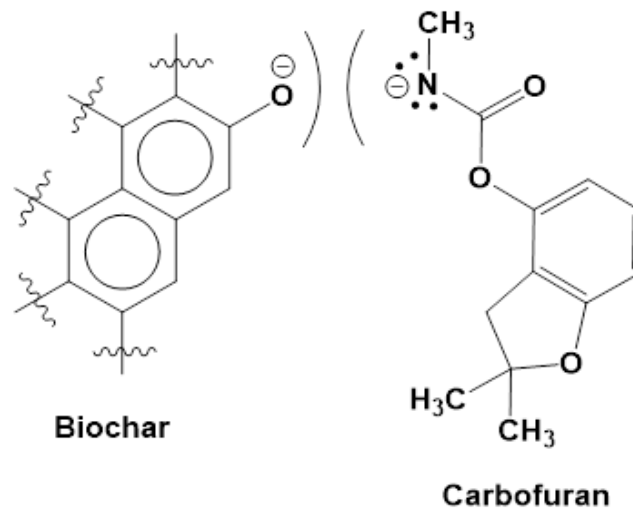
Figure 4.3 (g) Repulsion between carbofuran and biochar at strongly basic pH.
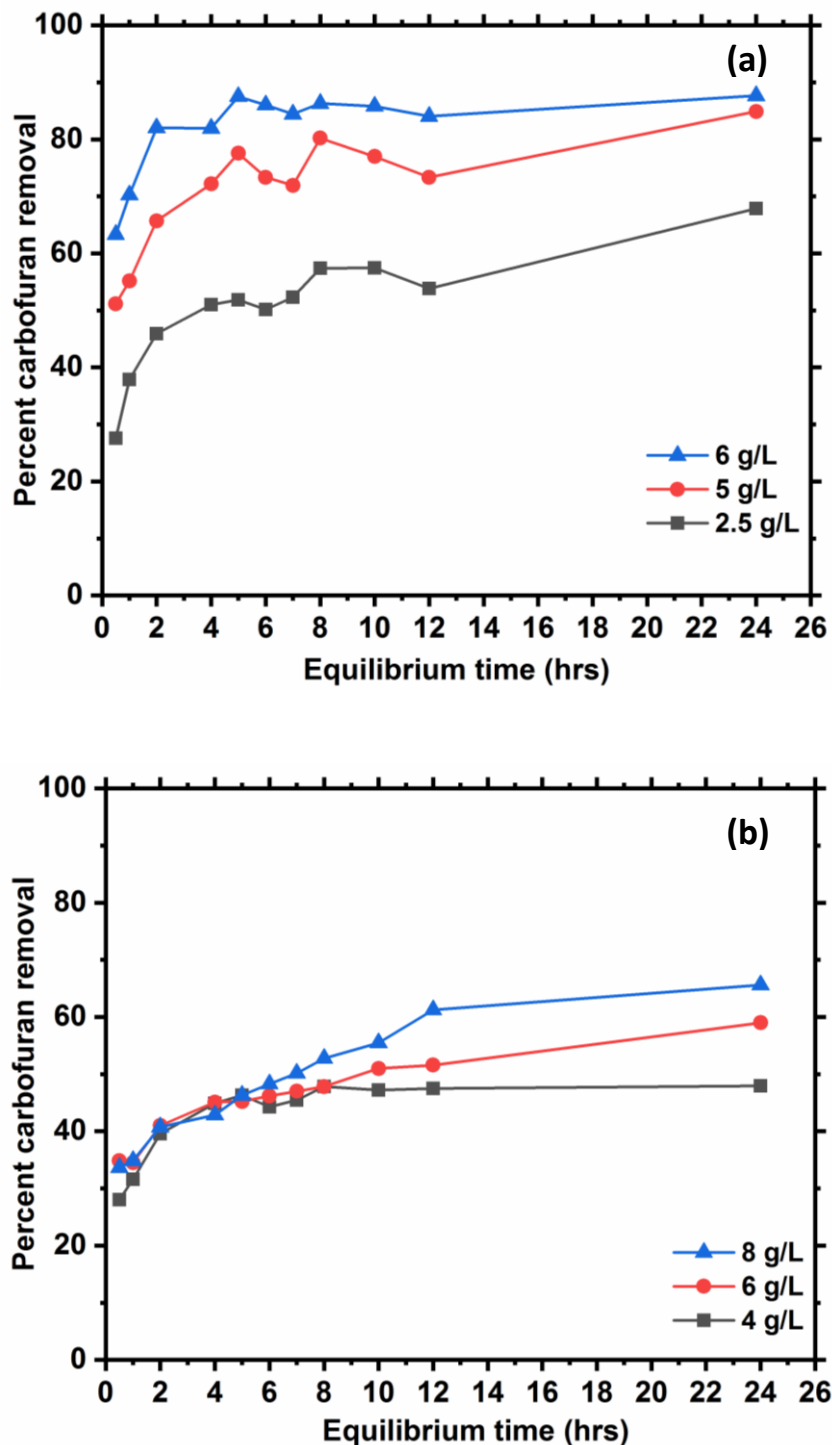
Figure 4.4 Effect of different adsorbent doses on carbofuran removal by (a) CSBC and (b) CCBC [pH= 6; initial carbofuran concentration= 10 mg/L; T= 25°C]
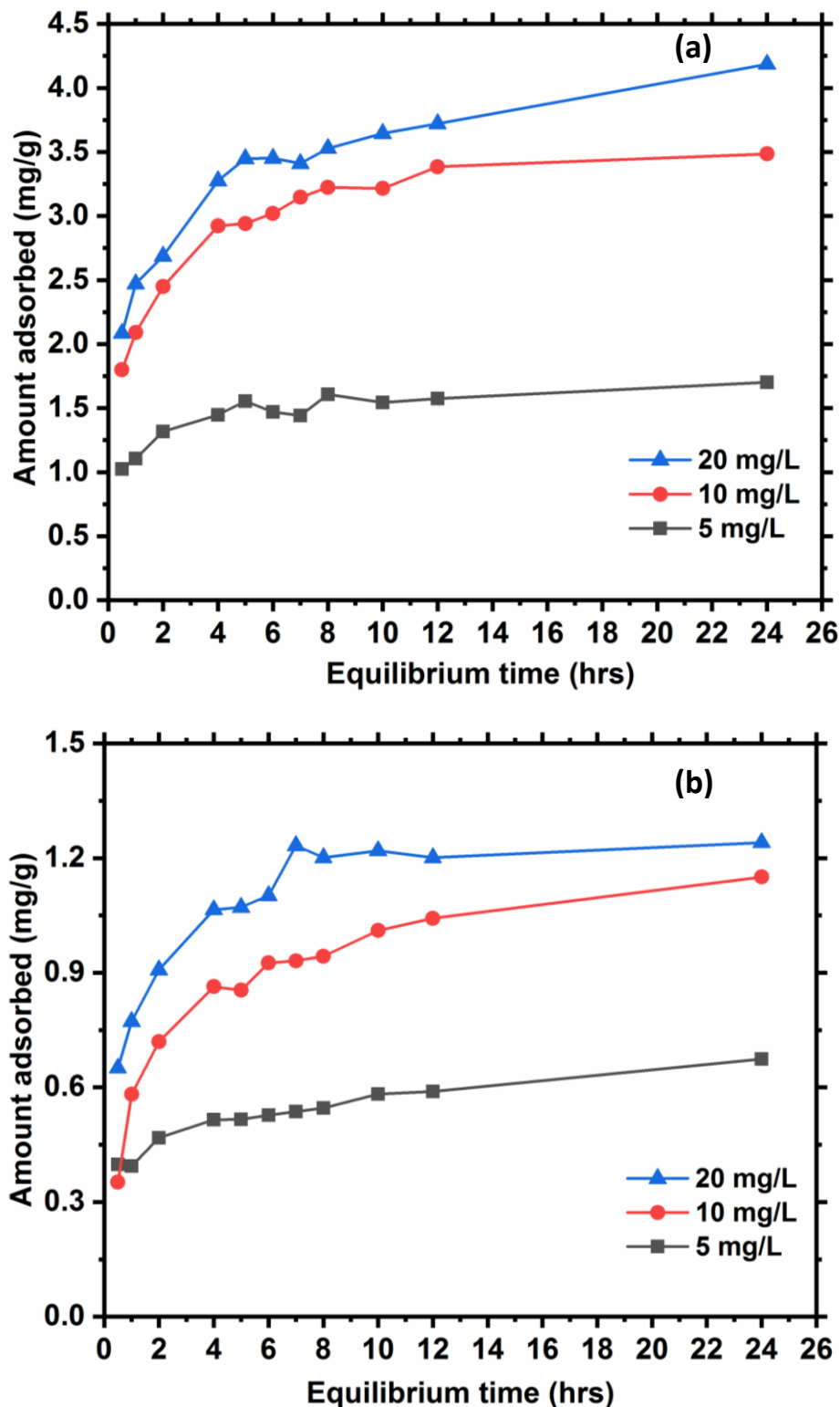
Figure 4.5 Effect of different initial concentration on carbofuran removal by (a) CSBC (dose= 5 g/L) and (b) CCBC (dose= 6g/L) [pH= 6; T= 25°C]
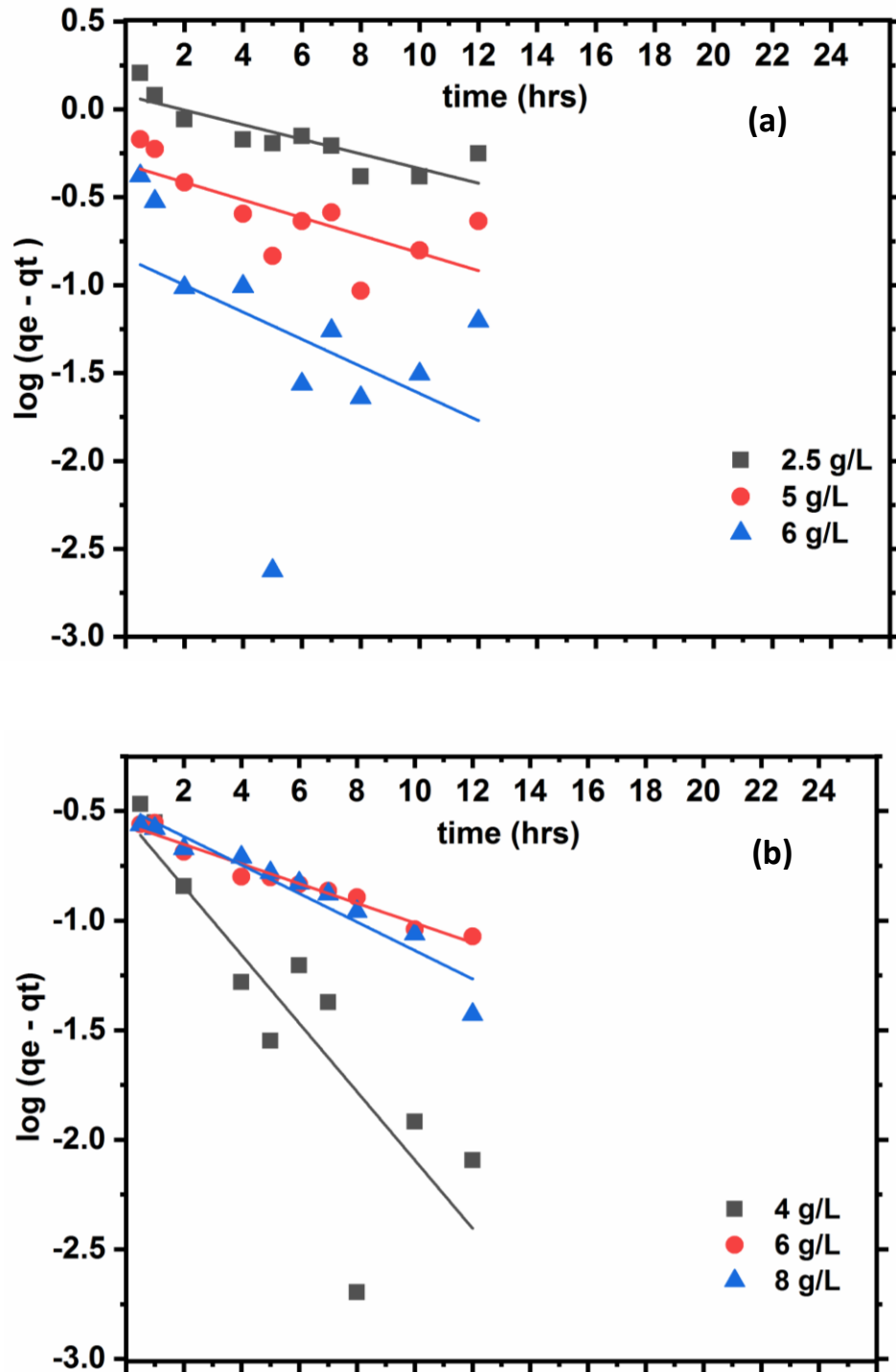
Figure 4.6 Pseudo-first-order kinetic plots for carbofuran removal by (a) CSBC and (b) CCBC at various adsorbent doses [pH= 6; initial carbofuran concentration= 10 mg/L; T= 25°C]
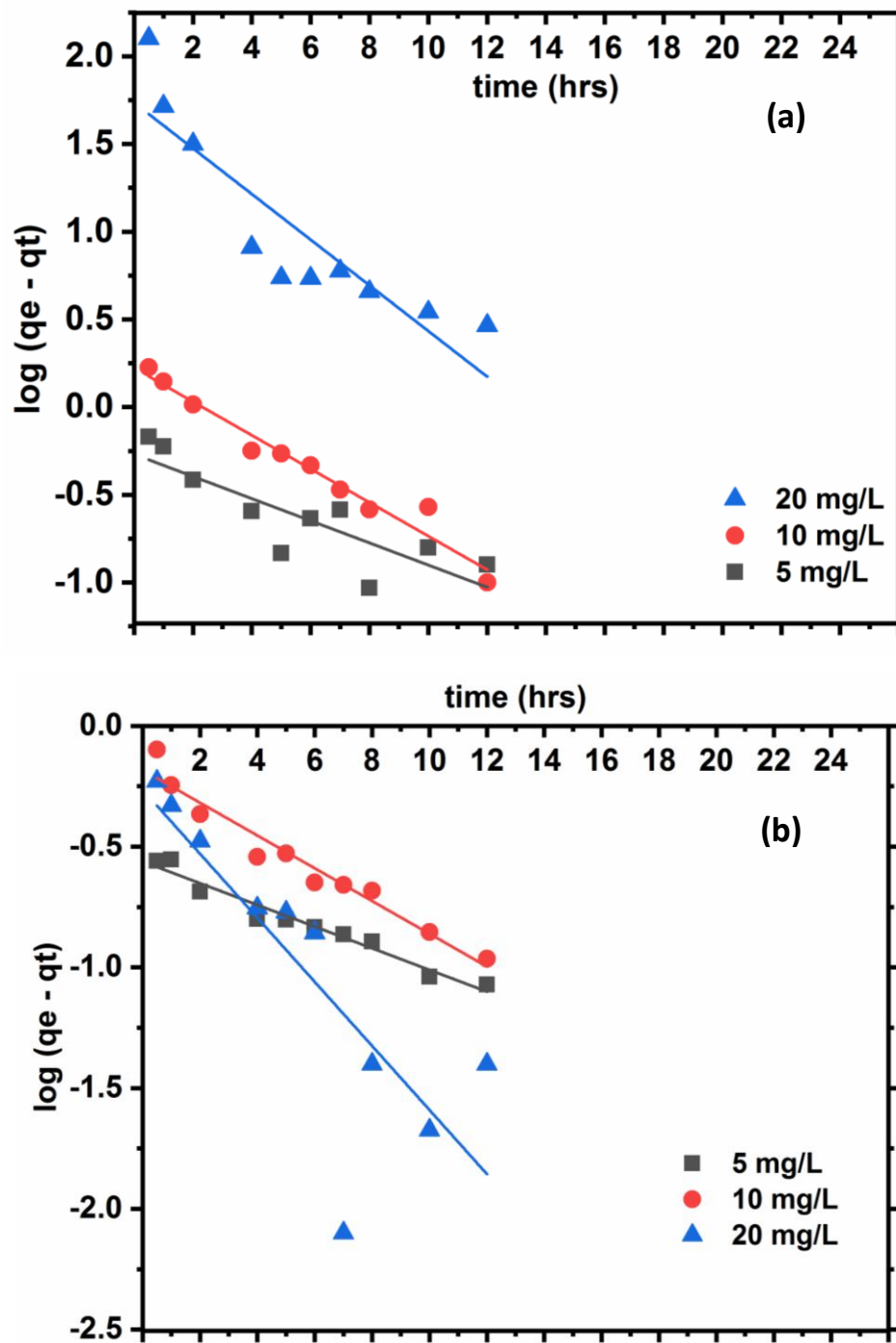
Figure 4.7 Pseudo-first-order kinetic plots for carbofuran removal by (a) CSBC (dose= 5 g/L and (b) CCBC (dose= 6 g/L) at different initial carbofuran concentration [pH= 6; T= 25°C]
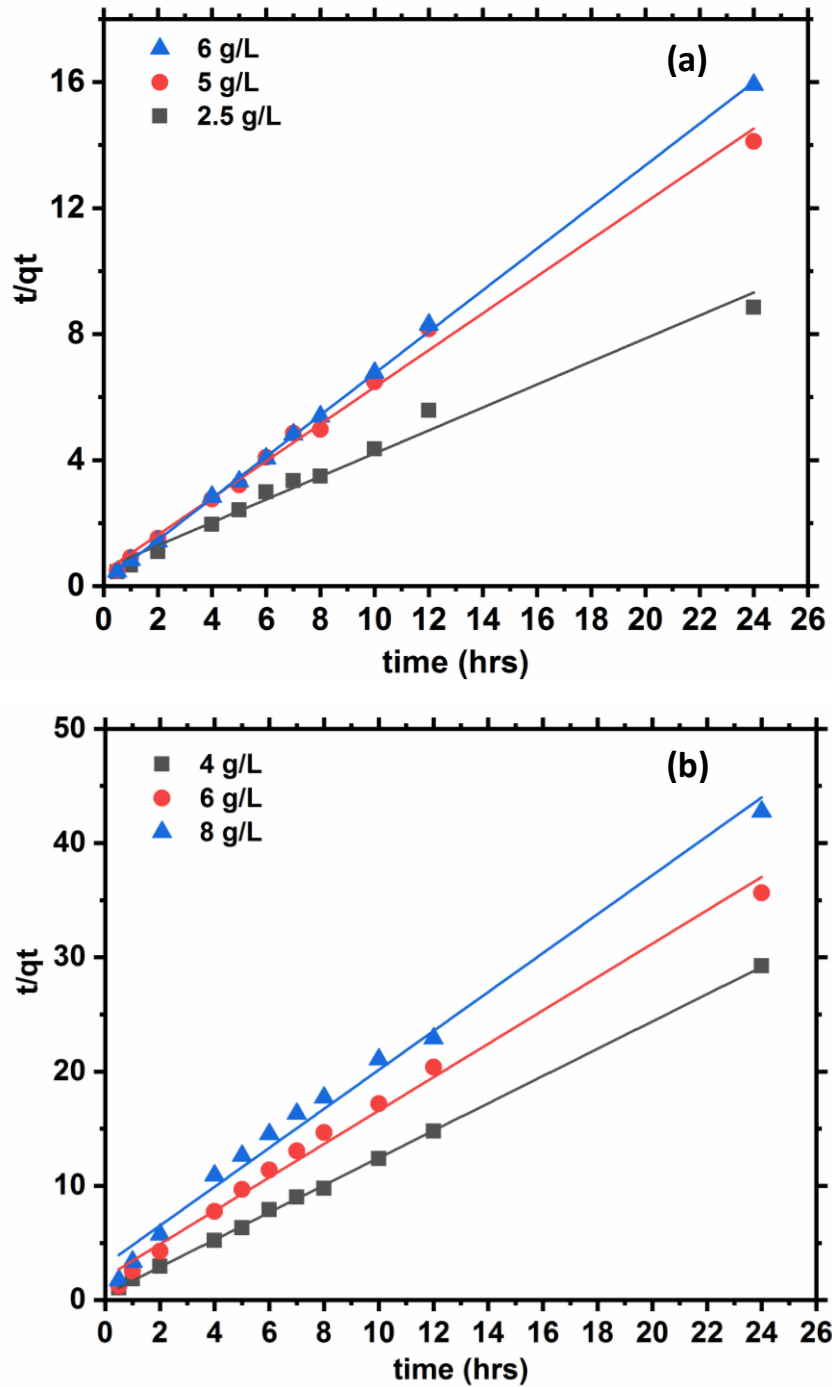
Figure 4.8 Pseudo-second-order kinetic plots for carbofuran removal by (a) CSBC and (b) CCBC at different adsorbent doses [pH= 6; initial carbofuran concentration= 10 mg/L; T= 25°C]
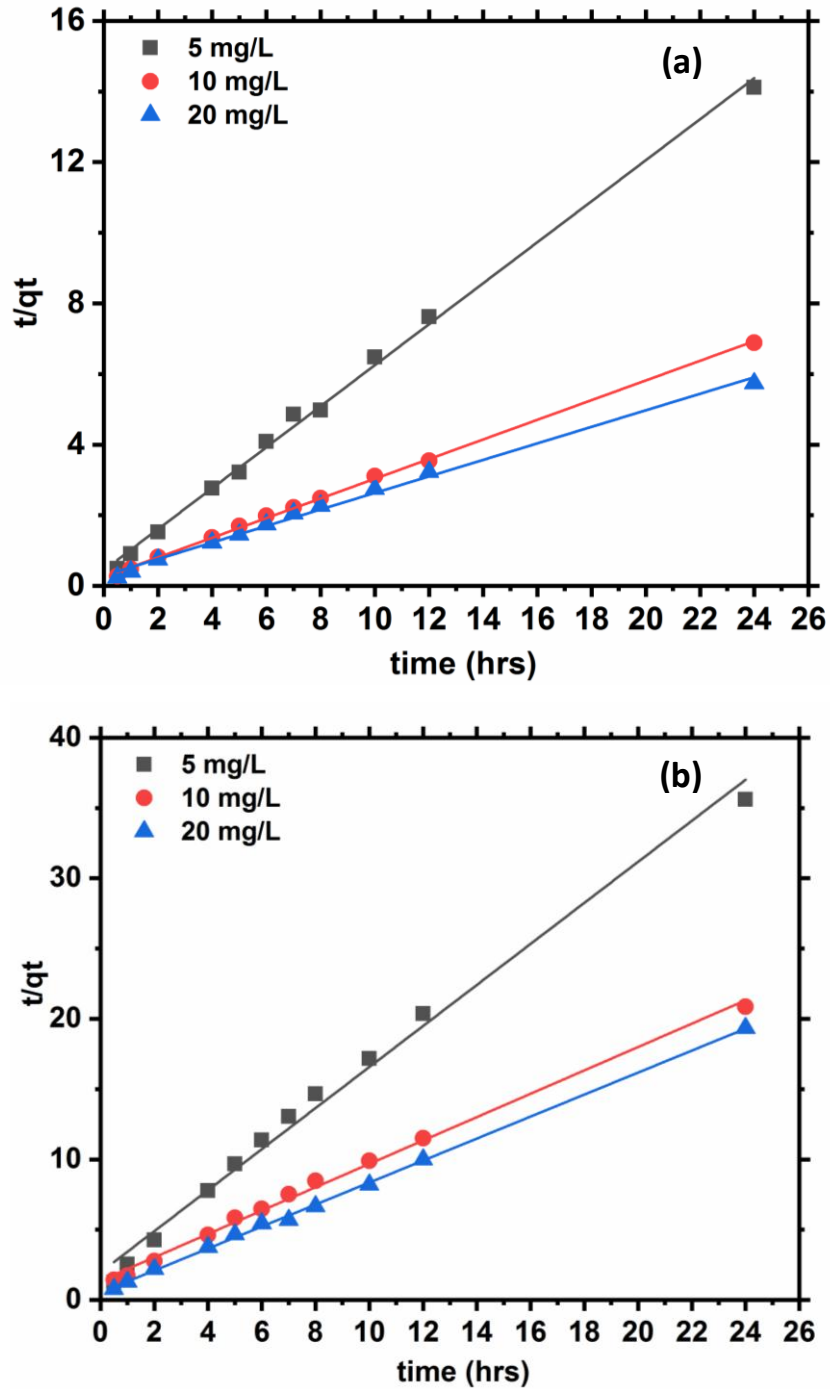
Figure 4.9 Pseudo-second-order kinetic plots for carbofuran removal by (a) CSBC (dose= 5 g/L and (b) CCBC (dose= 6 g/L) at different initial carbofuran concentration [pH= 6; T= 25°C]

Table 4.1 Pseudo-first order and pseudo-second order rate parameters and its comparison with experimental q_e for aqueous carbofuran removal of at different CSBC doses.

Dose (g/L)	Pseudo-first order rate constant, k_1 (h^{-1})	R^2	Pseudo-second order rate constant, k_2 ($g\,mg^{-1}\,h^{-1}$)	R^2	q_e experimental (mg/g)	q_e, calculated using first order kinetic model (mg/g)	q_e, calculated using second order kinetic model (mg/g)
2.5	0.0958	0.7274	13.3799	0.9840	2.71	1.2012	2.7397
5	0.1158	0.5153	5.7284	0.9940	1.70	2.0606	1.7391
6	0.1776	0.2165	16.1668	0.9995	1.51	6.9904	1.5152

Table 4.2 Pseudo-first order and pseudo-second order rate parameters and its comparison with experimental q_e for aqueous carbofuran removal of by CSBC at different initial concentrations.

Concentration (mg/L)	Pseudo-first order rate constant, k_1 (h^{-1})	R^2	Pseudo-second order rate constant, k_2 ($g\,mg^{-1}\,h^{-1}$)	R^2	q_e experimental (mg/g)	q_e, calculated using first order kinetic model (mg/g)	q_e, calculated using second order kinetic model (mg/g)
10	0.1455	0.7191	6.6927	0.9971	1.70	1.8561	1.72
20	0.2206	0.9625	51.8158	0.9990	3.48	1.6719	3.59
30	0.2999	0.7989	62.4157	0.9946	4.19	54.5004	4.27

Table 4.3 Pseudo-first order and pseudo-second order rate parameters and its comparison with experimental q_e for aqueous carbofuran removal at different CCBC doses.

Dose (g/L)	Pseudo-first order rate constant, k_1 (h^{-1})	R^2	Pseudo-second order rate constant, k_2 ($g\,mg^{-1}\,h^{-1}$)	R^2	q_e experimental (mg/g)	q_e, calculated using first order kinetic model (mg/g)	q_e, calculated using second order kinetic model (mg/g)
4	0.3590	0.725	1.6041	0.99	0.8206	3.4064	0.8373
6	0.1034	0.960	0.2373	0.99	0.6734	3.6425	0.6845
8	0.1496	0.920	0.1110	0.98	0.5615	3.0598	0.5869

Table 4.4 Pseudo-first order and pseudo-second order rate parameters and its comparison with experimental q_e for aqueous carbofuran removal by CCBC at different initial concentrations.

Concentration (mg/L)	Pseudo-first order rate constant, k_1 (h^{-1})	R^2	Pseudo-second order rate constant, k_2 ($g\,mg^{-1}\,h^{-1}$)	R^2	q_e experimental (mg/g)	q_e, calculated using first order kinetic model (mg/g)	q_e, calculated using second order kinetic model (mg/g)
5	0.0294	0.951	0.2384	0.99	0.6739	1.5205	0.6850
10	0.0195	0.960	1.0571	0.99	1.1508	3.6425	1.2031
20	0.0576	0.672	3.0923	0.99	1.2407	1.8335	1.2783
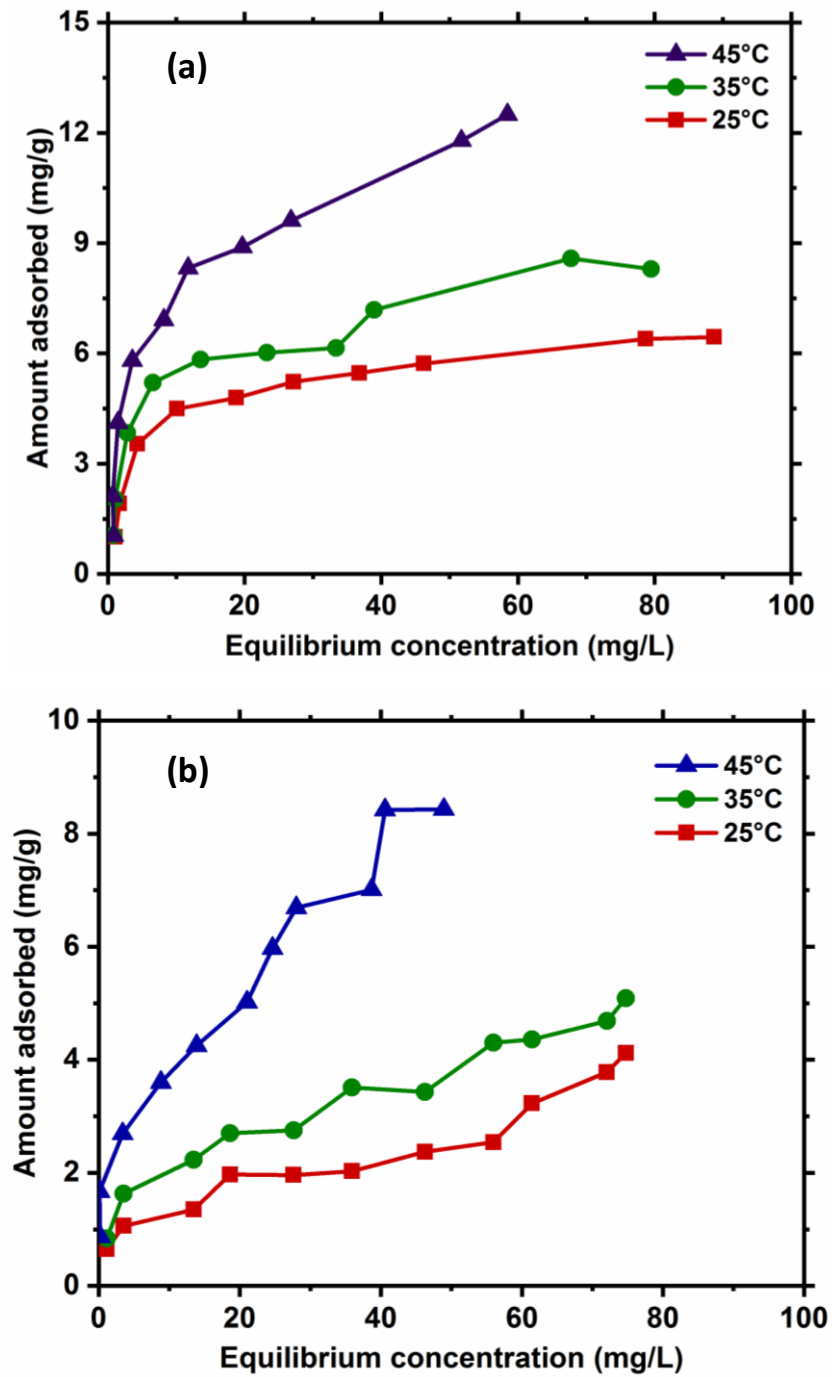
Figure 4.10 Effect of temperature on the carbofuran removal by (a) CSBC (initial carbofuran concentration= 5-110 mg/L; dose= 5 g/L) and (b) CCBC (Initial carbofuran concentration= 5-100 mg/L; dose= 6g/L) [pH=6; particle size= 30-50 BSS mesh]
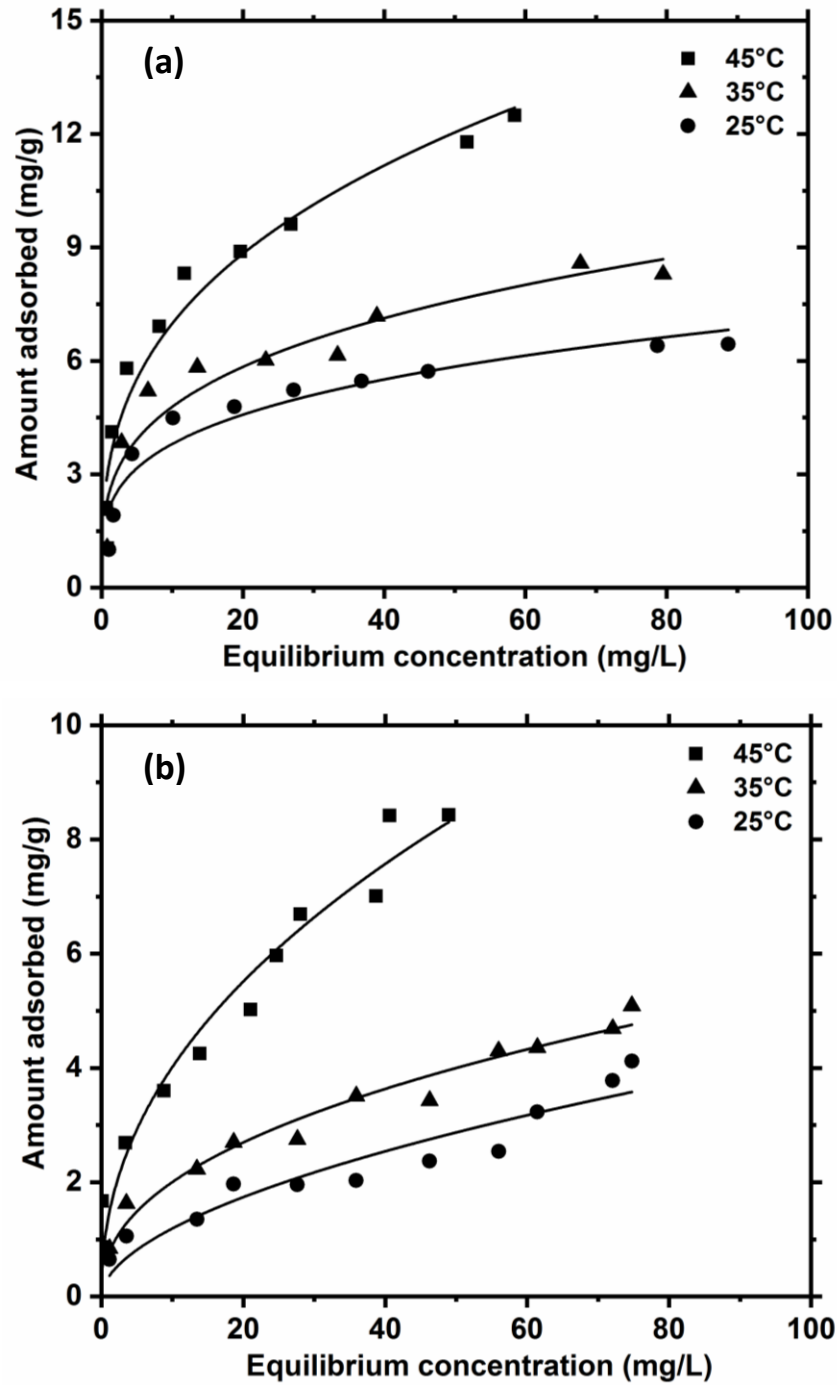
Figure 4.11 Freundlich adsorption isotherms of carbofuran by (a) CSBC (initial carbofuran concentration= 5-110 mg/L; dose= 5 g/L) and (b) CCBC (Initial carbofuran concentration= 5-100 mg/L; dose= 6g/L) [pH=6; particle size= 30-50 BSS mesh]
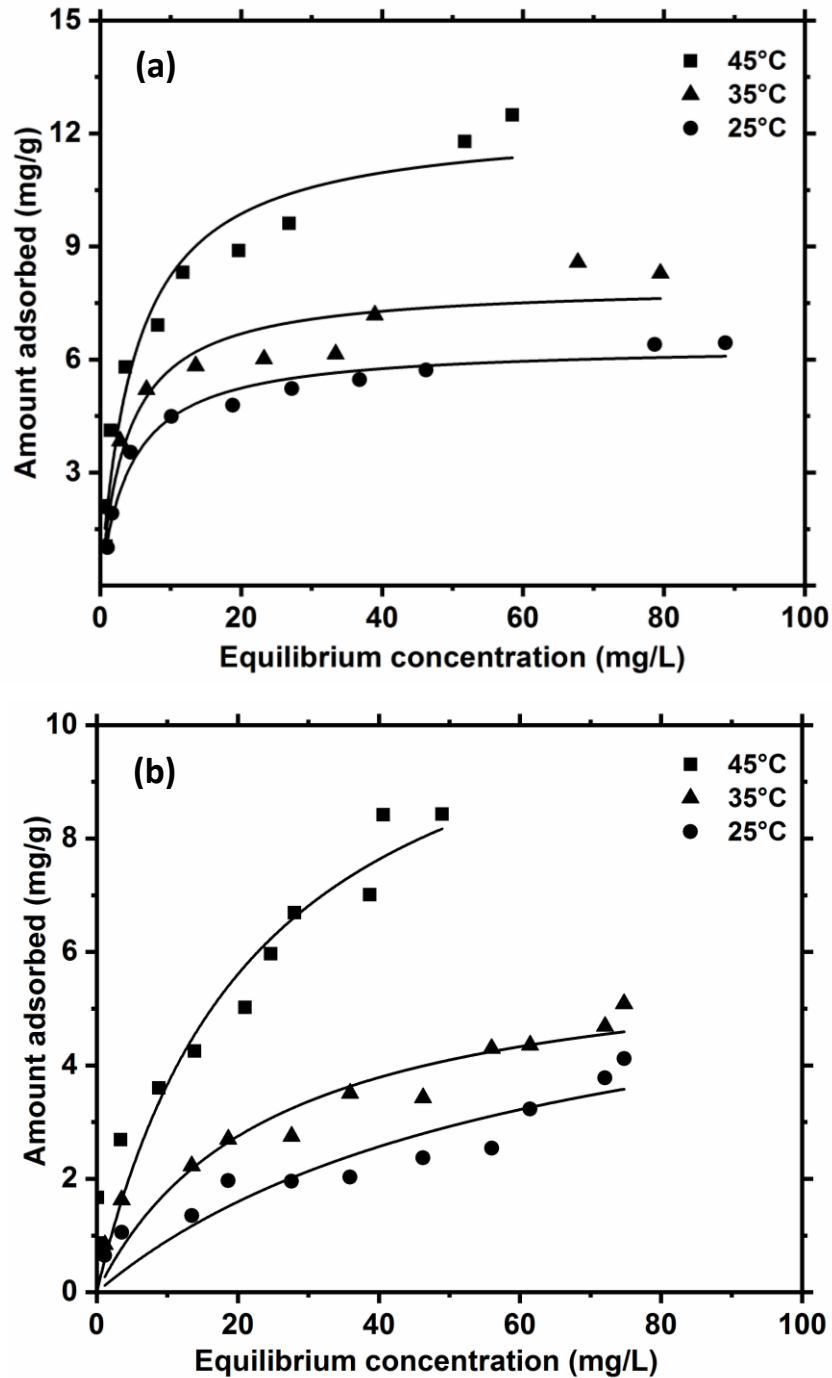
Figure 4.12 Langmuir adsorption isotherms of carbofuran by (a) CSBC (initial carbofuran concentration= 5-110 mg/L; dose= 5 g/L) and (b) CCBC (Initial carbofuran concentration= 5-100 mg/L; dose= 6g/L) [pH=6; particle size= 30-50 BSS mesh]
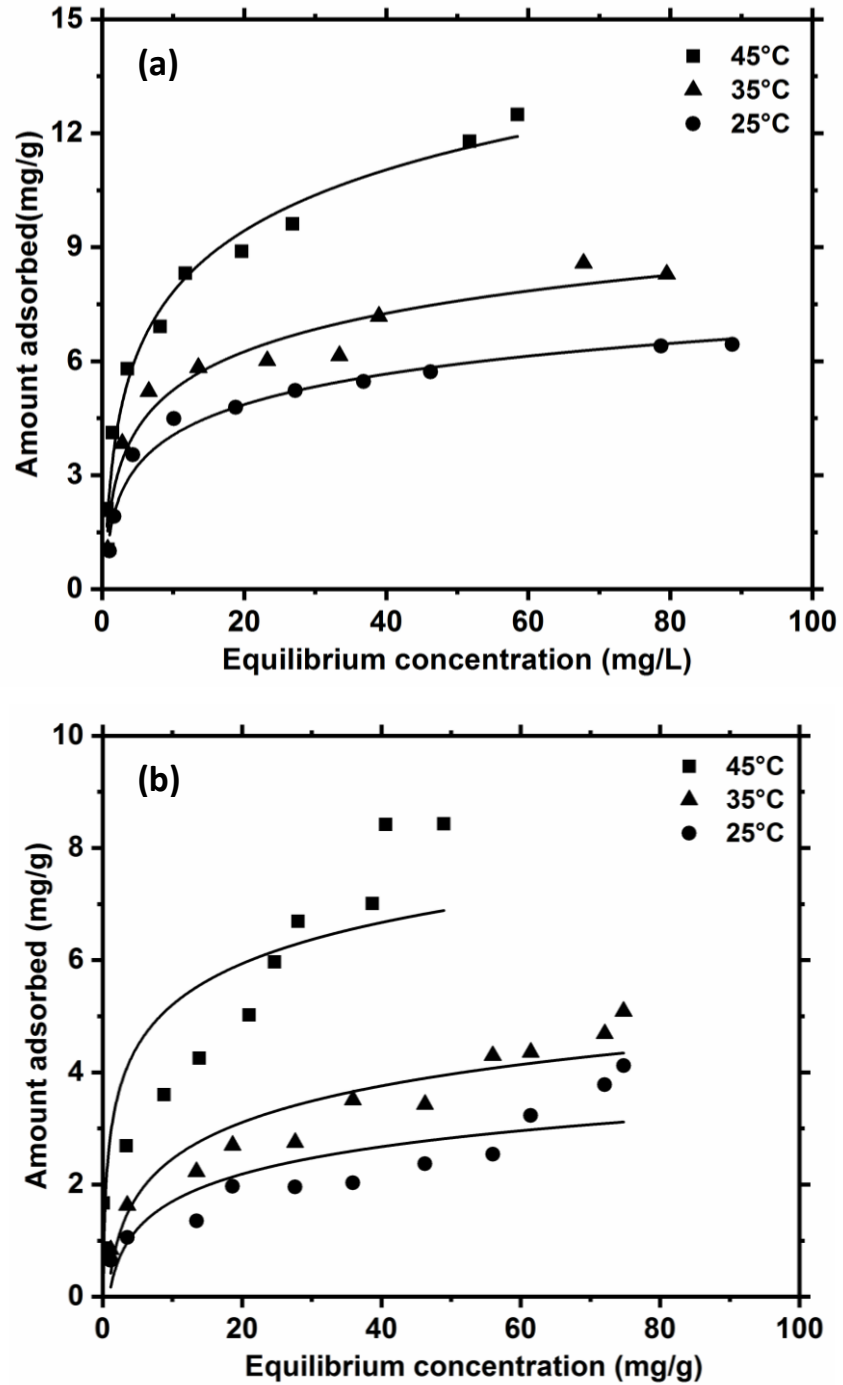
Figure 4.13 Temkin adsorption isotherms of carbofuran by (a) CSBC (initial carbofuran concentration= 5-110 mg/L; dose= 5 g/L) and (b) CCBC (Initial carbofuran concentration= 5-100 mg/L; dose= 6g/L) [pH=6; particle size= 30-50 BSS mesh]
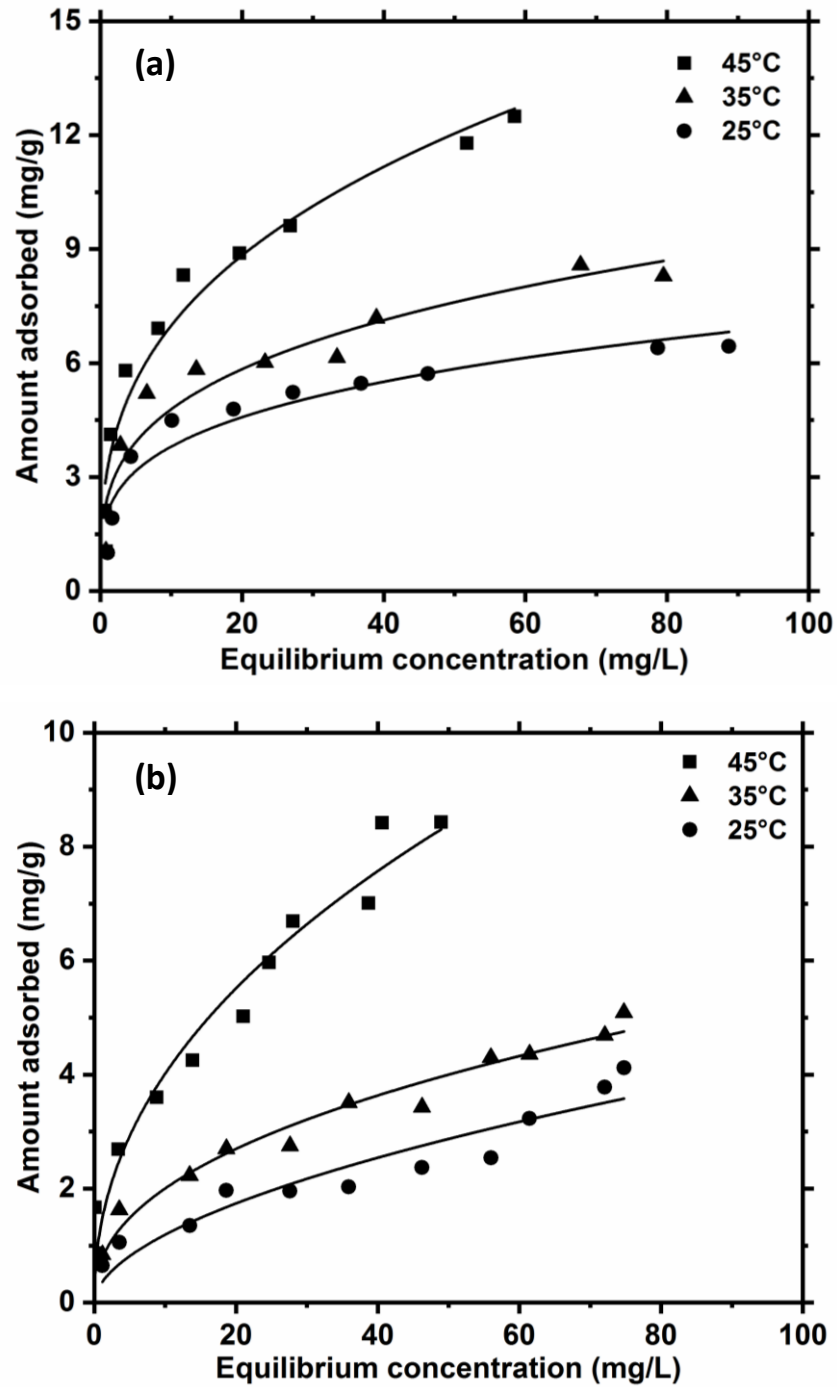
Figure 4.14 Sips adsorption isotherms of carbofuran by (a) CSBC (initial carbofuran concentration= 5-110 mg/L; dose= 5 g/L) and (b) CCBC (Initial carbofuran concentration= 5-100 mg/L; dose= 6g/L) [pH=6; particle size= 30-50 BSS mesh]
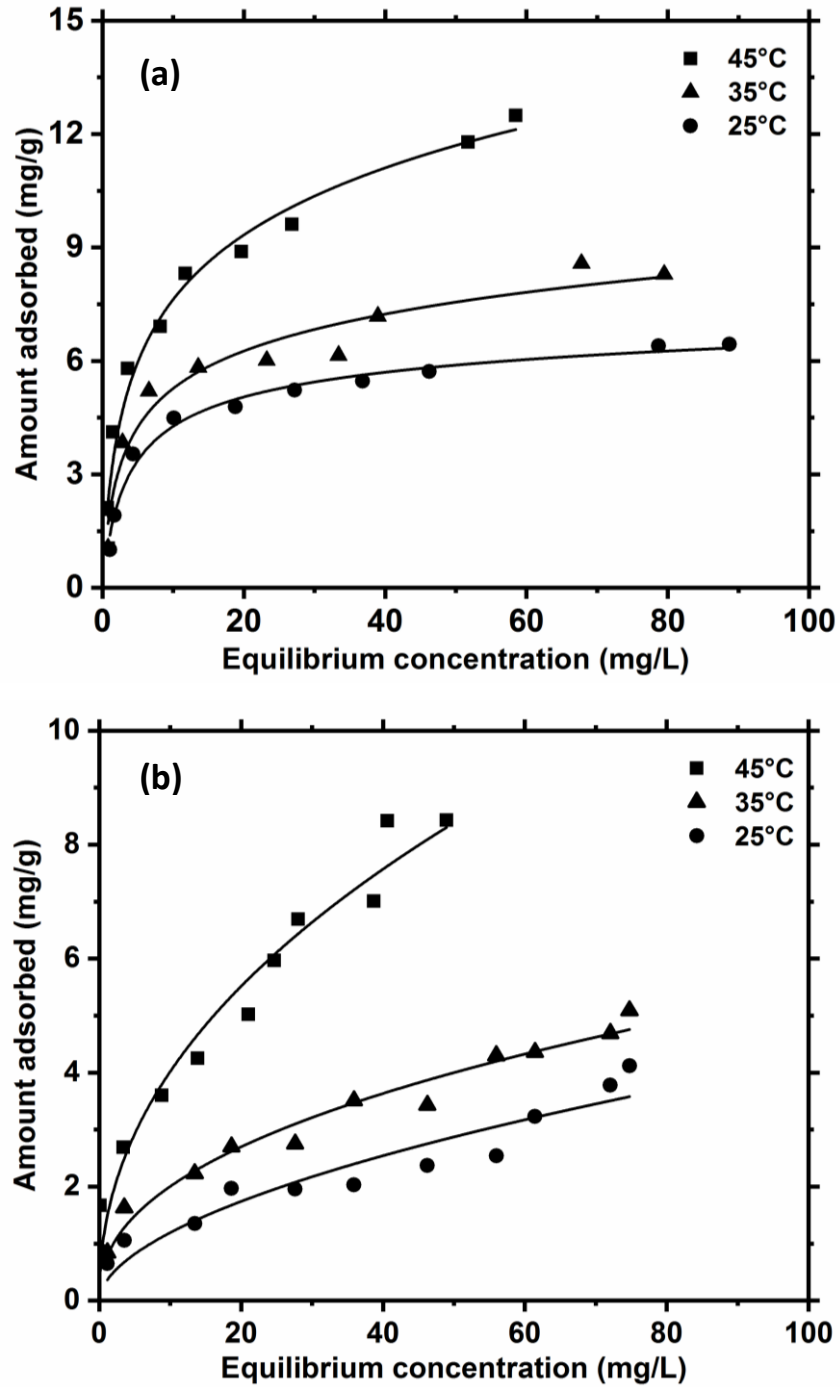
Figure 4.15 Redlich-Peterson adsorption isotherms of carbofuran by (a) CSBC (initial carbofuran concentration= 5-110 mg/L; dose= 5 g/L) and (b) CCBC (Initial carbofuran concentration= 5-100 mg/L; dose= 6g/L) [pH= 6; particle size= 30-50 BSS mesh]
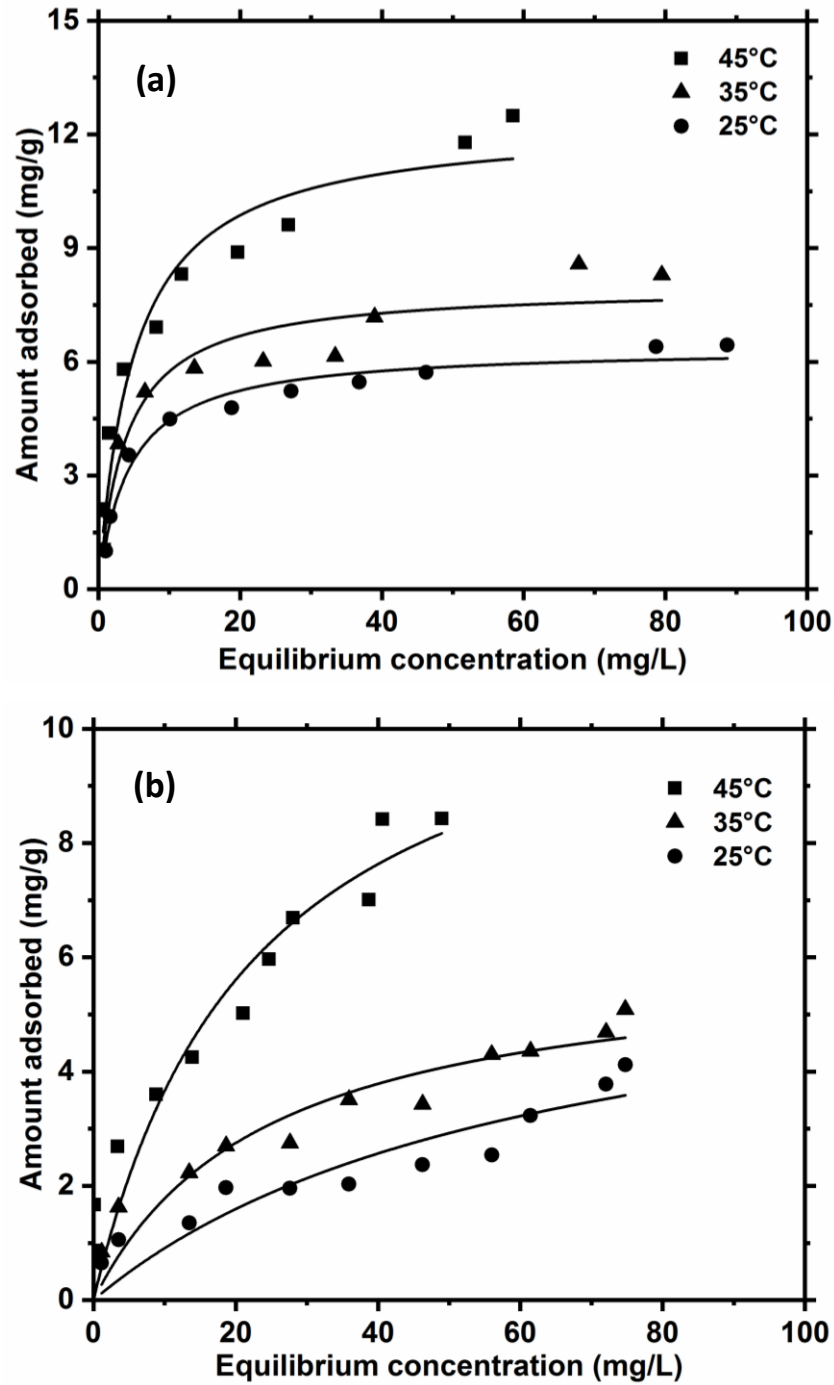
Figure 4.16 Toth adsorption isotherms of carbofuran by (a) CSBC (initial carbofuran concentration= 5-110 mg/L; dose= 5 g/L) and (b) CCBC (Initial carbofuran concentration= 5-100 mg/L; dose= 6g/L) [pH= 6; particle size= 30-50 BSS mesh]
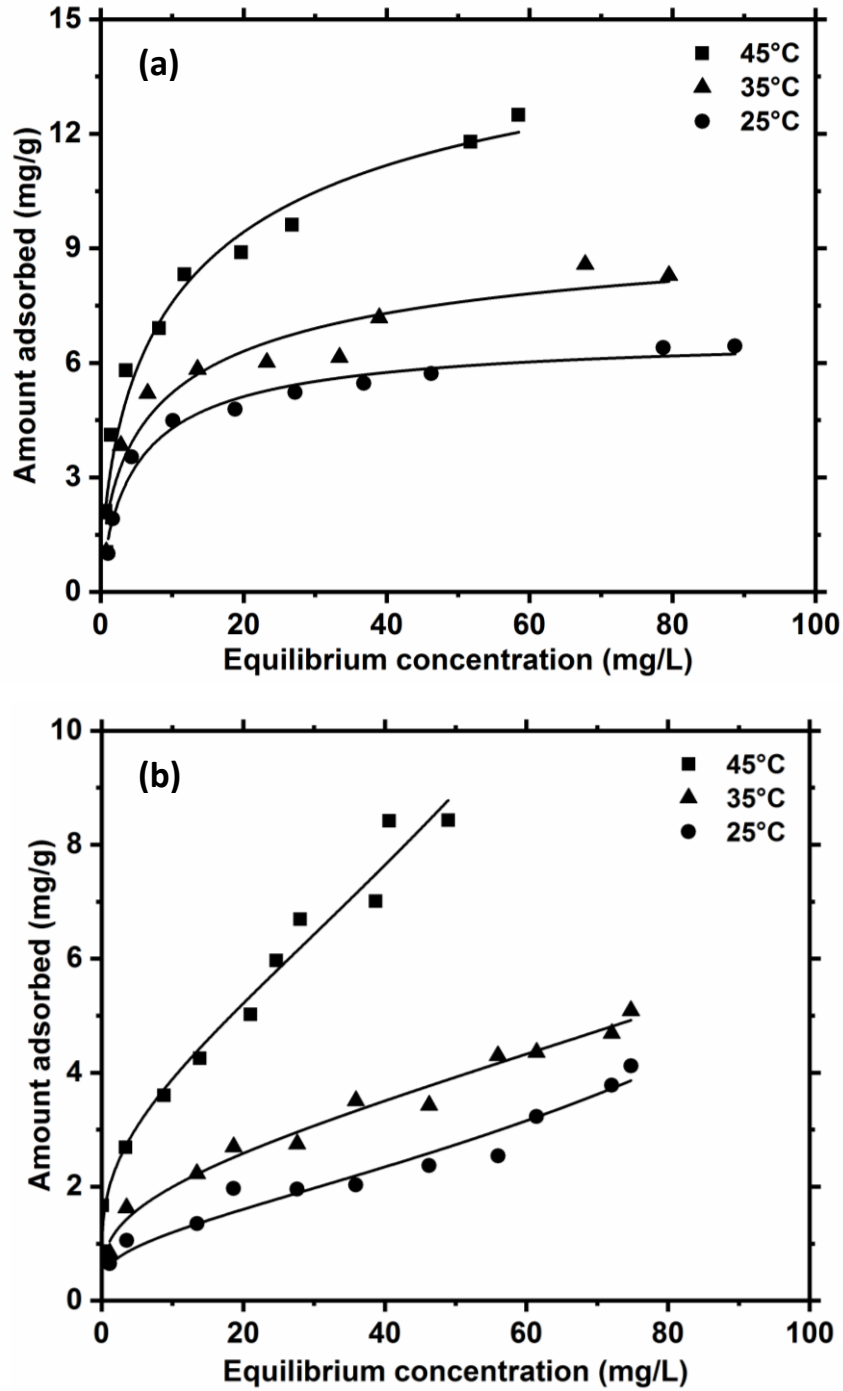
Figure 4.17 Koble-Corrigan adsorption isotherms of carbofuran by (a) CSBC (initial carbofuran concentration= 5-110 mg/L; dose= 5 g/L) and (b) CCBC (Initial carbofuran concentration= 5-100 mg/L; dose= 6g/L) [pH=6; particle size= 30-50 BSS mesh]
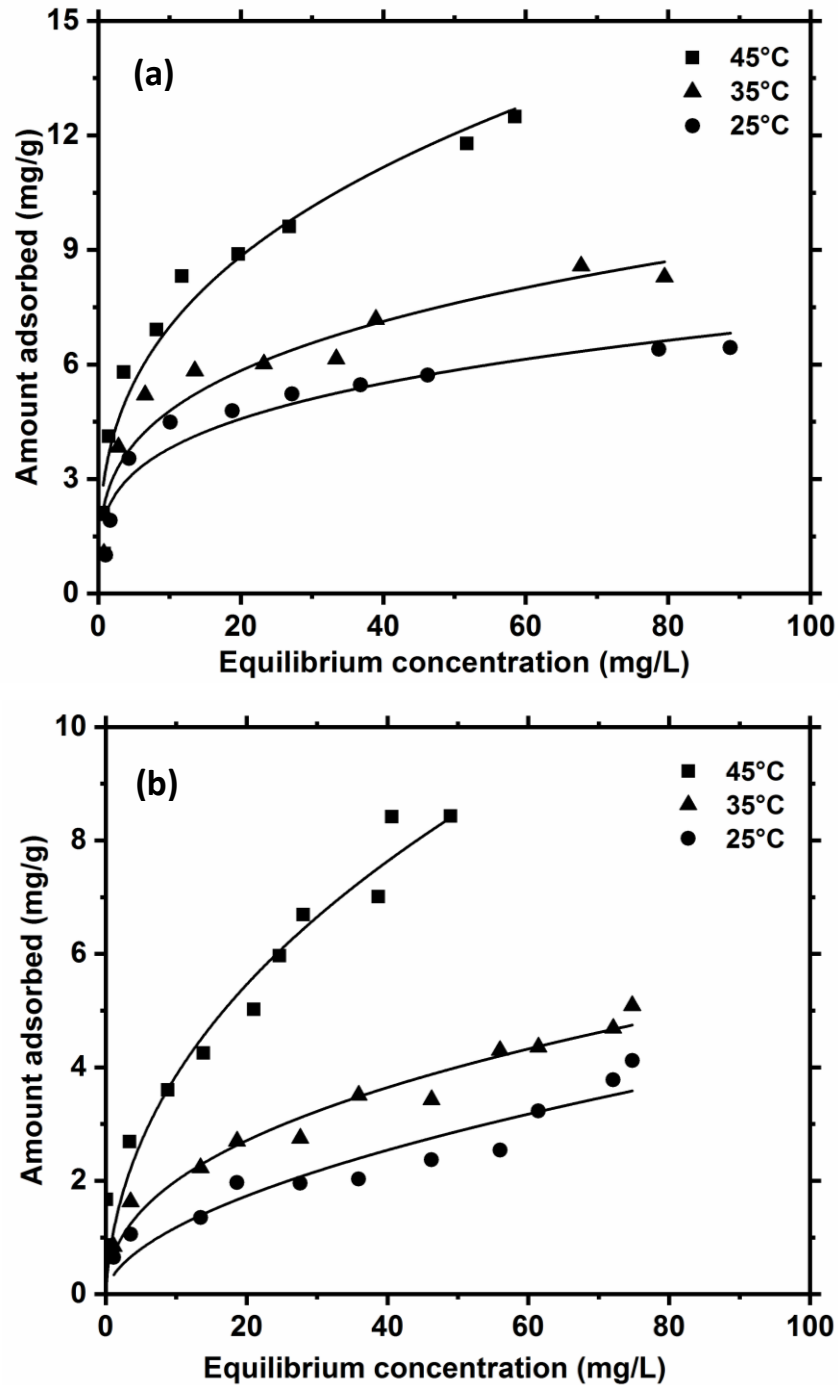
Figure 4.18 Radke-Prausnitz adsorption isotherms of carbofuran by (a) CSBC (initial carbofuran concentration= 5-110 mg/L; dose= 5 g/L) and (b) CCBC (Initial carbofuran concentration= 5-100 mg/L; dose= 6g/L) [pH=6; particle size= 30-50 BSS mesh]

Table 4.5 Adsorption isotherm parameters for adsorption of carbofuran from aqueous solution by CSBC and CCBC at different temperatures

Parameters	Carbofuran adsorption onto CSBC			Carbofuran adsorption onto CCBC		
	25°C	35°C	45°C	25°C	35°C	45°C
Freundlich						
K_F (mg/g)	2.0524	2.4647	3.2026	0.3374	0.7432	1.3989
$1/n$	0.2676	0.2879	0.3385	0.5474	0.4302	0.4577
R^2	0.9207	0.9280	0.9500	0.8950	0.9680	0.9541
Langmuir						
q (mg/g)	6.3876	7.9974	12.3280	6.5705	6.8129	11.9529
b	0.2284	0.2544	0.2003	0.0160	0.0413	0.0441
R^2	0.9753	0.9315	0.9486	0.8291	0.8940	0.9084
Temkin						
a_{Te}	3.2796	3.6420	2.9130	1.1136	1.3645	13.5758
b_{Te}	925.9221	762.7710	494.6891	1.6219	2.1635	2.4392
R^2	0.9795	0.9637	0.9770	0.7510	0.8866	0.7816
Sips						
K_{LF}	0.8619	1.1187	1.5757	0.0705	0.2417	0.5429
a_{LF}	1.9190	2.8063	4.2087	0.0869	0.2011	0.7143
η_{LF}	0.2676	0.2879	0.3385	0.5470	0.4302	0.4575
R^2	0.9208	0.9281	0.9500	0.8950	0.9680	0.9514
Redlich-Peterson						
K_{RP}	1.9435	3.6551	4.8211	10619.4275	12874.4027	157021.9760
a_{RP}	0.4326	0.8455	0.8251	31388.7980	17308.6563	112007.3625
B_{RP}	0.9148	0.8465	0.8098	0.4533	0.5700	0.5429
R^2	0.9850	0.9606	0.9745	0.8950	0.9680	0.9541
Toth						
K_T	1.4596	2.0350	2.4689	0.1052	0.2508	0.5277
B_T	0.2285	0.2545	0.2003	0.0160	0.0412	0.0441
β_T	0.01	0.01	0.01	0.0100	0.0100	0.0100
R^2	0.9753	0.9315	0.9486	0.8219	0.8940	0.9083
Koble- Corrigan						
A	1.6988	2.5393	3.1878	0.2491	0.6558	0.8306
b	0.2482	0.2445	0.1898	-0.5883	-0.3476	-0.5748
η_{KC}	0.8271	0.6154	0.6369	0.0988	0.1697	0.2246
R^2	0.9787	0.9488	0.9686	0.9520	0.9794	0.9733
Radhke-Prausnitz						
a	4.4055	6.0333	1.4578	3.0000	3.0000	3.0000
b	2.0506	2.4606	3.2028	0.3520	0.8393	1.6025
β	0.2679	0.2883	0.3385	0.5415	0.4064	0.4409
R^2	0.9208	0.9281	0.9500	0.8929	0.9642	0.9396

4.6 Thermodynamic parameters

Thermodynamic including change in standard enthalpy ($\Delta H°$), standard entropy ($\Delta S°$) and standard free energy ($\Delta G°$) were calculated. Thermodynamic parameters tells about the nature of adsorption process and its feasibility. Thermodynamic parameters for carbofuran adsorption on CSBC and CCBC are given in table 4.6. Positive value of $\Delta H°$ confirms that the carbofuran adsorption onto CSBC and CCBC was endothermic in nature. Change in standard free energy ($\Delta G°$) values obtained for carbofuran adsorption on CSBC and CCBC were negative at all temperatures. This negative value indicates the spontaneous nature of carbofuran adsorption onto CSBC and CCBC. Positive value of change in standard entropy ($\Delta S°$) shows the increase in randomness as solute and surface interacts (Njoku et al., 2014).

Table 4.6. Thermodynamic parameters for carbofuran adsorption on CSBC and CCBC

Biochars	$\Delta G°$ (KJ mol^{-1})			$\Delta H°$ (KJ mol^{-1})	$\Delta S°$ (KJ/mol^{-1}K^{-1})
	25°C	35°C	45°C		
CSBC	-30.57	-31.87	-32.28	21.18	0.17
CCBC	-23.98	-27.22	-28.28	72.36	0.33

CHAPTER 5

2,4-D ADSORPTION ON CSBC AND CCBC

5.0 Sorption studies for 2,4-Dichlorophenoxyacetic acid (2,4-D) removal

2,4-D sorption onto CSBC (corn stover biochar) and CCBC (corncob biochar) were studied in batch mode. Removal studies were conducted at different pHs, biochar dosages, initial concentration, reaction temperatures and contact time. Batch adsorption experiments were conducted to optimize conditions for 2,4-D adsorption and for describing the mechanisms involved in it.

5.1 Effect of pH

pH is one of the major parameter guiding the adsorption process. Aqueous removal of pesticide 2,4-D is also affected by the solution pH. As seen in Figure 5.1, there is not much variation in percent 2,4-D adsorption onto CSBC with increase in solution pH except for pH 2 to pH 4. But this reduction is comparatively smaller and in order of less than 10%. It is observed that the removal efficiency is 56.67 % at pH 2 and increases to 64.67% at pH 4. Afterwards this removal efficiency remains almost same at pH 6 and 8 i.e. 65.82 and 64.38%, respectively. At pH 10 too, the reduction in percent 2,4-D removal is quite less and hovers at 60.40%. On the other hand, 2,4-D adsorption onto CCBC seems distinct both in terms of trends as well as magnitude. As given in Figure 5.2, the percent 2,4-D adsorption increases from 50.50 % to 57.28% and later to 60.22 % with rise in pH of the solution from 2 to 6. Here, variation in 2,4-D removal efficiency is found to be of significant i.e. 4-10%. At pH beyond 6 i.e. 8 and 10 the removal efficiency takes a bigger dip of more than15% and falls sharply to 44.78 and 43.37%, respectively. The change in equilibrium pH have similar trends for either biochars i.e. slight or no increase, increase, and slight decrease for initial pH 2, pH range 4-8 and pH 10, respectively.

5.2 2,4-D adsorption mechanism onto CSBC and CCBC

Aqueous 2,4-D removal through adsorption onto CSBC and CCBC can be explained through different H-bonding, π-π interaction, porous diffusion and electrostatic interactions [Figure 5.3 (a-d)].

H-bonding between 2,4-D molecule and surface functional groups of CSBC and CCBC is one such mechanism (Essandoh et al., 2017). Oxygen bearing carboxylic and phenolic groups present on biochar surface can form hydrogen bond with carboxylic acid group of 2,4-D and its anion at different pH. Carboxylic acid (-COOH) group of CSBC

and CCBC can act as hydrogen donor as well as hydrogen acceptor using its hydroxyl hydrogen (-OH) and carbonyl oxygen (-C=O), respectively. Similar behavior can be shown by carboxylic acid group of a neutral 2,4-D molecule depending on the pH conditions. When lower pH, 2,4-D exist as neutral molecule and form donor-acceptor H-bond with CSBC and CCBC [Figure 5.3(a)]. Surface phenolic (Ar-OH) groups of biochars can also form donor/acceptor H-bond with 2,4-D at lower pH. Surface phenolic groups can either form donor or acceptor H-bond as they cannot phenolic hydrogen or oxygen at the same time due to stearic hindrance. With increase in solution pH to 4 and 6, the phenoxyacetate ion prevails which forms phenolic donor H-bond with biochars. Even at higher pH i.e. pH > pHzpc of biochars, 2,4-D forms carboxylate acceptor H-bond with biochars. But at higher pH, 2,4-D removal may also decrease sharply as anions of both biochars and 2,4-D are devoid of hydrogen required for H-bonding and due to effective repulsion caused by negative charge over them. Hydrogen bond between –OH and carboxylate or phenolate anions of biochars is stronger than that of between –OH and neutral carboxylic or phenolic groups. Apart from this, pH independent between graphene like surface of biochars and π-electrons of aromatic ring of 2,4-D can also assist in adsorption [Figure 5.3 (b)]. Adsorption of 2,4-D onto CSBC and CCBC is also assisted by porous diffusion. CSBC and CCBC with BET surface area 204.9 and 222.9 m^2/g, respectively and abundance of micro, meso and macro pores are very much effective in 2,4-D adsorption [Figure 5.3 (c)].

pKa value of 2,4-D (2.81) and net surface charge over CSBC and CCBC determined by their pHzpc are major factors affecting the electrostatic interactions. 2,4-D, being a weak acid tends to stay in neutral form at pH below 2.81 but beyond mentioned pH it dissociates into phenoxyacetate anion and becomes increasingly negative with increase in pH. CSBC (pHzpc-7.90) and CCBC (pHzpc-7.75), on the other hand have net positive surface charge at pH below their pHzpc and become negatively charged above it. At pH 2, the neutral 2,4-D molecule encounters insufficient attraction to positively charged biochar surface causing lesser percent 2,4-D removal. With increase in pH from 2-6, phenoxyacetate anion from 2,4-D dissociation (pH > pKa) is attracted to positively charged surfaces of CSBC and CCBC. Hence, gradual rise in 2,4-D removal is observed at this pH range. At pH 8 and onwards, the net charge over biochars becomes

negative and experiences repulsion from negatively charged 2,4-D anion which possibly causes fall in removal efficiency of CSBC and CCBC [Fig 5.3 (d)]. It may be concluded that the trend of variation in percent 2,4-D removal with change in pH is combined outcome of different H-bonding and π-π interactions along with electrostatic interactions.

5.3 Sorption kinetic studies for 2,4-D removal

Kinetic studies for 2,4-D adsorption onto CSBC and CCBC were carried out at different biochar doses and initial 2,4-D concentrations.

5.3.1 Effect of biochar doses on 2,4-D removal

Dose kinetic studies for 2,4-D removal by CSBC was carried out at adsorbent dose of 2.5, 5 and 7 g/L. Here, percent 2,4-D removal increased with time and reached up to 50, 67 and 76 % for the CSBC doses respectively after 24 hours [Figure 5.4 (a)]. Most of adsorption was completed within 8 hours but 2,4-D removal continued to increase with time afterwards. This trend can be attributed to the longer interaction between 2,4-D and biochar surfaces with rise in contact time. With increases in the dose from 2.5 to 5 g/L the adsorption capacity decreased from 2.21 to 1.50 mg/g. It further decreases from 1.50 to 1.22 mg/g with increases in CSBC dose from 5 to 7 g/L.

Dose kinetics studies for 2,4-D adsorption onto CCBC were conducted at 3, 5 and 7 g/L. Percent 2,4-D adsorption was 40% at CCBC dose of 3 g/L which increased up to 50% with increase in CCBC dose to 5 g/L. Further rise in biochar dose to 7 g/L resulted into 2,4-D removal increasing up to 60% [Figure 5.4 (b)]. Here too, the adsorption capacity decreases with increase in adsorbent dose i.e. 1.28, 0.89 and 0.64 mg/g at CCBC dose 3, 5 and 7 g/L, respectively (figure 5.4). The increase in percent 2,4-D removal by CSBC and CCBC can be attributed to more availability of specific adsorption sites at their higher doses. Similar results were obtained by Bazrafshan et al., 2013.

5.3.2 Effect of initial concentration on 2,4-D removal

In kinetic sorption studies at initial 2,4-D concentrations of 5, 10 and 20 mg/L, CSBC showed percent removal of 84, 76 and 73%, respectively at the end of 24 hours. Similar results were obtained for 2,4-D adsorption onto CCBC where percent removal shows a decrease from 75% to 62% with rise in concentration from 5 to 10 mg/L. On further increasing the initial conc. to 20 mg/L, this percent removal further dips to 59%

Increase in adsorption capacities of CSBC and CCBC were observed with rise in initial concentration. Adsorption capacity (qe) of CSBC was found to be 0.93, 1.37 and 1.92 mg/g at 2,4-D concentrations of 5, 10 and 20 mg/L [Figure 5.5 (a)]. Similarly, adsorption capacity of CCBC was found to be 0.50, 0.85 and 1.59 mg/g at 2,4-D concentration of 5, 10 and 20 mg/L, respectively [Figure 5.5 (b)]. Thus, biochars adsorption capacities were found to be in positive correlation with initial 2,4-D concentration. This relationship between the adsorption capacities of biochars and initial concentration can be attributed to the higher concentration gradient which drives the adsorption process to greater sorption capacities of biochars. Similar results were obtained by different research groups (Gupta et al., 2006; Essandoh et al., 2017). It was also observed that more than 50% of 2,4-D adsorption by CSBC and CCBC was complete by end of 8 hours with significant adsorption afterwards too.

5.4. Kinetic modelling

Pseudo-first order and Pseudo-second order kinetic equation were applied to the experimental kinetic data. The best fit equation was selected on the basis of agreement between experimental and theoretical values along with regression coefficients. The feasibility of sorption process along with nature of sorption i.e. physical adsorption or chemical adsorption is described by these kinetic models.

5.4.1 Pseudo-first order kinetic model

Results obtained from kinetic sorption studies at different biochar doses and initial 2,4-D concentration are assessed using pseudo-first order kinetic equation. The rate constants (K_1), adsorption capacities (qe) obtained through kinetic model and correlation coefficients (R^2) for adsorption of 2,4-D onto CSBC and CCBC are provided in Table 5.1-5.4. As mentioned in the tables, the experimental qe value doesn't seems to be near qe value obtained by pseudo-first order model. Also, the value of correlation coefficient is quite away from one which denotes that the experimental data is not in agreement with the data obtained through pseudo-first order rate equations. Linear pseudo first order kinetic plots [log (qe-qt) vs t] for 2,4-D adsorption onto CSBC and CCBC at different dose and initial concentration are given in Figure 5.7 (a, b) and 5.8 (a, b), respectively. Thus, pseudo-first order rate equation cannot explain 2,4-D adsorption kinetic onto CSBC and CCBC.

5.4.2 Pseudo-second order kinetic model

Results obtained from kinetic sorption studies at different biochar doses and initial conc. were also fitted to pseudo-second order kinetic equation. The rate constants (k_2), adsorption capacities (q_e) obtained through kinetic model and correlation coefficients (R^2) for adsorption of 2,4-D onto CSBC and CCBC are provided in Table 5.1-5.4. It is clear from these tables that experimental q_e value is very close to q_e value obtained by pseudo-second order model. Here value of correlation coefficient is found to be very close to unity ($R^2 > 0.99$) at almost all biochar doses and initial concentrations. Closeness of R^2 value to 1 suggests that the pseudo-second order rate model fits the kinetic data well. Thus, experimental data is in agreement with the data obtained through pseudo-second order rate equations.

Linear pseudo-second order kinetic plots [t/q_t vs t] for 2,4-D adsorption onto CSBC and CCBC at different dose and initial concentration are given in Figure 5.8 (a, b) and 5.9 (a, b), respectively. Thus, on the basis of better fitting of kinetic data to pseudo second order rate equation, it can be concluded that chemisorption is the rate limiting step in 2,4-D adsorption onto CSBC and CCBC.

5.5. Sorption isotherm studies for 2,4-D removal

2,4-D adsorption isotherm studies on CSBC and CCBC were conducted at 25, 35 and 45°C [Figure 5.10 (a, b). Isotherms studies for 2,4-D adsorption on CSBC and CCBC were performed at biochar dose of 7 g/L and initial conc. of 5-110 mg/L at pH 6. Optimized pH i.e. 6 was used for all the isotherm experiments. More than 50% of final absorption was completed within 8 hours. After 8 hours, adsorption process continued with slow pace till equilibrium was reached after 24 hour.

5.5.1 Isotherm modelling

Freundlich, Langmuir, Temkin, Sips, Redlich-Peterson, Toth, Koble-Corrigan and Radke-Prausnitz isotherm models were used to fit the data obtained from equilibrium studies.

The non-linear Freundlich plots for 2,4-D adsorption onto CSBC and CCBC are given in Figure 5.11 (a) and (b), respectively. Parameters from Freundlich and other isotherms for 2,4-D adsorption are given together in Table 5.5. Freundlich isotherm fits well to both 2,4-D adsorption onto CSBC as well as CCBC with regression coefficient,

R^2 being more than 0.96 at all temperatures. Also, chemisorption as driving step can be confirmed by value of 1/n being less than 1 (Foo and Hameed, 2010).

Non-linear Langmuir plots for 2,4-D adsorption onto CSBC and CCBC are given in Figure 5.12 (a) and (b), respectively. Langmuir isotherm model provide information about adsorption capacities of the adsorbent. Specific parameters acquired from this model is also useful in determining thermodynamic particulars of sorption process. As per assumptions Langmuir adsorption is monolayer. So, the adsorption capacity obtained through Langmuir isotherm is called monolayer adsorption capacity. Monolayer adsorption capacities for CSBC (6.77 mg/g at 25°C, 6.82 mg/g at 35°C and 8.18 mg/g at 45°C) and CCBC (5.17 mg/g at 25°C, 4.97 mg/g at 35°C and 5.29 mg/g at 45°C) were calculated. Increase in adsorption capacities with rise in temperature was not very significant. This small increase in adsorption with temperature indicates endothermic nature of adsorption. CCBC is better fitted to Langmuir isotherm model than CSBC at all temperatures. Similar results of minor change in adsorption capacities with increase in temperature has also been reported by Essandoh et al., 2017.

Temkin isotherm plots for biochars CSBC and CCBC are given in Figure 5.13 (a) and (b), respectively. 2,4-D adsorption onto CCBC ($R^2 > 0.96$) is better fitted to the Temkin isotherm model than 2,4-D adsorption onto CSBC ($R^2 < 0.92$). One significant inference derived from this model is endothermic nature of this adsorption process as value of b_{Te} is positive (Inam et al., 2017).

Plots with Sips isotherm fitting for 2,4-D adsorption on CSBC and CCBC are given in Figure 5.14 (a) and (b), respectively. It is observed that the Sips isotherm model fits the 2,4-D adsorption data well with $R^2 > 0.96$ for both the biochars and at all the temperatures. Adsorption data is excellently fitted by Redlich-Peterson ($R^2 > 0.98$), Koble-Corrigan ($R^2 > 0.98$) and Radke-Prausnitz ($R^2 > 0.98$) isotherms and are given in Figure [5.15 (a), (b)], [5.17 (a), (b)], and [5.18 (a), (b)] respectively. Toth [5.16 (a), (b)] isotherm model also fit the adsorption data with reasonable R^2 value which is more than 0.90 for both biochars and at all temperatures.
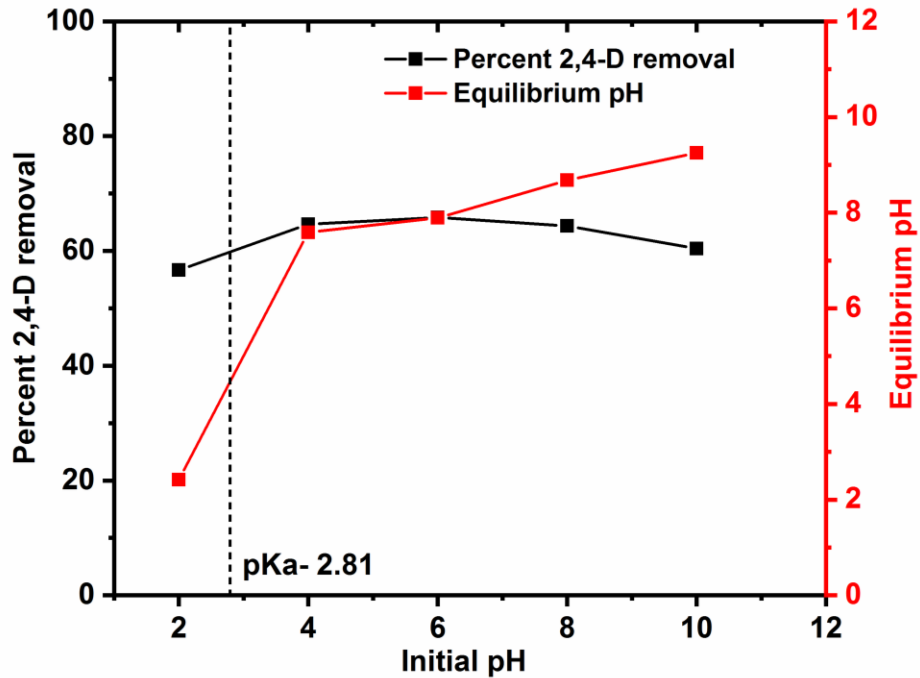
Figure 5.1 Effect of pH on 2,4-D removal by CSBC [Initial concentration= 10 mg/L; CSBC dose= 5 g/L;T= 25°C].
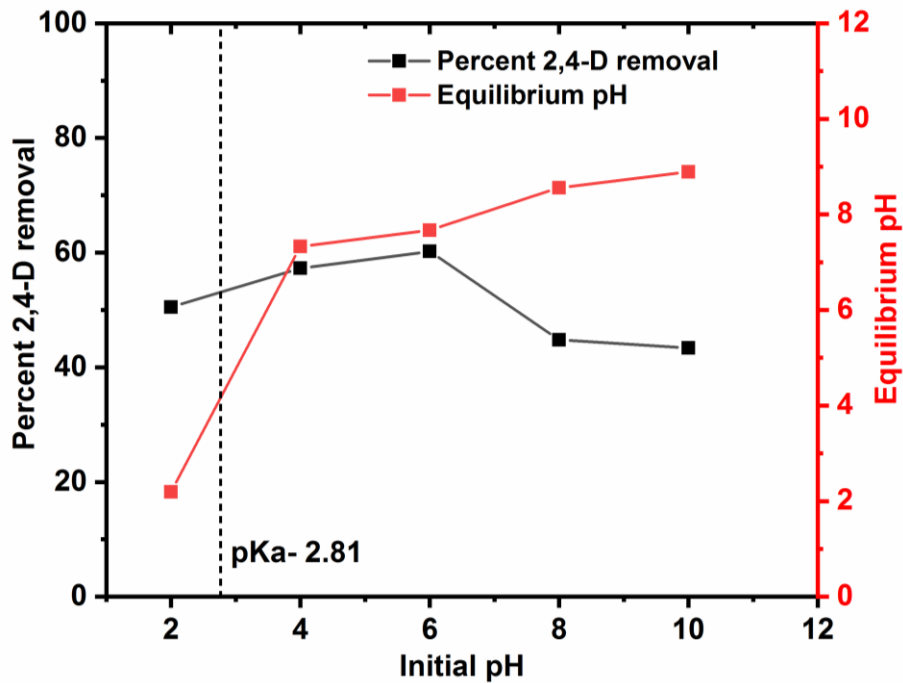
Figure 5.2 Effect of pH on 2,4-D removal by CCBC [Initial concentration= 10 mg/L; CSBC dose= 5 g/L;T= 25°C].

118
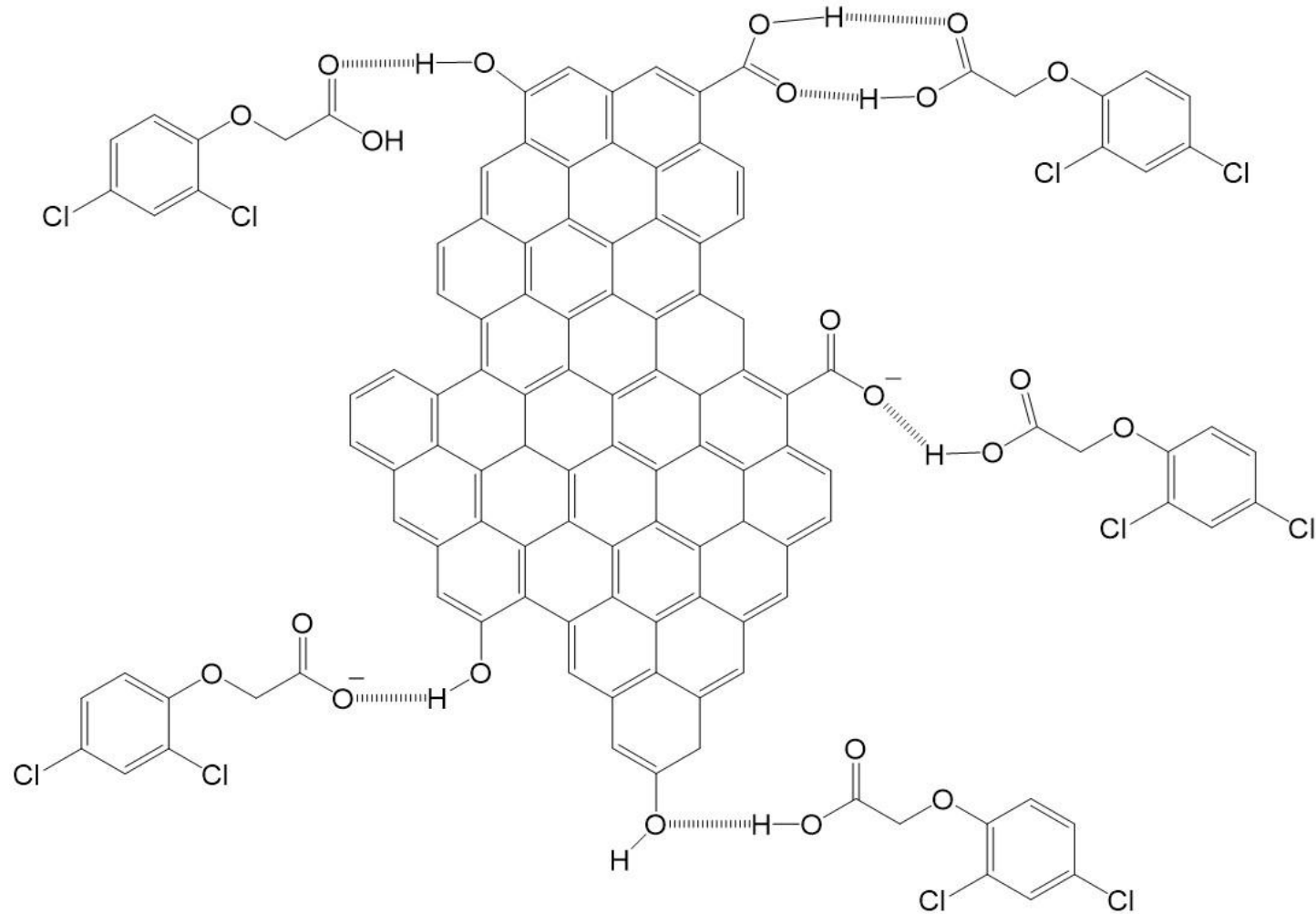
Figure 5.3 (a) Sorption of 2,4-D onto biochar surface through various H-bonding.
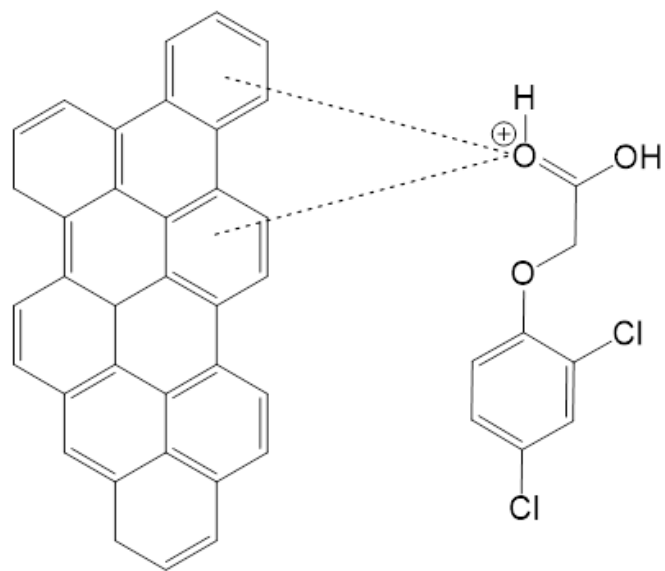
Figure 5.3 (b) Sorption of 2,4-D onto biochar through π-π interaction.
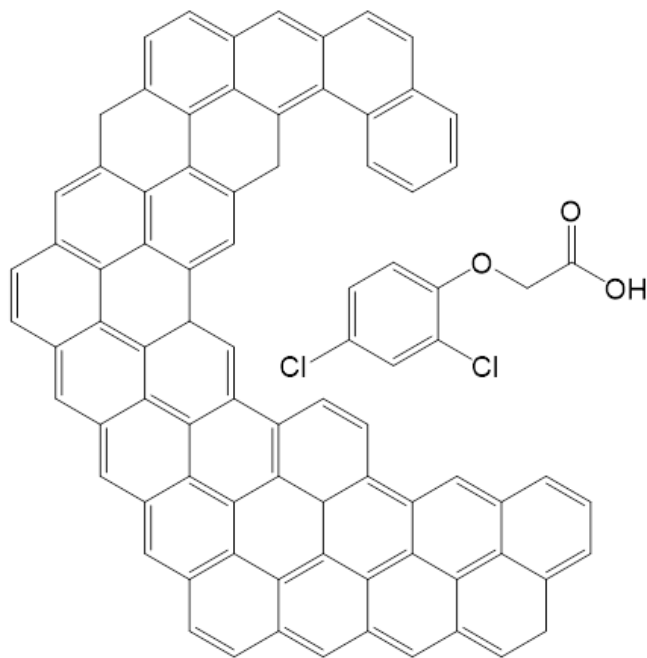
Figure 5.3 (c) Sorption of 2,4-D onto biochar through pore diffusion.
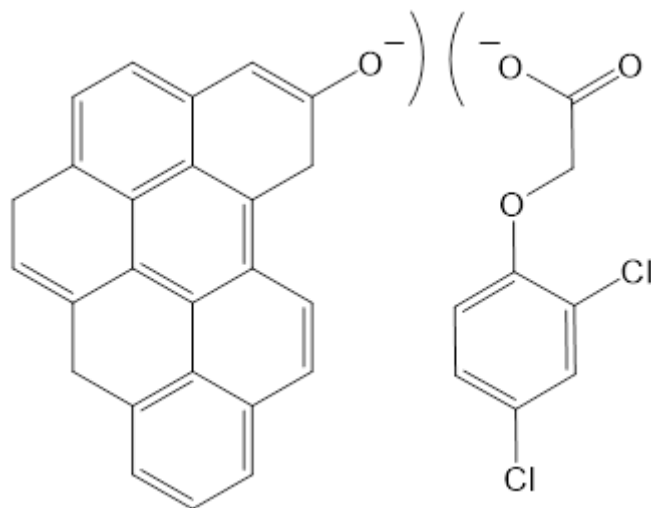
Figure 5.3 (d) Repulsion between 2,4-D and biochar at strongly basic pH
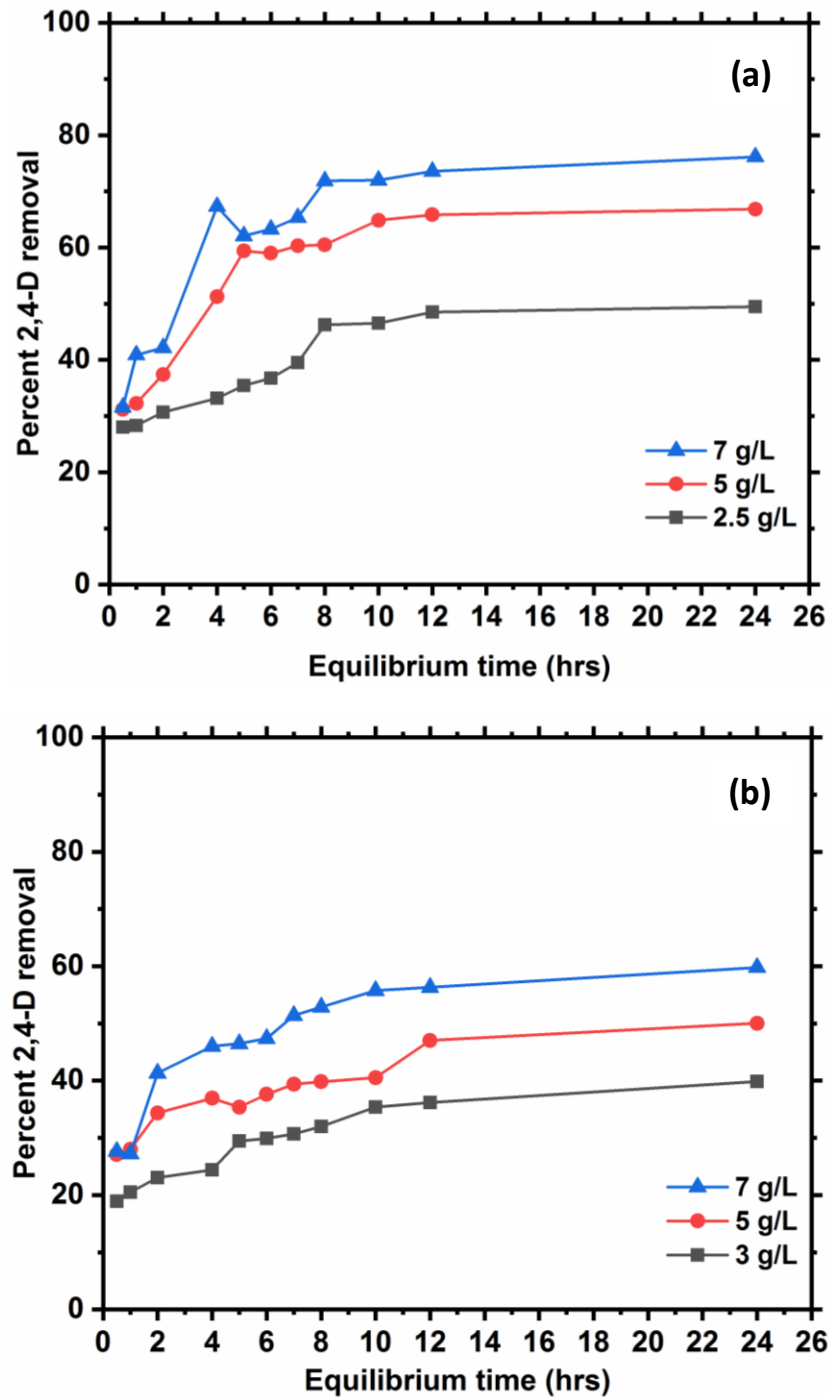
Figure 5.4 Effect of different adsorbent doses on 2,4-D removal by (a) CSBC and (b) CCBC [pH= 6; initial concentration= 10 mg/L; T= 25°C].
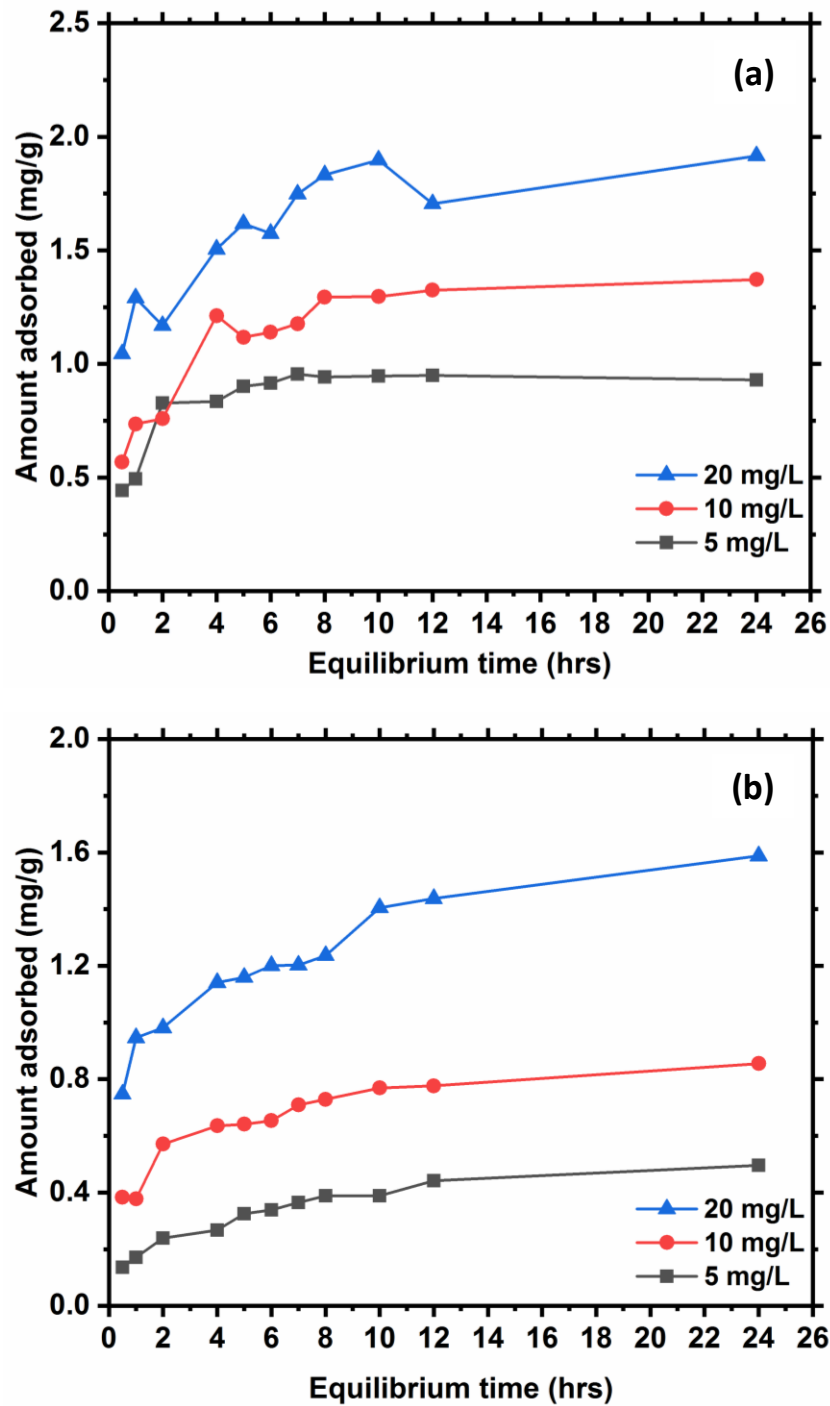
Figure 5.5 Effect of different initial concentration on 2,4-D removal by (a) CSBC (dose= 7 g/L)and (b) CCBC (dose= 7 g/L) [pH= 6; T= 25°C]
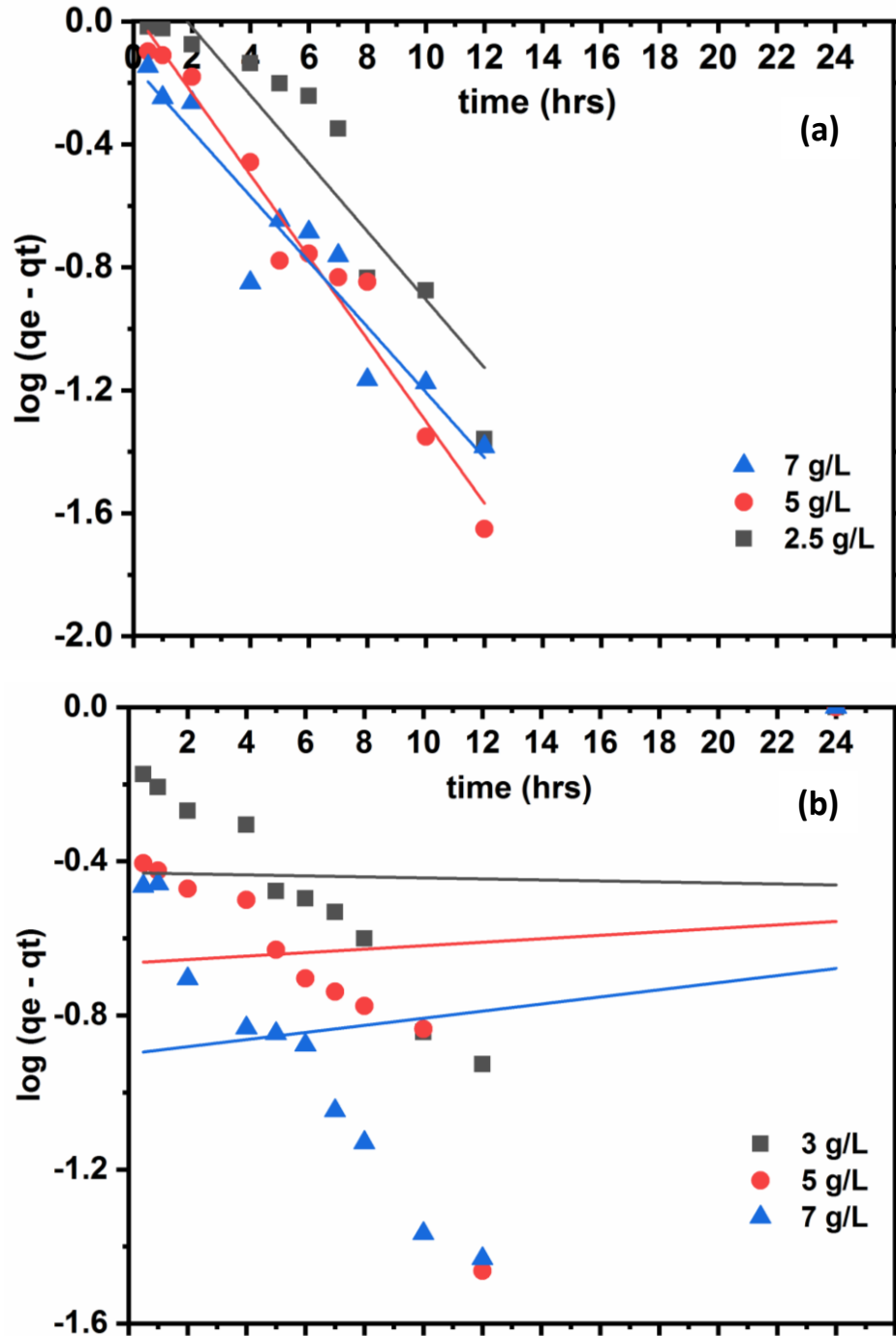
Figure 5.6 Pseudo-first order kinetic plots for 2,4-D removal by (a) CSBC and (b) CCBC at different adsorbent doses [pH= 6; initial concentration= 10 mg/L; T= 25°C]
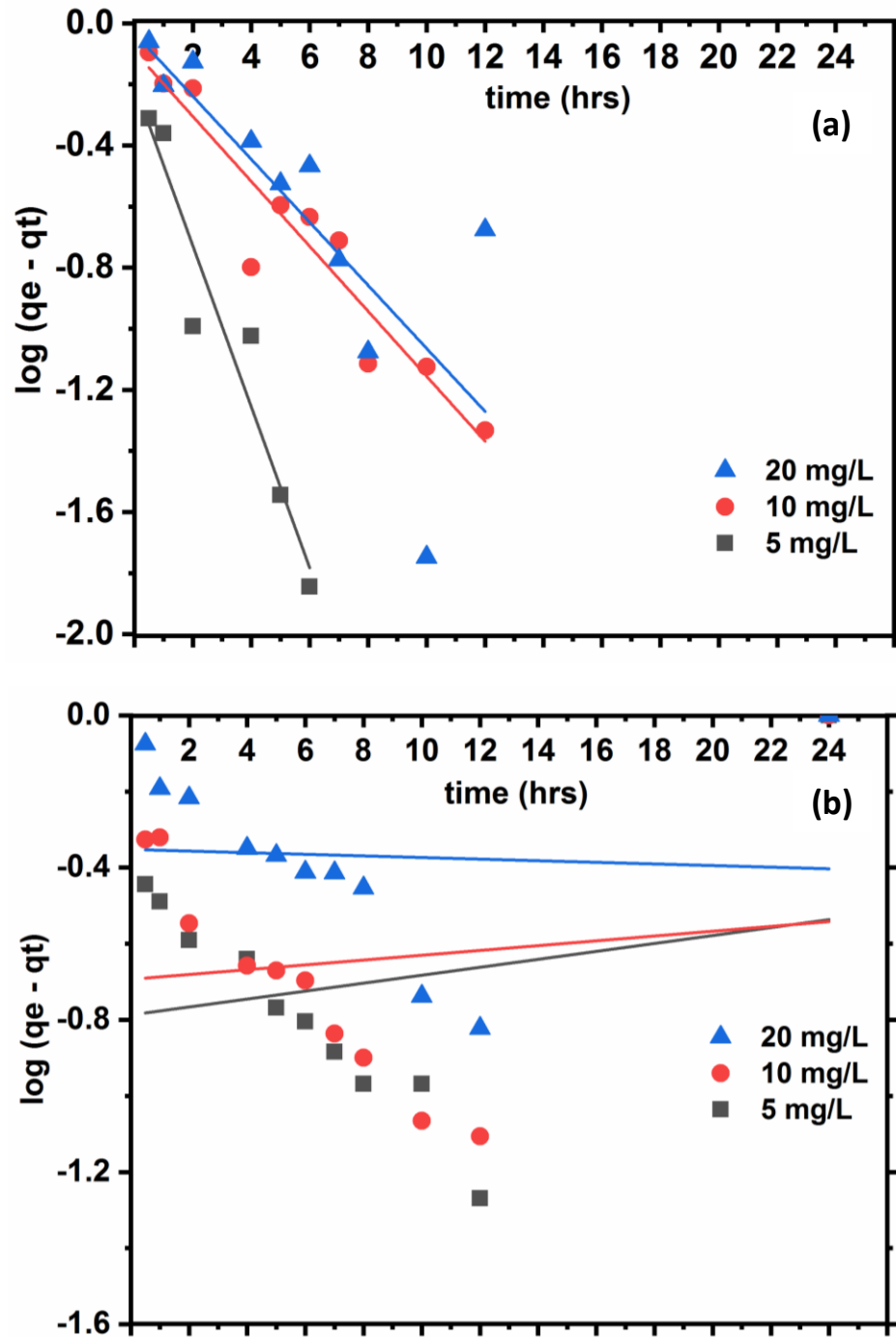
Figure 5.7 Pseudo-first order kinetic plots for 2,4-D removal by (a) CSBC (dose= 7 g/L) and (b) CCBC (dose= 7 g/L) at different initial concentration [pH= 6; T= 25°C]
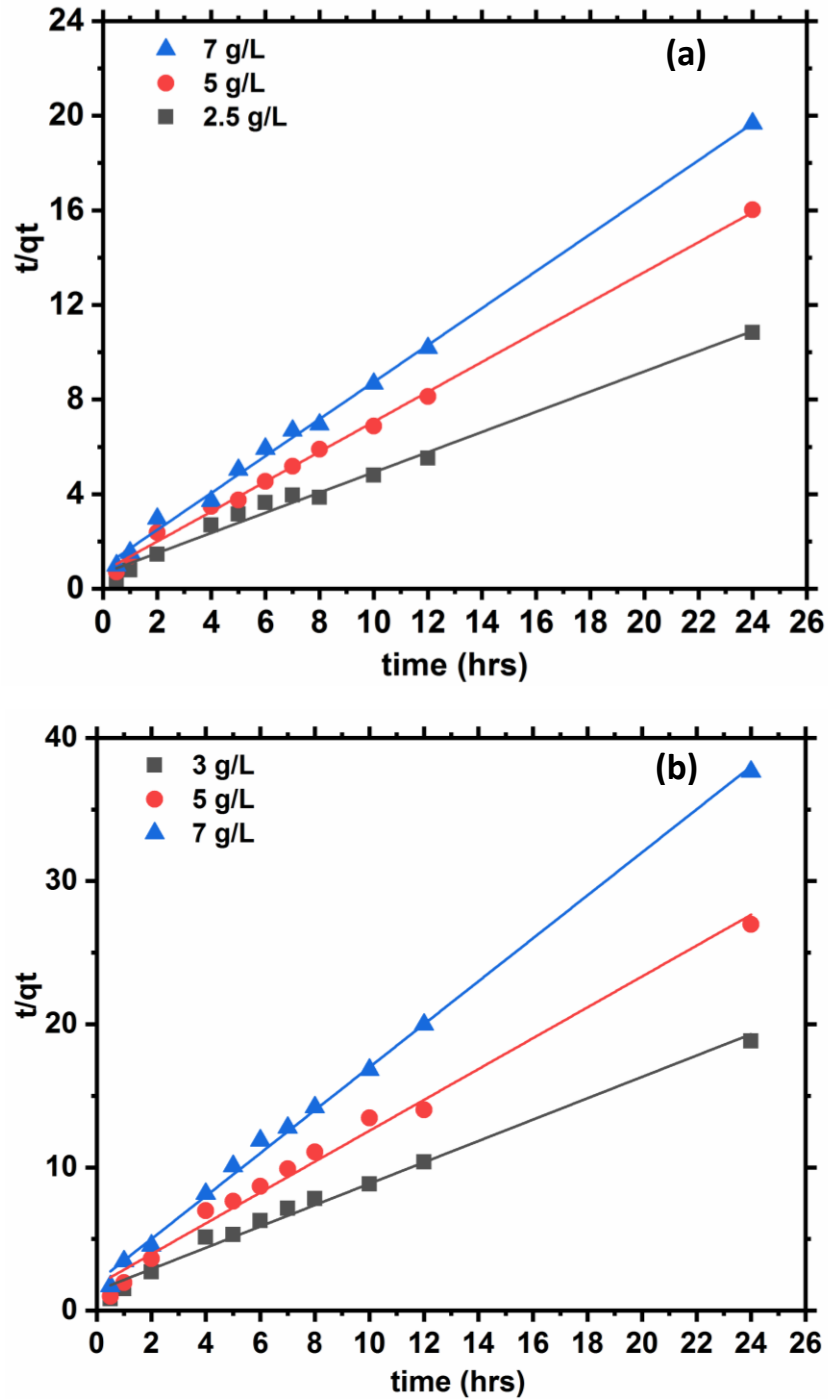
Figure 5.8 Pseudo-second order kinetic plots for 2,4-D removal by (a) CSBC and (b) CCBC at different adsorbent doses [pH= 6; initial concentration= 10 mg/L; T= 25°C]
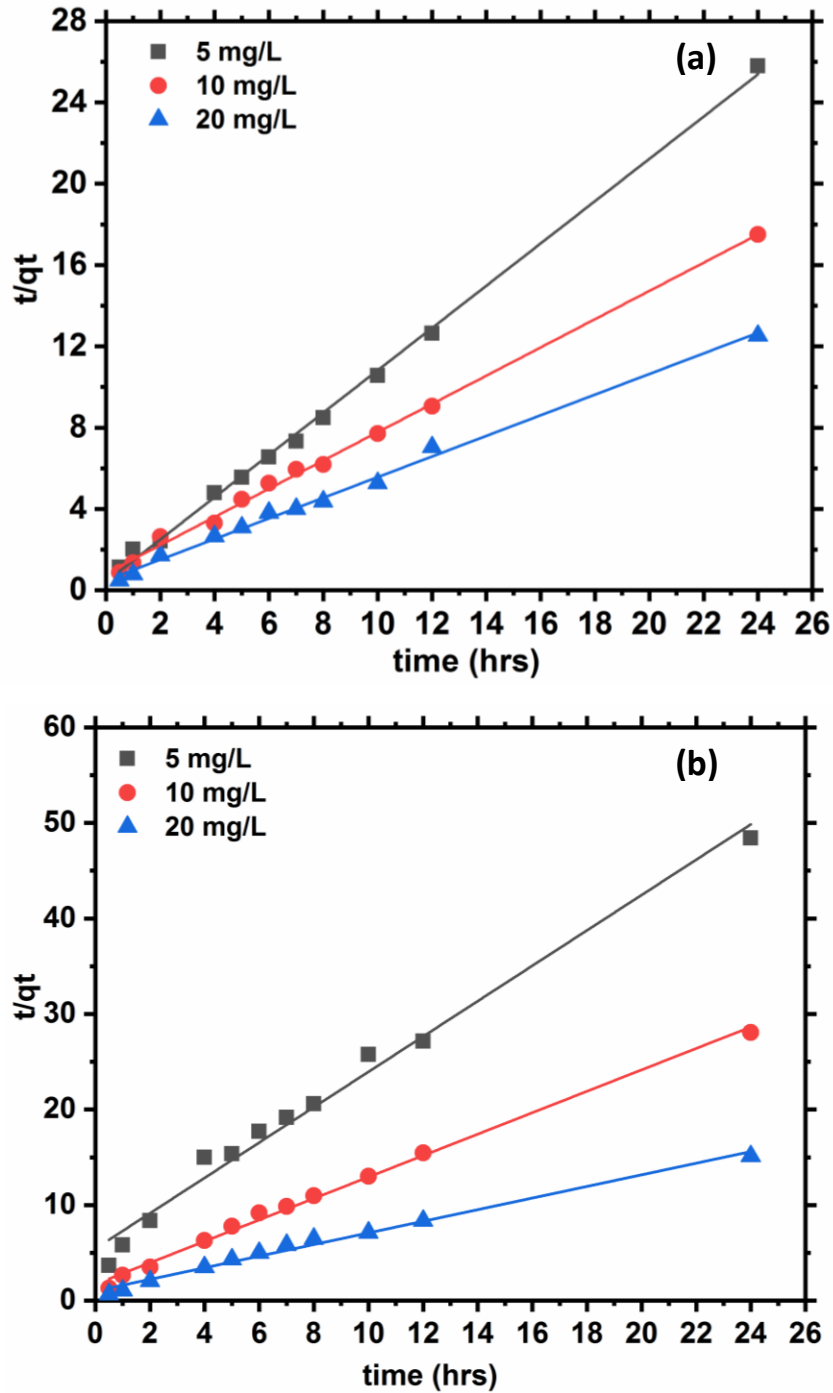
Figure 5.9 Pseudo-second order kinetic plots for 2,4-D removal by (a) CSBC (dose= 7 g/L) and (b) CCBC (dose= 7 g/L) at different initial concentration [pH= 6; T= 25°C]

Table 5.1 Pseudo-first order and pseudo-second order rate parameters and its comparison with experimental q_e for aqueous 2,4-D removal at different CSBC doses.

Dose (g/L)	Pseudo-first order rate constant, k_1 (h^{-1})	R^2	Pseudo-second order rate constant, k_2 (g mg^{-1} h^{-1})	R^2	q_e experimental (mg/g)	q_e, calculated using first order kinetic model (mg/g)	q_e, calculated using second order kinetic model (mg/g)
2.5	0.2552	0.8467	8.3851	0.9881	2.215	1.5988	2.3430
5	0.3075	0.9673	3.4145	0.9976	1.499	1.0829	1.5805
7	0.2448	0.9095	1.7747	0.9972	1.220	1.3893	1.2799

Table 5.2 Pseudo-first order and pseudo-second order rate parameters and its comparison with experimental q_e for aqueous 2,4-D removal of by CSBC at different initial concentration.

Conc. (mg/L)	Pseudo-first order rate constant, k_1 (h^{-1})	R^2	Pseudo-second order rate constant, k_2 (g mg^{-1} h^{-1})	R^2	q_e experimental (mg/g)	q_e, calculated using first order kinetic model (mg/g)	q_e, calculated using second order kinetic model (mg/g)
5	0.5446	0.9265	2.2418	0.9981	0.93	1.7246	0.9612
10	0.2450	0.9095	2.5160	0.9971	1.37	1.2345	1.4386
20	0.2377	0.6018	7.9416	0.9946	1.92	1.0760	1.9704

Table 5.3 Pseudo-first order and pseudo-second order rate parameters and its comparison with experimental q_e for aqueous 2,4-D removal at different CCBC doses.

Dose (g/L)	Pseudo-first order rate constant, k_1 (h^{-1})	R^2	Pseudo-second order rate constant, k_2 ($g\,mg^{-1}\,h^{-1}$)	R^2	q_e experimental (mg/g)	q_e, calculated using first order kinetic model (mg/g)	q_e, calculated using second order kinetic model (mg/g)
3	0.0030	0.0009	1.2811	0.9889	1.28	2.6910	1.3405
5	0.1036	0.0068	0.4835	0.9878	0.89	4.6132	0.9279
7	0.0212	0.0213	0.2232	0.9972	0.64	7.9360	0.6664

Table 5.4 Pseudo-first order and pseudo-second order rate parameters and its comparison with experimental q_e for aqueous 2,4-D removal by CCBC at different initial concentration.

Concentration (mg/L)	Pseudo-first order rate constant, k_1 (h^{-1})	R^2	Pseudo-second order rate constant, k_2 ($g\,mg^{-1}\,h^{-1}$)	R^2	q_e experimental (mg/g)	q_e, calculated using first order kinetic model (mg/g)	q_e, calculated using second order kinetic model (mg/g)
5	0.0240	0.0424	0.6294	0.9851	0.50	6.1250	0.5404
10	0.0145	0.0156	0.7314	0.9955	0.85	4.9374	0.8915
20	0.0048	0.0031	0.3661	0.9887	1.59	2.2500	1.6447
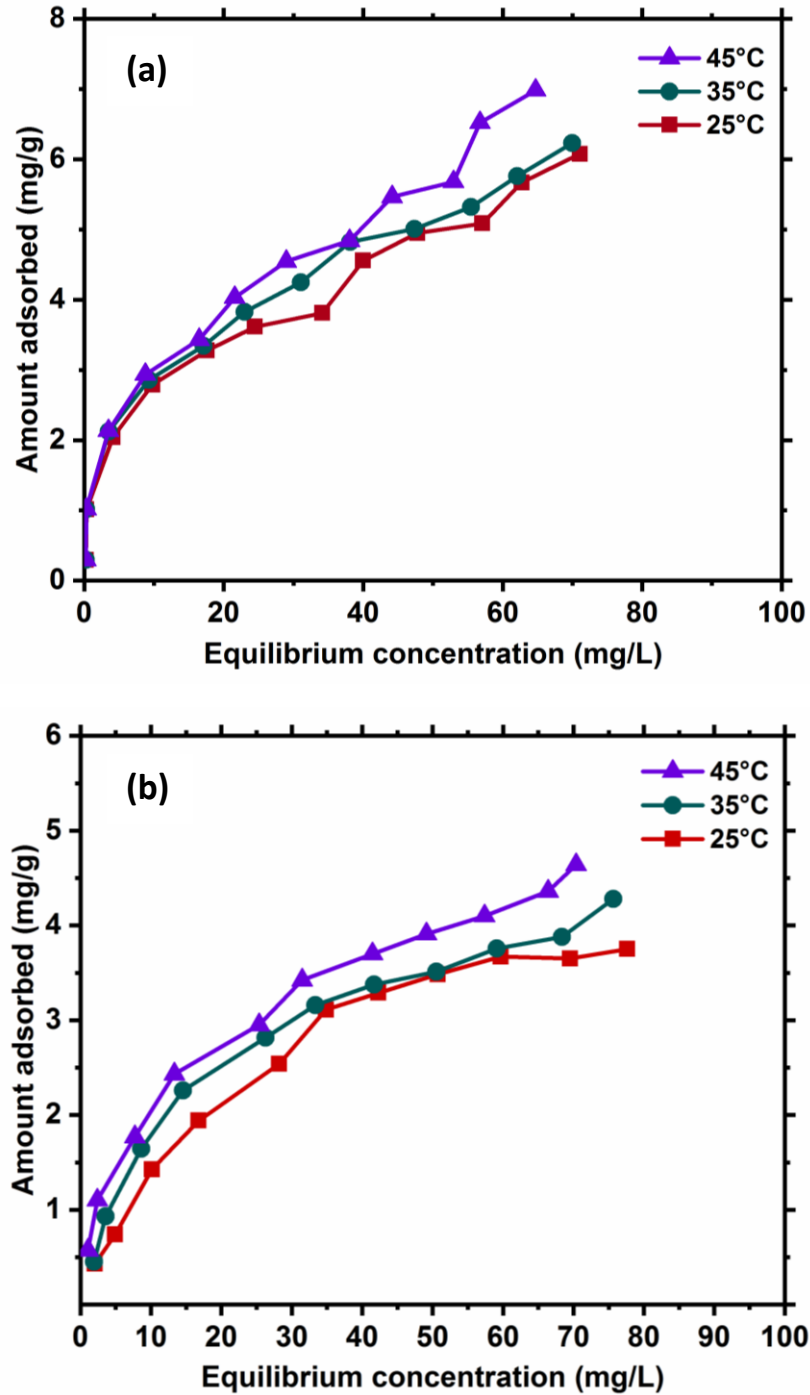
Figure 5.10 Effect of temperature on the 2,4-D removal by (a) CSBC (initial concentration= 5-110 mg/L; dose= 7 g/L) and (b) CCBC (Initial concentration= 5-105 mg/L; dose= 7 g/L) [pH=6; particle size= 30-50 BSS mesh]
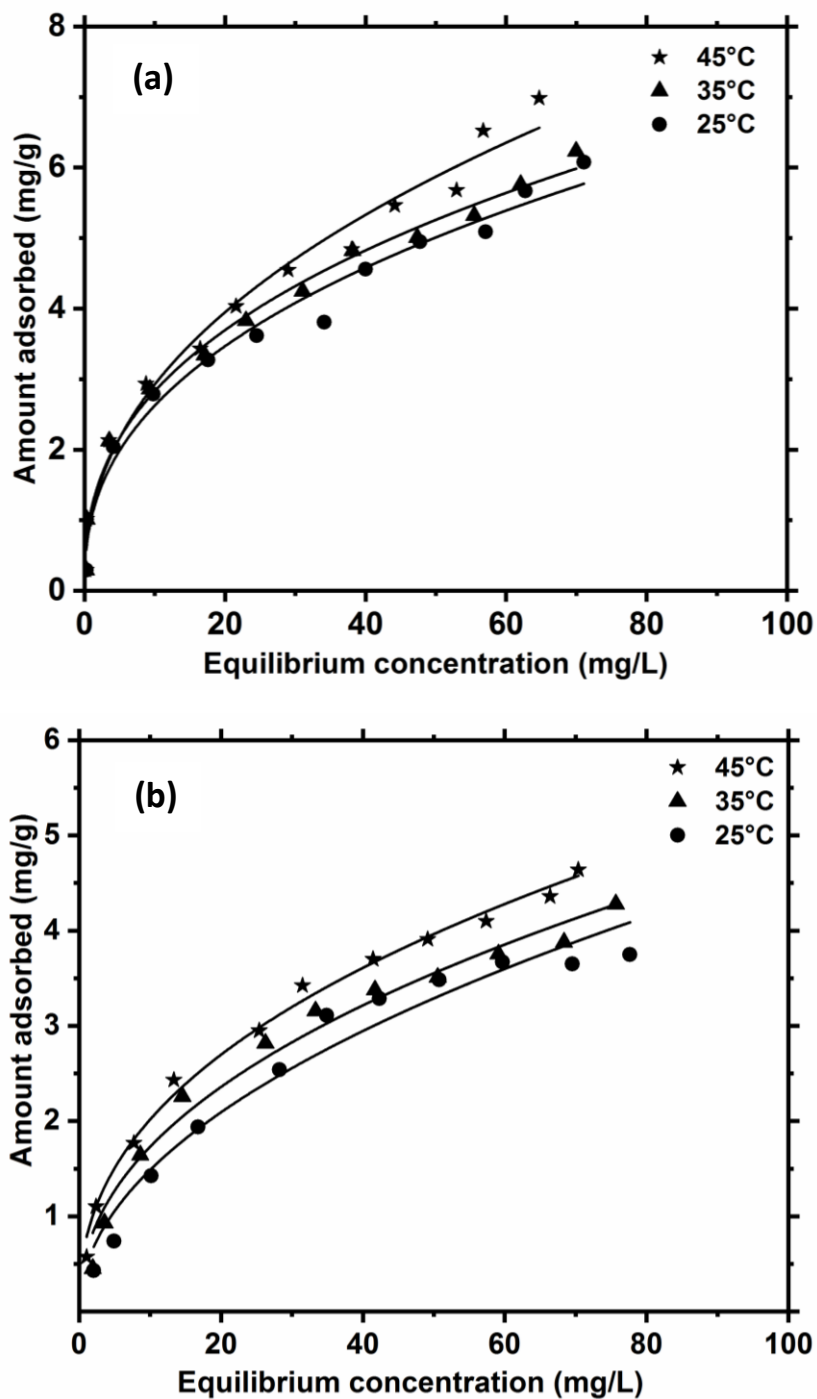
Figure 5.11 Freundlich adsorption isotherms of 2,4-D by (a) CSBC (initial concentration= 5-110 mg/L; dose= 7 g/L) and (b) CCBC (Initial concentration= 5-105 mg/L; dose= 7 g/L) [pH=6; particle size= 30-50 BSS mesh]
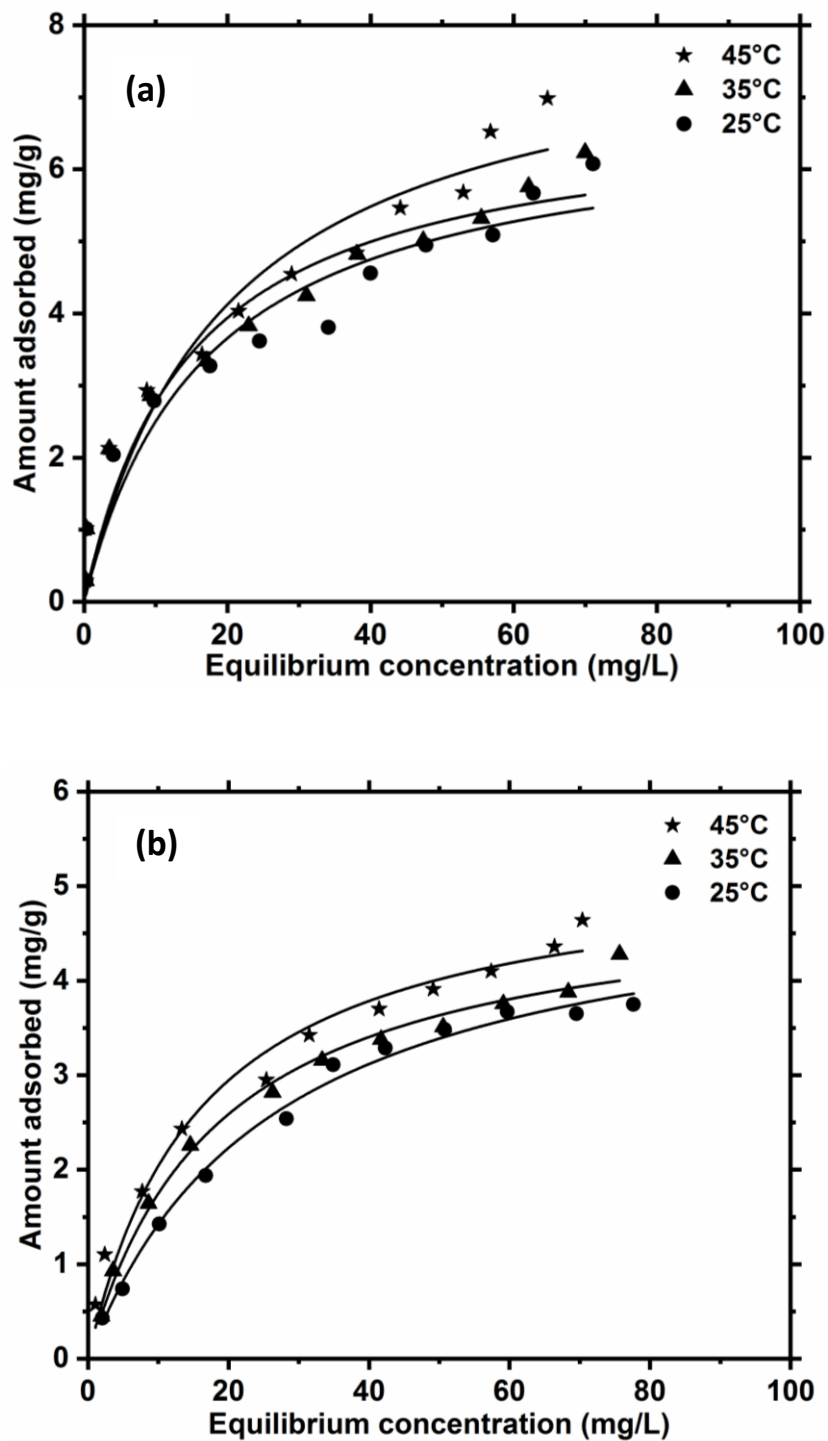
Figure 5.12 Langmuir adsorption isotherms of 2,4-D by (a) CSBC (initial concentration= 5-110 mg/L; dose= 7 g/L) and (b) CCBC(Initial concentration= 5-105 mg/L; dose= 7 g/L) [pH=6; particle size= 30-50 BSS mesh]
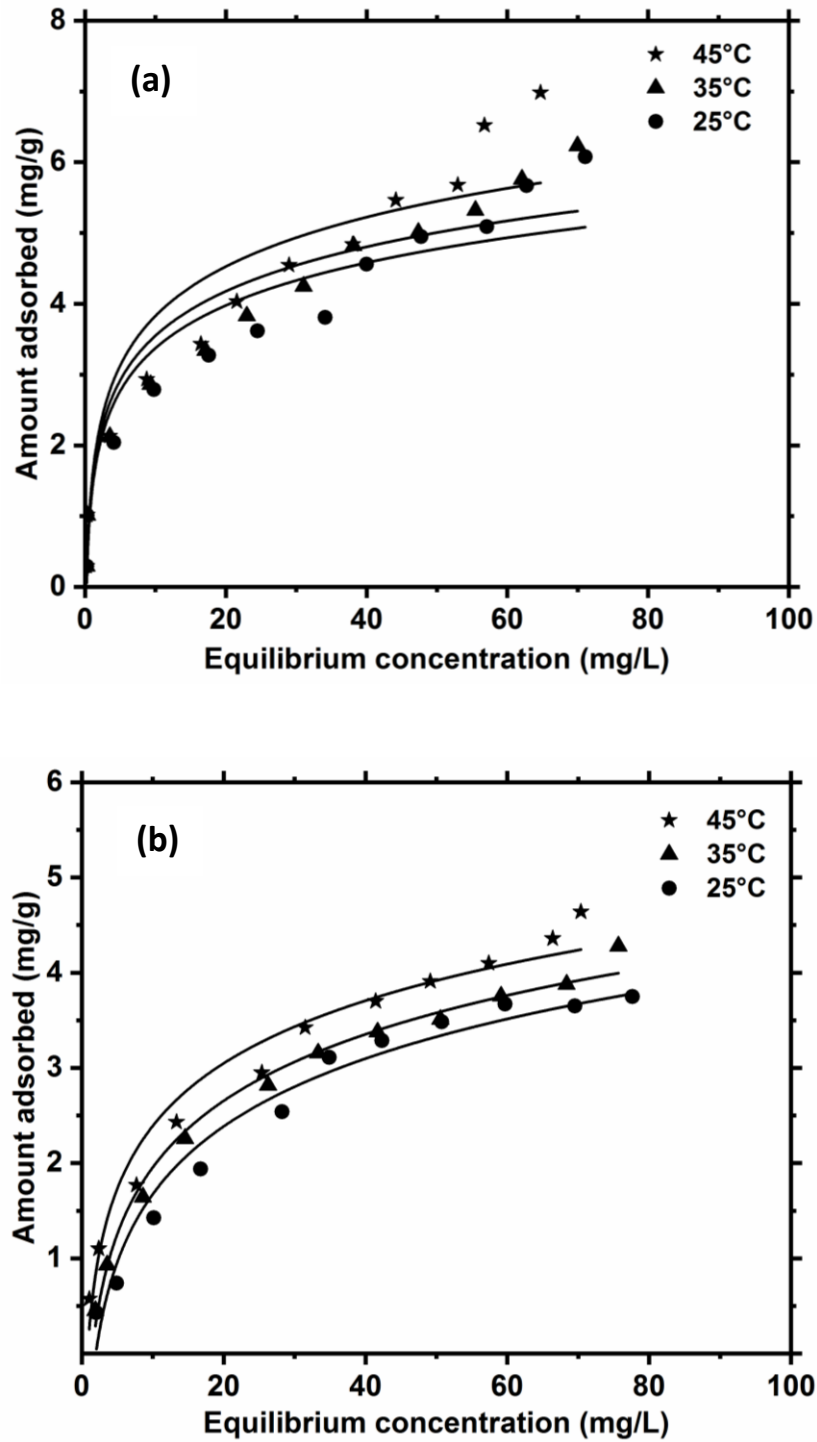
Figure 5.13 Temkin adsorption isotherms of 2,4-D by (a) CSBC (initial concentration= 5-110 mg/L; dose= 7 g/L) and (b) CCBC (Initial concentration= 5-105 mg/L; dose= 7 g/L) [pH=6; particle size= 30-50 BSS mesh]
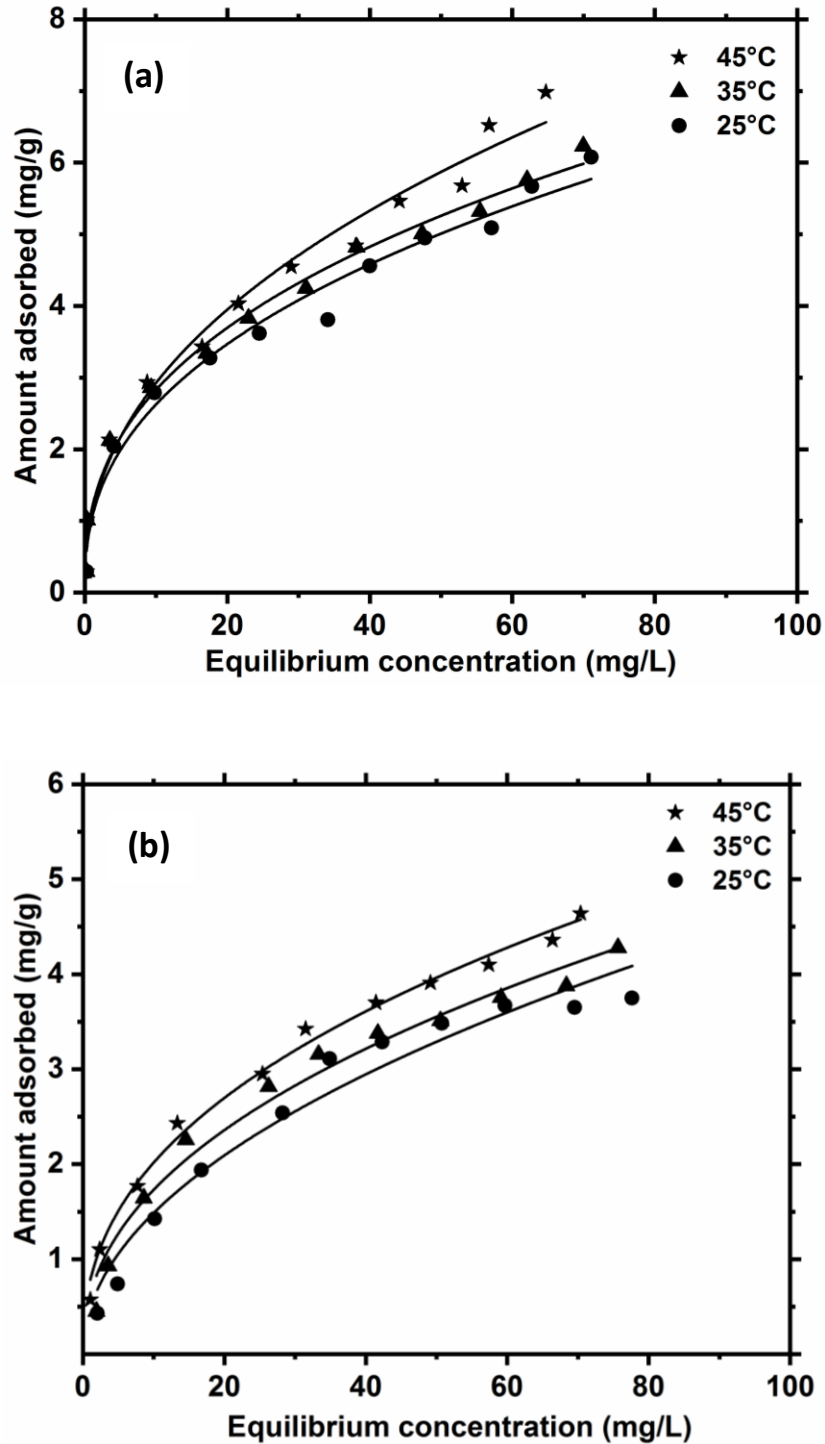
Figure 5.14 Sips adsorption isotherms of 2,4-D by (a) CSBC (initial concentration= 5-110 mg/L; dose= 7 g/L) and (b) CCBC (Initial concentration= 5-105 mg/L; dose= 7 g/L) [pH=6; particle size= 30-50 BSS mesh]
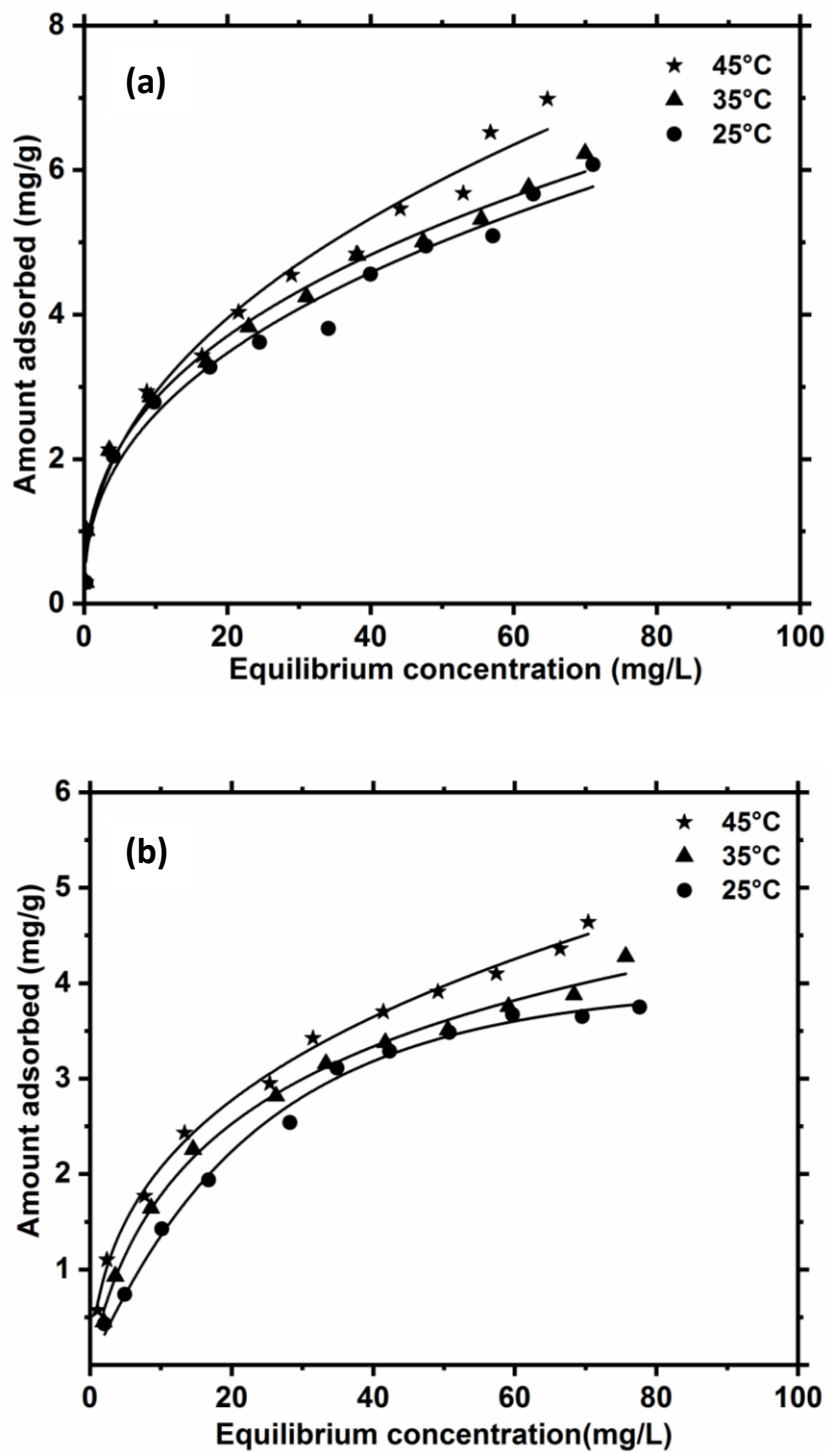
Figure 5.15 Redlich-Peterson adsorption isotherms of 2,4-D by (a) CSBC (initial concentration= 5-110 mg/L; dose= 7 g/L) and (b) CCBC (Initial concentration= 5-105 mg/L; dose= 7 g/L) [pH=6; particle size= 30-50 BSS mesh]
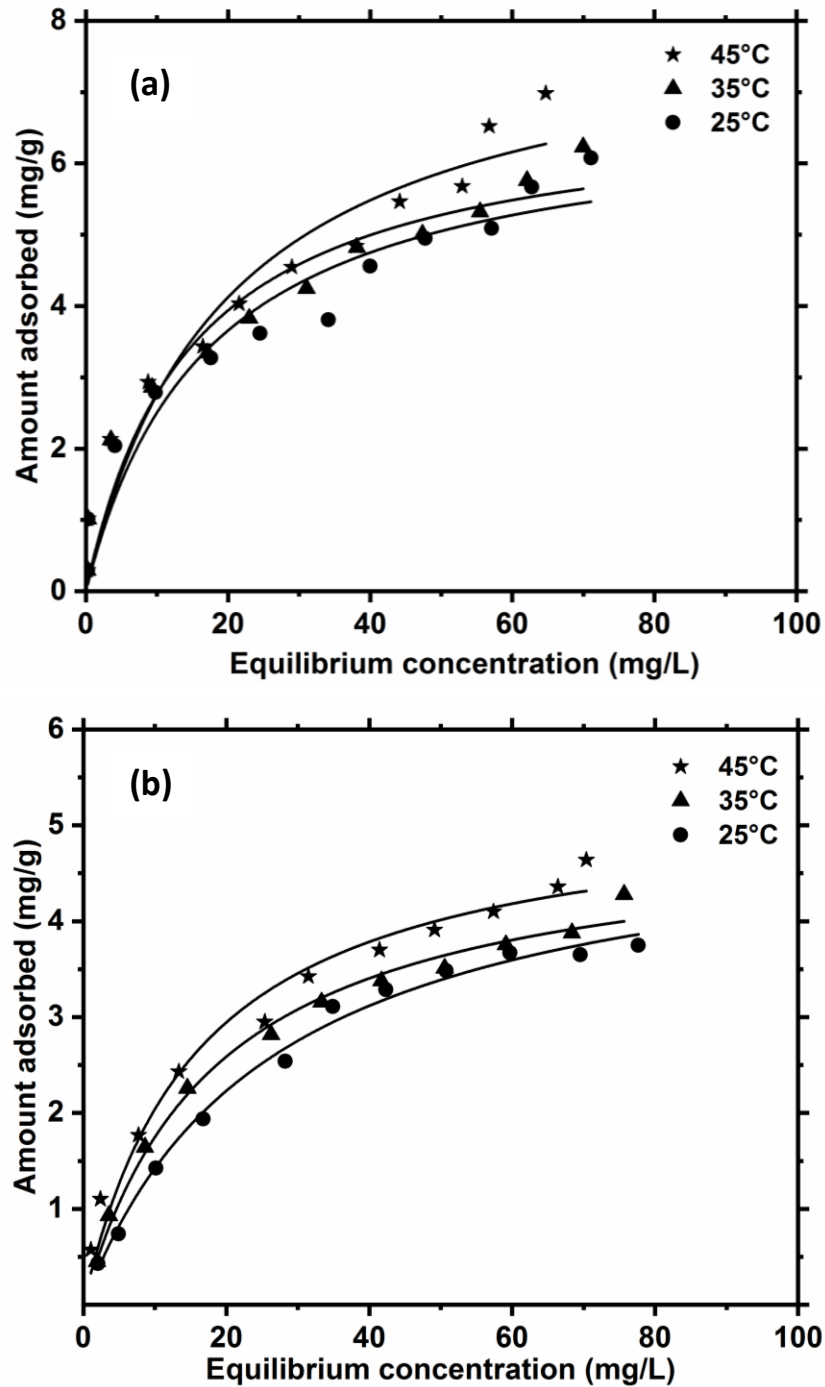
Figure 5.16 Toth adsorption isotherms of 2,4-D by (a) CSBC (initial concentration= 5-110 mg/L; dose= 7 g/L) and (b) CCBC(Initial concentration= 5-105 mg/L; dose= 7 g/L) [pH=6; particle size= 30-50 BSS mesh]
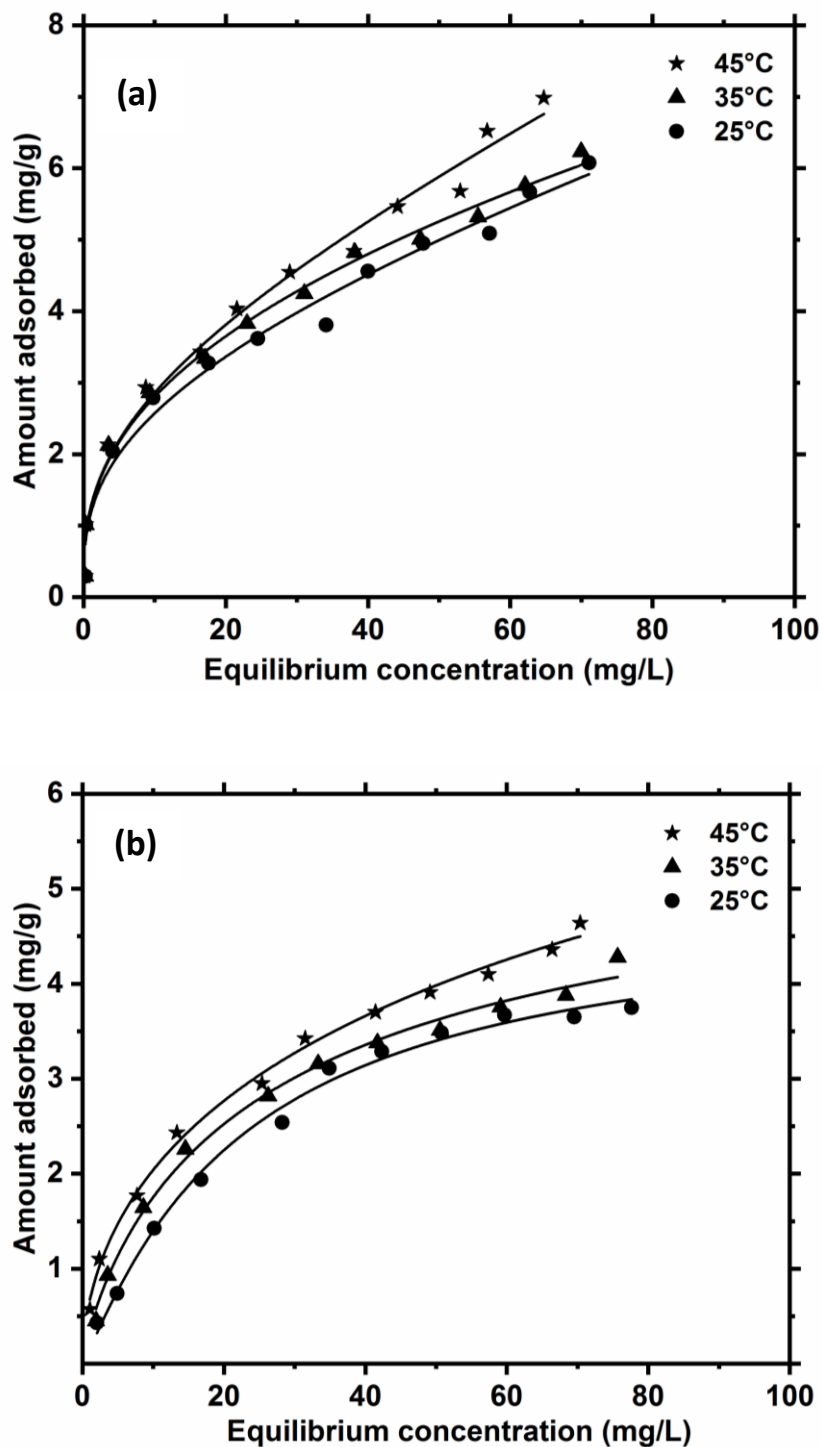
Figure 5.17 Koble-Corrigan adsorption isotherms of 2,4-D by (a) CSBC (initial concentration= 5-110 mg/L; dose= 7 g/L) and (b) CCBC (Initial concentration= 5-105 mg/L; dose= 7 g/L) [pH=6; particle size= 30-50 BSS mesh]
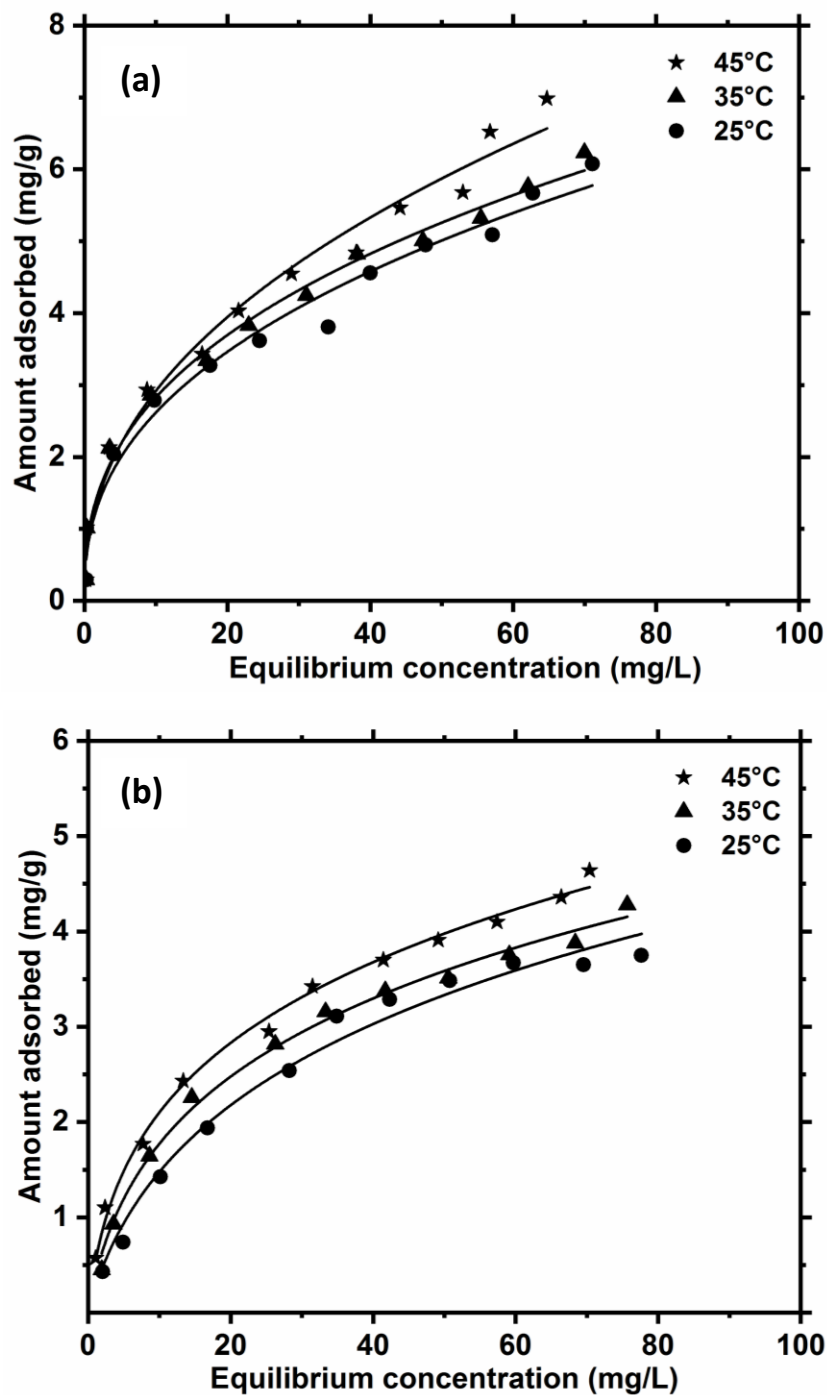
Figure 5.18 Radke-Prausnitz adsorption isotherms of 2,4-D by (a) CSBC (initial concentration= 5-110 mg/L; dose= 7 g/L) and (b) CCBC (Initial concentration= 5-105 mg/L; dose= 7 g/L) [pH=6; particle size= 30-50 BSS mesh]

Table 5.5 Adsorption isotherm parameters for 2,4-D adsorption from aqueous solution by CSBC and CCBC at different temperatures

Parameters	2,4-D adsorption onto CSBC			2,4-D adsorption onto CCBC		
	25°C	35°C	45°C	25°C	35°C	45°C
Freundlich						
K_F (mg/g)	1.0407	1.1650	1.0790	0.4746	0.6176	0.7656
$1/n$	0.4017	0.3852	0.4330	0.4938	0.4472	0.4203
R^2	0.9800	0.9889	0.9808	0.9629	0.9787	0.9933
Langmuir						
q (mg/g)	6.7752	6.8267	8.1828	5.1788	4.9755	5.2960
b	0.0586	0.0681	0.0755	0.0378	0.0541	0.0626
R^2	0.9261	0.9397	0.9338	0.9930	0.9911	0.9747
Temkin						
a_{Te}	4.7889	5.0198	4.4718	0.5089	0.6936	1.2386
b_{Te}	1234.0559	1226.8622	1139.6325	2.3668	2.3233	2.1861
R^2	0.8986	0.9205	0.8865	0.9697	0.9902	0.9676
Sips						
K_{LF}	0.3502	0.4026	0.3816	0.1196	0.1734	0.2399
a_{LF}	0.3978	0.4946	0.4350	0.1205	0.1629	0.2166
η_{LF}	0.4017	0.3852	0.4329	0.4938	0.4472	0.4203
R^2	0.9800	0.9887	0.9808	0.9629	0.9788	0.9933
Redlich-Peterson						
K_{RP}	13498.4835	56.6218	18723.7926	0.1601	0.3775	1.3650
a_{RP}	12963.0039	47.7793	17342.2173	0.0109	0.1679	1.2281
B_{RP}	0.5985	0.6187	0.5672	1.2285	0.8254	0.6592
R^2	0.9800	0.9889	0.9808	0.9950	0.9951	0.9962
Toth						
K_T	0.3970	0.4650	0.4152	0.1958	0.2693	0.3314
B_T	0.0586	0.0681	0.0507	0.0378	0.0541	0.0626
β_T	0.01	0.01	0.01	0.0100	0.0100	0.0100
R^2	0.9261	0.9397	0.9338	0.9930	0.9911	0.9747
Koble- Corrigan						
A	1.0059	1.5712	1.0572	0.1568	0.3735	0.6935
b	-0.1392	-0.0513	-0.1564	0.0325	0.0637	0.0567
η_{KC}	0.2753	0.3334	0.2787	1.0978	0.8225	0.5475
R^2	0.9833	0.9893	0.9852	0.9937	0.9937	0.9958
Radke-Prausnitz						
a	3.7158	1.3007	-8.3528	0.3175	0.4997	0.8157
b	1.0337	1.1650	1.0734	1.5000	1.5000	1.5000
β	0.4034	0.3852	0.4344	0.2643	0.2623	0.2755
R^2	0.9800	0.9889	0.9808	0.9836	0.9938	0.9949

5.6 Thermodynamic parameters

Thermodynamic parameters like change in standard enthalpy ($\Delta H°$), standard entropy ($\Delta S°$) and standard free energy ($\Delta G°$) were calculated for 2,4-D adsorption on biochars. These parameters tell about the nature of adsorption and its feasibility. Thermodynamic parameters calculated for 2,4-D adsorption on CSBC and CCBC are given in Table 5.6. Positive value of $\Delta H°$ confirms the endothermic nature of adsorption process. Change in standard free energy ($\Delta G°$) for 2,4-D adsorption on CSBC and CCBC was negative at all the temperatures. Negative value denotes the spontaneous nature of 2,4-D adsorption on CSBC and CCBC. Positive value of change in standard entropy ($\Delta S°$) shows the increase in randomness with 2,4-D adsorption on CSBC and CCBC.

Table 5.6 Thermodynamic parameters for 2,4-D adsorption on CSBC and CCBC

Biochars	$\Delta G°$ ($KJmol^{-1}$)			$\Delta H°$ ($KJ\ mol^{-1}$)	$\Delta S°$ ($KJmol^{-1}K^{-1}$)
	25°C	35°C	45°C		
CSBC	-27.00	-28.59	-29.70	22.25	0.16
CCBC	-26.12	-27.91	-29.20	27.36	0.18

CHAPTER 6

COLUMN ADSORPTION AND DESORPTION STUDIES

6.1 Introduction

An adsorption system can either be operated in batch mode or in continuous mode. Adsorption in continuous mode is also known as fixed-bed or column mode. In batch mode adsorbate and adsorbent are kept in contact for duration longer enough until equilibrium is reached (Ahmad and Hameed, 2010). Continuous studies on the other hand are real-time adsorption system. Here, adsorbate solution enters and leaves the adsorbent packed in column. Hence, equilibrium is not established initially between adsorbate present in solution and that present on adsorbent due to which this mode is also called dynamic equilibrium of sorption (Chowdhary et al., 2015). Continuous mode is also more successful as practical version of adsorption system due to industrial applicability. So, in order to scale up a fixed bed reactor of industrial scale from preliminary information provided by batch study column study in continuous mode is necessary (Low and Lee, 1991).

6.1.1. Continuous adsorption system

Continuous adsorption system can be, 1) Fixed-bed system which involves continuous flow of adsorbate solution through a static bed of adsorbent at constant speed, 2) Continuous moving bed sorption system where both adsorbent and adsorbate both are in moving state but adsorbent stays limited to particular section and 3) continuous fluidized bed sorption system where adsorbent bed is in free-flowing condition in adsorbate solution present in the column (Patel, 2019). Fixed bed system in continuous flow mode are more preferred as they ensure better utilization of adsorbent and inhibit concentration gradient based decline in adsorption process (Ali and Gupta, 2006). Fixed bed adsorption system may have down-flow or up-flow as inflow arrangement for adsorbate. It is observed that adsorption is fast and almost complete in the beginning with effluent concentration being least. But gradually the adsorption process reduces and rise in effluent concentration is observed with passage of more adsorbate solution (Goel at al., 2005). Also, equilibrium time in batch mode is different for equilibrium time in continuous mode (Ali and Gupta, 2006). So, column conditions optimization is necessary to design a column.

6.1.2 Breakthrough curve in continuous adsorption system

Efficiency of column can be explained through breakthrough curve. It is obtained by plotting concentration of adsorbate in effluent against volume of adsorbate solution passed through the column. Shape of the breakthrough curve along with the time of its appearance are major determinants of operational and dynamic responses of a column. Breakthrough curves help in determination of breakthrough, exhaustion and column capacity along with the degree of the column utilization. Breakthrough and exhaustion capacity are the adsorbate mass adsorbed onto the sorbent at break point and saturation point, respectively. Degree of column utilization is represented as the ratio of breakthrough capacity to exhaustion capacity.

Weber et al., 1972 described the relation between breakthrough curves and fixed bed adsorption system. According to them, solute from the adsorbate solution introduced in column is rapidly adsorbed by uppermost layers of the adsorbent at beginning. Rate of adsorption at uppermost layers is more as compared to next layers in column. It is such as they are in contact of initial concentration (C_o) which is maximum concentration available to them. Thus, formation of primary adsorption zone, PAZ (δ) takes place at the uppermost section of column. Solute remaining in the adsorbate solution after passing through PAZ is taken up by the next layers leaving the effluent concentration (C_e) zero initially. With the passage of time and steady flow of adsorbate solution uppermost layer of column gets saturated. Subsequently shifting of adsorption zone to lower layer of adsorbents in column also takes place. With the passage of more adsorbate solution, increase in size of saturated zone and downward shift adsorption zone also takes place. Due to both these changes in adsorbent layer in column adsorbate starts to escape adsorption as shown in Figure 6.1.

C_e/C_o plotted against time or volume of adsorbate solution passed at definite flow rate shows the increase in C_e/C_o ratio as zone moves along the column. Continuous or fixed bed adsorption studies are mostly characterized by "S" shaped breakthrough curves with varying degree of steepness. This curve steepness and breakpoint depends on the type of adsorbent material used, adsorbate solution concentration, dimension of column, flow rate and particle size of the adsorbent. Also, breakpoint time increases with the (a) high solution concentration (b) greater depth and width of the adsorbent bed, (c) slow

flow rate and (d) smaller particle size of the adsorbent as it increases the surface area for the adsorption.
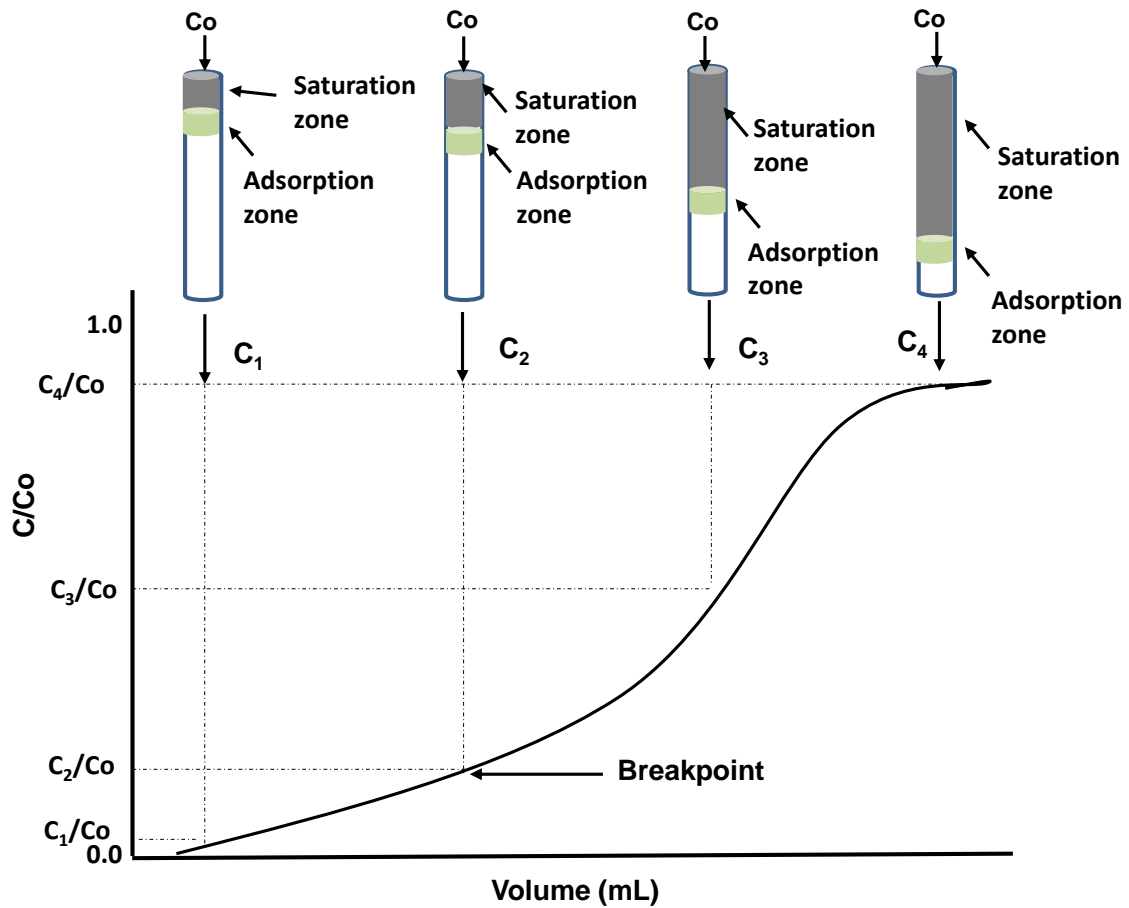
Figure 6.1: Schematic diagram showing shifting of adsorption zone and the breakthrough curve (Patel et al., 2019).

6.1.3 Designing a fixed bed reactor

Mass transfer model given by Weber (Weber, 1972) can be used for designing a fixed-bed reactor. An ideal breakthrough curve assumes the effluent concentration (C_f) leaving the column after passing through adsorbent bed to be zero, at the beginning of process. However, under practical conditions C_f isn't always zero, which may be due to eventual leakage (small though) at initial phase of operations. So, expression of an ideal breakthrough curve in the terms of C_f, total mass of solute free water, $\overline{V_e}$, passing through per unit cross sectional area of the adsorbent depends upon: (a) total effluent mass per unit adsorbent area at breakpoint, $\overline{V_b}$ and (b) curve's nature between $\overline{V_b}$ and $\overline{V_x}$, where $\overline{V_x}$ is total effluent's mass per unit adsorbent area, when adsorbent is approaching

towards the saturation. C_b and C_x are the effluent conconcentration at $\overline{V_b}$ and $\overline{V_x}$, respectively. Constant zone length (δ) is the part of the adsorbent bed, when the adsorbate's concentration decreased from C_x to C_b.
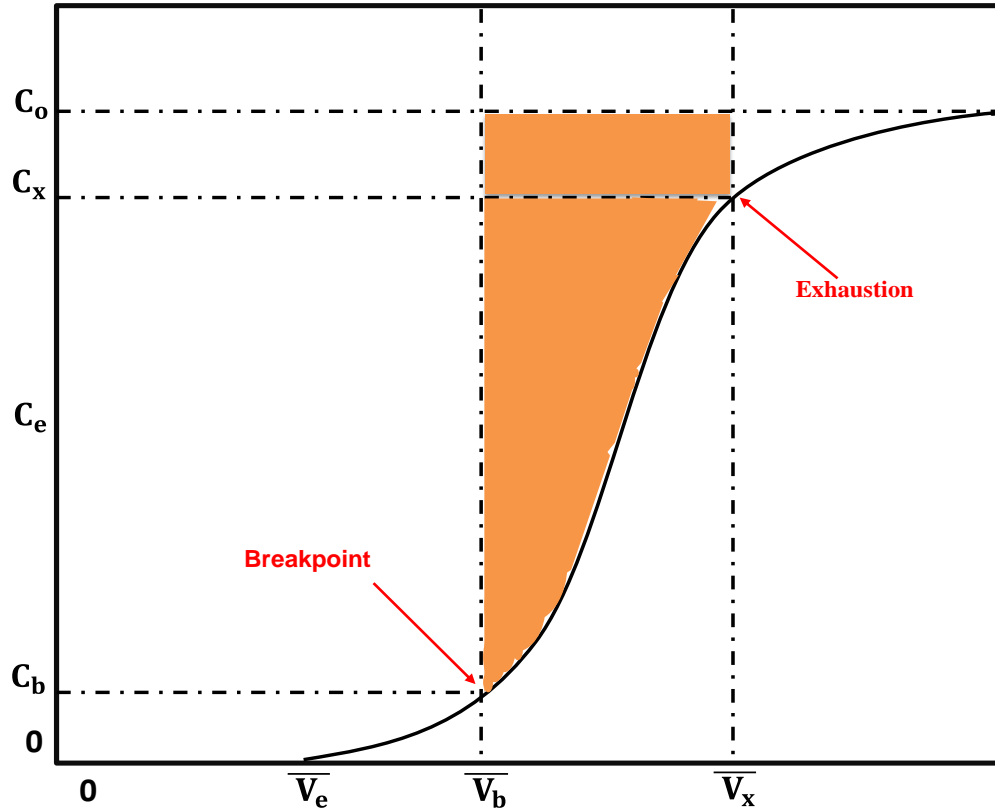
Figure 6.2 Ideal breakthrough curve with all design parameters (Patel et al., 2019)

The total time t_x, taken by primary adsorption zone can be calculated by equation 6.1.

$$t_x = \frac{\overline{V_x}}{F_m} \qquad (6.1)$$

where, F_m is the mass flow rate which is expressed as the mass per unit cross-sectional area of the bed.

The time (t_δ) required for the zone to move down to its own length in columnis calculated by equation 6.2.

$$T_\delta = \frac{\overline{V_x} - \overline{V_b}}{F_m} \qquad (6.2)$$

144

The ratio of biochar bed depth (D) to the time can be calculated by equation 6.3.

$$\frac{\delta}{D} = \frac{t_\delta}{t_x - t_b}$$ (6.3)

where, t_b is the time required for initial PAZ formation.

The fractional capacity (f) can be calculated using equation 6.4.

$$f = 1 - \frac{t_b}{t_\delta}$$ (6.4)

The length of the PAZ (δ) can be calculated by equation 6.5.

$$\delta = D\left(1 - \frac{t_b}{t_x}\right)$$ (6.5)

where, D is the biochar bed depth; t_b and t_x are time duration upto breakpoint and exhaustion point (in minutes), respectively.

The percent saturation can finally be calculated using equation 6.6.

$$\text{Percent saturation} = \frac{D + \delta(f-1)}{D} \times 100$$ (6.6)

Apart from these, total breakthrough capacity is estimated by calculating area between influent and effluent to the breakthrough point, and further divided by weight of the biochar used for fixed-bed preparation. Similarly, total column capacity is also calculated by determining total area up to the point where effluent curve joins the influent, and further divided by weight of the biochar. The obtained column capacity was also compared with the obtained batch capacity. In addition to the above parameters, bed volume, empty-bed-contact-time and biochar usage rate can be calculated using equation 6.7.

$$\text{Bed volume} = \frac{\text{Weight of biochar (Kg)}}{\text{Biochar bulk density }(\frac{Kg}{m^3})}$$ (6.7)

Empty Bed Contact Time (EBCT)

EBCT is the empty bed volume divided by the flow rate. It is explained as the total time for which the influent remainsin contact with the biochar bed in the column. EBCT can be calculated using the equation 6.8.

$$\text{EBCT} = \frac{\text{Bed volume}}{\text{Flow rate}}$$ (6.8)

The biochar usage rate can be calculated using equation 6.9.

$$\text{Biochar usage rate} = \frac{\text{Weight of biochar in column (g)}}{\text{Volume of breakthrough (L)}} \qquad (6.9)$$

6.2 Carbofuran and 2,4-D adsorption onto corn stover biochar (CSBC) in column mode

Carbofuran and 2,4-D adsorption on CSBC in continuous flow mode is carried out in two separate glass columns. These glass columns having length and internal diameter of 40 and 2 cm, respectively were packed with 3.0 g of biochar. The biochar bed height of 10 cm was measured in both the columns. Carbofuran and 2,4-D concentration used in this study were 4.48 and 4.71 mg/L, respectively. Initial pH of carbofuran and 2,4-D solutions were kept at 6. Steady flow rates of 1.1 and 1 mL/minute were maintained for carbofuran and 2,4-D solution respectively into packed column.

Special precautions were kept during loading of column as well as its operation. Biochar were degassed using warm water before its loading into the column. This slurry of biochar was poured into the column slowly to avoid trapping of air as bubbles. During continuous flow operation, pesticide solutions from overhead tanks were allowed to pass through respective columns under effect of gravity. Level of pesticide solution was always maintained above biochar bed height during entire operation. Special care was given to the flow rate maintenance as it was controlled manually using flow-control knob of the column. Complete experiment was carried out at room temperature and glass column were wrapped with aluminum foil to restrict light induced degradation of pesticides in column. Effluents samples were collected in test-tube at regular time intervals and analyzed for carbofuran and 2,4-D concentration using UV/visible spectrophotometer. Column operation were continued till stabilization of effluent concentration near influent concentration. Figure 6.3 shows the schematic diagram and image of the column study experimental set-up.

Breakthrough curves for carbofuran and 2,4-D adsorption on CSBC are given in Figure 6.4 and 6.5, respectively. Both the curves are "S" type but breakthrough curve for 2,4-D adsorption on CSBC is steeper than breakthrough curve of carbofuran adsorption on CSBC. These breakthrough curves were used to calculate the column capacity at the

time of exhaustion. Breakthrough and exhaustion capacity of CSBC for carbofuran adsorption in column mode is 0.75 and 1.46 mg/g, respectively. Similarly, breakthrough and exhaustion capacity of CSBC for 2,4-D adsorption in column mode is 0.15 and 1.00 mg/g, respectively. The results from column studies are in lines of batch studies where carbofuran is adsorbed better on CSBC than 2,4-D (Table 6.1). All the other column parameters are summarized in Table 6.2. The adsorption behavior of carbofuran on CSBC is different from that of 2,4-D on CSBC. So the column parameters calculated are also different.

The volume of pesticide solution flown through column till attainment of breakpoint (V_b) was significantly higher for carbofuran than for 2,4-D i.e. 496 and 128 mL respectively. Also, the volume of pesticide solution flown through column till attainment of exhaustion pint (V_x) was higher for carbofuran than for 2,4-D i.e. 1320 and 1214 mL respectively. The time to achieve the breakpoint (t_b) was more for carbofuran (440 minute) than it was for 2,4-D (100 minute). The time taken by adsorption zone to move along its length is less for carbofuran (735.6155) as compared to 2,4-D (1071.04). This is in accordance with length of primary adsorption zone for both of the biochar i.e. 6.65 and 9.16 cm, respectively. The fractional capacities of the column for carbofuran and 2,4-D adsorption were found to be 0.40 and 0.90, respectively. The percentage saturation for carbofuran and 2,4-D adsorption were calculated to be 61.12 and 91.44, respectively. These parameters can be used to design a full scale reactor.

6.3 Desorption studies

Adsorption of carbofuran and 2,4-D on the biochar in the column study is followed by their desorption studies. These studies are important as desorption lead to regeneration of column making it available for the next round of adsorption. High desorption capacities of 82% and 95% were obtained by using ethanol as eluent for carbofuran desorption from date seed activated carbon (Salman, 2013) and palm fronds activated carbon (Salman et al., 2011), respectively. Similarly, Mandal et al., (2017) obtained limited desorption efficiencies of 4.4-21.5% by using deionized water as eluent for 2,4-D removal from biochars used as adsorbent. Koner et al., (2012) also reported 75 and 80% 2,4-D desorption from surface modified silica gel waste (SMSGW) using

ethanol and acetone as eluent, respectively. Thus, ethanol can be used as common eluent for both carbofuran and 2,4-D desorption.

Here in this study, 10 ml ethanol was passed through the saturated columns which were not showing any further adsorption and was collected again as effluent. This step was repeated again and again till no carbofuran and 2,4-D were obtained in the effluents from respective columns. 8 aliquots of 10 mL each were used to desorb carbofuran and 2,4-D from respective saturated column. Almost 83.18% carbofuran desorption was achieved by first two aliquots of ethanol. Similarly 88.12% 2,4-D desorption was achieved by first 3 aliquots of ethanol. Desorption curves of carbofuran and 2,4-D for CSBC are given in Figures 6.6 (a) and (b), respectively.

Table 6.1 Comparative table shows the column capacities of CSBC for carbofuran and 2,4-D adsorption along with their adsorption capacities in batch mode.

Adsorbate	Batch capacity (at 25°C)	Column capacity	Ref
Carbofuran	6.38	1.46	This study
2,4-D	6.77	1.00	This study

Table 6.2 Column parameters for carbofuran and 2,4-D adsorption onto CSBC.

Parameters	Carbofuran adsorption on CSBC	2,4-D adsorption on CSBC
C_o (mg mL^{-1})	0.00448	0.004711
C_x (mg mL^{-1})	0.00435	0.004622
C_b (mg mL^{-1})	0.000267	0.000267
V_x (mg cm^{-2})	1.82866	1.78697
V_b (mg cm^{-2})	0.70766	0.19204
F_m (mg cm^{-2} min^{-1})	0.001523	0.001489
D (cm)	10.5	10
t_x (min)	1200	1200
t_δ (min)	735.6155	1071.04
t_b (min)	440	100
F	0.40186	0.907
δ (cm)	6.65	9.16
Saturation (%)	62.12	91.44
Usage rate (kg L^{-1})	0.006048387	0.02343
EBCT (min)	9.54545	31.4
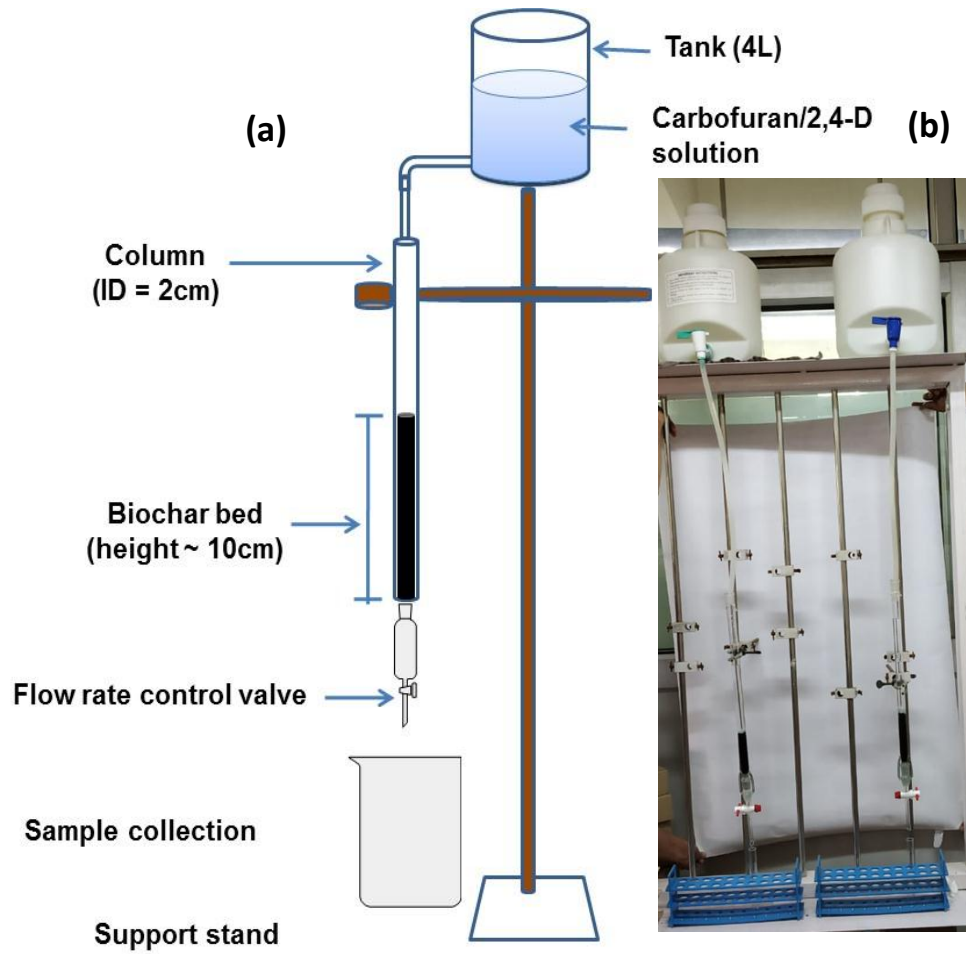
Figure 6.3 Schematic diagram (a) and image (b) of pesticide adsorption study in column model
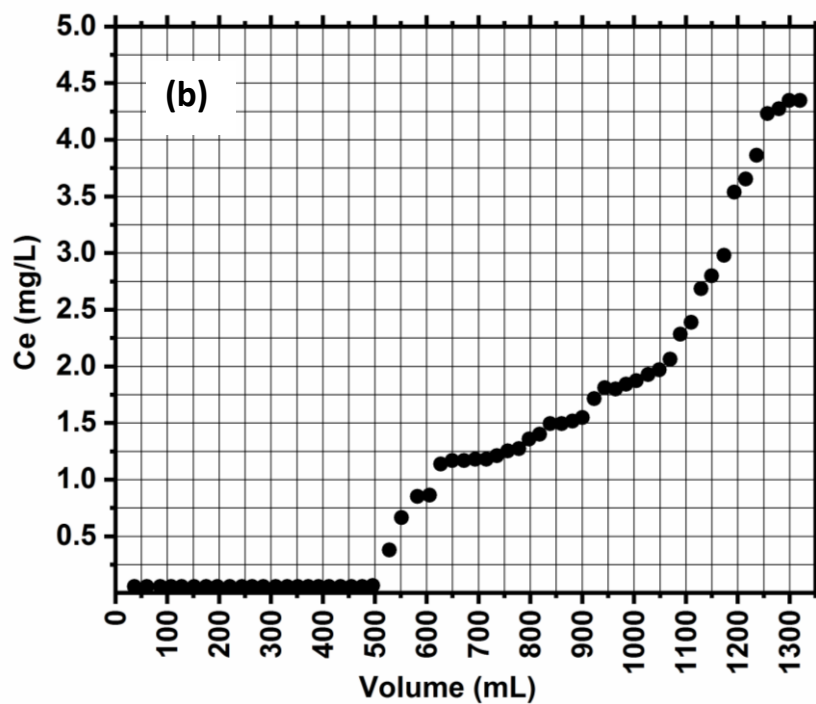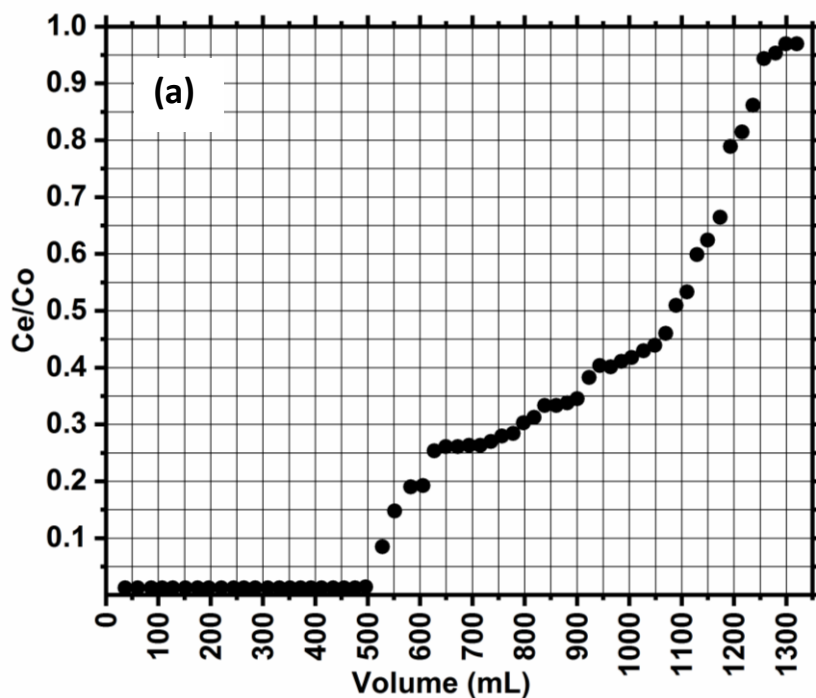
Figure 6.4 Breakthrough curves for carbofuran adsorption on CSBC (a) Volume vs Ce/Co and (b) Volume vs Ce [pH= 6.0; carbofuran concentration= 4.48 mg/L].
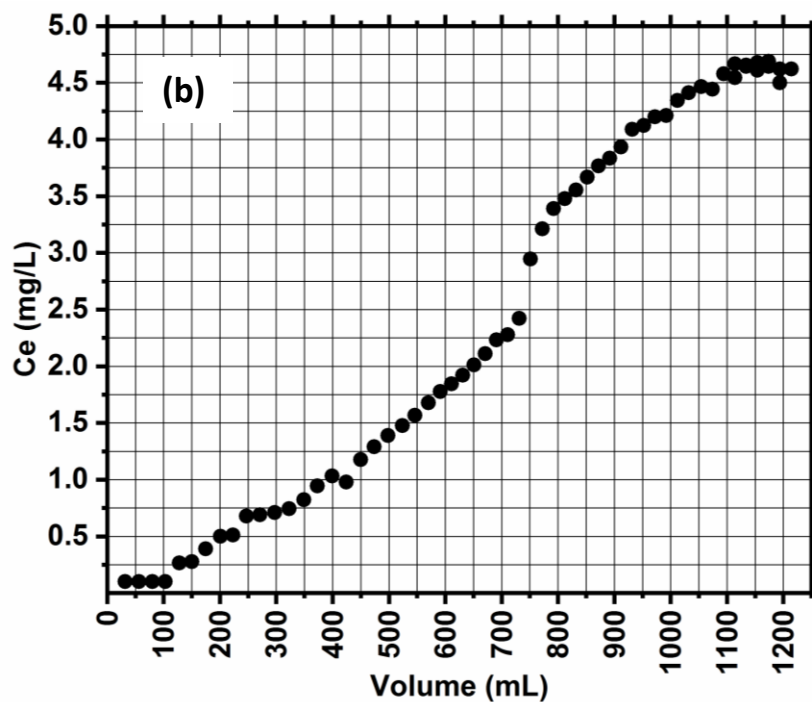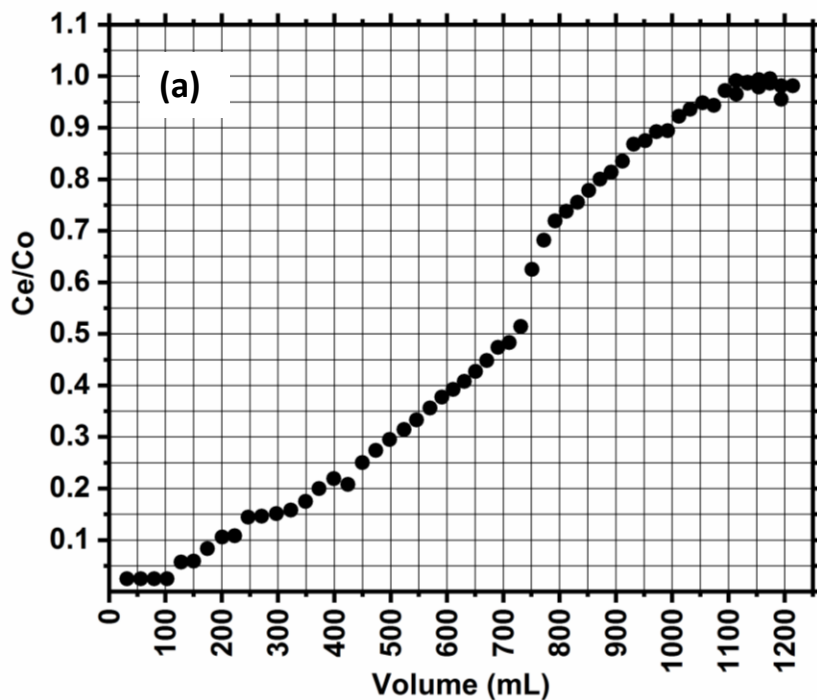
Figure 6.5 Breakthrough curves for 2,4-D adsorption on CSBC (a) Volume vs C_e/C_o and (b) Volume vs C_e [pH= 6.0; 2,4-D concentration= 4.71 mg/L]
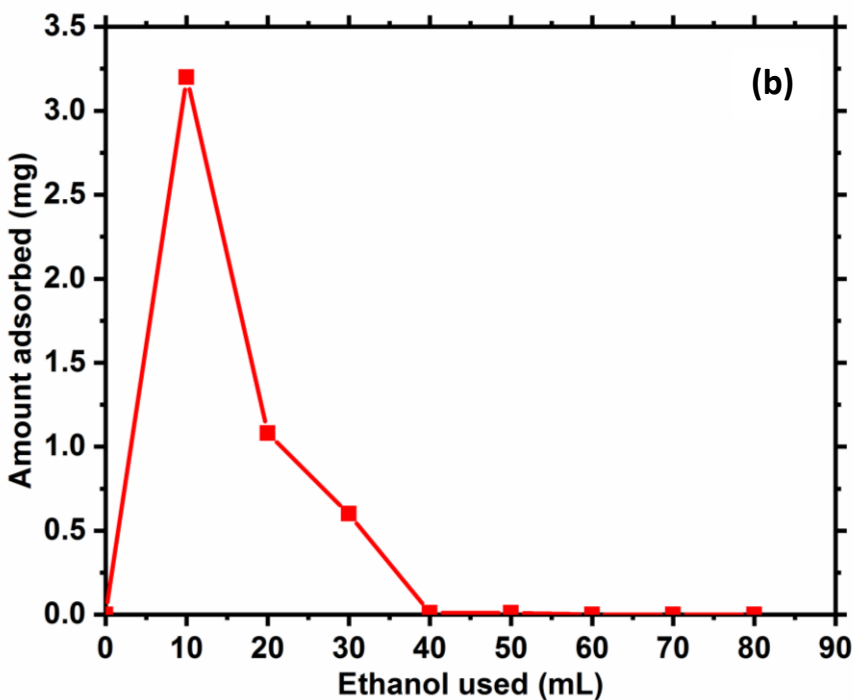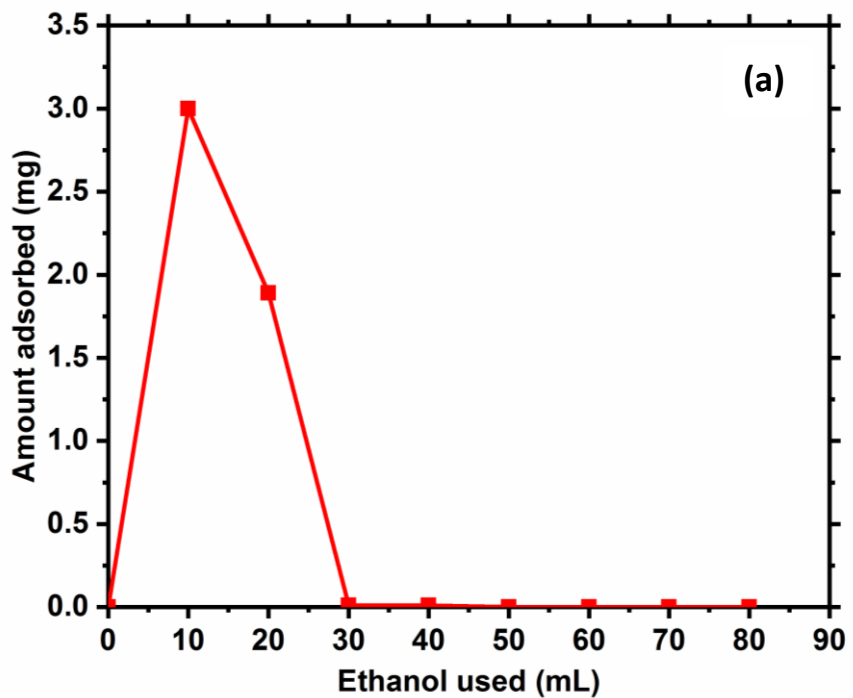
Figure 6.6 Desorption curve of (a) carbofuran and (b) 2,4-D for CSBC

CHAPTER 7

CONCLUSIONS AND RECOMMENDATIONS

7.1 Conclusions

In the present study, sustainable biochars i.e. Corn stover biochar (CSBC) and Corn con biochar (CCBC) were developed. Surface area assessment of these biochars were carried out using BET surface area analyzer. Elemental composition of biochars were determined using CHNS analysis and ICP-AES. Afterwards, theses biochars were characterized for surface morphology, physical and chemical characteristic using SEM, SEM-EDS, SEM mapping, TEM, FTIR, and XRD.

CSBC and CCBC were used as adsorbents for aqueous carbofuran and 2,4-Dichlorophenoxyacetic acid (2,4-D) removal. Adsorption studies for pesticides removal were carried out in batch as well as column modes. Equilibrium and kinetic studies were carried out for optimization of solution pH, adsorbent dose, initial adsorbate concentration and temperature. Data obtained from equilibrium studies were fitted to Freundlich, Langmuir, Temkin, Sips, Redlich-Peterson, Toth, Koble-Corrigan and Radke-Prausnitz isotherm equations. Results obtained from kinetic studies were fitted to pseudo first order and pseudo second order rate equations. Following important points are concluded:

1. CSBC and CCBC were developed from slow pyrolysis of agricultural byproducts like corn stover and corn cob at 900°C.

2. Zero point charge (pHzpc) for CSBC (7.90) was more than CCBC (7.75).

3. Surface area (S_{BET}) of CSBC (204.9 m^2/g) was slightly less than that of CCBC (222.9 m^2/g). The average pore diameter of biochar particles were less than 2 nm. Thus, both the biochars have abundance of micropores.

4. Carbofuran and 2,4-D adsorption onto CSBC and CCBC were maximum at pH 6.

5. Kinetic study showed that adsorption of carbofuran and 2,4-D on either biochars was slow and took hours to reach equilibrium. Most of the Carbofuran and 2,4-D adsorption on CSBC and CCBC was completed in 5 and 8 hours, respectively.

6. Data obtained from kinetic studies were best fitted to pseudo second order rate equation.

7. Carbofuran adsorption equilibrium data were best fitted to Redlich-Peterson (CSBC) and Koble-Corrigan (CCBC) models. Also, equilibrium data from 2,4-D adsorption on CSBC and CCBC were best fitted to Sips and Redlich-Peterson isotherms, respectively.

8. Carbofuran Langmuir adsorption capacities of 12.32 mg/g (45°C) and 11.95 mg/g (45°C) were obtained for CSBC and CCBC, respectively. Maximum 2,4-D adsorption capacities of 8.18 mg/g and 5.29 mg/g were obtained for CSBC and CCBC, respectively at 45°C.

9. Increase in adsorption capacity with increase in temperature was observed for carbofuran and 2,4-D uptake on biochars. The increase in uptake was more significant for carbofuran versus 2,4-D adsorption.

10. H-bonding, electrostatic and electrophilic interactions; π-π interactions along with porous diffusion were determined to be dominating mechanism for carbofuran and 2,4-D adsorption on biochars.

11. Standard enthalpy change ($\Delta H°$) was positive for carbofuran and 2,4-D adsorption on either biochars. Change in standard free energy (°G) for carbofuran and 2,4-D adsorption on biochars was negative at all temperatures. It suggests that carbofuran and 2,4-D adsorption onto biochars is an endothermic process and spontaneous at all temperatures.

12. Carbofuran and 2,4-D adsorption on CSBC were also done in column mode at pH 6.

13. Column capacity of CSBC was higher for carbofuran adsorption (1.46 mg/g) than the 2,4-D adsorption (1.00 mg/g).

14. Desorption studies were carried out for regeneration of carbofuran/2,4-D saturated biochar using ethanol as eluent.

15. About 83.18% of carbofuran desorption was obtained using 2 aliquots of 10 mL each. Similarly, ~88.12% 2,4-D desorption was obtained using 3 aliquots of 10 mL ethanol. Carbofuran and 2,4-D desorption was scanty after second and third aliquot, respectively.

16. Adsorption capacities of other biochars used for carbofuran and 2,4-D removal were compared with adsorption capacities CSBC and CCBC.

7.2 Recommendations

1. Applicability of CSBC and CCBC in carbofuran and 2,4-D adsorption from natural water should be attempted.

2. Magnetized CSBC and CCBC should be developed and used for carbofuran and 2,4-D removal.

3. Life cycle assessment of these biochars should be done.

Table 7.1 Comparison of adsorption capacities of CSBC and CCBC with other biochars used for carbofuran removal from water

Adsorbents	Name	Temp (°C)	pH	Conc. Range (mg/L)	Adsorption capacity (mg/g)	Surface area (m²/g)	Adsorption capacity per surface area	Ref
Corn stover biochar	CSBC	25 35 45	6	5-110	6.38 7.99 12.32	204.9	0.03 0.04 0.06	This study
Corn cob biochar	CCBC	25 35 45	6	5-100	6.57 6.81 11.95	222.9	0.03 0.03 0.05	This study
Sugarcane bagasse biochar	SB500	25 35 45		1-100	3.7 6.8 18.9	148	0.02 0.04 0.13	Vimal et al., 2019
Tea waste biochar	TWBC700	25	5	50	10.74	342	0.03	Vithanage et al., 2015
Rice husk biochar	RHBC700	25	5		23.86	377	0.06	
Tea waste biochar	TWBC300 TWBC500 TWBC700	30	5	5-100	54.71 48.73 22.74	2.3 1.6 342	23.99 31.04 0.06	Mayakaduwa et al., 2016a
Rice husk biochar	RHBC300 RHBC500 RHBC700	30	5	5-100	30.73 48.75 132.87	69 170 237	0.45 0.29 0.56	Mayakaduwa et al., 2016b
Rice husk biochar (steam modified)	RHBC700S	30	5		160.77	252	0.64	

156

Table 7.2 Comparison of adsorption capacities of CSBC and CCBC with other biochars used for 2,4-D removal from water

Adsorbents	Name	Temp (°C)	pH	Conc. Range (mg/L)	Adsorption capacity (mg/g)	Surface area (m²/g)	Adsorption capacity per surface area	Ref
Corn stover biochar	CSBC	25 35 45	6	5-110	6.77 6.82 8.18	204.9	0.03 0.03 0.04	This study
Corn cob biochar	CCBC	25 35 45	6	5-105	5.17 4.97 5.29	222.9	0.02 0.02 0.02	This study
Rice straw biochar	RS200 RS350 RS500	25	3-3.5	60-300	13.48 19.80 8.8	2.1 20.6 128	6.41 0.96 0.06	Lu et al., 2012
Poplar wood biochar	PW200 PW350 PW500	25	3-3.5	60-300	10 24 11	1.0 4.3 30.6	10.00 5.21 0.36	Li et al., 2013
Groundnut shell char	GSC	30	pH >7	100	3.0	43	0.07	Trivedi et al., 2016a
Cotton plant char	CPC	30	pH >7	100	3.9	109	0.03	Trivedi et al., 2016b
Tea waste biochar Tea waste steam modified Burcucumber biochar Oakwood biochar Bamboo biochar	TWBC TWBCS BUBC OWBC BBC	23	7	100	10.05 58.85 28.92 42.67 26.26	421.3 576.1 2.3 270.7 475.6	0.02 0.10 12.57 0.15 0.05	Mandal et al., 2017
Switchgrass biochar	-	25 35 45	2	25-400	133 134 129	1.1	120.90 121.81 117.27	Essandoh et al., 2017
Wood chips biochar Bamboo biochar Corn cob biochar Rice straw biochar Basudha biochar	-	25	7	1	42.7 19.5 1.1 1.2 54.6	516 510 2.3 128 404	0.08 0.04 0.47 0.01 0.14	Kearns et al., 2014

REFERENCES

Abigail, E. A., & Chidambaram, R. (2017). Nanotechnology in herbicide resistance. Nanostructured Materials: Fabrication to Applications, 207.

Abo-Amer, A. E. (2012). Characterization of a strain of Pseudomonas putida isolated from agricultural soil that degrades cadusafos (an organophosphorus pesticide). World Journal of Microbiology and Biotechnology, 28(3), 805-814.

Agrawal, A., Pandey, R. S., & Sharma, B. (2010). Water pollution with special reference to pesticide contamination in India. Journal of Water Resource and Protection, 2(05), 432-448.

Agrawal, O., and Gupta, V. K. (1999). Sub-Parts-per-Million Spectrophotometric Determination of Phenol and Related Pesticides Using Diazotized Aminoacetophenone. Microchemical Journal. 62, 147-153.

Ahmad, A. A., & Hameed, B. H. (2010). Fixed-bed adsorption of reactive azo dye onto granular activated carbon prepared from waste. Journal of hazardous materials, 175(1-3), 298-303.

Ahmed, M. B., Zhou, J. L., Ngo, H. H., & Guo, W. (2016). Insight into biochar properties and its cost analysis. Biomass and Bioenergy, 84, 76-86.

Ahmed, S., Rasul, M. G., Brown, R., & Hashib, M. A. (2011). Influence of parameters on the heterogeneous photocatalytic degradation of pesticides and phenolic contaminants in wastewater: a short review. Journal of environmental management, 92(3), 311-330.

Akçay, G., Akçay, M., & Yurdakoç, K. (2005). Removal of 2, 4-dichlorophenoxyacetic acid from aqueous solutions by partially characterized organophilic sepiolite: thermodynamic and kinetic calculations. Journal of colloid and interface science, 281(1), 27-32.

Akhtar, M., Mahboob, S., Sultana, S., & Sultana, T. (2014). Pesticides in the river Ravi and its tributaries between its stretches from Shahdara to Balloki headworks, Punjab-Pakistan. Water Environment Research, 86(1), 13-19.

Aksu, Z. (2005). Application of biosorption for the removal of organic pollutants: a review. Process biochemistry, 40(3-4), 997-1026.

Aksu, Z., & Kabasakal, E. (2004). Batch adsorption of 2, 4-dichlorophenoxy-acetic acid (2, 4-D) from aqueous solution by granular activated carbon. Separation and Purification Technology, 35(3), 223-240.

Aktar, W., Sengupta, D., & Chowdhury, A. (2009). Impact of pesticides use in agriculture: their benefits and hazards. Interdisciplinary toxicology, 2(1), 1-12.

Alam, J. B., Dikshit, A. K., & Bandyopadhyay, M. (2000). Efficacy of adsorbents for 2, 4-D and atrazine removal from water environment. Global nest: Int. J, 2(2), 139-148.

Alam, J. B., Dikshit, A. K., & Bandyopadhyay, M. (2000). Efficacy of adsorbents for 2, 4-D and atrazine removal from water environment. GlobalNEST International Journal, 2(2), 139-148.

Alam, M. J., Daoxian, Y., Jiang, Y. J., Yuchuan, S., Yong, L., & Xin, X. (2014). Sources and transports of organochlorine pesticides in the Nanshan underground river, China. Environmental earth sciences, 71(4), 1977-1987.

Aleem, A., & Malik, A. (2005). Genotoxicity of the Yamuna river water at Okhla (Delhi), India. Ecotoxicology and environmental safety, 61(3), 404-412.

Al-Hatim, H. Y., Alrajhi, D., & Al-Rajab, A. J. (2015). Detection of pesticide residue in dams and well water in Jazan area, Saudi Arabia. American Journal of Environmental Sciences, 11(5), 358.

Ali, I., & Gupta, V. K. (2006). Advances in water treatment by adsorption technology. Nature protocols, 1(6), 2661.

Ali, N., Khan, S., ur Rahman, I., & Muhammad, S. (2018). Human Health Risk Assessment through Consumption of Organophosphate Pesticide-Contaminated Water of Peshawar Basin, Pakistan. Exposure and Health, 10(4), 259-272.

Alonso, L. L., Demetrio, P. M., Etchegoyen, M. A., & Marino, D. J. (2018). Glyphosate and atrazine in rainfall and soils in agroproductive areas of the pampas region in Argentina. Science of the Total Environment, 645, 89-96.

Al-Wabel, M. I., Al-Omran, A., El-Naggar, A. H., Nadeem, M., & Usman, A. R. (2013). Pyrolysis temperature induced changes in characteristics and chemical composition of biochar produced from conocarpus wastes. Bioresource Technology, 131, 374-379.

Al-Wabel, M., El-Saeid, M. H., El-Naggar, A. H., Al-Romian, F. A., Osman, K., Elnazi, K., & Sallam, A. S. (2016). Spatial distribution of pesticide residues in the groundwater of a condensed agricultural area. Arabian Journal of Geosciences, 9(2), 120.

Alza Camacho, W. R., García Colmenares, J. M., & Chaparro Acuña, S. P. (2016). Risk estimate of water sources contamination of pesticides (Mancozeb and Carbofuran) in Ventaquemada, Boyacá-Colombia. Acta Agronómica, 65(4), 368-374.

Angın, D., Altintig, E., & Köse, T. E. (2013). Influence of process parameters on the surface and chemical properties of activated carbon obtained from biochar by chemical activation. Bioresource Technology, 148, 542-549.

Aravinna, P., Priyantha, N., Pitawala, A., & Yatigammana, S. K. (2017). Use pattern of pesticides and their predicted mobility into shallow groundwater and surface water bodies of paddy lands in Mahaweli river basin in Sri Lanka. Journal of Environmental Science and Health, Part B, 52(1), 37-47.

Arias-Estévez, M., López-Periago, E., Martínez-Carballo, E., Simal-Gándara, J., Mejuto, J. C., & García-Río, L. (2008). The mobility and degradation of pesticides in soils and the pollution of groundwater resources. Agriculture, Ecosystems & Environment. 123, 247-260.

Ayranci, E., & Hoda, N. (2004). Studies on removal of metribuzin, bromacil, 2, 4-D and atrazine from water by adsorption on high area carbon cloth. Journal of hazardous materials, 112(1-2), 163-168.

Azizullah, A., Richter, P., & Häder, D. P. (2011). Comparative toxicity of the pesticides carbofuran and malathion to the freshwater flagellate Euglena gracilis. Ecotoxicology. 20, 1442-1454.

Babu, S. S., Kumar, S., Roychowdhury, T., Vidyadharan, V., Roychowdhury, N., Samanta, J., & Bhowmick, S (2015). Occurrence and impacts of fluoride in drinking water-a review. Indian Groundwater, 5, 40-54

Badawy, M. I., Ghaly, M. Y., & Gad-Allah, T. A. (2006). Advanced oxidation processes for the removal of organophosphorus pesticides from wastewater. Desalination, 194(1-3), 166-175.

Bai, Y., Ruan, X., & van der Hoek, J. P. (2018). Residues of organochlorine pesticides (OCPs) in aquatic environment and risk assessment along Shaying River, China. Environmental geochemistry and health, 40(6), 2525-2538.

Bailey, G. W., & White, J. L. (1970). Factors influencing the adsorption, desorption, and movement of pesticides in soil. In Single Pesticide Volume: The Triazine Herbicides (pp. 29-92). Springer, New York, NY.

Balakrishna, K., Rath, A., Praveenkumarreddy, Y., Guruge, K. S., & Subedi, B. (2017). A review of the occurrence of pharmaceuticals and personal care products in Indian water bodies. Ecotoxicology and environmental safety, 137, 113-120.

Bandurski, R. S. (1947). Spectrophotometric method for determination of 2, 4 dichlorophenoxyacetic acid. Botanical Gazette, 108(3), 446-449.

Barbosa, G. V., Zaghete, M. A., Amoresi, R. A. C., da Silva, M. S., Cavalheiro, A. A., & da Silva, R. C. D. L. (2017). Structural Analysis of Magnesium-Aluminium Hydrotalcites Modified with Iron III Obtained by Hydroxide Precipitation Method. Materials Sciences and Applications, 8(11), 784.

Barbusiński, K., & Filipek, K. (2001). Use of Fenton's reagent for removal of pesticides from industrial wastewater. Polish Journal of Environmental Studies, 10(4), 207-212.

Bartolomeu, M., Neves, M. G. P. M. S., Faustino, M. A. F., & Almeida, A. (2018). Wastewater chemical contaminants: remediation by advanced oxidation processes. Photochemical & Photobiological Sciences, 17(11), 1573-1598.

Bazrafshan, E., Mostafapour, F. K., Faridi, H., Farzadkia, M., Sargazi, S., & Sohrabi, A. (2013). Removal of 2, 4-dichlorophenoxyacetic acid (2, 4-D) from aqueous environments using single-walled carbon nanotubes. Health Scope, 2(1), 39-46.

Becker J.G. and Seagren E.A. (2010). Biorremediation of hazardous organics. In: Environmental microbiology (R. Mitchell y G. Ji-Dong, Ed.). Wiley-Blackwell, New Jersey, United States of America, pp. 177-212.

Bedmar, F., Gianelli, V., Angelini, H., & Viglianchino, L. (2015). Risk of pesticide contamination of groundwater in the basin of the El Cardalito stream, Argentina. RIA, Revista de Investigaciones Agropecuarias, 41(1), 70-82.

Bernardes, M. F. F., Pazin, M., Pereira, L. C., & Dorta, D. J. (2015). Impact of pesticides on environmental and human health. Toxicology Studies-Cells, Drugs and Environment (Andreazza C y Scola G Eds.). InTech, Croacia, 195-233.

Berton, A., Brugnera, M. F., & Dores, E. F. (2018). Grab and passive sampling applied to pesticide analysis in the São Lourenço river headwater in Campo Verde–MT, Brazil. Journal of Environmental Science and Health, Part B, 53(4), 237-245.

Bhargavi, O., Kiran, K., Suvardhan, K., Rekha, D., Janardhanam, K., Chiranjeevi, P. (2006). A Sensitive Determination of Carbofuran by Spectrophotometer using 4, 4-azo-bis-3, 3′ 5, 5′-tetra bromoaniline in various Environmental Samples. Journal of Chemistry. 3, 68-77.

Bhattacharya, A. (2006). Remediation of Pesticide-Polluted Waters Through Membranes. Separation and Purification Reviews, 35(1), 1-38.

Bhowmick, S., Pramanik, S., Singh, P., Mondal, P., Chatterjee, D., & Nriagu, J. (2018). Arsenic in groundwater of West Bengal, India: a review of human health risks and assessment of possible intervention options. Science of the Total Environment, 612, 148-169.

Bilal, M., Rasheed, T., Sosa-Hernández, J., Raza, A., Nabeel, F., & Iqbal, H. (2018). Biosorption: an interplay between marine algae and potentially toxic elements—a review. Marine drugs, 16(2), 65.

Bourke, J., Manley-Harris, M., Fushimi, C., Dowaki, K., Nunoura, T., & Antal, M. J. (2007). Do all carbonized charcoals have the same chemical structure? 2. A model of the chemical structure of carbonized charcoal. Industrial & Engineering Chemistry Research, 46(18), 5954-5967.

Bouya, H., Errami, M., Salghi, R., Bazzi, L., Zarrouk, A., Al-Deyab, S. S., Hammouti, B., Bazzi, L., & Chakir, A. (2012). Electrochemical degradation of cypermethrin pesticide on a SnO2 anode. International Journal of Electrochemical Science, 7(4), 7453.

Bovey, R. W., & Young, A. L. (1980). The science of 2, 4, 5-T and associated phenoxy herbicides. Wiley publications.

Bragg, W. H. (1913). The Reflection of X-rays by Crystals.(II.). Proceedings of the Royal Society of London. Series A, Containing Papers of a Mathematical and Physical Character, 89(610), 246-248.

Brame, J., & Griggs, C. (2016). Surface Area Analysis Using the Brunauer-Emmett-Teller (BET) Method: Standard Operating Procedure Series: SOP-C (No. ERDC/EL-SR-16-3). US Army Engineer Research and Development Center-Environmental Laboratory Vicksburg United States.

Brauns, B., Jakobsen, R., Song, X., & Bjerg, P. L. (2018). Pesticide use in the wheat-maize double cropping systems of the North China Plain: Assessment, field study, and implications. Science of the Total Environment, 616, 1307-1316.

Broséus, R., Vincent, S., Aboulfadl, K., Daneshvar, A., Sauvé, S., Barbeau, B., & Prévost, M. (2009). Ozone oxidation of pharmaceuticals, endocrine disruptors and pesticides during drinking water treatment. Water Research, 43(18), 4707-4717.

Brown, R. (2012). Biochar production technology. In Biochar for environmental management (pp. 159-178). Routledge.

Budavari, S. (1989). Merck index- encyclopedia of chemicals, drugs and biological, New Jersey:Merck and Co., Inc.

Çagler, E., Donar, Y. O., Sinag, A., Birogul, İ., Bilge, S., Aydincak, K., & Pliekhov, O. (2018). Adsorption of anionic and cationic dyes on biochars, produced by hydrothermal carbonization of waste biomass: effect of surface functionalization and ionic strength. Turkish Journal of Chemistry, 42(1), 86-99.

Cansado, I. P. P., Mourão, P. A. M., Gomes, J. A. F. L., & Almodôvar, V. (2017). Adsorption of MCPA, 2, 4-D and diuron onto activated carbons from wood composites. Ciência & Tecnologia dos Materiais, 29(1), e224-e228.

Cantrell, K. B., Hunt, P. G., Uchimiya, M., Novak, J. M., Ro, K. S. (2012). Impact of pyrolysis temperature and manure source on physicochemical characteristics of biochar. Bioresource Technology. 107, 419-428.

Cassardo, C., & Jones, J. A. A. (2011). Managing water in a changing world. Water, 3, 618-628.

Cebi, U. K., Çakir, R., & Tok, H. H. (2016). Evaluation of the effects of 2,6-dinitro-N, N-dipropyl-4-trifluoromethylanil herbicide on the groundwater contamination in the Thrace region. Journal of Environmental Protection and Ecology, 17(2), 445-452.

CGWB, (2014). Concept note on Geogenic contamination of Groundwater in India with a special note on nitrate, 2014, Central Ground Water Board, Ministry of water resources, Government of India.

Chamkasem, N., & Morris, C. (2016). Direct Determination of 2, 4-dichlorophenoxyacetic acid in Soybean and Corn by Liquid chromatography/tandem mass spectrometry. Journal of Regulatory Science, 4(2), 9-18.

Chang, K. L., Lin, J. H., Chen, S. T. (2011). Adsorption studies on the removal of pesticides (Carbofuran) using activated carbon from rice straw agricultural waste. World Academy of Science and Engineering Technology. 76, 348-351

Chang, Q. (2016). Colloid and interface chemistry for water quality control. Academic Press.

Charles, J. M., Cunny, H. C., Wilson, R. D., & Bus, J. S. (1996). Comparative subchronic studies on 2, 4-dichlorophenoxyacetic acid, amine, and ester in rats. Fundamental and Applied Toxicology, 33(2), 161-165.

Chau, N. D. G., Sebesvari, Z., Amelung, W., & Renaud, F. G. (2015). Pesticide pollution of multiple drinking water sources in the Mekong Delta, Vietnam: evidence from two provinces. Environmental Science and Pollution Research, 22(12), 9042-9058.

Chaza, C., Sopheak, N., Mariam, H., David, D., Baghdad, O., & Moomen, B. (2018). Assessment of pesticide contamination in Akkar groundwater, northern Lebanon. Environmental Science and Pollution Research, 25(15), 14302-14312.

Chen, D., Wang, L., Ma, Y., & Yang, W. (2016). Super-adsorbent material based on functional polymer particles with a multilevel porous structure. NPG Asia Materials, 8(8), e301.

Chen, J. Q., Hu, Z. J., & Ji, R. (2012). Removal of carbofuran from aqueous solution by orange peel. Desalination and Water Treatment, 49(1-3), 106-114.

Chinalia, F. A., Regali-Seleghin, M. H., & Correa, E. M. (2007). 2, 4-D toxicity: cause, effect and control. Terrestrial and Aquatic Environmental Toxicology, 1(2), 24-33.

Chingombe, P., Saha, B., & Wakeman, R. J. (2006). Effect of surface modification of an engineered activated carbon on the sorption of 2, 4-dichlorophenoxy acetic acid and benazolin from water. Journal of Colloid and Interface Science, 297(2), 434-442.

Chiou, C. T., Sheng, G., & Manes, M. (2001). A partition-limited model for the plant uptake of organic contaminants from soil and water. Environmental Science & Technology, 35(7), 1437-1444.

Choudhury, P.P., Singh, R., Ghosh, D. and Sharma, A.R. (2016) Herbicide Use in Indian Agriculture. ICAR - Directorate of Weed Research, Jabalpur, Madhya Pradesh, 110 p.

Chouhan, S., & Flora, S. J. S. (2010). Arsenic and fluoride: two major ground water pollutants. Indian Journal of Experimental Biology. 18, 666-678.

Chowdhury, Z. Z., Hamid, S. B. A., & Zain, S. M. (2015). Evaluating design parameters for breakthrough curve analysis and kinetics of fixed bed columns for Cu (II) cations using lignocellulosic wastes. BioResources, 10(1), 732-749.

Claoston, N., Samsuri, A. W., Ahmad Husni, M. H., & Mohd Amran, M. S. (2014). Effects of pyrolysis temperature on the physicochemical properties of empty fruit bunch and rice husk biochars. Waste Management & Research, 32(4), 331-339.

Climent, M. J., Sánchez-Martín, M. J., Rodríguez-Cruz, M. S., Pedreros, P., Urrutia, R., & Herrero-Hernández, E. (2018). Determination of pesticides in river surface waters of Central Chile using spe-GC-MS multi-residue method. Journal of the Chilean Chemical Society, 63(2), 4023-4031.

Coates, J. (2006). Interpretation of infrared spectra, a practical approach. Encyclopedia of analytical chemistry: applications, theory and instrumentation. R.A. Meyers (Ed.) Copyright, John Wiley & Sons Ltd

CPCB, (2010). Annual Report. Central Pollution Control Board, Ministry of Environment & Forests, Government of India, New Delhi.

Crosby, D. G. (1973). The fate of pesticides in the environment. Annual Review of Plant Physiology, 24(1), 467-492.

Daioglou, V., Stehfest, E., Wicke, B., Faaij, A., & Van Vuuren, D. P. (2016). Projections of the availability and cost of residues from agriculture and forestry. Gcb Bioenergy, 8(2), 456-470.

Damalas, C. A., & Eleftherohorinos, I. G. (2011). Pesticide exposure, safety issues, and risk assessment indicators. International Journal of Environmental Research and Public Health, 8(5), 1402-1419.

Darapu, S. S. K., Sudhakar, B., Krishna, K. S. R., Rao, P. V., & Sekhar, M. C. (2011). Determining water quality index for the evaluation of water quality of river Godavari. International Journal of Environmental Research and Application, 1, 174-18.

Das, R. (2018). Carbon nanotubes for clean water, carbon nanostructures. Springer international publishing AG. pp 12. https://doi.org/10.10071978-3-319-95603-92.

de Aragão, B. J., & Messaddeq, Y. (2008). Peak separation by derivative spectroscopy applied to FTIR analysis of hydrolized silica. Journal of the Brazilian chemical Society, 19(8), 1582-1594.

De Gerónimo, E., Aparicio, V. C., Bárbaro, S., Portocarrero, R., Jaime, S., & Costa, J. L. (2014). Presence of pesticides in surface water from four sub-basins in Argentina. Chemosphere, 107, 423-431.

Dehghani, M. H., Sanaei, D., Ali, I., & Bhatnagar, A. (2016). Removal of chromium (VI) from aqueous solution using treated waste newspaper as a low-cost adsorbent: kinetic modeling and isotherm studies. Journal of molecular liquids, 215, 671-679.

Dehghani, M., Nasseri, S., & Karamimanesh, M. (2014). Removal of 2, 4-Dichlorophenolyxacetic acid (2, 4-D) herbicide in the aqueous phase using modified granular activated carbon. Journal of Environmental Health Science and Engineering, 12(1), 28.

Deng, S., Ma, R., Yu, Q., Huang, J., Yu, G. (2009). Enhanced removal of pentachlorophenol and 2, 4-D from aqueous solution by an aminated biosorbent. Journal of Hazardous Materials. 165, 408-414.

Department of agriculture, cooperation and farmers welfare (2018). Annual report (2017-18) ministry of agriculture and farmers welfare, Government of India, New Delhi-110001 (retrieved from http://www.agricoop.nic.in/sites/default/files/Krishi%20AR%202017-18-1%20for%20web.pdf).

Dequaire, M., Degrand, C., & Limoges, B. (1999). An immunomagnetic electrochemical sensor based on a perfluorosulfonate-coated screen-printed electrode for the determination of 2, 4-dichlorophenoxyacetic acid. Analytical Chemistry, 71(13), 2571-2577.

Deuel, L. E., Price, J. D., Turner, F. T., Brown, K. W. (1979). Persistence of carbofuran and its metabolites, 3-keto and 3-hydroxy carbofuran, under flooded rice culture. Journal of Environmental Quality. 8, 23-26.

Devipriya, S., & Yesodharan, S. (2005). Photocatalytic degradation of pesticide contaminants in water. Solar Energy Materials and Solar Cells, 86(3), 309-348.

Diaz-Flores, P. E., Leyva-Ramos, R., Rangel-Mendez, J. R., Ortiz, M. M., Guerrero-Coronado, R. M., & Mendoza-Barron, J. (2006). Adsorption of 2, 4-dichlorophenoxyacetic acid from aqueous solution on activated carbon cloth. Journal of Environmental Engineering and Management, 16(4), 249-257.

Diwan, V., Hanna, N., Purohit, M., Chandran, S., Riggi, E., Parashar, V., Tamhankar, A. and Stålsby Lundborg, C. (2018). Seasonal Variations in Water-Quality, Antibiotic Residues, Resistant Bacteria and Antibiotic Resistance Genes of Escherichia coli Isolates from Water and Sediments of the Kshipra River in Central India. International Journal of Environmental Research and Public Health, 15(6), 1281.

Doczekalska, B., Kuśmierek, K., Świątkowski, A., & Bartkowiak, M. (2018). Adsorption of 2, 4-dichlorophenoxyacetic acid and 4-chloro-2-metylphenoxyacetic acid onto activated carbons derived from various lignocellulosic materials. Journal of Environmental Science and Health, Part B, 53(5), 290-297.

Dong, H., Zeng, G., Tang, L., Fan, C., Zhang, C., He, X., & He, Y. (2015). An overview on limitations of TiO2-based particles for photocatalytic degradation of organic pollutants and the corresponding countermeasures. Water research, 79, 128-146.

Dressing, S.A., Meals, D.W., Harcum, J.B., Spooner, J., Stribling, J.B., Richards, R.P., Millard, C.J., Lanberg, S.A. and O'Donnell, J.G. (2016). Monitoring and Evaluating Nonpoint Source Watershed Projects. EPA 841-R-16-010. US Environmental Protection Agency, Washington, DC. Accessed December 4, 2018. https://www. epa.gov/nps/monitoring-and-evaluating-nonpoint-source-watershed-projects.

Du Plessis, A. (2017). Freshwater Challenges of South Africa and its Upper Vaal River. Springer. DOI 10.1007/978-3-319-49502-6_1

Dume, B., Berecha, G., & Tulu, S. (2015). Characterization of biochar produced at different temperatures and its effect on acidic nitosol of Jimma, Southwest Ethiopia. International Journal of Soil Science, 10(2), 63-73.

EBC (2012) 'European Biochar Certificate - Guidelines for a Sustainable Production of Biochar.' European Biochar Foundation (EBC), Arbaz, Switzerland. http://www.europeanbiochar.org/en/download. Version 6.2E of 04th February 2016, DOI:10.13140/RG.2.1.4658.7043.

Ebenstein, A. (2012). The consequences of industrialization: evidence from water pollution and digestive cancers in China. Review of Economics and Statistics, 94(1), 186-201.

Eckert, M. (2012). Max von Laue and the discovery of X-ray diffraction in 1912. Annalen der Physik, 524(5), A83-A85.

Eisler, R. 1985. Carbofuran hazards to fish, wildlife, and invertebrates: a synoptic review. U.S. Fish and Wildlife Service Biological Report 85 (1.3). 36.

El-Beshlawy, A. M., El-Alfy, M. S., Sari, T. T., Chan, L. L., & Tricta, F. (2014). Continuation of deferiprone therapy in patients with mild neutropenia may not lead to a more severe drop in neutrophil count. European journal of haematology, 92(4), 337-340.

El-Osmani, R., Net, S., Dumoulin, D., Baroudi, M., Bakkour, H., & Ouddane, B. (2014). Solid phase extraction of organochlorine pesticides residues in groundwater (akkar plain, north Lebanon). International Journal of Environmental Research, 8(4), 903-912.

Essandoh, M., Wolgemuth, D., Pittman Jr, C. U., Mohan, D., & Mlsna, T. (2017). Phenoxy herbicide removal from aqueous solutions using fast pyrolysis switchgrass biochar. Chemosphere, 174, 49-57.

European Environmental Agency, EEA (2018) retrieved https://www.eea.europa.eu/archived/archived-content-water-topic/water-pollution/point-sources/point-sources on 7 december, 2018.

Evert, S. (2002). Environmental fate of Carbofuran. California Environmental Protection Agency, Department of Pesticide Regulation, Sacramento.

Farahani, G. H. N., Sahid, I. B., Zakaria, Z., Kuntom, A., Omar, D. (2008). Study on the downward movement of carbofuran in two Malaysian soils. Bulletin of Environmental Contamination and Toxicology. 81, 294-298.

Fiol, N., & Villaescusa, I. (2009). Determination of sorbent point zero charge: usefulness in sorption studies. Environmental Chemistry Letters, 7(1), 79-84.

Foo, K. Y. (2016). Value-added utilization of maize cobs waste as an environmental friendly solution for the innovative treatment of carbofuran. Process Safety and Environmental Protection, 100, 295-304.

Foo, K. Y. (2016). Value-added utilization of maize cobs waste as an environmental friendly solution for the innovative treatment of carbofuran. Process Safety and Environmental Protection, 100, 295-304.

Foo, K. Y., & Hameed, B. H. (2010). Detoxification of pesticide waste via activated carbon adsorption process. Journal of Hazardous Materials, 175(1), 1-11.

Foo, K. Y., & Hameed, B. H. (2010). Insights into the modeling of adsorption isotherm systems. Chemical Engineering Journal, 156(1), 2-10.

Frank, L., Hovorka, M., Mikmeková, Š., Mikmeková, E., Müllerová, I., & Pokorná, Z. (2012). Scanning electron microscopy with samples in an electric field. Materials, 5(12), 2731-2756.

Freundlich, H. (1907). Über die adsorption in lösungen. Zeitschrift für physikalische Chemie, 57(1), 385-470.

Fu, X., Liang, Y., Qin, L., Zeng, H., Mo, L., Wang, D., & Qin, L. (2018). Distribution of organochlorine pesticides（OCPs）in the water body of huixian karst wetland of guilin and environmental risk assessment of OCP mixtures. Journal of Agro-Environment Science, 37(5), 974-983.

Fukuto, T. R. (1990). Mechanism of action of organophosphorus and carbamate insecticides. Environmental Health Perspectives. 87, 245.

Gadd, G. M. (2009). Biosorption: critical review of scientific rationale, environmental importance and significance for pollution treatment. Journal of Chemical Technology & Biotechnology: International Research in Process, Environmental & Clean Technology, 84(1), 13-28.

Gavrilescu, M. (2005). Fate of pesticides in the environment and its bioremediation. Engineering in Life Sciences, 5(6), 497-526.

Gholizadeh, A., Kermani, M., Gholami, M., & Farzadkia, M. (2013). Kinetic and isotherm studies of adsorption and biosorption processes in the removal of phenolic compounds from aqueous solutions: comparative study. Journal of Environmental Health Science and Engineering, 11(1), 29.

Gitari, M. W., & Mudzielwana, R. (2018). Mineralogical and Chemical Characteristics of Raw and Modified Clays and Their Application in Arsenic and Fluoride Removal. Current Topics in the Utilization of Clay in Industrial and Medical Applications, 45.

Głowacki, M., & Ciesielczuk, T. (2014). Assessment of pahs and selected pesticides in shallow groundwater in the highest protected areas in the Opole region, Poland. Journal of Ecological Engineering, 15(2).

Goel, A., and Aggarwal. P. (2007). Pesticide Poisoning, The National Medical Journal of India. 20,182-191.

Goel, J., Kadirvelu, K., Rajagopal, C., & Garg, V. K. (2005). Removal of lead (II) by adsorption using treated granular activated carbon: batch and column studies. Journal of Hazardous Materials, 125(1), 211-220.

Gong, W., Mowlem, M., Kraft, M., & Morgan, H. (2009). A simple, low-cost double beam spectrophotometer for colorimetric detection of nitrite in seawater. IEEE Sensors Journal, 9(7), 862-869.

Greig, J. B. (1995). Veterans and Agent Orange: Health Effects of Herbicides Used in Vietnam. Occupational and Environmental Medicine, 52(2), 144.

Grossmann, K. (2010). Auxin herbicides: current status of mechanism and mode of action. Pest Management Science, 66(2), 113-120.

Grützmacher, G., Kumar, P. S., Rustler, M., Hannappel, S., & Sauer, U. (2013). Geogenic groundwater contamination—Definition, occurrence and relevance for drinking water production. Zbl Geol Paläont Teil I, 1, 69-75.

Gupta, A., Bhatnagar, P., & Bakre, P. P. (2016). Residues of organochlorine insecticides in water and sediment from Ramgarh water reservoir, Jaipur, Rajastan. Journal of Entomology and Zoology Studies, 4, 397-401.

Gupta, R. C. (1994). Carbofuran toxicity. Journal of Toxicology and Environmental Health, Part A Current Issues. 43, 383-418.

Gupta, V. K., Ali, I., & Saini, V. K. (2006). Adsorption of 2, 4-D and carbofuran pesticides using fertilizer and steel industry wastes. Journal of Colloid and Interface Science, 299(2), 556-563.

Gupta, V. K., Gupta, B., Rastogi, A., Agarwal, S., & Nayak, A. (2011). Pesticides removal from waste water by activated carbon prepared from waste rubber tire. Water Research, 45(13), 4047-4055.

Gwenzi, W., & Chaukura, N. (2018). Organic contaminants in African aquatic systems: current knowledge, health risks, and future research directions. Science of the Total Environment, 619, 1493-1514.

Hadian, Z., & Eslamizad, S. (2018). Pesticide residues analysis in Iranian fruits and vegetables by Gas Chromatography-Mass Spectrometry (winter 2019). Iranian Journal of Pharmaceutical Research. 18 (1), 275-285. DOI: 10.22037/IJPR.2019.2333.

Hall G.L., Mourer C.R., and Shibamoto, T. (1997). Development of Determination Method for Carbofuran and Oxydemeton-methyl in Ambient Air, Journal of Agricultural and Food Chemicals. 45, 4347-4350.

Hameed, B. H., Salman, J. M., & Ahmad, A. L. (2009). Adsorption isotherm and kinetic modeling of 2, 4-D pesticide on activated carbon derived from date stones. Journal of Hazardous Materials, 163(1), 121-126.

Hardesty, J. H., & Attili, B. (2010). Spectrophotometry and the Beer-Lambert Law: An Important Analytical Technique in Chemistry. Collin College: Collin, TX, USA.

Harikishna, V., and Naidu, N. V. S. (2005). Facile and Sensitive Spectrophotometric Technique for the Determination of Carbofuran in its Formulations, Water and Grain Samples with Substituted Anilines. Journal of Chemistry. 2, 218-223.

Health and Welfare Canada. Guidelines for Canadian drinking water quality (1987). 3d ed. Prepared by the Federal–Provincial Subcommittee on Drinking Water of the Federal–Provincial Advisory Committee on Environmental and Occupational Health.

Herath, I., Kumarathilaka, P., Al-Wabel, M. I., Abduljabbar, A., Ahmad, M., Usman, A. R., & Vithanage, M. (2016). Mechanistic modeling of glyphosate interaction with rice husk derived engineered biochar. Microporous and Mesoporous Materials, 225, 280-288.

Herrero-Hernández, E., Pose-Juan, E., Sánchez-Martín, M. J., Andrades, M. S., & Rodríguez-Cruz, M. S. (2016). Intra-annual trends of fungicide residues in waters from vineyard areas in La Rioja region of northern Spain. Environmental Science and Pollution Research, 23(22), 22924-22936.

Hiloidhari, M., Das, D., & Baruah, D. C. (2014). Bioenergy potential from crop residue biomass in India. Renewable and Sustainable Energy Reviews, 32, 504-512.

Ho, Y. S., & McKay, G. (1999). Pseudo-second order model for sorption processes. Process Biochemistry, 34(5), 451-465.

Hodgson, E., Roe, R., Motoyama, N. (1991). Pesticides and the Future: Toxicological studies of risks and benefits. Rev. Pesticide Toxicology. 1, 3-12.

Holm, T. R., Machesky, M. L., & Scott, J. W. (2014). Sorption of Polycyclic Aromatic Hydrocarbons (PAHs) to Biochar and Estimates of PAH Bioavailability. Champaign, IL: Illinois Sustainable Technology Center.

Humbert, H., Gallard, H., Suty, H., & Croué, J. P. (2008). Natural organic matter (NOM) and pesticides removal using a combination of ion exchange resin and powdered activated carbon (PAC). Water Research, 42(6-7), 1635-1643.

Hussein, M. H., Abdullah, A. M., Badr El-Din, N. I., & Mishaqa, E. S. I. (2017). Biosorption potential of the microchlorophyte chlorella vulgaris for some pesticides. Journal of Fertilizers & Pesticides, 8(01).

Idrees, N., Tabassum, B., Abd_Allah, E. F., Hashem, A., Sarah, R., & Hashim, M. (2018). Groundwater contamination with cadmium concentrations in some West UP Regions, India. Saudi Journal of Biological Sciences, 25(7), 1365-1368.

Ikehata, K., & Gamal El-Din, M. (2005). Aqueous pesticide degradation by ozonation and ozone-based advanced oxidation processes: a review (Part I). Ozone: Science and Engineering, 27(2), 83-114.

Inam, E., Etim, U. J., Akpabio, E. G., & Umoren, S. A. (2017). Process optimization for the application of carbon from plantain peels in dye abstraction. Journal of Taibah University for Science, 11(1), 173-185.

International Agency for Research on Cancer. Volume 113: DDT, lindane and 2,4-D. IARC Working Group. Lyon; 2–9 June 2015. IARC Monogr Eval Carcinog Risks Hum.

International Biochar Initiative. (2015). Standardized product definition and product testing guidelines for biochar that is used in soil: version number 2.1 [online], [cited 14 November 2016]. Available from Internet: http://www.biochar-international.org/sites/default/files/IBI_Biochar_Standards_V2.1_Final.pdf.

Jaggi, N., & Vij, D. R. (2006). Fourier transform infrared spectroscopy. In Handbook of Applied Solid State Spectroscopy (pp. 411-450). Springer, Boston, MA.

Jan, M. R., Shah, J., Khan, H. (2003). Investigation of new indirect spectrophotometric method for the determination of carbofuran in carbamate pesticides. Chemosphere. 52, 1623-1626.

Jayasumana, C., Paranagama, P., Agampodi, S., Wijewardane, C., Gunatilake, S., & Siribaddana, S. (2015). Drinking well water and occupational exposure to Herbicides is associated with chronic kidney disease, in Padavi-Sripura, Sri Lanka. Environmental Health, 14(1), 6.

Jiang, N., Shang, R., Heijman, S. G., & Rietveld, L. C. (2018). High-silica zeolites for adsorption of organic micro-pollutants in water treatment: A review. Water research, 144, 145-161.

Jiménez, J. J. (2013). Simultaneous liquid–liquid extraction and dispersive solid-phase extraction as a sample preparation method to determine acidic contaminants in river water by gas chromatography/mass spectrometry. Talanta, 116, 678-687.

Jindo, K., Mizumoto, H., Sawada, Y., Sanchez-Monedero, M. A., & Sonoki, T. (2014). Physical and chemical characterization of biochars derived from different agricultural residues. Biogeosciences, 11(23), 6613-6621.

Jung, B. K., Hasan, Z., & Jhung, S. H. (2013). Adsorptive removal of 2, 4-dichlorophenoxyacetic acid (2, 4-D) from water with a metal–organic framework. Chemical engineering journal, 234, 99-105.

Kaech, A. (2002). An introduction to electron microscopy instrumentation, imaging and preparation. Cent. Microsc. Image Anal, 1-26.

Kammerer, J., Carle, R., & Kammerer, D. R. (2010). Adsorption and ion exchange: basic principles and their application in food processing. Journal of Agricultural and Food Chemistry, 59(1), 22-42.

Karabelas, A., & Plakas, K. (2011). Membrane treatment of potable water for pesticides removal. In Herbicides, theory and applications. InTech. 369-408.

Kashyap, S. M., Pandya, G. H., Kondawar, V. K., & Gabhane, S. S. (2005). Rapid analysis of 2, 4-D in soil samples by modified Soxhlet apparatus using HPLC with UV detection. Journal of Chromatographic Science, 43(2), 81-86.

Katsumata, H., Kobayashi, T., Kaneco, S., Suzuki, T., & Ohta, K. (2011). Degradation of linuron by ultrasound combined with photo-Fenton treatment. Chemical Engineering Journal, 166(2), 468-473.

Katz, B. G., Berndt, M. P., & Crandall, C. A. (2014). Factors affecting the movement and persistence of nitrate and pesticides in the surficial and upper Floridan aquifers in two agricultural areas in the southeastern United States. Environmental Earth Sciences, 71(6), 2779-2795.

Kearns, J. P., Wellborn, L. S., Summers, R. S., & Knappe, D. R. U. (2014). 2, 4-D adsorption to biochars: Effect of preparation conditions on equilibrium adsorption capacity and comparison with commercial activated carbon literature data. Water research, 62, 20-28.

Keiluweit, M., Nico, P. S., Johnson, M. G., & Kleber, M. (2010). Dynamic molecular structure of plant biomass-derived black carbon (biochar). Environmental Science & Technology, 44(4), 1247-1253.

Kibona, D., Kidulile, G., & Rwabukambara, F. (2009). Environment, climate warming and water management. Transition Studies Review, 16(2), 484-500.

King, P. L., Ramsey, M. S., McMillan, P. F., & Swayze, G. (2004). Laboratory Fourier transform infrared spectroscopy methods for geologic samples. Infrared Spectroscopy in Geochemistry, Exploration, and Remote Sensing, 33, 57-91.

Klarich, K. L., Pflug, N. C., DeWald, E. M., Hladik, M. L., Kolpin, D. W., Cwiertny, D. M., & LeFevre, G. H. (2017). Occurrence of neonicotinoid insecticides in finished drinking water and fate during drinking water treatment. Environmental Science & Technology Letters, 4(5), 168-173.

Koble, R. A., & Corrigan, T. E. (1952). Adsorption isotherms for pure hydrocarbons. Industrial & Engineering Chemistry, 44(2), 383-387.

Köck-Schulmeyer, M., Ginebreda, A., Postigo, C., Garrido, T., Fraile, J., de Alda, M. L., & Barceló, D. (2014). Four-year advanced monitoring program of polar pesticides in groundwater of Catalonia (NE-Spain). Science of the Total Environment, 470, 1087-1098.

Koner, S., Pal, A., & Adak, A. (2013). Adsorption of 2, 4-D herbicide from water environment on modified silica gel factory waste. Water Environment Research, 85(11), 2147-2156.

Krasner, S. W., Croué, J. P., Buffle, J., & Perdue, E. M. (1996). Three approaches for characterizing NOM. Journal-American Water Works Association, 88(6), 66-79.

Kumar, S., & Jain, S. (2013). History, introduction, and kinetics of ion exchange materials. Journal of Chemistry, 2013. http://dx.doi.org/10.1155/2013/957647.

Kumar, S., Kaushik, G., & Villarreal-Chiu, J. F. (2016). Scenario of organophosphate pollution and toxicity in India: A review. Environmental Science and Pollution Research, 23(10), 9480-9491.

Kumari, K., Singh, R. P., & Saxena, S. K. (1988). Adsorption thermodynamics of carbofuran on fly ash. Colloids and Surfaces, 33, 55-61.

Kundu, S., Coumar, M. V., Rajendiran, S., & Rao, A. S. (2015). Phosphates from detergents and eutrophication of surface water ecosystem in India. Current Science, 108, 1320-1325.

Kyriakopoulos, G. G., Hourdakis, A. A., & Doulia, D. D. (2003). Adsorption of pesticides on resins. Journal of Environmental Science and Health, Part B, 38(2), 157-168.

Lagergren, S. (1898). Zur theorie der sogenannten adsorption geloster stoffe. Kungliga svenska vetenskapsakademiens. Handlingar, 24, 1-39.

Langmuir, I. (1918). The adsorption of gases on plane surfaces of glass, mica and platinum. Journal of the American Chemical society, 40(9), 1361-1403.

Lapworth, D.J., Das, P., Shaw, A., Mukherjee, A., Civil, W., Petersen, J.O., Gooddy, D.C., Wakefield, O., Finlayson, A., Krishan, G. and Sengupta, P. (2018). Deep urban groundwater vulnerability in India revealed through the use of emerging organic contaminants and residence time tracers. Environmental Pollution, 240, 938-949.

Lata, S., Singh, P. K., & Samadder, S. R. (2015). Regeneration of adsorbents and recovery of heavy metals: a review. International Journal of Environmental Science and Technology, 12(4), 1461-1478.

Lazic, S., Sunjka D., Milovanovic, I., Jovanov, P., & Grahovac, N. (2013). Determination of pesticide residues in drainage water. Proceedings of the 13th International Conference of Environmental Science and Technology Athens, Greece, 5-7 September 2013

Legrouri, A., Lakraimi, M., Barroug, A., De Roy, A., & Besse, J. P. (2005). Removal of the herbicide 2, 4-dichlorophenoxyacetate from water to zinc–aluminium–chloride layered double hydroxides. Water Research, 39(15), 3441-3448.

Lehmann, E., Fargues, M., Dibié, J. J. N., Konaté, Y., & de Alencastro, L. F. (2018). Assessment of water resource contamination by pesticides in vegetable-producing areas in Burkina Faso. Environmental Science and Pollution Research, 25(4), 3681-3694.

Lehmann, E., Fargues, M., Dibié, J. J. N., Konaté, Y., & de Alencastro, L. F. (2018). Assessment of water resource contamination by pesticides in vegetable-producing areas in Burkina Faso. Environmental Science and Pollution Research, 25(4), 3681-3694.

Lehmann, J., & Joseph, S. (Eds.). (2015). Biochar for environmental management: science, technology and implementation. Routledge.

Lehmann, J., Gaunt, J., & Rondon, M. (2006). Bio-char sequestration in terrestrial ecosystems–a review. Mitigation and Adaptation Strategies for Global Change, 11(2), 403-427.

Lei, H., Pan, H., Xi, B., Xu, T. (2014). Composition and potential risks of agricultural chemical pesticides presented in the potential drinking water sources of groundwater from rural area. BioTechnology: An Indian Journal 10(12), 5966-5971.

Li, H., Feng, Y., Li, X., & Zeng, D. (2018). Analytical Confirmation of Various Herbicides in Drinking Water Resources in Sugarcane Production Regions of Guangxi, China. Bulletin of Environmental Contamination and Toxicology, 100(6), 815-820.

Li, J. L., Zhang, C. X., Wang, Y. X., Liao, X. P., Yao, L. L., Liu, M., & Xu, L. (2015c). Pollution characteristics and distribution of polycyclic aromatic hydrocarbons and organochlorine pesticides in groundwater at Xiaodian Sewage Irrigation Area, Taiyuan City. Huan jing ke xue Huanjing kexue, 36(1), 172-178.

Li, J., Li, F., & Liu, Q. (2015a). Sources, concentrations and risk factors of organochlorine pesticides in soil, water and sediment in the Yellow River estuary. Marine Pollution Bulletin, 100(1), 516-522.

Li, J., Li, Y., Wu, M., Zhang, Z., & Lü, J. (2013). Effectiveness of low-temperature biochar in controlling the release and leaching of herbicides in soil. Plant and Soil, 370(1-2), 333-344.

Li, Q., Sun, J., Ren, T., Guo, L., Yang, Z., Yang, Q., & Chen, H. (2018). Adsorption mechanism of 2, 4-dichlorophenoxyacetic acid onto nitric-acid-modified activated carbon fiber. Environmental technology, 39(7), 895-906.

Li, X., Rao, Z., Yang, Z., Guo, X., Huang, Y., Zhang, J., Guo, F. and Liu, C. (2015b). A survey of 42 semi-volatile organic contaminants in groundwater along the grand canal from Hangzhou to Beijing, East China. International Journal of Environmental Research and Public Health, 12(12), 16070-16081.

Li, Y., & Yu, J. (2014). New stories of zeolite structures: their descriptions, determinations, predictions, and evaluations. Chemical reviews, 114(14), 7268-7316.

Lima, I., Bigner, R., & Wright, M. (2017). Conversion of sweet sorghum bagasse into value-added biochar. Sugar Tech, 19(5), 553-561.

Lin, P. C., Lin, S., Wang, P. C., & Sridhar, R. (2014). Techniques for physicochemical characterization of nanomaterials. Biotechnology Advances, 32(4), 711-726.

Liu, N., Zhu, M., Wang, H., & Ma, H. (2016). Adsorption characteristics of Direct Red 23 from aqueous solution by biochar. Journal of Molecular Liquids, 223, 335-342.

Low, K. S., & Lee, C. K. (1991). Cadmium uptake by the moss, Calymperes delessertii, Besch. Bioresource Technology, 38(1), 1-6.

Lü, J., Li, J., Li, Y., Chen, B., & Bao, Z. (2012). Use of rice straw biochar simultaneously as the sustained release carrier of herbicides and soil amendment for their reduced leaching. Journal of agricultural and food chemistry, 60(26), 6463-6470.

Majewski, M. S., & Capel, P. D. (1995). Pesticides in the atmosphere: distribution, trends, and governing factors. CRC Press.

Mandal, S., Sarkar, B., Igalavithana, A. D., Ok, Y. S., Yang, X., Lombi, E., & Bolan, N. (2017). Mechanistic insights of 2, 4-D sorption onto biochar: Influence of feedstock materials and biochar properties. Bioresource technology, 246, 160-167.

Marturi, N. (2013). Vision and visual servoing for nanomanipulation and nanocharacterization in scanning electron microscope (Doctoral dissertation).

Mašek, O., Brownsort, P., Cross, A., Sohi, S. (2013). Influence of production conditions on the yield and environmental stability of biochar. Fuel. 103, 151-155.

Masoud, A. A., Abdel-Wahab Arafa, N. A., & El-Bouraie, M. (2018). Patterns and Trends of the Pesticide Pollution of the Shallow Nile Delta Aquifer (Egypt). Water, Air, & Soil Pollution, 229, 1-23.

Matsumura, F. (1982). Degradation of pesticides in the environment by microorganisms and sunlight. In Biodegradation of Pesticides (pp. 67-87). Springer, Boston, MA.

Mawussi, G., Júnior, R. P. S., Dossa, E. L., & Alaté, K. K. A. (2014). Insecticide residues in soil and water in coastal areas of vegetable production in Togo. Environmental Monitoring and Assessment, 186(11), 7379-7385.

Mayakaduwa, S. S., Herath, I., Ok, Y. S., Mohan, D., & Vithanage, M. (2017). Insights into aqueous carbofuran removal by modified and non-modified rice husk biochars. Environmental Science and Pollution Research, 24(29), 22755-22763.

Mayakaduwa, S. S., Herath, I., Ok, Y. S., Mohan, D., & Vithanage, M. (2016b). Insights into aqueous carbofuran removal by modified and non-modified rice husk biochars. Environmental Science and Pollution Research, 24(29), 22755-22763.

Mayakaduwa, S. S., Vithanage, M., Karunarathna, A., Mohan, D., & Ok, Y. S. (2016a). Interface interactions between insecticide carbofuran and tea waste biochars produced at different pyrolysis temperatures. Chemical Speciation & Bioavailability, 28(1-4), 110-118.

McLaughlin, H., Anderson, P. S., Shields, F. E., & Reed, T. B. (2009, August). All biochars are not created equal, and how to tell them apart. In Proceedings, North American Biochar Conference, Boulder, Colorado, 1-36.

McNabb, D. E. (2017). Water Resource Management: Sustainability in an Era of Climate Change. Springer.

Meffe, R., & de Bustamante, I. (2014). Emerging organic contaminants in surface water and groundwater: a first overview of the situation in Italy. Science of the Total Environment, 481, 280-295.

Megharaj, M., Ramakrishnan, B., Venkateswarlu, K., Sethunathan, N., & Naidu, R. (2011). Bioremediation approaches for organic pollutants: a critical perspective. Environment International, 37(8), 1362-1375.

Meleiro-Porto A.L., Zelayarán M. G., Consiglio-Kasemod-el M. and Nitschke M. (2011). Biodegradation of Pes-ticides. In: Pesticides in the Modern World-Pesticides Use and Management. (M. Stoytcheva, Ed.). InTech. Croatia, 408-438.

Memon, G. Z., Bhanger, M. I., & Akhtar, M. (2007). The removal efficiency of chestnut shells for selected pesticides from aqueous solutions. Journal of Colloid and Interface Science, 315(1), 33-40.

Memon, G. Z., Moghal, M., Memon, J. R., Memon, N. N., & Bhanger, M. I. (2014). Adsorption of selected pesticides from aqueous solutions using cost effective walnut shells. Adsorption, 4(10).

Memon, S., Memon, N., & Memon, S. (2015). Removal of carbofuran and methylparathion from aqueous media through calix [4] arene-based impregnated resin. Desalination and Water Treatment, 54(3), 802-812.

Memon, S., Memon, S., & Memon, N. (2014b). An efficient p-tetranitrocalix [4] arene based adsorbent for the removal of carbofuran from aqueous media. Journal of the Iranian Chemical Society, 11(6), 1599-1608.

Menchen, A., De las Heras, J., & Alday, J. J. G. (2017). Pesticide contamination in groundwater bodies in the Júcar River European Union pilot basin (SE Spain). Environmental monitoring and assessment, 189(4), 146.

Minnesota Department of Health (MDH), Health Risk Assessment Unit, 2,4-D and drinking water (2016)

Mitchell, C., Brodie, J., & White, I. (2005). Sediments, nutrients and pesticide residues in event flow conditions in streams of the Mackay Whitsunday Region, Australia. Marine Pollution Bulletin, 51(1-4), 23-36.

Mittal, S., Kaur, G., & Vishwakarma, G. S. (2014). Effects of environmental pesticides on the health of rural communities in the Malwa Region of Punjab, India: a review. Human and Ecological Risk Assessment: An International Journal, 20(2), 366-387.

Mohammed, A. M. (2018). UV-Visible Spectrophotometric Method and Validation of Organic Compounds. European Journal of Engineering Research and Science, 3(3), 8-11.

Mohan, D., Abhishek, K., Sarswat, A., Patel, M., Singh, P., & Pittman, C. U. (2018). Biochar production and applications in soil fertility and carbon sequestration–a sustainable solution to crop-residue burning in India. RSC Advances, 8(1), 508-520.

Mohan, D., Kumar, S., & Srivastava, A. (2014). Fluoride removal from ground water using magnetic and nonmagnetic corn stover biochars. Ecological Engineering, 73, 798-808.

Montory, M., Ferrer, J., Rivera, D., Villouta, M. V., & Grimalt, J. O. (2017). First report on organochlorine pesticides in water in a highly productive agro-industrial basin of the Central Valley, Chile. Chemosphere, 174, 148-156.

Moses, M., Johnson, E. S., Anger, W. K., Burse, V. W., Horstman, S. W., Jackson, R. J., Lewis, R. G., Maddy, K. T., McConnell, R., Meggs, W. J. (1992). Environmental equity and pesticide exposure. Toxicology and Industrial Health. 9, 913-959.

Munira, S., Farenhorst, A., Sapkota, K., Nilsson, D., & Sheedy, C. (2018). Auxin Herbicides and Pesticide Mixtures in Groundwater of a Canadian Prairie Province. Journal of Environmental Quality, 47(6), 1462-1467.

Munro, I.C., Carlo, G.L., Orr, J.C., Sund, K.G., Wilson, R.M., Kennepohl, E., Lynch, B.S. and Jablinske, M. (1992). A comprehensive, integrated review and evaluation of the scientific evidence relating to the safety of the herbicide 2, 4-D. Journal of the American College of Toxicology, 11(5), 559-664.

Murali, S., Shrivastava, R., & Saxena, M. (2008). Quantification of agricultural residues for energy generation—a case study. Journal of the Institution of Public Health Engineers, 3, 27.

Murthy, H. M., and Manonmani, H. K. (2007). Aerobic degradation of technical hexachlorocyclohexane by a defined microbial consortium. Journal of Hazardous Materials. 149, 18-25.

Nagaraja, P., and Bhaskara, B. L. (2006). Sensitive spectrophotometric assessment of carbofuran using dapsone as a new chromogenic reagent in formulations and environmental samples. Eclética Química. 31, 43-48.

Nair, D. R., Burken, J. G., Licht, L. A., & Schnoor, J. L. (1993). Mineralization and uptake of triazine pesticide in soil-plant systems. Journal of Environmental Engineering, 119(5), 842-854.

Nanakoudis, A. (2019) SEM and TEM: what's the difference? Thermo-Fisher scientific. (Retrieved from https://blog.phenom-world.com/sem-tem-difference on 9th june, 2019)

Navarrete, I. A., Tee, K. A. M., Unson, J. R. S., & Hallare, A. V. (2018). Organochlorine pesticide residues in surface water and groundwater along Pampanga River, Philippines. Environmental Monitoring and Assessment, 190(5), 289.

Ndunda, E. N., Madadi, V. O., & Wandiga, S. O. (2018). Organochlorine pesticide residues in sediment and water from Nairobi River, Kenya: levels, distribution, and ecological risk assessment. Environmental Science and Pollution Research, 25(34), 34510-34518.

Nethaji, S., Sivasamy, A., & Mandal, A. B. (2013). Adsorption isotherms, kinetics and mechanism for the adsorption of cationic and anionic dyes onto carbonaceous particles prepared from Juglans regia shell biomass. International Journal of Environmental Science and Technology, 10(2), 231-242.

Nguyen, J., Sison, C. M., Lorenzi, V., Asvapathanagul, P., & Pham, N. M. Monitoring Organochlorine Pesticides, Polychlorinated Biphenyls, and Polyaromatic Hydrocarbons in Wastewater and Groundwater. In World Environmental and Water Resources Congress 2017 (pp. 183-192).

Nicolopoulou-Stamati, P., Maipas, S., Kotampasi, C., Stamatis, P., & Hens, L. (2016). Chemical pesticides and human health: the urgent need for a new concept in agriculture. Frontiers in Public Health, 4, 148.

Niti, C., Sunita, S., Kamlesh, K., & Rakesh, K. (2013). Bioremediation: An emerging technology for remediation of pesticides. Research Journal of Chemistry and Environment 17(4), 88-105.

Njoku, V. O., & Hameed, B. H. (2011). Preparation and characterization of activated carbon from corncob by chemical activation with H3PO4 for 2, 4-dichlorophenoxyacetic acid adsorption. Chemical Engineering Journal, 173(2), 391-399.

Njoku, V. O., Islam, M. A., Asif, M., & Hameed, B. H. (2014). Preparation of mesoporous activated carbon from coconut frond for the adsorption of carbofuran insecticide. Journal of Analytical and Applied Pyrolysis, 110, 172-180.

Njoku, V. O., Islam, M. A., Asif, M., & Hameed, B. H. (2015). Adsorption of 2, 4-dichlorophenoxyacetic acid by mesoporous activated carbon prepared from H3PO4-activated langsat empty fruit bunch. Journal of Environmental Management, 154, 138-144.

Novak, J. M., Lima, I., Xing, B., Gaskin, J. W., Steiner, C., Das, K. C., Ahmedna, M., Rehrah, D., Watts, D.W., Busscher, W.J., Schomberg, H. (2009). Characterization of designer biochar produced at different temperatures and their effects on a loamy sand. Annals of Environmental Science. 3, 195-206.

O'Brien, R. D., Hilton, B. D., Gilmour, L. (1966). The reaction of carbamates with cholinesterase. Molecular Pharmacology. 2, 593-605.

O'Connor, G. A., Elliott, H. A., & Bastian, R. K. (2008). Degraded water reuse: an overview. Journal of Environmental Quality, 37(5_Supplement), S-157.

Odette, M. V., & Yin-Ping, H. (2014). Effects of Pyrolization Temperature of Bamboo Biochars on the Germination and Growth Rates of Zea Maize L. and Brassica Rapa. Journal of Technology 29(4), 239-249.

Ogbeide, O., Tongo, I., & Ezemonye, L. (2015). Risk assessment of agricultural pesticides in water, sediment, and fish from Owan River, Edo State, Nigeria. Environmental monitoring and assessment, 187(10), 654.

Ok, Y. S., Chang, S. X., Gao, B., & Chung, H. J. (2015). SMART biochar technology—a shifting paradigm towards advanced materials and healthcare research. Environmental Technology & Innovation, 4, 206-209.

Okada, E., Pérez, D., De Gerónimo, E., Aparicio, V., Massone, H., & Costa, J. L. (2018). Non-point source pollution of glyphosate and AMPA in a rural basin from the southeast Pampas, Argentina. Environmental Science and Pollution Research, 25(15), 15120-15132.

Ortiz-Hernadez, M. L., Sanchez-Salinas, E., Castrejon Godinez, M. L., Dantan Gonzalez, E., & Popoca Ursino, E. C. (2013). Mechanisms and strategies for pesticide biodegradation: opportunity for waste, soils and water cleaning. Revista Internacional de Contaminación Ambiental, 29.

Ortiz-Hernández M.L., Sánchez-Salinas E., Olvera-Velona A. and Folch-Mallol J.L. (2011). Pesticides in the Envi-ronment: Impacts and its Biodegradation as a Strategy for Residues Treatment. En: Pesticides-Formulations, Effects, Fate. (M. Stoytcheva, Ed.). InTech. Croatia, pp. 551-574.

Otieno, P. O., Lalah, J. O., Virani, M., Jondiko, I. O., Schramm, K. W. (2010b). Soil and water contamination with carbofuran residues in agricultural farmlands in Kenya following the application of the technical formulation Furadan. Journal of Environmental Science and Health Part B. 45, 137-144.

Otieno, P. O., Lalah, J. O., Virani, M., Jondiko, I. O., Schramm, K. W. (2010a). Carbofuran and its toxic metabolites provide forensic evidence for Furadan exposure in vultures (Gyps africanus) in Kenya. Bulletin of Environmental Contamination and Toxicology. 84, 536-544.

Otieno, P., Okinda Owuor, P., Lalah, J. O., Pfister, G., & Schramm, K. W. (2015). Monitoring the occurrence and distribution of selected organophosphates and carbamate pesticide residues in the ecosystem of Lake Naivasha, Kenya. Toxicological & Environmental Chemistry, 97(1), 51-61.

Page, D., Miotliński, K., Gonzalez, D., Barry, K., Dillon, P., & Gallen, C. (2014). Environmental monitoring of selected pesticides and organic chemicals in urban stormwater recycling systems using passive sampling techniques. Journal of Contaminant Hydrology, 158, 65-77.

Pan, H., Lei, H., He, X., Xi, B., & Xu, Q. (2017). Spatial distribution of organochlorine and organophosphorus pesticides in soil-groundwater systems and their associated risks in the middle reaches of the Yangtze River Basin. Environmental Geochemistry and Health, 1-13. doi: 10.1007/s10653-017-9970-1.

Park, S. J., & Seo, M. K. (2011). Interface science and composites (Vol. 18). Academic Press.

Patel, H. (2019). Fixed-bed column adsorption study: a comprehensive review. Applied Water Science, 9(3), 45.

Pavlovic, I., Barriga, C., Hermosín, M. C., Cornejo, J., & Ulibarri, M. A. (2005). Adsorption of acidic pesticides 2, 4-D, Clopyralid and Picloram on calcined hydrotalcite. Applied Clay Science, 30(2), 125-133.

Peiris, N. (2014). Microwave-assisted processing of solid materials for sustainable energy related electronic and optoelectronic applications (Doctoral dissertation, © TA Nirmal Peiris).

Perreault, F., De Faria, A. F., & Elimelech, M. (2015). Environmental applications of graphene-based nanomaterials. Chemical Society Reviews, 44(16), 5861-5896.

Petropoulou, S. S. E., Tsarbopoulos, A., Siskos, P. A. (2006). Determination of carbofuran, carbaryl and their main metabolites in plasma samples of agricultural populations using gas chromatography–tandem mass spectrometry. Analytical and Bioanalytical Chemistry. 385, 1444-1456.

Pitarch, E., Cervera, M.I., Portolés, T., Ibáñez, M., Barreda, M., Renau-Pruñonosa, A., Morell, I., López, F., Albarrán, F. and Hernández, F. (2016). Comprehensive monitoring of organic micro-pollutants in surface and groundwater in the surrounding of a solid-waste treatment plant of Castellón, Spain. Science of the Total Environment, 548, 211-220.

Plangklang, P., and Reunsang, A. (2010). Bioaugmentation of Carbofuran by Burkholderia cepacia PCL3 in a bioslurry phase sequencing batch reactor, Process Biochemistry. 45, 230-238.

Popp, J., Pető, K., & Nagy, J. (2013). Pesticide productivity and food security. A review. Agronomy for Sustainable Development, 33(1), 243-255.

Pozo, K., Oyola, G., Estellano, V.H., Harner, T., Rudolph, A., Prybilova, P., Kukucka, P., Audi, O., Klánová, J., Metzdorff, A. and Focardi, S. (2017). Persistent Organic Pollutants (POPs) in the atmosphere of three Chilean cities using passive air samplers. Science of the Total Environment, 586, 107-114.

Qian, K., Kumar, A., Zhang, H., Bellmer, D., & Huhnke, R. (2015). Recent advances in utilization of biochar. Renewable and Sustainable Energy Reviews, 42, 1055-1064.

Qiu, Y. P., Chen, J. L., Li, A. M., Zhang, Q. X., & Huang, M. S. (2005). Adsorption of 2, 4-D on modified hypercrosslinked polystyrene (NDA-99) and XAD-4 resin. Chinese journal of polymer science, 23(04), 435-440.

Qureshi, M. N., & Rahman, I. (2017) "Quantification of pesticide residues in drinking water in different areas of district Charsadda, Pakistan." Pakistan Journal of Scientific and Industrial Research Series A: Physical Sciences, 60, 2, 101-105

Qurratu, A., & Reehan, A. (2016). A Review of 2, 4-Dichlorophenoxyacetic Acid (2, 4-D) Derivatives: 2, 4-D Dimethylamine Salt and 2, 4-D Butyl Ester. International Journal of Applied Engineering Research, 11(19), 9946-9955.

Rades, S., Hodoroaba, V. D., Salge, T., Wirth, T., Lobera, M. P., Labrador, R. H., Natte, K., Behnke, T., Gross, T., & Unger, W. E. (2014). High-resolution imaging with SEM/T-SEM, EDX and SAM as a combined methodical approach for morphological and elemental analyses of single engineered nanoparticles. Rsc Advances, 4(91), 49577-49587.

Radke, C. J., & Prausnitz, J. M. (1972). Adsorption of organic solutes from dilute aqueous solution of activated carbon. Industrial & Engineering Chemistry Fundamentals, 11(4), 445-451.

Radović, T., Grujić, S., Petković, A., Dimkić, M., & Laušević, M. (2015). Determination of pharmaceuticals and pesticides in river sediments and corresponding surface and ground water in the Danube River and tributaries in Serbia. Environmental Monitoring and Assessment, 187(1), 4092.

Rajkovich, S., Enders, A., Hanley, K., Hyland, C., Zimmerman, A. R., & Lehmann, J. (2012). Corn growth and nitrogen nutrition after additions of biochars with varying properties to a temperate soil. Biology and Fertility of Soils, 48(3), 271-284.

Raks, V. A., Turchin, V. A., & Zaitsev, V. N. (2015). Chromatographic determination of pesticide 2, 4-D in water bodies. Journal of Water Chemistry and Technology, 37(6), 295-298.

Ramdane, H., El Rhilassi, A., Mourabet, M., Bennani-Ziatni, M., Elabidi, A., Zinedine, A., & Taitai, A. (2014). Calcium phosphates as adsorbents for the controlled release of carbofuran. Journal Material and Environmental Sciences 5 (6), 1715-1726.

Rangasamy, S., Purushothaman, G., Alagirisamy, B., & Santiago, M. (2015). Chromium contamination in soil and groundwater due to tannery wastes disposals at Vellore district of Tamil Nadu. International Journal of Environmental Sciences, 6(1), 114.

Rawlings, N.C., Cook, S.J., Waldbillig,D (1998). Effects of the pesticides carbofuran, chlorpyrifos, dimethoate, lindane, triallate, trifluralin, 2, 4-D, and pentachlorophenol on the metabolic endocrine and reproductive endocrine system in ewes. Journal of Toxicology and Environmental Health Part A, 54(1), 21-36.

Redlich, O. J. D. L., & Peterson, D. L. (1959). A useful adsorption isotherm. Journal of Physical Chemistry, 63(6), 1024-1024.

Rendón-von Osten, J., & Dzul-Caamal, R. (2017). Glyphosate residues in groundwater, drinking water and urine of subsistence farmers from intensive agriculture localities: a survey in Hopelchén, Campeche, Mexico. International Journal of Environmental Research and Public Health, 14(6), 595.

Richards, R. P., Kramer, J. W., Baker, D. B., Krieger, K. A. (1987). Pesticides in rainwater in the northeastern United States. Nature. 327, 129.

Rodríguez Correa, C., Stollovsky, M., Hehr, T., Rauscher, Y., Rolli, B., & Kruse, A. (2017). Influence of the carbonization process on activated carbon properties from lignin and lignin-rich biomasses. ACS Sustainable Chemistry & Engineering, 5(9), 8222-8233.

Rodríguez, A. G. P., López, M. I. R., Casillas, Á. D., León, J. A. A., & Banik, S. D. (2018). Impact of pesticides in karst groundwater. Review of recent trends in Yucatan, Mexico. Groundwater for Sustainable Development. 7, 20-29

Rossatto, D. R., Silva, L. C. R., Sternberg, L. S. L., & Franco, A. C. (2014). Do woody and herbaceous species compete for soil water across topographic gradients? Evidence for niche partitioning in a Neotropical savanna. South African Journal of Botany, 91, 14-18.

Roudani, A., Mamouni, R., Saffaj, N., Laknifli, A., Gharby, S., & Faouzi, A. (2014). Removal of Carbofuran pesticide from aqueous solution by adsorption onto animal bone meal as new low cost adsorbent. Chemical and Process Engineering Research, 28, 2014.

Ruiz-Toledo, J., Castro, R., Rivero-Pérez, N., Bello-Mendoza, R., & Sánchez, D. (2014). Occurrence of glyphosate in water bodies derived from intensive agriculture in a tropical region of southern Mexico. Bulletin of Environmental Contamination and Toxicology, 93(3), 289-293.

Sahoo, S., Borpatragohain, B., Rai, Ashish (2019). Sorption, desorption, and degradation of pesticides in biochar amended agricultural soils. International Journal of Chemical Studies, 7(3): 5106-5111

Salman, J. M. (2012). Batch study for insecticide carbofuran adsorption onto palm-oil-fronds-activated carbon. Journal of Chemistry, 2013.

Salman, J. M. (2013). Batch study for insecticide carbofuran adsorption onto palm-oil-fronds-activated carbon. Journal of Chemistry, 1-5. http://dx.doi.org/10.1155/2013/630371.

Salman, J. M., & Al-Saad, K. A. (2012). Adsorption of 2, 4-dichlorophenoxyacetic acid onto date seeds activated carbon: equilibrium, kinetic and thermodynamic studies. International Journal of Chemical Science, 10(2), 677-690.

Salman, J. M., Abd, F. M., Muhammed, A. A. (2011a). Adsorption of carbofuran insecticide from aqueous solution using commercial activated carbon. International Journal of Chemical Sciences. 9, 557-564.

Salman, J. M., and Hameed, B. H. (2010a). Removal of insecticide carbofuran from aqueous solutions by banana stalks activated carbon. Journal of Hazardous Materials, 176, 814-819.

Salman, J. M., and Hameed, B. H. (2010b). Adsorption of 2, 4-dichlorophenoxyacetic acid and carbofuran pesticides onto granular activated carbon. Desalination. 256, 129-135.

Salman, J. M., Njoku, V. O., & Hameed, B. H. (2011a). Batch and fixed-bed adsorption of 2, 4-dichlorophenoxyacetic acid onto oil palm frond activated carbon. Chemical Engineering Journal, 174(1), 33-40.

Salman, J. M., Njoku, V. O., Hameed, B. H. (2011b). Bentazon and carbofuran adsorption onto date seed activated carbon: kinetics and equilibrium. Chemical Engineering Journal. 173, 361-368.

Samiey, B., Cheng, C. H., & Wu, J. (2014). Organic-inorganic hybrid polymers as adsorbents for removal of heavy metal ions from solutions: a review. Materials, 7(2), 673-726.

Sassine, L., La Salle, C. L. G., Khaska, M., Verdoux, P., Meffre, P., Benfodda, Z., & Roig, B. (2017). Spatial distribution of triazine residues in a shallow alluvial aquifer linked to groundwater residence time. Environmental Science and Pollution Research, 24(8), 6878-6888.

Satapathy, S., Singh, R. K., Kumar, C., Negi, R., Mishra, K., & Bhuyan, K. (2017). Biostrategic removal of sulphur contamination in groundwater with sulphur-reducing bacteria: a review. Air, Soil and Water Research, 10, 1-7.

Scimeca, M., Bischetti, S., Lamsira, H. K., Bonfiglio, R., & Bonanno, E. (2018). Energy Dispersive X-ray (EDX) microanalysis: A powerful tool in biomedical research and diagnosis. European Journal of Histochemistry: EJH, 62(1).

Shackley, S., Carter, S., Knowles, T., Middelink, E., Haefele, S., Sohi, S., & Haszeldine, S. (2012). Sustainable gasification–biochar systems? A case-study of rice-husk gasification in Cambodia, Part I: Context, chemical properties, environmental and health and safety issues. Energy Policy, 42, 49-58.

Shah, J., Rasul Jan, M., & Bashir, N. (2006). Flow Injection Spectrophotometric Determination of 2, 4-D Herbicide. Journal of the Chinese Chemical Society, 53(4), 845-850.

Sharma, R., Sarswat, A., Pittman, C. U., & Mohan, D. (2017). Cadmium and lead remediation using magnetic and non-magnetic sustainable biosorbents derived from Bauhinia purpurea pods. RSC Advances, 7(14), 8606-8624.

Shi, H., Zhao, G., Liu, M., & Zhu, Z. (2011). A novel photoelectrochemical sensor based on molecularly imprinted polymer modified TiO_2 nanotubes and its highly selective detection of 2, 4-dichlorophenoxyacetic acid. Electrochemistry Communications, 13(12), 1404-1407.

Siddaramappa, R., Tirol, A. C., Seiber, J. N., Heinrichs, E. A., Watanabe, I. (1978). The degradation of carbofuran in paddy water and flooded soil of untreated and retreated rice fields. Journal of Environmental Science & Health Part B. 13, 369-380.

Sikhlomanov, I.A., Rodda, J.C. (2003). World Water Resources at the Beginning of Twenty-First Century, Cambridge University Press, Cambridge.

Simon-Delso, N., Amaral-Rogers, V., Belzunces, L.P., Bonmatin, J.M., Chagnon, M., Downs, C., Furlan, L., Gibbons, D.W., Giorio, C., Girolami, V. and Goulson, D. (2015). Systemic insecticides (neonicotinoids and fipronil): trends, uses, mode of action and metabolites. Environmental Science and Pollution Research, 22(1), 5-34.

Singh, B. K., & Walker, A. (2006). Microbial degradation of organophosphorus compounds. FEMS Microbiology Reviews, 30(3), 428-471.

Singh, D. K., Mohan, S., Kumar, V., & Hasan, S. H. (2016). Kinetic, isotherm and thermodynamic studies of adsorption behaviour of CNT/CuO nanocomposite for the removal of As (III) and As (V) from water. RSC Advances, 6(2), 1218-1230.

Singh, R. (2006). Hybrid Membrane Systems for Water Purification: Technology, Systems Design and Operations, Elsevier Science & Technology Books, Oxford, UK https://doi.org/10.1016/B978-185617442-8/50002-6.

Sips, R. (1948). On the structure of a catalyst surface. The Journal of Chemical Physics, 16(5), 490-495.

Soler, C., Mañes, J., Picó, Y. (2008). The role of the liquid chromatography-mass spectrometry in pesticide residue determination in food. Critical Reviews in Analytical Chemistry. 38, 93-117.

Somashekar, K. M., Mahima, M. R., & Manjunath, K. C. (2015). Contamination of Water Sources in Mysore City by Pesticide Residues and Plasticizer–A Cause of Health Concern. Aquatic Procedia, 4, 1181-1188.

Song, Y. (2014). Insight into the mode of action of 2, 4-dichlorophenoxyacetic acid (2, 4-D) as an herbicide. Journal of Integrative Plant Biology, 56(2), 106-113.

Sriramachari, S. (2004).The Bhopal gas tragedy: An Environmental Disaster Current Science. 86(7), 905-920.

Stănescu, M.D. (2014) Pesticides: Synthesis, Activity and Environmental Aspects. Printech, Bucharest, Hungry. DOI:10.13140/RG.2.1.3434.6007.

Steven, S. R., Heskett, M. D., & Spengler, S. C. (2018). Glyphosate in runoff from urban, mixed-use and agricultural watersheds in hawaii, USA. WIT Transactions on Ecology and the Environment, 228, 65-77.

Strathmann, H. (2012). Membranes and Membrane Separation Processes, 1. Principles. Encyclopaedia of Industrial Chemistry, 413-454.

Suett, D.L. (1986) Effects of formation of dimethylamine and dietheylamine in soils treated with pesticides. Crop Protection. 5, 16-167.

Suhag, R. (2016). Overview of ground water in India. Retrieved from https://www.prsindia.org/administrator/uploads/general/1455682937~~Overview%20of%20Ground%20Water%20in%20India.pdf] on 7th December 2018.

Sumon, K. A., Rico, A., Ter Horst, M. M., Van den Brink, P. J., Haque, M. M., & Rashid, H. (2016). Risk assessment of pesticides used in rice-prawn concurrent systems in Bangladesh. Science of the Total Environment, 568, 498-506.

Sun, S., Chen, Y., Lin, Y., & An, D. (2018). Occurrence, spatial distribution, and seasonal variation of emerging trace organic pollutants in source water for Shanghai, China. Science of the Total Environment, 639, 1-7.

Sun, X., Shan, R., Li, X., Pan, J., Liu, X., Deng, R., & Song, J. (2017). Characterization of 60 types of Chinese biomass waste and resultant biochars in terms of their candidacy for soil application. Gcb Bioenergy, 9(9), 1423-1435.

Swinehart, D. F. (1962). The beer-lambert law. Journal of Chemical Education, 39(7), 333.

Székács , A., Mörtl, M., & Darvas, B. (2015). Monitoring pesticide residues in surface and ground water in Hungary: surveys in 1990–2015. Journal of Chemistry, 2015. doi.org/10.1155/2015/717948.

Tadiboyina, R., & Ptsrk, P. R. (2016). Trace Analysis of Heavy Metals in Ground Waters of Vijayawada Industrial Area. International Journal of Environmental and Science Education, 11(10), 3215-3229.

Taghizade Firozjaee, T., Mehrdadi, N., Baghdadi, M., & Nabi Bidhendi, G. R. (2018). Application of nanotechnology in pesticides removal from aqueous solutions-a review. International Journal of Nanoscience and Nanotechnology, 14(1), 43-56.

Takaya, C. A., Fletcher, L. A., Singh, S., Okwuosa, U. C., & Ross, A. B. (2016). Recovery of phosphate with chemically modified biochars. Journal of environmental chemical engineering, 4(1), 1156-1165.

Tamrakar, U., Pillai, A. K., Gupta, V. K. (2007). A simple colorimetric method for the determination of carbofuran and its application in environmental and biological samples. Journal of the Brazilian Chemical Society. 18, 337-341.

Tan, Z., Zou, J., Zhang, L., & Huang, Q. (2018). Morphology, pore size distribution, and nutrient characteristics in biochars under different pyrolysis temperatures and atmospheres. Journal of Material Cycles and Waste Management, 20(2), 1036-1049.

Tang, L., Zhang, S., Zeng, G. M., Zhang, Y., Yang, G. D., Chen, & Deng, Y. C. (2015). Rapid adsorption of 2, 4-dichlorophenoxyacetic acid by iron oxide nanoparticles-doped carboxylic ordered mesoporous carbon. Journal of colloid and interface science, 445, 1-8.

Tariq, M. I., Afzal, S., Hussain, I. (2004). Pesticides in shallow groundwater of Bahawalnagar, Muzafargarh, DG Khan and Rajan Pur districts of Punjab, Pakistan. Environment International. 30, 471-479.

Tempkin, M. I., & Pyzhev, V. (1940). Kinetics of ammonia synthesis on promoted iron catalyst. Acta Phys. Chim. USSR, 12(1), 327.

Tiryaki, O., & Temur, C. (2010). The fate of pesticide in the environment. J. Biol. Environ. Sci, 4(10), 29-38.

Titus, M. T., Victor, O., Thompson, N. E., Moses, S., Joseph, N. O., James, K., Emmanuel, G.C. (2013). Adsorption of carbofuran on Granulated Activated carbon from Canarium Schweinfurthii seed shell. International Journal of Scientific and Engineering Research. 4, 2370-2373.

Tóth, J. (2000). Calculation of the BET-compatible surface area from any type I isotherms measured above the critical temperature. Journal of Colloid and Interface Science, 225(2), 378-383.

Trazzi, P. A., Leahy, J. J., Hayes, M. H., & Kwapinski, W. (2016). Adsorption and desorption of phosphate on biochars. Journal of environmental chemical engineering, 4(1), 37-46.

Trivedi, N. S., Kharkar, R. A., & Mandavgane, S. A. (2016a). 2, 4-Dichlorophenoxyacetic acid adsorption on adsorbent prepared from groundnut shell: Effect of preparation conditions on equilibrium adsorption capacity. Arabian Journal of Chemistry. https://doi.org/10.1016/j.arabjc.2016.07.022

Trivedi, N. S., Kharkar, R. A., & Mandavgane, S. A. (2016b). Utilization of cotton plant ash and char for removal of 2, 4-dichlorophenoxyacetic acid. Resource-Efficient Technologies, 2, S39-S46.

Trotter, D.M., Kent, R.A., Wong, M.P. (1991) Aquatic fate and effect of Carbofuran. Critical Reviews in Environmental Control. 21, 137-176.

U. N. (2015). Wastewater Management-A UN-Water Analytical Brief. World Meteorological Organization in Geneva, Switzerland, 1-52.

Uddin, M. K. (2017). A review on the adsorption of heavy metals by clay minerals, with special focus on the past decade. Chemical Engineering Journal, 308, 438-462.

Ugwu, I. M., & Igbokwe, O. A. (2019). Sorption of Heavy Metals on Clay Minerals and Oxides: A Review. In Advanced Sorption Process Applications. IntechOpen.

United States Environmental Protection Agency (USEPA) (2001). The Incorporation of Water Treatment Effects on Pesticide Removal and Transformation in Food Quality Protection Act (FQPA) Drinking Water Assessments. Office of Pesticide Programs 50 pp.

United States Environmental protection agency, USEPA (2003) retrieved from https://nepis.epa.gov/Exe/ZyPDF.cgi/P10039OH.PDF?Dockey=P10039OH.PDF on 7th December 2018.

United States Environmental protection agency, USEPA (2005) retrieved from https://nepis.epa.gov/Exe/ZyPDF.cgi/P10039OH.PDF?Dockey=P10039OH.PDF on 7th December 2018.

USEPA (2014). United States Environment Protection Agency (2014, May 10) Retrieved from EPA website http://www.epa.gov/pesticides/about/index.htm.

USEPA, (2018) United States Environment Protection Agency (2018, June 10) Retrieved from EPA website https://www.epa.gov/ingredients-used-pesticide-products/basic-information-about pesticide-ingredients.

Valix, M., Cheung, W. H., & Mckay, G. (2004). Preparation of activated carbon using low temperature carbonisation and physical activation of high ash raw bagasse for acid dye adsorption. Chemosphere, 56(5), 493-501.

Van den Berg, H., Zaim, M., Yadav, R.S., Soares, A., Ameneshewa, B., Mnzava, A., Hii, J., Dash, A.P. and Ejov, M. (2012). Global trends in the use of insecticides to control vector-borne diseases. Environmental Health Perspectives, 120(4), 577.

Van Stempvoort, D. R., Spoelstra, J., Senger, N. D., Brown, S. J., Post, R., & Struger, J. (2016). Glyphosate residues in rural groundwater, Nottawasaga River watershed, Ontario, Canada. Pest Management Science, 72(10), 1862-1872.

Verheijen, F., Jeffery, S., Bastos, A. C., Van der Velde, M., & Diafas, I. (2010). Biochar application to soils. A critical scientific review of effects on soil properties, processes, and functions. EUR, 24099, 162.

Vetrimurugan, E., Brindha, K., Elango, L., & Ndwandwe, O. M. (2017). Human exposure risk to heavy metals through groundwater used for drinking in an intensively irrigated river delta. Applied Water Science, 7(6), 3267-3280.

Vieira, D. C., Noldin, J. A., Deschamps, F. C., & Resgalla Jr, C. (2016). Ecological risk analysis of pesticides used on irrigated rice crops in southern Brazil. Chemosphere, 162, 48-54.

Vimal, V., Patel, M., & Mohan, D. (2019). Aqueous carbofuran removal using slow pyrolysed sugarcane bagasse biochar: equilibrium and fixed-bed studies. RSC advances (accepted/in press)

Vithanage, M., Mayakaduwa, S. S., Herath, I., Ok, Y. S., & Mohan, D. (2016). Kinetics, thermodynamics and mechanistic studies of carbofuran removal using biochars from tea waste and rice husks. Chemosphere, 150, 781-789.

Volesky, B. (2007). Biosorption and me. Water Research, 41(18), 4017-4029.

Von Gunten, U. (2003). Ozonation of drinking water: Part I. Oxidation kinetics and product formation. Water Research, 37(7), 1443-1467.

Vulliet, E., Tournier, M., Vauchez, A., Wiest, L., Baudot, R., Lafay, F., Kiss, A. and Cren-Olivé, C. (2014). Survey regarding the occurrence of selected organic micropollutants in the groundwaters of overseas departments. Environmental Science and Pollution Research, 21(12), 7512-7521.

Wafa, T., Nadia, K., Amel, N., Ikbal, C., Insaf, T., Asma, K., & Mohamed, H. (2013). Oxidative stress, hematological and biochemical alterations in farmers exposed to pesticides. Journal of Environmental Science and Health, Part B, 48(12), 1058-1069.

Walker, L. C. (1998). The North American forests: geography, ecology, and silviculture. CRC press.

Walters, J. (1999). Environmental fate of 2, 4-dichlorophenoxyacetic acid. Department of pesticide regulations, Sacramento, CA, 18.

Wang, J. W., Zhang, C. X., Pan, Z. Z., Liao, X. P., Liu, Y., Lü, Y., & Tang, M. (2017). Distribution Characteristics and Influencing Factors of Organophosphorus Pesticides in Typical Soil Environment of Jianghan Plain. Huan jing ke xue= Huanjing kexue, 38(4), 1597-1605.

Wang, J., & Chen, C. (2006). Biosorption of heavy metals by Saccharomyces cerevisiae: a review. Biotechnology Advances, 24(5), 427-451.

Wang, S., & Peng, Y. (2010). Natural zeolites as effective adsorbents in water and wastewater treatment. Chemical Engineering Journal, 156(1), 11-24.

Wang, S., Gao, B., Zimmerman, A. R., Li, Y., Ma, L., Harris, W. G., & Migliaccio, K. W. (2015). Physicochemical and sorptive properties of biochars derived from woody and herbaceous biomass. Chemosphere, 134, 257-262.

Wang, S., Zhao, X., Xing, G., & Yang, L. (2013). Large-scale biochar production from crop residue: A new idea and the biogas-energy pyrolysis system. BioResources, 8(1), 8-11.

Waseem, A., Yaqoob, M., Nabi, A. (2007). Flow-injection determination of carbaryl and carbofuran based on KMnO4–Na2SO3 chemiluminescence detection. Luminescence. 22, 349-354.

Weber, W. J. (1972). Physicochemical processes for water quality control. Wiley Interscience.

Wheeler, W. B. (Ed.). (2002). Pesticides in Agriculture and the Environment. CRC Press.

WHO, 1997. Water Pollution Control- A Guide to the use of Water Quality Management Principles. Great Britain: WHO/UNEP.

WHO, 2004. Carbofuran in drinking water- Background document for development of WHO guidelines for drinking water quality, http://www.who.int/water_sanitation_health/dwq/chemicals/carbofuran.pdf (dated 6 june 2014).

Wilson, I.B., and Harrison, M. A. (1961). Turnover number of acetylcholinesterase. Journal of Biological Chemistry. 236, 2292-2295.

Wong, L., and Fisher, F. M. (1975). Determination of carbofuran and its toxic metabolites in animal tissue by gas chromatography of their N-trifluoroacetyl derivatives. Journal of Agricultural and Food Chemistry. 23, 315-318.

World Health Organization (WHO). (2017). Guidelines for drinking-water quality: fourth edition incorporating the first addendum.Geneva:. Licence: CC BY-NC-SA 3.0 IGO.

World Health Organization. (2004). Back ground document for development of WHO Guidelines for drinking water quality.

Wu, C., Luo, Y., Gui, T., & Huang, Y. (2014a). Concentrations and potential health hazards of organochlorine pesticides in shallow groundwater of Taihu Lake region, China. Science of the Total Environment, 470, 1047-1055.

Wu, C., Luo, Y., Gui, T., & Yan, S. (2014b). Characteristics and Potential Health Hazards of Organochlorine Pesticides in Shallow Groundwater of Two Cities in the Yangtze River Delta. CLEAN–Soil, Air, Water, 42(7), 923-931.

Wu, J., & Yu, H. Q. (2007). Biosorption of 2, 4-dichlorophenol by immobilized white-rot fungus Phanerochaete chrysosporium from aqueous solutions. Bioresource Technology, 98(2), 253-259.

Wu, W., Yang, M., Feng, Q., McGrouther, K., Wang, H., Lu, H., & Chen, Y. (2012). Chemical characterization of rice straw-derived biochar for soil amendment. Biomass and bioenergy, 47, 268-276.

WWAP (United Nations World Water Assessment Programme) (2015). The United Nations World Water Development Report 2015: Water for a Sustainable World. Paris, UNESCO.

Xi, Y., Mallavarapu, M., & Naidu, R. (2010). Adsorption of the herbicide 2, 4-D on organo-palygorskite. Applied Clay Science, 49(3), 255-261.

Yadav, I. S., & Devi, N. L. (2017). Pesticides Classification and its Impact on Human and Environment. Environment Science and Engineering, 6.

Yang, S. B., & Hu, H. Q. (2000). Development of Surface Area and Pore Structure of Carbon Adsorbent with Large Surface Area. Journal of Fuel Chemistry and Technology, 28(5), 473-477.

Youssef, L., Younes, G., Kouzayha, A., & Jaber, F. (2015). Occurrence and levels of pesticides in South Lebanon water. Chemical Speciation & Bioavailability, 27(2), 62-70.

Zama, E. F., Zhu, Y. G., Reid, B. J., & Sun, G. X. (2017). The role of biochar properties in influencing the sorption and desorption of Pb (II), Cd (II) and As (III) in aqueous solution. Journal of cleaner production, 148, 127-136.

Zdravkov, B. D., Čermák, J. J., Šefara, M., & Janků, J. (2007). Pore classification in the characterization of porous materials: A perspective. Central European Journal of Chemistry, 5(2), 385-395.

Zhang, M., Sun, Y. C., Xie, Z. L., Yu, Q., & Xu, X. (2016). Distribution Characteristics and Source Identification of Organochlorine Pesticides in the Karst Groundwater System. Huan jing ke xue= Huanjing kexue, 37(9), 3356-3364.

Zhang, W. (2018). Global pesticide use: Profile, trend, cost/benefit and more. Proceedings of the International Academy of Ecology and Environmental Sciences, 8(1), 1-27.

Zhang, X., Luo, Y., & Goh, K. S. (2018). Modeling spray drift and runoff-related inputs of pesticides to receiving water. Environmental Pollution, 234, 48-58.

Zhang, Z.-Y., Liu, X.-J., & Hong, X.-Y. (2007). Effects of home preparation on pesticide residues in cabbage. Food Control, 18(12), 1484-1487.

Zhao, S. X., Ta, N., & Wang, X. D. (2017). Effect of temperature on the structural and physicochemical properties of biochar with apple tree branches as feedstock material. Energies, 10(9), 1293.

Zhu, L., Lei, H., Wang, L., Yadavalli, G., Zhang, X., Wei, & Ahring, B. (2015). Biochar of corn stover: Microwave-assisted pyrolysis condition induced changes in surface functional groups and characteristics. Journal of Analytical and Applied Pyrolysis, 115, 149-156.

Zolgharnein, J., Shahmoradi, A., Ghasemi, J. (2011) Pesticides Removal Using Conventional and Low-Cost Adsorbents: A Review, Clean – Soil, Air, Water. 39, 1105–1119.